MINISTRY OF EDUCATION AND SCIENCE UKRAINE

ODESSA I. I. MECHNIKOV NATIONAL UNIVERSITY

ФОТОЭЛЕКТРОНИКА

PHOTOELECTRONICS
INTER-UNIVERSITIES SCIENTIFIC ARTICLES

Founded in 1986

Number 28

ODESSA
ONU
2019

«PHOTOELECTRONICS»
№ 2 8 – 2 0 1 9

INTER-UNIVERSITIES SCIENTIFIC ARTICLES

Founded in 1986

Certificate of State Registration
KB № 15953

«ФОТОЭЛЕКТРОНИКА»
№ 28–2019

МЕЖВЕДОМСТВЕННЫЙ НАУЧНЫЙ СБОРНИК

Основан в 1986 г.

Свидетельство о Государственной регистрации КВ № 15953

UDC 621.315.592:621.383.51:537.221

The results of theoretical and experimental studies in problems of the semiconductor and micro-electronic devices physics, opto- and qantum electronics, quantum optics, spectroscopy and photophysics of nucleus, atoms, molecules and solids are presented in the issue. New directions in the photoelectronics, stimulated by problems of the super intense laser radiation interaction with nuclei, atomic systems and substance, are considered. Scientific articles «Photoelectronics» collection abstracted in ВИНИТИ and «Джерело».

Scientific articles «Photoelectronics» collection abstracted in: Scientific Periodicals in National Library of Ukraine Vernadsky, Ukrainian Abstract Journal, Україніка наукова, ВИНИТИ, Джерело, Українські наукові журнали: The issue is introduced to the List of special editions of the Ukrainian Higher Certification Com¬mission in physics-mathematics and technical sciences.

For lecturers, scientists, post-graduates and students.

У збірнику наведено результати теоретичних і експериментальних досліджень з питань фізики напівпровідників та мікроелектронних приладів, опто- та квантової електроніки, квантової оптики, спектроскопії та фотофізики ядра, атомів, молекул та твердих тіл. Розглянуто нові напрямки розвитку фотоелектроніки, пов'язані із задачами взаємодії надінтенсивного лазерного випромінювання з ядром, атомними системами, речовиною.

Збірник включено до Переліку спеціальних видань ВАК України з фізико-математичних та технічних наук.

Збірник реферується: Scientific Periodicals in National Library of Ukraine Vernadsky, Ukrainian Abstract Journal, Україніка наукова, ВИНИТИ, Джерело, Українські наукові журнали.

Для викладачів, наукових працівників, аспіранів, студентів.

В сборнике приведены результаты теоретических и экспериментальных исследований по вопросам физики полупроводников и микроэлектронных приборов, опто- и квантовой электроники, квантовой оптики, спектроскопии и фотофизики ядра, атомов, молекул и твердых тел. Рассмотрены новые направ¬ления развития фотоэлектроники, связанные с задачами взаимодействия сверхинтенсивного лазерного излучения с ядром, атомными системами, веществом.

Сборник включен в Список специальных изданий ВАК Украины по физико-математическим и тех¬ническим наукам. Сборник «Photoelectronics» реферируется в Scientific Periodicals in National Library of Ukraine Vernadsky, Ukrainian Abstract Journal, Україніка наукова, ВИНИТИ, Джерело, Українські наукові журнали.

Для преподавателей, научных работников, аспирантов, студентов.

Address of editorial board:
Odessa I. I. Mechnikov National University 42, Pasteur str., Odessa, 65026, Ukraine
Information is on the site: http://phys.onu.edu.ua/journals/photoele/
http://experiment.onu.edu.ua/exp_ru/files/?
e-mail: photoelectronics@onu.edu.ua.

TABLE OF CONTENTS:

UDC 621.315.592

Yu. A. Nitsuk, Yu. F. Vaksman, I. V. Tepliakova, V. A. Smyntyna, G. V. Korenkova, Ie. V. Brytavskyi

I. I. Mechnikov Odesa National University
e-mail: nitsuk@onu.edu.ua

OPTICAL PROPERTIES OF OF ZnS:Fe NANOCHRYSTALLS OBTAINED BY COLLOIDAL METHOD

Iron doped zinc sulfide nanocrystals were obtained by colloidal synthesis using gelatin, lactose or polyvinyl alcohol as a stabilizing matrix. The structure of the nanocrystals was determined using X-ray diffraction (XRD). The influence of the concentration effect on the size and properties of ZnS nanocrystals, the optical absorption spectra and photoluminescence spectra were studied, and the types of optical transitions in these nanocrystals were determined.

I. Introduction

In recent years, researchers' interest in colloidal methods for the synthesis of semiconductor nanoparticles has been growing. These particles have a number of unique characteristics determined by their shape and size. In this regard, the widespread practical use of nanoparticles is constrained by the possibility of obtaining nanoparticles with a controlled shape and size.

Among II-VI semiconductor compounds, zinc sulfide has the largest band gap. Another more important advantage of ZnS is non-toxicity, which makes the use of ZnS nanocrystals as luminescent markers in medicine promising [1,2]. The radiation of such markers should be localized in the area of maximum transparency of living tissues (0.65-1.5 μm). Our studies on semiconductor ZnS:Fe single crystals [3] indicate the presence of broad absorption bands and photoluminescence (0.5-0.8 μm) that are effectively excited by light from the impurity absorption region.

The purpose of this work is to develop a technique for obtaining ZnS:Fe nanocrystals in which the spectra of optical absorption and photoluminescence are in the near infrared region. To determine the nature of the optical and radiation transitions, the results of the study of the optical properties of ZnS: Fe single crystals are given.

II. Experimental

ZnS, ZnS: Fe nanocrystals were obtained by chemical synthesis in a matrix of polyvinyl alcohol, gelatin or lactose. Pure zinc sulphide nanocrystals were obtained by reaction of:

$$ZnCl_2+Na_2S\rightarrow ZnS+2NaCl. \quad (1)$$

Fe doped ZnS nanocrystals were obtained by reaction of:

$$ZnCl_2+Na_2S+Fe_2Cl_3\rightarrow ZnS:Fe:Cl+ +2NaCl+Cl_2\uparrow. \quad (2)$$

Commercial reagents from Beijing were used for the synthesis.

After synthesis, the solution was dried on a quartz or glass substrate. As a result, ZnS, ZnS:Fe nanocrystals were obtained in a transparent solid polymer matrix. The structure analysis of the obtained ZnS nanoparticles was carried out by X-ray diffraction (Fig. 1). The diffraction peaks 2θ correspond to the plane (111) in zinc sulfide.

III. Experiment and results

The optical absorption spectra of undoped nanocrystals are shown in Fig. 2, curve 1. The band gap of zinc sulfide single crystals is 3.6 eV. The nanocrystals obtained are characterized by bandgap values E_g of 5.07 eV at Na_2S and $ZnCl_2$ concentrations of 10%, respectively.

The optical absorption spectra of ZnS:Fe nanocrystals show an offset of the absorption edge towards lower energies compared to undoped samples (Fig. 2, curves 2-4). The magnitude of the shift is 0.2 eV with increasing

Fe_2Cl_3 concentration from 0.1 to 0.5%, this may be due to an increase in the Fe content in the samples, or an increase in the size of the nanocrystals.

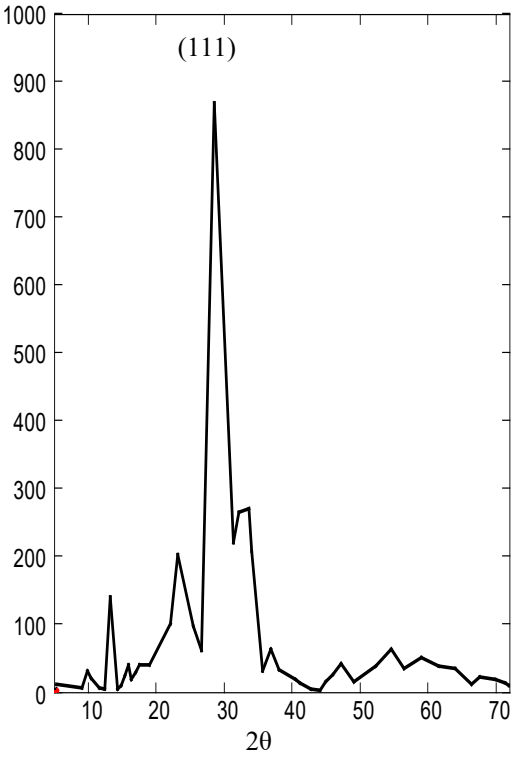

Fig.1. XRD-pattern of ZnS:Fe nanocrystals.

The size of nanocrystals was estimated by the difference of their bandgap and bulk single crystals using the ratio [4]:

$$R = \frac{h}{\sqrt{8\mu\Delta E_g}}, \qquad (3)$$

h - Planck constant, $\mu=((m_e)^{-1}+(m_h)^{-1})^{-1}$ – reduced mass, $m_e=0.27m_0$, $m_h=0.58m_0$, respectively, the effective masses of electrons and holes in zinc sulfide, m_0 – mass of free electron, ΔE_g - the difference between the bandgap of the nanocrystals (3.63eV). As shown in the Table 1, the size of the nanocrystallites does not change significantly.

The optical absorption spectra of ZnS:Fe nanocrystals in the region of 1.6 - 4.0 eV are characterized by the presence of a considerable number of absorption lines (Fig. 3). Increasing the concentration of Fe leads to an increase in the absorption in this region with the unchanged arrangement of the maxima of the absorption lines. This indicates the intracenter nature of the absorption lines in ZnS:Fe nanocrystals. Similar absorption lines were observed previously in bulk ZnS:Fe crystals [3].

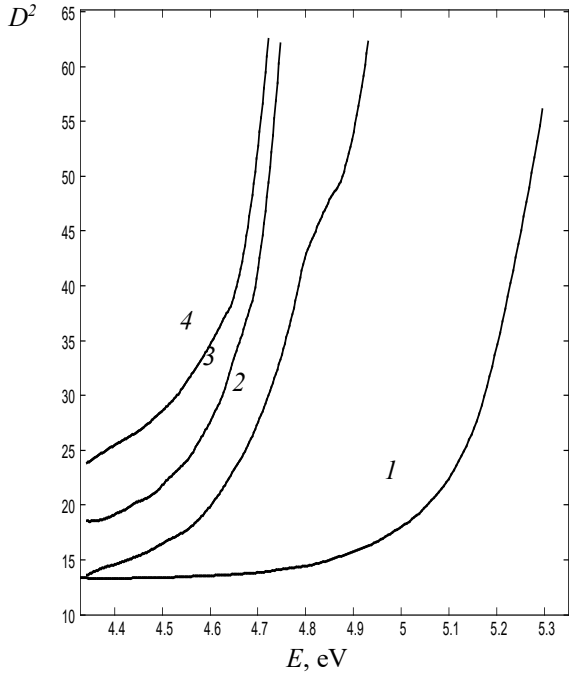

Fig.2 Optical absorption spectra of ZnS (1), ZnS:Fe(2-4) nanocrystals, T=300 K.

Table 2 summarizes the energies and interpretation of optical transitions in bulk and ZnS:Fe nanocrystals. The middle column shows the calculations of the energy states of Fe^{2+} ions in the approximation of the nearest tetrahedral environment at the crystal field parameters Δ = 3500 cm^{-1} and B = 600 cm^{-1}. In this case, light absorption occurs through optical transitions from the ground ^5E (D) to the excited states of the Fe^{2+} ion. As shown in Table 2, the calculations are equally good for
both bulk and nanocrystals, which testifies to the validity of the crystal field theory, according to which the ions of transition elements are affected by the closest tetrahedral environment whose size is smaller than the size of the

Table 2. Optical transitions involving Fe^{2+} ions

№	Type of crystal	ZnS:Fe bulk		Culc	ZnS:Fe nano	
Transition		$E_{exp.\ abs.}$, eV	$E_{PL,}\ eV$	$E_{culc.abs.,}\ eV$	$E_{exp.\ abs.}$, eV	$E_{PL,}\ eV$
1	$^5E(D) \rightleftarrows {}^1T_2(F)$	---	---	---	3.87	---
2	$^5E(D) \rightleftarrows {}^1T_2(F)$	---	---	---	3.84	---
3	$^5E(D) \rightleftarrows {}^1A_2(F)$	---	---	---	3.72	---
4	$^5E(D) \rightleftarrows {}^1A_1(S)$	---	---	---	3.66	---
5	$^5E(D) \rightleftarrows {}^1T_2(D)$	---	---	---	3.48	---
6	$^5E(D) \rightleftarrows {}^1T_1(G)$	---	---	3.34	3.37	---
7	$^5E(D) \rightleftarrows {}^1E(D)$	---	---	3.22	3.21	---
8	$^5E(D) \rightleftarrows {}^1A_1(G)$	3.18	---	3.19	3.14	---
9	$^5E(D) \rightleftarrows {}^1E(G)$	3.06	---	3.06	3.05	---
10	$^5E(D) \rightleftarrows {}^1T_2(G)$	2.94	---	2.97	2.97	---
11	$^5E(D) \rightleftarrows {}^3T_2(D)$	2.84	---	2.82	2.84	---
12	$^5E(D) \rightleftarrows {}^3E(D)$	2.78	---	2.75	2.78	---
13	$^5E(D) \rightleftarrows {}^1T_1(I)$	2.72	2.7	2.72	2.7	---
14	$^5E(D) \rightleftarrows {}^1T_2(I)$	---	---	2.65	2.65	---
15	$^5E(D) \rightleftarrows {}^1A_1(I)$	---	2.58	2.64	2.62	---
16	$^5E(D) \rightleftarrows {}^3T_1(P)$	2.60	---	2.60	2.58	2.55
17	$^5E(D) \rightleftarrows {}^3T_2(G)$	---	2.48	2.52	2.50	2.47
18	$^5E(D) \rightleftarrows {}^1A_2(I)$	2.50	2.36	2.51	2.45	---
19	$^5E(D) \rightleftarrows {}^3T_1(G)$	2.39	2.28	2.38	2.41	---
20	$^5E(D) \rightleftarrows {}^1T_2(I)$	2.30	2.25	2.34	2.38	2.31
21	$^5E(D) \rightleftarrows {}^1E(I)$	---	---	2.33	2.33	---
22	$^5E(D) \rightleftarrows {}^3T_2(F)$	---	2.20	2.24	2.26	2.25
23	$^5E(D) \rightleftarrows {}^3E(G)$	2.22	2.09	2.23	2.18	2.17
24	$^5E(D) \rightleftarrows {}^3T_1(F)$	2.11	1.99	2.08	2.07	2.05
25	$^5E(D) \rightleftarrows {}^3A_1(G)$	2.03	1.88	2.03	2.0	---
26	$^5E(D) \rightleftarrows {}^3A_2(F)$	1.94	---	1.97	1.91	1.91
27	$^5E(D) \rightleftarrows {}^3T_2(H)$	1.85	---	1.84	1.84	1.83
28	$^5E(D) \rightleftarrows {}^3T_1(H)$	1.82	---	1.82	1.77	1.75
29	$^5E(D) \rightleftarrows {}^3E(H)$	1.75	---	1.73	1.71	---
30	$^5E(D) \rightleftarrows {}^3T_1(H)$	1.35	1.30	1.37	---	---
31	$^5E(D) \rightleftarrows {}^5T_2(D)$	0.45	0.68	0.45	--	---

nanocrystallites (lattice period) ZnS is 5.6 Å and nanocrystallite size is 3-5 nm).

Photoluminescence of the undoped ZnS nanocrystals wasn't observed in the region of 1.6-3.5 eV. The doping of ZnS nanocrystals leads to the formation of a broad structured photoluminescence band in the 1.6-2.8 eV region (Fig. 4). The same structured photoluminescence bands were observed previously in bulk ZnS:Fe crystals. With increasing Fe concentrations, the luminescence spectrum expands toward lower energies.

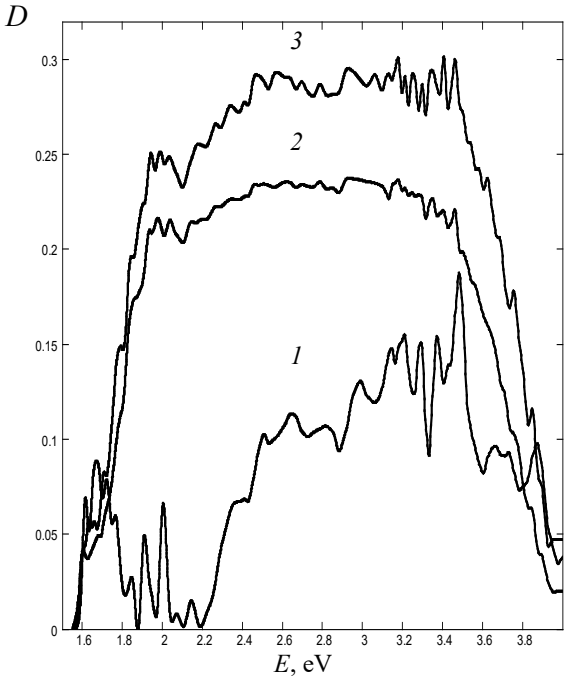

Fig.3. Optical density spectra of ZnS:Fe nanocrystals. [Fe]=0.1(1), 0.3(2), 0.5%(3). *T*=300 K.

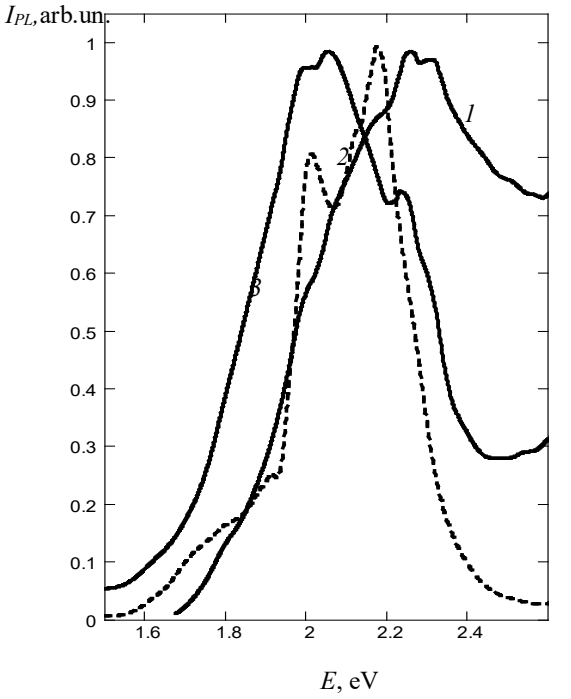

Fig.4. Photoluminescence spectra of ZnS:Fe nanocrystals. [Fe]=0.1(1), 0.3(2) та 0.5%(3). T=300 K.

Conclusions

Iron-doped zinc sulfide nanocrystals were obtained. A comparative analysis of the optical absorption and photoluminescence spectra of iron-doped zinc sulfide nano- and single crystals was performed.

The nature of intracenter optical transitions that determine the optical properties of ZnS: Fe nanocrystals is established. The crystal field theory that the splitting of the energy states of Fe^{2+} ions occurs under the action of the closest tetrahedral environment is confirmed.

ZnS: Fe nanocrystals have a photoluminescence spectrum corresponding to the transparency of living tissues. This allows the use of ZnS: Fe nanocrystals as fluorescent markers in medical diagnostics

References

1. Rosdi I., Saleh M-H., Norsal K., Malek M. Z.- A., Sulaiman M. - A. and Baharom M. -A. Synthesis of Fe^{2+} ion Doped ZnS Nanoparticles // Advanced Materials Research. – 2014. – V. 879. – P.155-163.

2. Kumar S., Singhal M., Sharma J. K. Functionalization and characterization of ZnS quantum dots using biocompatible L –cysteine// J. Mater Sci: Mater Electron. - 2013. - V. 24. - P.3875–3880.

3. Nitsuk Yu.A., Vaksman Yu.F., Yatsun V.V., Purtov Yu.N. Optical absorption and diffusion of iron in ZnS single crystals// Functional Materials. - 2012. - V.19, No.2.- P.182-186.

4. Гусев А.И., Рempель А.А. Нанокристаллические материалы.- М:Физматлит.-2000.-С.224.

UDC 621.315.592

Yu. A. Nitsuk, Yu. F. Vaksman, I. V. Tepliakova, V. A. SMyntyna, G. V. Korenkova, Ie. V. Brytavskyi

I. I. Mechnikov Odesa National University
e-mail: nitsuk@onu.edu.ua

OPTICAL PROPERTIES OF OF ZnS:Fe NANOCHRYSTALLS OBTAINED BY COLLOIDAL METHOD

Abstract – iron doped zinc sulfide nanocrystals were obtained by colloidal synthesis using gelatin, lactose or polyvinyl alcohol as a stabilizing matrix. The structure of the nanocrystals was determined using X-ray diffraction (XRD). The influence of the concentration effect on the size and properties of ZnS nanocrystals, the optical absorption spectra and photoluminescence spectra were studied, and the types of optical transitions in these nanocrystals were determined.

Key words – Zinc Sulfide, Nanocrystals, Absorption Edge, Photoluminescence.

УДК 621.315.592

Ю. А. Ніцук, Ю. Ф. Ваксман, І. В. Теплякова, В. А. Сминтина, Г. В. Коренкова, Є. В. Бритавський

Одеський національний університет імені І. І. Мечникова
e-mail: nitsuk@onu.edu.ua

ОПТИЧНІ ВЛАСТИВОСТІ НАНОКРИСТАЛІВ ZnS:Fe ОТРИМАНИХ КОЛОЇДНИМ МЕТОДОМ

Анотація– Нанокристали сульфіду цинку легованого залізом були отримані шляхом колоїдного синтезу з використанням желатину, лактози або полівінілового спирту в якості стабілізуючої матриці. Структура нанокристалів визначена за допомогою рентгенівської дифракції (XRD). Вивчено вплив концентраційного ефекту на розмір і властивості нанокристалів ZnS, спектри оптичного поглинання і фотолюмінесценції, визначено типи оптичних переходів в даних нанокристалах.

Ключові слова – Сульфід цинку, нанокристали, край поглинання, фотолюмінесценція.

УДК 621.315.592

Ю. А. Ницук, Ю. Ф. Ваксман, И. В. Теплякова, В. А. Смынтына, А. В. Коренкова, Е. В. Бритавский

Одесский национальний университет имени И. И. Мечникова
e-mail: nitsuk@onu.edu.ua

ОПТИЧЕСКИЕ СВОЙСТВА НАНОКРИСТАЛЛОВ ZnS:Fe ПОЛУЧЕННЫХ КОЛЛОИДНЫМ МЕТОДОМ

Аннотация – Нанокристаллы сульфида цинка легированного железом были получены путем коллоидного синтеза с использованием желатина, лактозы или поливинилового спирта в качестве стабилизирующей матрицы. Структура нанокристаллов определена при помощи рентгеновской дифракции (XRD). Изучены влияние концентрационного эффекта на размер и свойства нанокристаллов ZnS, спектры оптического поглощения и фотолюминесценции, определены типы оптических переходов в данных нанокристаллах.

Ключевые слова – Сульфид цинка, нанокристаллы, край поглощения, фотолюминесценция.

PACS 73.61.Le, 73.63.Bd

Y. I. Bulyga, A. P. Chebanenko, V. S. Grinevych, L. M. Filevska

Odessa Mechnikov National University, Odessa, Dvorianskaya str., 2, Odessa 65082, Ukraine,
e-mail: lfilevska@gmail.com

ELECTROPHYSICAL PROPERTIES OF ZINC OXIDE THIN FILMS OBTAINED BY CHEMICAL METHODS

The electrophysical characteristics comparative studies were carried out for ZnO films obtained by chemical precipitation from zinc acetate solutions and thermal oxidation of zinc films. The ZnO films showed optical absorption and band gap (2.9 to 3.2 eV) specific for this material, which indicates the presence of crystalline structure in them. The use of polyvinyl alcohol made it possible to obtain samples with the highest values of Eg and electrical resistance, which is caused by the nanosize crystallites of the films. The investigated electrophysical characteristics of the ZnO films made it possible to establish the contribution of their own defects and surface states to the conductivity.

Introduction

Recently, interest in zinc oxide has increased due to the possibility of using this material to create cathodoluminophores, electroluminescent screens, acoustoelectronic amplifiers, gas detectors, various types of photo- and optoelectronic devices [1,2], as well as in the composition of electronic materials [3]. Often this is possible due to the special properties of the surface and grain boundaries of the material, which can be further modified by targeted alloying, as well as by change in the synthesis conditions. [4-6]. High values of transparency and refractive index of ZnO films in the visible spectrum region makes it possible to use them as illuminating coatings for interference optical elements, as well as to create a transparent conductive electrode in solar cells. [7,8]. Currently, interest to ZnO films has increased due to their possible application to photoelectronic devices such as LEDs with ultraviolet radiation, blue fluorescent ultraviolet emitters and lasers [9]. The need to reduce the costs and to improve the quality of optoelectronic devices necessitates the development of new methods in the manufacturing of ZnO films.

Known from the literature methods for producing thin films of zinc oxide are: atomic layer deposition technique [10,11], and magnetron sputtering in many of its modifications [12,13]. However, these methods require quite energy-intensive technical support. Another used method is sol-gel technology, which, unfortunately, involves the application of relatively expensive and at the same time harmful reagents, such as α-terpineol, 2-methoxyethanol, 2-aminoethanol, etc.

In this paper zinc oxide films were obtained by relatively simple methods, in particular, chemical precipitation from zinc acetate solutions, thermal oxidation of zinc films, and subsequent comparative studies of their electrophysical characteristics.

Samples preparation

The studied zinc oxide films were obtained in three different ways, which are hereinafter arbitrarily designated as groups A, B and C. To obtain samples of group A, an aqueous solution of zinc acetate ($Zn(O_2CCH_3)_2$) with a concentration of 0.25 mol was used. Glass substrates were immersed in an aqueous solution of zinc acetate, dried at room temperature in air, and again immersed in the solution. After that, the obtained films were annealed in an air atmosphere at a temperature of 310 °C for 20-60 min.

Samples of group B were also obtained from an aqueous solution of zinc acetate, but with the addition of an aqueous 1% solution of polyvinyl alcohol (C_2H_4O - PVA) for the purpose of additional structuring of the films, in equal proportions of 2 ml each. Then, the substrates were immersed several times in the solution according to the procedure described above and annealed

in air at a temperature of 310 °C for 60 min.

To obtain group C samples, thin films of zinc metal were deposited on a cleaned glass substrate by thermal spraying in high vacuum. Further, zinc films were annealed in a muffle furnace in air at 570 °C for 10-30 min. As a result, the oxidation process occurred and translucent whitish zinc oxide films were created.

For conducting electrophysical measurements, samples of each of the groups of zinc oxide films were provided with ohmic contacts. For this, indium in the form of parallel strips was deposited on the samples by thermal spraying in high vacuum.

Results and Discussion

A typical edge of the optical absorption spectra of ZnO films (group A) is shown on Fig.1. The satisfactory straightening in the coordinates of D^2-hυ (here D is the optical density) is evident. This fact indicates direct allowed optical transitions in the films. The extrapolation of the linear section of the dependences to the energy axis gives the band gap for various samples ranging from 3.02 to 3.06 eV, which satisfactorily coincides with the band gap data for zinc oxide films either calculated [14] or obtained from optical measurements [15,16] by other authors. Extrapolation was carried out taking into account the subtraction of the apparent absorption, which is due to scattering and reflection of the incident light from the film surface. The plateau near the absorption edge at low energies is due to the presence of an amorphous phase in the studied ZnO films.

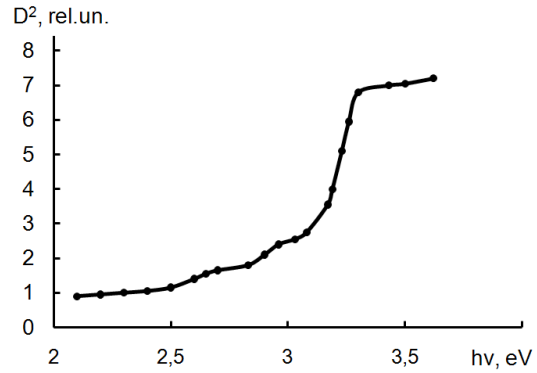

Fig. 1. Typical spectra of the optical absorption of ZnO films (group A)

Figure 2 shows a typical absorption spectrum of a zinc oxide film (group B). The band gap, E_g = (3.15-3.2) eV was found by extrapolating its linear section to the energy axis. It can be argued that it is noticeably larger than the band gap of the group A zinc oxide films. This means that the sizes of ZnO crystallites obtained in a solution of zinc acetate with polyvinyl alcohol impurities are smaller than crystallites of ZnO films obtained from a solution without PVA impurities.

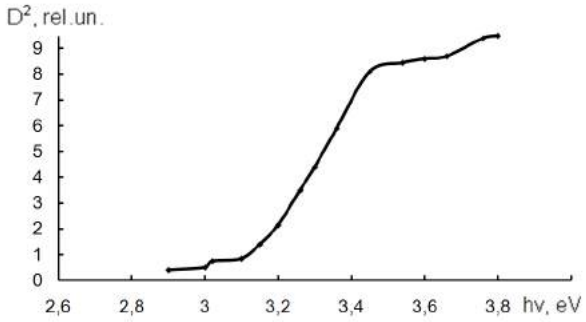

Fig. 2. Typical spectra of the optical absorption of ZnO films (group B).

Figure 3 shows a typical edge of the absorption spectra of zinc oxide films (group C). The band gap, obtained from the extrapolation of their straight section is (2.9-2.96) eV. Thus, the zinc oxide films obtained by oxidizing a metal zinc film in air atmosphere have the smallest band gap. However, the shape of the optical absorption edge indicates their most perfect crystalline structure compared to films obtained from a solution of zinc acetate.

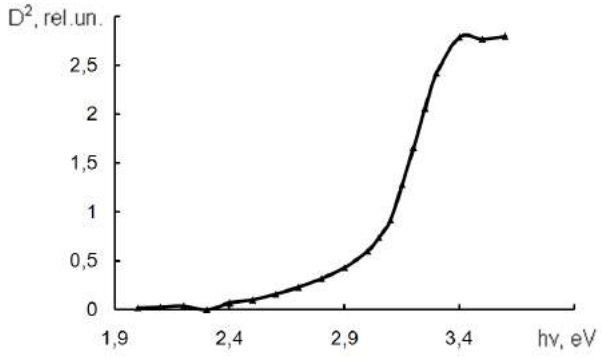

Fig. 3. Typical spectra of the optical absorption of ZnO films (group C).

The band gap of ZnO films obtained with PVA admixture is greater than that of similar films obtained without PVA admixture. The reason is that the PVA polymer matrix limits the size of the reaction volumes where zinc oxide crystallites are synthesized, and thus inhibits the growth of ZnO crystallites.

The current-voltage characteristics and the dark current temperature dependences were investigated in order to assess the electrophysical properties and the presence of their own defects in the band gap of zinc oxide films

Current-voltage characteristic (CVC) of the ZnO film (group A), measured in air (Fig. 4), shows the current linear dependence on the applied voltage, which indicates the electrical uniformity of the film. The inter electrode resistance calculated from the CVC is about $4 \cdot 10^7$ Ohms.

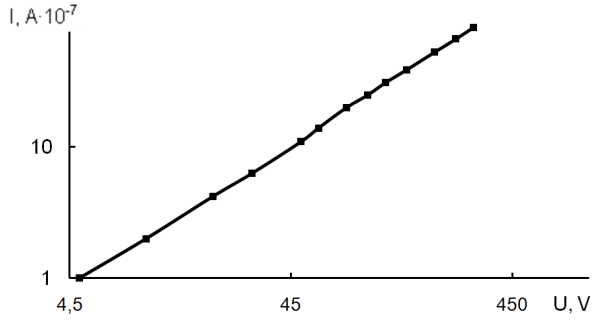

Fig. 4. Current-voltage characteristic of ZnO film (group A), measured in air (T = 293K)

The dark current temperature dependence of ZnO film (group A), measured in vacuum at heating of the film is shown at Fig.5. It can be distinguished three characteristic areas. The current at all these sites grows with temperature exponentially. The first section, located in the low-temperature region, has the conductivity activation energy of 0.08 eV, which, with increasing temperature, changes the line slope to the activation energy of 0.16 eV. At a temperature of about 105 °C, this section is replaced by a section with a sharp rise of current with the conductivity activation energy of 1.6 eV.

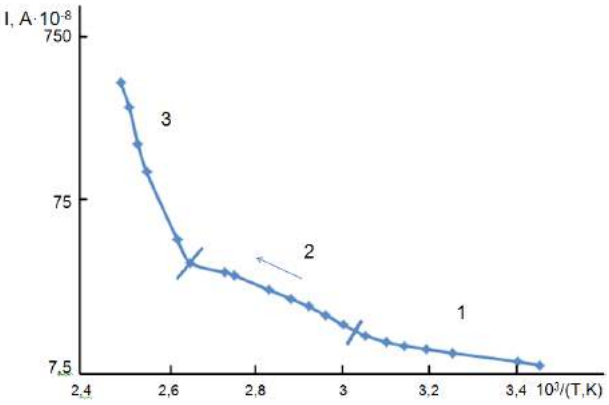

Fig. 5. The dark current temperature dependence of the ZnO film (group A) measured in vacuum. (U = 10 V).

The first and the second temperature-dependent regions may correspond to donor levels formed in the films' volume by single- and double-ionized oxygen vacancies, just as in the case with tin dioxide films. The sharp increase in the current at a temperature above 105 °C is caused by oxygen desorption from the surface of ZnO films. It is known that an oxygen atom adsorbed on the surface of a ZnO film captures one electron from the conduction band thus transforming into a single negatively charged ion, or captures two electrons and becomes a twice negatively charged ion. This leads to a current locking type bending of the surface energy zones and to the appearance of local levels (0.7-0.76) eV and (1.4-1.6) eV, respectively with energy distances from the bottom of the conduction band on the surface of the film. At high temperatures electrons, trapped by oxygen atoms, are thermally released into the conduction band, and oxygen atoms are desorbed from the film surface.

The current–voltage characteristic of the ZnO film (group B) (Fig. 6) is slightly superlinear and has a tendency to an exponential current –voltage dependence. Such dependence is inherent to the barrier current flow mechanism. That is, in the films obtained with PVA admixtures, the intercrystalline potential barriers affecting the current flow are more pronounced. The average value of the inter-electrode resistance, calculated from the initial linear section of the CVC, is

about 2.8 · 10^9 Ohms. Therefore, the presence of PVA impurity increases the film resistance by almost 2 orders of magnitude. The reason is, that the PVA evaporates during the annealing, thus increasing the porosity of these films, and they become nanostructured with a more developed surface. Nanometer crystallites can create a quantum well effect for carriers [17], which also lead to greater resistance.

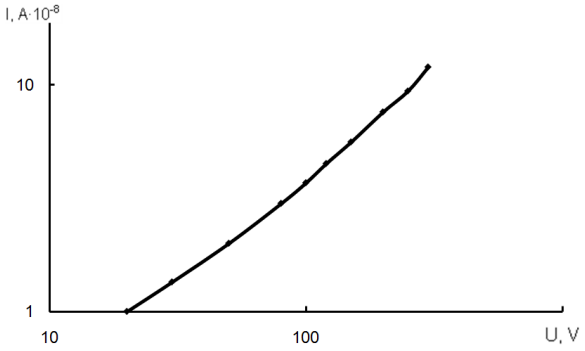

Fig 6. The CVC of the ZnO film (group B) measured in air (T = 293K).

Fig. 7 shows the temperature dependence of the current measured during heating and cooling of the ZnO film (group B). It also contains low-temperature sections with activation energies of 0.08 eV and 0.15 eV associated with oxygen vacancies. There is also a high-temperature region with an activation energy of about 1.6 eV, caused by the desorption of double charged oxygen ions from the ZnO film surface. At the same time, the only one section with activation energy (0.14-0.16) eV is observed in the current temperature dependence curve, measured at cooling. If the film is being cooled to room temperature, then the current remains almost 60 times greater than at heating. This is due to the fact that, when the film is heated in vacuum oxygen desorbes and the conductivity is controlled only by donor vacancies of oxygen in the volume of the film. However, when the air is let into the chamber, then the current decreases to almost the original value. Moreover, the decrease of the current strength in "e" times occurs very rapidly over a period of about 35 s. (Fig. 7).

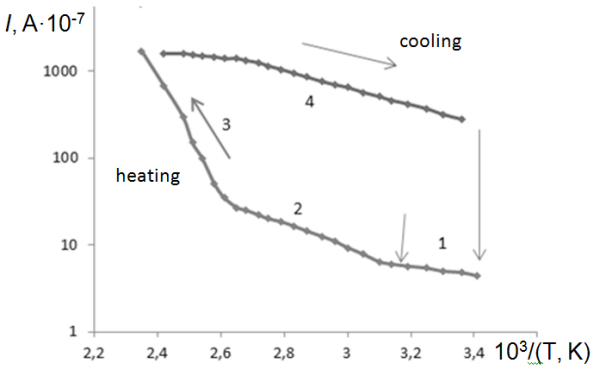

Fig. 7. The dark current temperature dependence of the ZnO film (group B)

When in the Fig. 8 a slower relaxation region is observed, then the straightening of the curve in the coordinates (ln I - t) indicates that relaxation follows the law $I(t) = I_0 exp^{-\frac{t}{\tau}}$, where the characteristic time constant τ is 150 s.

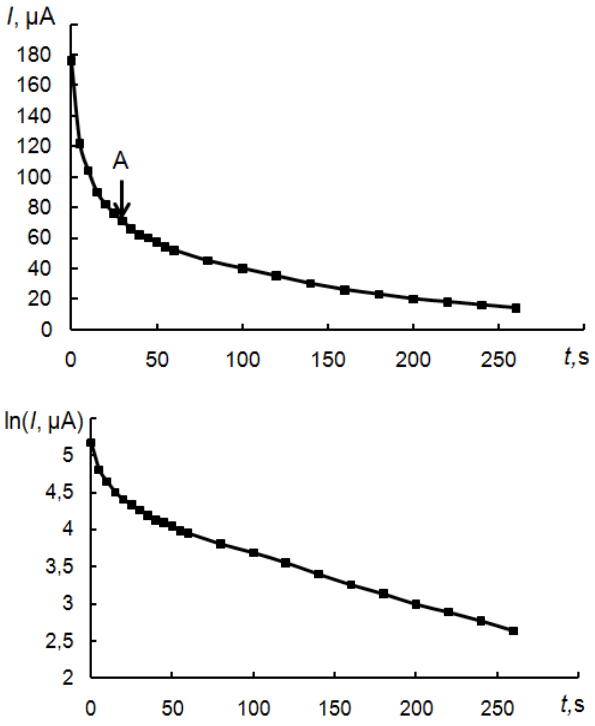

Fig. 8. Relaxation of the current in the film (group B) at letting the ambient air into the chamber (T = 298 K, U = 150 V).

The interelectrode resistance of zinc oxide (Group C) films calculated from the current-

voltage characteristic (Fig. 9) has of about 2 · 10^5 Ohms, which is also much lower than for Group A and Group B films.

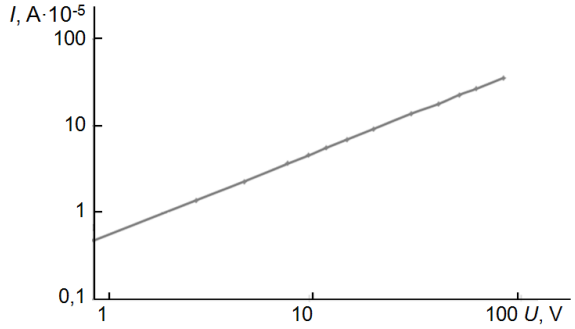

Fig. 9. The CVC of the ZnO film (group C) measured in air (T = 290 K).

Comparison of the calculation results for zinc oxide films' parameters obtained by different chemical methods is shown in table 1.

Table 1

Type of films	A	B	C
Bandwidth	(3,06-3,02) eV	(3,15-3,2) eV	(2,9-2,96) eV
Inter-electrode resistance	$4 \cdot 10^7$ Ohm	$2{,}8 \cdot 10^9$ Ohm	$2 \cdot 10^5$ Ohm

Zinc oxide films obtained from a solution of zinc acetate with admixtures of polyvinyl alcohol have a much higher resistance than similar films obtained without PVA admixture. This happens in the process of high-temperature annealing of PVA, playing the role of a polymer matrix, with the consequent evaporation of the decay products and hence, the zinc oxide films become porous with a more developed surface.

The ZnO film, obtained by oxidation of zinc metal films appeared low-resistance and have the smallest band gap. However, the shape of the optical absorption edge indicates their most perfect crystalline structure compared to films obtained from a solution of zinc acetate.

Conclision

The zinc oxide films obtained by three different methods showed typical for them optical absorption and bandgap (2.9 to 3.2 eV) characteristic for this material, which indicates the presence of crystalline structure in them. Moreover, the use of polyvinyl alcohol made it possible to obtain samples with the highest values of E_g and electrical resistance, which is caused by the nanosize crystallites of group C films. The investigated electrophysical characteristics of the obtained zinc oxide films made it possible to establish the contribution to the conductivity of their own defects and surface states.

References

1. C. D. Geddes. Reviews in Fluorescence 2009, Springer Science & Business Media.-2011.- 392 p.
2. C. Klingshirn, Past, Present and Future Applications, in book: C.F. Klingshirn, B.K. Meyer, A. Waag, A. Hoffmann, J. Geurts. Zinc Oxide. From Fundamental Properties Towards Novel Applications // N. Y., Springer.- 2010.- P.325-345.
3. Я.І. Лепіх, Т.І. Лавренова, Н.М. Садова, В.А. Борщак, А.П. Балабан, Н.П. Затовська. Структурно-фазові перетворення і електрофізичні властивості композиційних матеріалів на базі системи "SiO_2-B_2O_3-Bi_2O_3-ZnO-BaO" // Sensor electronics and Microsystem Technologies.–2018.–Vol.15,№ 4.–P.77-84
4. И.А. Пронин, Б.В. Донкова, Д.Ц. Димитров, И.А. Аверин, Ж.А. Пенчева, В.А. Мошников. Взаимосвязь фотокаталитических и фото-люминесцентных свойств оксида цинка, легированного медью и марганцем. // Физика и техника полупроводников.–2014ю-Т.48,№7.-С.868-874.
5. В.П. Папуша, А.К. Савин, О.С. Литвин. Люминесцентные и структурные свойства пленок ZnO−Ag. В.С. Хомченко, В.И. Кушниренкою // Физика и техника полупроводников.-2010.-Т.44,№5.-С.713-717.
6. Н.М. Лядов, А.И. Гумаров, Р.Н. Кашапов, А.И. Носков, В.Ф. Валеев, В.И. Нуждин, Базаров, Р.И. Хайбуллин, И.А. Файзрахманов. Структура и оптические свойства

ZnO с наночастицами серебра. // Физика и техника полупроводников, 2016.- Т.50, № 1.-С.44-50.
7. D. Lee, W. K. Bae, I. Park, D. Y. Yoon, S. Lee, C. Lee. Transparent electrode with ZnO nanoparticles in tandem organic solar cells // Solar Energy Materials and Solar Cells.- 2011.- V.95,N 1.-P.365-368.
8. G. P. Agus Sumiarna, Irmansyah, Akhiruddin Maddu, Dye-sensitized Solar Cell Based on Flower-like ZnO Nanoparticles as Photoanode and Natural Dye as Photosensitizer // J. Nano- Electron. Phys.-2016.-V.8, No 2.- 02012.
9. H. Liu, Y. Liu, P. Xiong, et al. Aluminum-doped zinc oxide transparent electrode prepared by atomic layer deposition for organic light emitting devices. // IEEE Trans Nanotechnol.-2017.-V.16.-P.634-638
10. T. Krajeski, E. Guziewicz, M. Godlewski et al. The influence of growth temperature and precursors' doses on electrical parameters of ZnO thin films grown by atomic layer deposition technique. // Microelectron. J.-2009.- V.40.-P.293–295.
11. G. Luka, M. Godlewski, E. Guziewicz, P. Stahira, V. Cherpak and D. Volonyuk. ZnO films grown by atomic layer deposition for organic electronics. // Semicond. Sci. Technol.-2012.-V.27.-P. 074006–074013.
12. P. Y. Dave, K. H. Patel, K. V. Chauhan, A. K. Chawla, S. K. Rawal, Examination of Zinc Oxide Films Prepared by Magnetron Sputtering // Procedia Technology.- 2016. V.23.- P.328-335
13. A. Sh. Asvarov, S. Sh. Makhmudov, A. Kh. Abduev, et al., Structural and Optical Properties of Mg Doped ZnO Thin Films Deposited by DC Magnetron Sputtering. // J. Nano- Electron. Phys.-2016.-V.8,No 4(2).- 04053.
14. N. Bouchenak Khelladi, N.E. Chabane Sari: Optical properties of ZnO thin film// Advances in Materials Science.- 2013.-V. 13, No 1(35).- P. 21-29.
15. C. Gümüş, O. M. Ozkendir, H. Kavak, Y. Ufuktepe, Structural and optical properties of zinc oxide thin films prepared by spray pyrolysis method // Optoelectronics and Adv. Mat.- rapid Commun.- 2006.-8(1).- P.299-303.
16. H. Nezzari, R. Saidi, A. Taabouche, M. Messaoudi, M. Salah Aida, Substrate Temperature Effect on Structural and Optical Properties of ZnO Thin Films Deposited by Spray Pyrolysis.// Defect and Diffusion Forum.- September 2019.- V. 397.- P.1-7.
17. V.N. Ermakov, S.P. Kruchinin, A. Fujiwara. Electronic nanosensors based on nanotransistor with bistability behaviour, in book: Electron Transport in Nanosystems, Springer, Dordrecht, 2008.- P. 341-349.

PACS 73.61.Le, 73.63.Bd

ELECTROPHYSICAL PROPERTIES OF ZINC OXIDE THIN FILMS OBTAINED BY CHEMICAL METHODS

Y. I. Bulyga, A. P. Chebanenko, V. S. Grinevych, L. M. Filevska

Summary

The electrophysical characteristics comparative studies were carried out for ZnO films obtained by chemical precipitation from zinc acetate solutions and thermal oxidation of zinc films. The ZnO films showed optical absorption and band gap (2.9 to 3.2 eV) specific for this material, which indicates the presence of crystalline structure in them. The use of polyvinyl alcohol made it possible to obtain samples with the highest values of E_g and electrical resistance, which is caused by the nanosize crystallites of the films. The investigated electrophysical characteristics of the ZnO films made it possible to establish the contribution of their own defects and surface states to the conductivity.

Key words: zinc oxide, thin films, electrophysical properties

PACS 73.61.Le, 73.63.Bd

ЭЛЕКТРОФИЗИЧЕСКИЕ СВОЙСТВА ТОНКИХ ПЛЕНОК ОКСИДА ЦИНКА, ПОЛУЧЕННЫХ ХИМИЧЕСКИМИ МЕТОДАМИ

Ю. И. Булыга, А. П. Чебаненко, В. С. Гриневич, Л. Н. Филевская

Резюме

Проведены сравнительные исследования электрофизических характеристик пленок ZnO, полученных химическим осаждением из растворов ацетата цинка и термическим окислением пленок цинка. Пленки ZnO показали оптическое поглощение и ширину запрещенной зоны (2,9-3,2 эВ), характерные для этого материала, что свидетельствует о наличии в них кристаллической структуры. Использование поливинилового спирта позволило получить образцы с наибольшими значениями E_g и электросопротивления, что обусловлено наноразмером кристаллитов в пленках. Исследованные электрофизические характеристики пленок ZnO позволили установить вклад собственных дефектов и поверхностных состояний в проводимость.

Ключевые слова: оксид цинка, тонкие пленки, электрофизические свойства

PACS 73.61.Le, 73.63.Bd

ЕЛЕКТРОФІЗИЧНІ ВЛАСТИВОСТІ ТОНКИХ ПЛІВОК ОКСИДУ ЦИНКУ, ОТРИМАНИХ ХІМІЧНИМИ МЕТОДАМИ

Ю. І. Булига, А. П. Чебаненко, В. С. Гріневич, Л. М. Філевська

Резюме

Проведено порівняльні дослідження електрофізичних характеристик плівок ZnO, отриманих шляхом хімічного осадження з розчинів ацетату цинку та термічного окислення плівок цинку. Плівки оксиду цинку демонстрували специфічне для цього матеріалу оптичне поглинання та ширину забороненої зони (2,9-3,2 еВ), що вказує на наявність у них кристалічної структури. Використання полівінілового спирту дозволило отримати зразки з найвищими значеннями E_g та електричного опору, що спричинені нанорозміром кристалітів плівок. Досліджені електрофізичні характеристики плівок ZnO дали змогу встановити внесок власних дефектів та станів поверхні в електропровідність.

Ключові слова: оксид цинку, тонкі плівки, електрофізичні властивості

PACS 31.15.Ne, 31.10.1z

A. O. Makarova, A. A. Buyadzhi, O. V. Dubrovsky

Odessa National Maritime Academy, Odessa, 4, Didrikhsona str., Odessa, Ukraine
e-mail: buyadzhiaa@gmail.com

SPECTROSCOPY AND DYNAMICS OF MULTIELECTRON ATOM IN A MAGNETIC FIELD: NEW APPROACH

Spectroscopy and dynamics of multielectron atomic system in a magnetic field is numerically investigated. It is presented a new quantum-mechanical approach to calculating the energies and widths of some states for the multielectron atomic system in in a homogeneous magnetic field. The approach is based on the numerical difference solution of the Schrödinger equation, the model potential method and the operator perturbation theory formalism. As illustration, the data for energies of the electronic excited and ground state of the lithium atom in dependence upon the magnetic field strength are listed and compared with available theoretical results, obtained on the basis of alternative Hartree-Fock method.

1. Introduction

The hydrogen atom in a constant magnetic field has been considered in a fairly large number of studies, however, many of the results turn out to be either unsuitable for specific applications or even incomplete until recently (see, for example, [1-5]). In the case of many-electron (non-hydrogen-like) atomic systems in a magnetic field, the situation looks dramatic enough. The fact is that generalizing the model to the case of many-electron atoms is quite problematic. Traditional methods such as perturbation theory, models based on asymptotic expansions in the magnitude of the field B, quasiclassical approaches (see, [1–14]) encounter significant problems when generalizing to the case of many-electron systems. Particularly acute is the problem of describing the dynamics of an atomic system in the intermediate region of magnetic field strengths, where it is necessary to consider the Coulomb and magnetic interactions on an equal footing. The problem is also relevant for the field of strong and superstrong fields, where today there are no sufficiently reliable data on the energy characteristics of atomic systems in the field. On the whole, at present, sufficiently convenient universal data for arbitrary states of many-electron atomic systems are absent for any values of the magnetic field B. Among modern methods for describing atomic spectroscopy in a magnetic field, a series of papers [4-18] should be distinguished, where perturbation theory methods, various schemes, and algorithms have been developed based on the numerical solution of the Schrödinger equation in the Hartree–Fock and other approximations. Based on them, it was possible to obtain a lot of useful numerical data regarding the energies of various states of a number of many-electron atoms at various magnetic field intensities. At the same time, in a number of cases, as the authors admit [3,8], their data require clarification due to the neglect of correlation effects, relativistic corrections, and other factors. Also relevant is the problem of describing the stochastic behavior of an atomic system in a magnetic field. It should be noted that various aspects of stochasticity in systems and the main features of quantum chaos that take place in the dynamics of many-electron atomic systems of atomic systems in a magnetic field are currently either partially or completely not studied, at least at a detailed quantitative level [14]. Naturally, therefore, the solution of the problem of a quantitative description of the elements of quantum chaos in the behavior of many-electron atomic systems in a static magnetic field seems extremely urgent and quite complicated (see [2]).

In this paper we shortly present a new quantum-mechanical approach to calculating the energies and widths of some states for the multielectron atomic system in in a homogeneous magnetic field. The approach is based on the numerical difference solution of the Schrödinger equation, the model potential method and the operator perturbation theory formalism.

2. Theoretical approach

The Hamiltonian of a multielectron atom in a magnetic field B differs from the operator of the hydrogen atom by the presence of the Coulomb interaction operator, which naturally aggravates the problem of separation of variables in the Schrödinger equation. Introducing a cylindrical coordinate system (ρ, φ, z), with the axis Oz || B and taking into account that the dependence of the wave function on the rotation angle φ around the z axis is trivial:

$$\Psi \sim e^{iM\varphi}\,\psi(\rho,z) \tag{1}$$

one should write the Schrödinger equation for the one-electron function of an atomic system (atomic units are used here $e=h=m=1$) as:

$$[\frac{\partial^2}{\partial\rho^2}+\frac{1}{\rho}\frac{\partial}{\partial\rho}+\frac{\partial^2}{\partial z^2}-\frac{M^2}{\rho^2}-4\gamma^2\rho^2+ \\ +\frac{4}{r}+V_c(r)+(\frac{E}{R_y}-\gamma M)]\Psi(\rho,z)=0 \tag{2}$$

where V_c (r) is the potential that describes the effect of all other electrons on the given one. Naturally, it is absent for the hydrogen atom. As the potential Vc, we use the Green-like potential (c.g.[2]), which approximates the Hartree potential quite accurately:

$$V=-\frac{(N_c-1)\Omega(r)}{r} \tag{3}$$

where function $\Omega(r)=1/[H\exp(r/d-1)+1]$ is the shielding function and H, d are the parameters of the potential. The required parameters, as a rule, are selected from the condition of the best fitting of the experimental values of the energy levels of free atoms (c.g. [2]). Note that a potential of type (2) was used intensively in calculating the energy levels and oscillator strengths of various atomic systems, including Li,Be, B, C, N, O, F, Ne, and others (see [17-20]). To take into account the exchange corrections, the exchange potential was taken in the simplest Slater approximation and added to potential (3) [19]. The two-dimensional equation (2) is naturally not solved analytically in a general form. The terms appearing in it: the potential of the Coulomb interaction, which contains $r=(\rho^2+z^2)^{1/2}$, potential V $[(\rho^2+z^2)^{1/2}]$ prevents the separation of variables. One could rewrite the Schrödinger equation as follows:

$$H\,\psi(\rho,z)=E\psi(\rho,z) \tag{4}$$

$$H=-1/2(\partial^2/\partial\rho^2+1/\rho\partial/\partial\rho+ \\ +\partial^2/\partial z^2-m^2/\rho^2),V(\rho,z),$$

$$V(\rho,z)=-(\rho^2+z^2)^{-1/2}+(N_c-1)\cdot \\ \Omega(\rho^2+z^2)^{-1/2}+1/8\gamma^2\rho^2+\gamma m/2, \tag{5}$$

The potential $1/8\gamma^2\rho^2$ limits the movement in the direction perpendicular to the field direction. Similarly, in the region $\gamma >> 1$, the motion of an electron across a magnetic field is determined by the size of its cyclotron orbit, $\lambda=(\hbar c/eM)^{1/2}$ and along the field by a modified Coulomb interaction, which takes into account the non-Coulomb character of the potential field in which an electron moves in a many-electron atom [18]. Note that calculations of multielectron atomic systems with introduced potentials are quite well known in the literature (see [2,18-20]); moreover, computational schemes based on them have been tested several times and tested for a number of atoms in the free state. The potential (3) was successfully used in calculating the energies and forces of atomic oscillators of the 1st period of the periodic table (see review in [21]). For solution of the Schrödinger equation with hamiltonian equations (7) we constructed the finite differences scheme which is in some aspects similar to method [2]. An infinite region is exchanged by a rectangular region: $0<\rho< L_\rho$, $0<z< L_Z$. It has sufficiently large size; inside it a rectangular uniform grid with steps h_ρ, h_Z was constructed. The external boundary condition, as usually, is: $(\partial\Psi\partial n)_r=0$. The knowledge of the asymptotic behaviour of wave function in the infinity allows to get numeral estimates for L_ρ, L_Z. A wave function has an asymptotic of the kind as: $exp[-(-2E)^{1/2}r]$, where $(-E)$ is the ionization energy from stationary state to lowest Landau level. Then L is estimated as $L\sim 9(-2E)^{-1/2}$. The more exact estimate is found empirically. The three-point symmetric differences scheme is used for second derivative on z. The derivatives on □ are approximated by $(2m+1)$-point symmetric differences scheme with the use of the Lagrange interpolation formula differentiation. To calculate the values of the width G for resonances in atomic spectra in a magnetic field one can use the modified operator perturba-

tion theory method (see details in Ref.[12,13]). Note that the imaginary part of the state energy in the lowest PT order is:

$$\text{Im } E = G/2 = \pi < \Psi_{Б} \mid H \mid \Psi_{Б} >^2 \qquad (8)$$

with the total Hamiltonian of system in a magnetic field. The state functions Ψ_{Eb} and Ψ_{Es} are assumed to be normalized to unity and by the δ(k -k')-condition, accordingly. Other calculation details can be found in Refs. [2, 19-21].

3. Illustration results and conclusion

As illustration, below we present the data (tables 1 and 2) for energies of the electronic excited and ground state of the lithium atom in dependence upon the magnetic field strength (parameter γ) and compared with available theoretical results, obtained on the basis of alternative methods. Parameter γ varies within: $\gamma = B/Bo$=0.00-10, where $B_0 = m^2 e^3 c / h^3 Z^3$. In Table 1 there are listed the energies of the ground state of the lithium atom in dependence upon the parameter γ. For the lithium atom there are available the results of calculations for the ground state and a few low-lying states of the Li atom at the regime of weak and intermediate fields. In particular, the Hartree-Fock (HF) calculation results are in the Refs. [6,7]. As the ground state analysis shows, in whole our data are corresponding to the alternative HF results, however, indeed, they lie a little lower for a weak field regime and more substantially lower in the intermediate regime of the magnetic parameter. In table 2 similar data are listed for the Li excited state.

Table 1.

Total energies (in a.u.) of the ground state of Li atom in a magnetic field with strength γ: HF-mesh- the Hartree-Fock data from [6], HF – data from [7], MP- this work;

γ	$1s^2 2s$ HF-mesh	$1s^2 2s$ HF	$1s^2 2s$ MP
0.000	27.4328	27.4327	27.4329
0.002	27.4338		27.4340
0.009	27.4371	27.4371	27.4373
0.020	27.4421		27.4424
0.126	27.4741	27.4739	27.4745
0.200	27.4840		27.4843
0.900	27.4250	27.4240	27.4253
1.800	27.2460	27.2446	27.2464
2.000	27.1962		27.1967
2.500	27.0562		27.0568
3.600	26.6787	26.6640	26.6793
5.000	26.0881		26.0887
5.400	25.9011	25.8772	25.9018
7.000	25.0891		25.0902

Table 2.

Total energies (in a.u.) of the excited state of the Li atom in the magnetic field with the strength γ: HF-mesh- the Hartree-Fock data from [6], HF – data from [7], MP- this work

γ	$1s^2 2p_{-1}$ HF-mesh	$1s^2 2p_{-1}$ HF	$1s^2 2p_{-1}$ MP
0.000	27.3651	27.3651	27.3652
0.002	27.3671		27.3673
0.009	27.3739	27.3738	27.3741
0.020	27.3840		27.3843
0.126	27.4565	27.4565	27.4568
0.200	27.4922		27.4925
0.900	27.6563	27.6563	27.6567
1.800	27.6766	27.6747	27.6770
2.000	27.6625		27.6631
2.500	27.6035		27.6041
3.600	27.3764	27.3627	27.3771
5.000	26.9423		26.9430
5.400	26.7952	26.7747	26.7959
7.000	26.1267		26.1279

The difference between the listed data can be explained by the partial account of electron correlation corrections, which is absent in the HF calculation.

References

1. Lisitsa, V.S. New results on the Stark and Zeeman effects in the hydrogen atom. *Sov. Phys. Usp.* **1987,** *30*, 927-960.
2. Glushkov, A.V. *Atom in an electromagnetic field*. KNT: Kiev, **2005**.
3. Ignatenko, A., Svinarenko A., Prepelitsa, G.P., Perelygina, T.B. Optical bi-stability effect for multi-photon absorption in atomic ensembles in a strong laser field. *Photoelectronics*. **2009**, *18*, 103-105.
4. Rao,J., Liu, W., Li, B. Theoretical complex Stark energies of hydrogen by a complex-scaling plus B-spline approach. *Phys. Rev. A*. **1994**, *50,* 1916-1919.
5. Rao, J.; Li, B. Resonances of hydrogen atom in strong parallel magnetic and electric fields. Phys.Rev.A. **1995,** *51,* 4526
6. Ivanov, M.V., Schmelcher, P. Ground state of the lithium atom in strong magnetic fields. *Phys.Rev.A*. **1998,** *57*, 3793-3800.
7. Jones, M., Ortiz, G., Ceperley, D. Hartree-Fock studies of atoms in strong magnetic fields. *Phys. Rev. A*. **1996,** *54,* 219-231.
8. Gadiyak G., Lozovik Yu.E., Mashchenko A., Obrecht M. Hydrogen-like and helium-like systems in a superstrong magnetic field. Opt. Spectr. **1984**, *56* (1), 26-32
9. Khetselius, O., Lopatkin Y., Dubrovskaya, Y., Svinarenko A. Sensing hyperfine-structure, electroweak interaction and parity non-conservation effect in heavy atoms and nuclei: New nuclear-QED approach. *Sensor Electr. and Microsyst. Techn*. **2010,** 7(2), 11-19.
10. Glushkov, A., Malinovskaya, S, Ambrosov S., Shpinareva I, Troitskaya O. Resonances in quantum systems in strong external fields: consistent quantum approach. *J. Techn.Phys*. **1997**, *38*(2), 215-218.
11. Ambrosov S., Ignatenko V., Korchevsky D., Kozlovskaya V. Sensing stochasticity of atomic systems in crossed electric and magnetic fields by analysis of level statistics for continuous energy spectra. *Sensor Electr. and Microsyst. Techn*. **2005**, Issue 2, 19-23.
12. Glushkov, A.; Ambrosov, S.; Ignatenko, A. Non-hydrogenic atoms and Wannier-Mott excitons in a DC electric field: Photoionization, Stark effect, Resonances in ionization continuum and stochasticity. *Photoelectronics,* **2001,** *10*, 103-106.
13. Glushkov A.V.; Ivanov, L.N. DC strong-field Stark effect: consistent quantum-mechanical approach. *J. Phys. B: At. Mol. Opt. Phys.* **1993,** *26,* L379-386.
14. Rusov V., Glushkov A., Vaschenko V., Korchevsky D., Ignatenko A. Stochastic dynamics of the atomic systems in the crossed electric and magnetic field: the rubidium atom recurrence spectra. *Bull.of Kiev Nat. Univ.* **2004**, N4, 433.
15. Khetselius, O. Relativistic perturbation theory calculation of the hyperfine structure parameters for some heavy-element isotopes. *Int. J. Quant.Chem.* **2009,** *109,* 3330-3335.
16. Glushkov, A.; Gurskaya, M.; Ignatenko, A.; Smirnov, A.; Serga, I.; Svinarenko, A.; Ternovsky E. Computational code in atomic and nuclear quantum optics: Ad-vanced computing multiphoton resonance parameters for atoms in a strong laser field. *J. Phys.: Conf. Ser*. **2017**, *905*, 012004.
17. Buyadzhi, V., Zaichko, P., Antoshkina, O., Kulakli, T., Prepelitsa, P., Ternovsky, V., Mansarliysky, V. Computing of radiation parameters for atoms and multicharged ions within relativistic energy approach: Advanced Code. *J. Phys.: Conf. Ser*. **2017**, *905*(1), 012003.
18. Svinarenko, A., Glushkov, A., Khetselius, O., Ternovsky,V., Dubrovskaya, Yu., Kuznetsova, A., Buyadzhi, V. Theoretical spectroscopy of rare-earth elements: spectra and autoionization resonances. *Rare Earth Element*, InTech. **2017**, 83-104
19. Glushkov, A., Khetselius, O., Svinarenko A.A., Buyadzhi, V.V., Ternovsky, V., Kuznetsova, A., Bashkarev, P. Relativistic perturbation theory formalism to computing spectra and radiation characteristics: application to heavy element. *Recent Studies in Perturbation Theory*. InTech. **2017**, 131-150.
20. Glushkov A.V., Khetselius O.Yu., Svinarenko A.A., Buyadzhi V.V., *Methods of computational mathematics and mathematical physics*. TES: Odessa, **2015**
21. Khetselius, O., Gurnitskaya, E., Loboda, A., Vitavetskaya, L. Consistent quantum approach to quarkony energy spectrum and semiconductor superatom and in external electric field *Photoelectron*. **2008**, *17*, 127.

PACS 31.15.Ne, 31.10.1z

A. O. Makarova, A. A. Buyadzhi, O. V. Dubrovsky

SPECTROSCOPY AND DYNAMICS OF MULTIELECTRON ATOM IN A MAGNETIC FIELD: NEW APPROACH

Summary. Spectroscopy of multielectron atomic system in a magnetic field is numerically investigated. It is presented a new quantum approach to calculating energies and widths of states for multi-electron atomic system in a homogeneous magnetic field. The approach is based on numerical difference solution of the Schrödinger equation, model potential method and operator perturbation theory. The data for energies of electronic excited and ground state of the lithium atom in dependence upon the magnetic field strength are listed and compared with available theoretical results, obtained on the basis of alternative Hartree-Fock method.

Key words: atomic system, magnetic field, spectroscopy and dynamics

PACS 31.15.Ne, 31.10.1z

А. О Макарова, А. А. Буяджи, О. В. Дубровский

СПЕКТРОСКОПИЯ И ДИНАМИКА МНОГОЭЛЕКТРОННОГО АТОМА В МАГНИТНОМ ПОЛЕ: НОВЫЙ ПОДХОД

Резюме. Изучается спектроскопия многоэлектронных атомных систем в магнитном поле. Представлен новый квантовый подход к расчету энергий и ширин состояний для многоэлектронного атома в однородном магнитном поле. Метод основан на численном разностном решении уравнения Шредингера, методе модельного потенциала и операторной теории возмущений. Приведены расчетные данные для энергий основного и возбужденного состояний атома лития в зависимости от напряженности магнитного поля и проведено сравнение с имеющимися теоретическими результатами, полученными на основе альтернативного метода Хартри-Фока.

Ключевые слова: атомная система, магнитное поле, спектроскопия и динамика

PACS 31.15.Ne, 31.10.1z

О. О. Макарова, Г. А. Буяджи, О. В. Дубровський

СПЕКТРОСКОПІЯ І ДИНАМІКА БАГАТОЕЛЕКТРОННОГО АТОМА У МАГНІТНОМУ ПОЛІ: НОВИЙ ПІДХІД

Резюме. Вивчається спектроскопія багато електронних атомних систем в магнітному полі. Представлений новий квантовий підхід до розрахунку енергій і ширин станів для багатоелектронного атома в однорідному магнітному полі. Метод заснований на чисельному різницевому рішенні рівняння Шредінгера, методі модельного потенціалу та операторній теорії збурень. Наведені розрахункові дані для енергій основного та збудженого станів атома літію в залежності від напруженості магнітного поля і проведено порівняння з наявними теоретичними результатами, отриманими на основі альтернативного методу Хартрі-Фока.

Ключові слова: атомна система, магнітне поле, спектроскопія та динаміка

PACS 31.15.A-; 32.30.-r

E. A. Efimova, A. S. Chernyshev, V. V. Buyadzhi, L. V. Nikola

I. I. Mechnikov Odessa National University, Dvoryanskaya str., 2, Odessa, 65000
E-mail: buyadzhivv@gmail.com

THEORETICAL AUGER SPECTROSCOPY OF THE NEON: TRANSITION ENERGIES AND WIDTHS

The combined relativistic energy approach and relativistic many-body perturbation theory with the zeroth order density functional approximation is applied to determination of the energy and spectral parameters of the resonant Auger decay for neon atomic system. The results are compared with reported experimental results as well as with those obtained by semiempirical and ab initio Hartree-Fock methods. The important point is linked with an accurate accounting for the complex exchange-correlation (polarization) effect contributions and using the optimized one-quasiparticle representation in the relativistic many-body perturbation theory zeroth order that significantly provides a physically reasonable agreement between theory and experiment.

1. Introduction

The research in many fields of modern atomic physics (spectroscopy, spectral lines theory, theory of atomic collisions etc), astrophysics, plasma physics, laser physics and quantum and photo-electronics requires an availability of sets of correct data on the energetic, spectroscopic and structural properties of atoms. The Auger electron spectroscopy remains an effective method to study the chemical composition of solid surfaces and near-surface layers [1-8].

As it is well known [11], the Auger process is a radiationless transition of an atom from an initial state possessing an inner-shell vacancy to a final state in which the inner vacancy is filled by an outer-shell electron with the simultaneous ejection of another outer-shell electron, resulting in two new vacancies. The kinetic energy of the ejected Auger electron is measured by Auger-electron spectroscopy (AES). Sensing the Auger spectra in atomic systems and solids gives the important data for the whole number of scientific and technological applications. So called two-step model is used most widely when calculating the Auger decay characteristics [1-5]. Since the vacancy lifetime in an inner atomic shell is rather long (about 10^{-17} to 10^{-14}s), the atom ionization and the Auger emission are considered to be two independent processes. In the more correct dynamic theory of the Auger effect [2,3] the processes are not believed to be independent from one another. The fact is taken into account that the relaxation processes due to Coulomb interaction between electrons and resulting in the electron distribution in the vacancy field have no time to be over prior to the transition.

In fact, a consistent Auger decay theory has to take into account correctly a number of correlation effects, including the energy dependence of the vacancy mass operator, the continuum pressure, spreading of the initial state over a set of configurations etc [1-19]. The most widespread theoretical studying the Auger spectra parameters is based on using the multi-configuration Dirac-Fock (MCDF) calculation [2,3]. The theoretical predictions based on MCDF calculations have been carried out within different approximations and remained hitherto nonsatisfactory in many relations. Earlier [8-13] it has been proposed relativistic perturbation theory (PT) method of the Auger decay characteristics for complex atoms, which is based on the Gell-Mann and Low S-matrix formalism energy approach) and QED PT formalism [4-7]. The novel element consists in using the optimal basis of the electron state functions derived from the minimization condition for the calibration-non-invariant contribution (the second order PT polarization diagrams contribution) to the imaginary part of the multi-electron system energy already at the first non-disappearing approxima-

tion of the PT. Earlier it has been applied in studying the Auger decay characteristics for a set of neutral atoms, quasi-molecules and solids. Besides, the ionization cross-sections of inner shells in various atoms and the Auger electron energies in solids were estimated. Here we apply the combined relativistic energy approach and relativistic many-body perturbation theory with the zeroth order density functional approximation is applied to determination of the energy and spectral parameters of the resonant Auger decay for neon atomic system.

2. The theoretical method

In Refs. [8-17] the fundamentals of the relativistic many-body PT formalism have been in detail presented, so further we are limited only by the novel elements. Let us remind that the majority of complex atomic systems possess a dense energy spectrum of interacting states. In Refs. [3-13, 19-33] there is realized field procedure for calculating the energy shifts ΔE of degenerate states, which is connected with the secular matrix M diagonalization. The whole calculation of the energies and decay probabilities of a non-degenerate excited state is reduced to the calculation and diagonalization of the M. The complex secular matrix M is represented in the form [9,10]:

$$M = M^{(0)} + M^{(1)} + M^{(2)} + M^{(3)}. \qquad (1)$$

where $M^{(0)}$ is the contribution of the vacuum diagrams of all order of PT, and $M^{(1)}$, $M^{(2)}$, $M^{(3)}$ those of the one-, two- and three-QP diagrams respectively. The diagonal matrix $M^{(1)}$ can be presented as a sum of the independent 1QP contributions. The optimized 1-QP representation is the best one to determine the zeroth approximation. In the relativistic energy approach [4-9], which has received a great applications during solving numerous problems of atomic, molecular and nuclear physics (e.g., see Refs. [10-13]), the imaginary part of electron energy shift of an atom is directly connected with the radiation decay possibility (transition probability). An approach, using the Gell-Mann and Low formula with the QED scattering matrix, is used in treating the relativistic atom. The total energy shift of the state is usually presented in the form:

$$\Delta E = \mathrm{Re}\Delta E + i\,\Gamma/2\,, \qquad (2)$$

where Γ is interpreted as the level width, and the decay possibility P = Γ. The imaginary part of electron energy of the system, which is defined in the lowest order of perturbation theory as [4]:

$$\mathrm{Im}\,\Delta E(B) = -\frac{e^2}{4\pi} \sum_{\substack{\alpha>n>f \\ [\alpha<n\le f]}} V^{|\omega_{\alpha n}|}_{\alpha n \alpha n}\,, \qquad (3)$$

where (α>n>f) for electron and (α<n<f) for vacancy. Under calculating the matrix elements (3) one should use the angle symmetry of the task and write the expansion for potential $\sin|\omega|r_{12}/r_{12}$ on spherical functions as follows [4]:

$$\frac{\sin|\omega|r_{12}}{r_{12}} = \frac{\pi}{2\sqrt{r_1 r_2}} \sum_{\lambda=0}^{\infty} (\lambda) J_{\lambda+1/2}(|\omega| r_1) J_{\lambda+1/2}(|\omega| r_2) P_\lambda(\cos r_1 r_2)\,.$$

$$\cdot \frac{\sin|\omega|r_{12}}{r_{12}} = \frac{\pi}{2\sqrt{r_1 r_2}} \sum_{\lambda=0}^{\infty} (\lambda) J_{\lambda+1/2}(|\omega| r_1) J_{\lambda+1/2}(|\omega| r_2) P_\lambda(\cos r_1 r_2)\,, \qquad (4)$$

where J is the Bessel function of first kind and (λ)= 2λ + 1. This expansion is corresponding to usual multipole one for probability of radiative decay.

Within the frame of QED PT approach the Auger transition probability and the Auger line intensity are defined by the square of an electron interaction matrix element having the form [4]:

$$V^{\omega}_{1234} = [(j_1)(j_2)(j_3)(j_4)]^{1/2} \sum_{\mu} (-1)^{\mu} \begin{pmatrix} j_1 & j_3 & \lambda \\ m_1 & -m_3 & \mu \end{pmatrix} \times \mathrm{R}\; Q_\lambda(1234);$$

$$Q_\lambda = Q_\lambda^{\mathrm{Qul}} + Q_\lambda^{\mathrm{B}}\,. \qquad (5)$$

The terms Q_λ^{Qul} and Q_λ^{B} correspond to subdivision of the potential into Coulomb part $cos|\omega|r_{12}/r_{12}$ and Breat one, $cos|\omega|r_{12}\alpha_1\alpha_2/r_{12}$. The real part of the electron interaction matrix element is determined using expansion in terms of Bessel functions:

$$\frac{\cos|\omega|r_{12}}{r_{12}} = \frac{\pi}{2\sqrt{r_1 r_2}} \sum_{\lambda=0} (\lambda) J_{\lambda+1/2}(|\omega| r_<) J_{-\lambda-1/2}(|\omega| r_>) P_\lambda(\cos \mathbf{r}_1 \mathbf{r}_2) \quad (6)$$

where J is the 1st order Bessel function, $(\lambda)=2\lambda+1$.

The Coulomb part Q_λ^{Qul} is expressed in terms of radial integrals R_λ, angular coefficients S_λ [4]:

$$\mathrm{Re}\,Q_\lambda^{\mathrm{Qul}} = \frac{1}{Z}\mathrm{Re}\{R_l(1243)S_\lambda(1243) + R_\lambda(\tilde{1}243)S_\lambda(\tilde{1}243) +$$

$$+ R_\lambda(1\tilde{2}43)S_\lambda(1\tilde{2}43) + R_\lambda(\tilde{1}\tilde{2}43)S_\lambda(\tilde{1}\tilde{2}43)\}. \quad (7)$$

As a result, the Auger decay probability is expressed in terms of $\mathrm{Re}\,Q_\lambda(1243)$ matrix elements:

$$\mathrm{R}\ R_\lambda(1243) = \int dr_1 r_1^2 r_2^2 f_1(r_1) f_3(r_1) f_2(r_2) f_4(r_2) Z_\lambda^{(1)}(r_<) Z_\lambda^{(1)}(r_>) \quad (8)$$

where f is the large component of radial part of single electron state Dirac function; function Z and angular coefficient are defined in Refs. [4-7]. The other items in (7) include small components of the Dirac functions; the sign «~» means that in (7) the large radial component f_i is to be changed by the small g_i one and the moment l_i is to be changed by $\tilde{l}_i = l_i - 1$ for Dirac number æ$_1$> 0 and l_i+1 for æ$_i$<0.

The Breat interaction is known to change considerably the Auger decay dynamics in some cases. The Breat part of Q is defined in [4,11]. The Auger width is obtained from the adiabatic Gell-Mann and Low formula for the energy shift [4]. The direct contribution to the Auger level width with a vacancy $n_\alpha l_\alpha j_\alpha m_\alpha$ is as follows:

$$\sum_\lambda \frac{2}{(\lambda)(j_\alpha)} \sum_{\beta} \sum_{f<k>f} Q_\lambda(\alpha k \beta) Q_\lambda(\beta k \alpha), \quad (9)$$

while the exchange diagram contribution is:

$$\frac{2}{(j_\alpha)} \sum_{\lambda_1 \lambda_2} \sum_{\beta} \sum_{f<k>f} Q_{\lambda_1}(\alpha k \beta) Q_{\lambda_2}(\beta k \alpha) \begin{Bmatrix} j_\alpha & j_\gamma & \lambda_2 \\ j_k & j_\beta & \lambda_1 \end{Bmatrix}. \quad (10)$$

The partial items of the $\sum_\beta \sum_k$ sum answer to contributions of $\alpha^{-1}\gamma(\beta\gamma)^{-1}K$ channels resulting in formation of two new vacancies βγ and one free electron k: $\omega_k=\omega_\alpha+\omega_\beta-\omega_\alpha$. The final expression for the width in the representation of jj-coupling scheme of single-electron moments has the form:

$$\Gamma(2j_1^o l_1^o, 2j_2^o l_2^o; J) = 2 \sum_{j_k l_k} |\Gamma(2j_1^o l_1^o, 2j_2^o l_2^o; 1 I_o, kjl)|^2 \quad (11)$$

The calculating of all matrix elements, wave functions, Bessel functions etc is reduced to solving the system of differential equations. The formulas for the autoionization (Auger) decay probability include the radial integrals $R_\alpha(\alpha k \gamma \beta)$, where one of the functions describes electron in the continuum state. When calculating this integral, the correct normalization of the wave functions is very important, namely, they should have the following asymptotic at $r \to 0$:

$$\left.\begin{matrix} f \\ g \end{matrix}\right\} \to (\lambda\omega)^{-1/2} \begin{cases} [\omega + (\alpha Z)^{-2}]^{-1/2} \sin(kr + \delta), \\ [\omega - (\alpha Z)^{-2}]^{-1/2} \cos(kr + \delta). \end{cases} \quad (12)$$

The important aspect of the whole procedure is an accurate accounting for the exchange-correlation effects. We have used the generalized relativistic Kohn-Sham density functional [8-17] in the zeroth approximation of relativistic PT; naturally, the perturbation operator contents the operator (7) minus the cited Kohn-Sham density functional. Further the wave functions are corrected by accounting of the first order PT contribution. Besides, we realize the procedure of optimization of relativistic orbitals base. The main idea is based on using ab initio optimization procedure, which is reduced to minimization of the gauge dependent multielectron contribution $Im\Delta E_{ninv}$ of the lowest QED PT corrections to the radiation widths of atomic levels. The formulae for the Auger decay probability include the radial integrals $R_\alpha(\alpha k \gamma \beta)$, where one of the functions describes electron in the continuum state. The energy of an electron formed due to a transition jkl is defined by the difference between energies of atom with a hole at j level and double-ionized atom at kl levels in final state:

$$E_A(jkl, {}^{2S+1}L_J) = E_A^+(j) - E_A^{2+}(k, {}^{2S+1}L_J) \quad (13)$$

To single out the above-mentioned correlation effects, the equation (13) can be presented as [8,9]:

$$E_A(jkl, {}^{2S+1}L_J) = E(j) - E(k) - E(l) - \Delta(k, l; {}^{2S+1}L_J), \quad (14)$$

where the item Δ takes into account the dynamic correlation effects (relaxation due to hole screening with electrons etc.) To take these effects into account, the set of procedures elaborated in the atomic theory [8-13] is used. All calculations are performed on the basis of the modified numeral code Superatom (version 93).

3. Results and conclusion

In tables 1 we present the data on the transition energies and angular anisotropy parameter β (for each parent state) for the resonant Auger decay to the $2s^12p^5(^{1.3}P)$ np and $2s^0p^6\ ^2S$ np (n=3,4) states of Ne^+. There are listed experimental data by De Fanis et al [18] and Pahler et al [15], theoretical ab initio Hartree-Fock results [18] and our data, obtained within the relativistic many-body PT with using the gauge-invariant QED PT method for generating relativistic functions basis's. In table 2 we the data on the widths (meV) for the $2s^12p^5(^{1.3}P)$np and $2s^0p^6$ (^1S) np (n=3,4) slates of Ne^+. There are listed experimental data by [18], theoretical ab initio multi configuration Hartree-Fock results by Sinanis et al [16], single-configuration Hartree-Fock data by Armen-Larkins [17] and our data, obtained within the relativistic many-body PT.

Table 1.

Transition energies E_k (for each parent state for the resonant Auger decay to the $2s^12p^5(^{1.3}P)$ np and $2s^0p^6\ ^2S$ np (n=3,4) states of Ne^+: the experimental data [18,15], theoretical ab initio Hartree-Fock results [18] and our data

Final state A=$2s^12p^5$ B=$2s^02p^6$	Exp. E_k, [18]	Theory: E_k, [18]	Theory: E_k, [7]	Theory: E_k, this
A(^{1}P)3p ^{2}S	778.79	776.43	778.52	778.61
A(^{1}P)3p ^{2}P	778.54	776.40	778.27	778.39
A(^{1}P)3p ^{2}D	778.81	776.66	778.57	778.68
A(^{1}P)3p ^{2}S	788.16	786.51	787.88	787.97
A(^{1}P)3p ^{2}P	788.90	787.52	788.69	788.75
A(^{1}P)3p ^{2}D	789.01	787.64	788.82	788.93
A(^{1}P)4p ^{2}S	773.60	-	-	773.52
A(^{1}P)4p ^{2}P	773.48	-	-	773.33
A(^{1}P)4p ^{2}D	773.56	-	-	773.41
A(^{3}P)4p ^{2}S	783.72	-	-	783.62
A(^{3}P)4p ^{2}P	783.95	-	-	783.81
A(^{3}P)4p ^{2}D	784.01	-	-	783.90
B(^{1}S)3p ^{2}P	-	-	-	754.99
B(^{1}S)4p ^{2}P	-	-	-	749.92

The analysis of the presented results in tables 1-3 allows to conclude that the précised description of the Auger processes requires the detailed accurate accounting for the exchange-correlation effects, including the particle-hole interaction, screening effects and iterations of the mass operator. The relativistic many-body PT approach provides more accurate results due to a considerable extent to more correct accounting for complex inter electron exchange-correlation effects. It is important to note that using more correct gauge-invariant procedure of generating the relativistic orbital bases is directly linked with correctness of accounting for the correlation effects.

Table 2.

Widths (meV) for $2s^12p^5(^{1.3}P)$np and $2s^0p^6$ (^1S) np (n=3,4) states of Ne^+: experiment [18]; theory: ab initio multi configuration Hartree-Fock [16], 1-configuration Hartree-Fock [17] and this work

final state	Exp. [18]/[15]	Th. [17]	Th. [16]	Th. this
A(^{1}P)3p ^{2}S	530±50 410±50	687	510	524
A(^{1}P)3p ^{2}P	42±3	20.7	-	38
A(^{1}P)3p ^{2}D	34±4	40.2	-	32
A(^{3}P)3p ^{2}S	120±10 110±40	18.8	122	118
A(^{3}P)3p ^{2}P	19±5	10.3	-	16
A(^{3}P)3p ^{2}D	80±10	62.3	-	72

References

1. Aberg, T., Hewat, G. *Theory of Auger effect*. Springer-Verlag: Berlin, **1979**.
2. Aglitsky, E., Safronova, U. *Spectroscopy*

of autoionization states of atomic systems. Energoat: Moscow, **1992**.
3. Glushkov, A.V., Khetselius, O.Yu., Svinarenko, A.A., Buyadzhi, V.V., *Spectroscopy of autoionization states of heavy atoms and multiply charged ions*. TEC: Odessa, **2015**.
4. Chernyakova, Y., Ignatenko, A., Vitavetskaya, L.A. Sensing the tokamak plasma parameters by means high resolution x-ray theoretical spectroscopy method: new scheme. *Sensor Electr. and Microsyst. Techn*. **2004**, *1*, 20-24.
5. Buyadzhi, V., Kuznetsova, A., Buyadzhi, A., Ternovsky, E., Tkach, T. Advanced quantum approach in radiative and collisional spectroscopy of multicharged ions in plasmas. *Adv. in Quant. Chem*. **2019**, *78*, 171-191.
6. Glushkov, A., Buyadzhi, V., Svinarenko, A., Ternovsky, E. Advanced relativistic energy approach in electron-collisional spectroscopy of multicharged ions in plasma. *Concepts, Methods, Applications of Quantum Systems in Chemistry and Physics* (Springer). **2018**, *31*, 55-69.
7. Glushkov, A., Ambrosov, S., Prepelitsa, G., Kozlovskaya, V. Auger effect in atoms and solids: Calculation of characteristics of Auger decay in atoms, quasi-molecules and solids with apllication to surface composition analysis. *Funct. Materials*. **2003**, *10*, 206.
8. Nikola, L. Resonant Auger spectroscopy of the atoms of inert gases. *Photoelectr*. **2011**, *20*, 104.
9. Khetselius, O.Yu. Quantum Geometry: New approach to quantization of quasistationary states of Dirac equation for superheavy ion and calculating hyperfine structure parameters. *Proc. Int. Geometry Center*. **2012**, *5*(3-4), 39-45.
10. Ivanov, L.N., Ivanova, E.P., Aglitsky, E. Modern trends in the spectroscopy of multicharged ions. *Phys. Rep.* **1988,** *166.*
11. Svinarenko, A., Khetselius, O., Buyadzhi, V., Florko, T., Zaichko, P., Ponomarenko E. Spectroscopy of Rydberg atoms in a Black-body radiation field: Relativistic theory of excitation and ionization. *J. Phys.: Conf. Ser*. **2014**, *548*, 012048.
12. Glushkov A.V., Ivanov, L.N. DC strong-field Stark effect: consistent quantum-mechanical approach. *J. Phys. B: At. Mol. Opt. Phys.* **1993,** *26,* L379-386.
13. Glushkov, A. Spectroscopy of atom and nucleus in a strong laser field: Stark effect and multiphoton resonances. *J. Phys.: Conf. Ser*. **2014**, *548*, 012020.
14. Osmekhin, S., Fritzsche, S., Grum-Grzhimailo, A.N., Huttula1, M., Aksela, H., Aksela S. Angle-resolved study of the Ar $2p^{-1}_{1/2}3d$ resonant Auger decay. *J. Phys. B: At. Phys*. **2008**, *41*, 145003.
15. Pahler, M., Caldwell, C., Schaphorst, S., Krause, M. Intrinsic linewidths of neon $2s2p^5(^{1,3}P)nl^2L$ correlation satellites. *J. Phys. B. At. Phys*. **1993,** *26,* 1617-1622.
16. Sinanis, C., Aspromallis, G., Nicolaides, C. Electron correlation in Auger spectra of the Ne^+ K $2s2p^5(^{3,1}P^0)3p^2S$ satellites. J. Phys. B. At. Phys. **1995**, *28*, L423-428.
17. Armen, G.B., Larkins, F.P. Valence Auger and X-ray participator and spectator processes for neon and argon atoms. *J. Phys. B. At. Mol. Opt. Phys*. **1991**, *24*, 741-760.
18. De Fanis, A., Tamenori, Y., Kitajima, M., Tanaka, H., Ueda, K. Doopler-free resonant Auger Raman spectroscopy on atoms and molecules at Spring-8. *J. Phys.: Conf. Ser*. **2004**, 183, 63-72.
19. Glushkov, A.V. Relativistic and correlation effects in spectra of atomic systems. Astroprint: Odessa, **2006**.
20. Glushkov A, Spectroscopy of cooperative muon-gamma-nuclear processes: Energy and spectral parameters *J. Phys.: Conf. Ser.* **2012,** *397,* 012011.
21. Khetselius, O.Yu. Hyperfine structure of atomic spectra.-Odessa: Astroprint, **2008.**
22. Dubrovskaya, Yu., Khetselius, O.Yu., Vitavetskaya, L., Ternovsky, V., Serga, I. Quantum chemistry and spectroscopy of pionic atomic systems with accounting for relativistic, radiative, and strong interaction effects. *Adv. Quantum Chem.* **2019,** *78*, 193-222.
23. Khetselius, O.Yu., Glushkov, A.V., Dubrovskaya, Yu., Chernyakova, Yu., Ignatenko, A., Serga, I., Vitavetskaya, L. Relativistic quantum chemistry and

spectroscopy of exotic atomic systems with accounting for strong interaction effects. In: *Concepts, Methods and Applications of Quantum Systems in Chem. and Phys.* Springer. **2018,** *31*, 71.
24. Khetselius, O. Relativistic perturbation theory calculation of the hyperfine structure parameters for some heavy-element isotopes. *Int. J. Quant. Chem.* **2009,** *109,* 3330–3335.
25. Buyadzhi, V.V., Chernyakova, Yu.G., Antoshkina, O., Tkach, T. Spectroscopy of multicharged ions in plasmas: Oscillator strengths of Be-like ion Fe. *Photoelectronics*. **2017,** *26,* 94-102.
26. Malinovskaya, S., Dubrovskaya, Yu., Zelentzova, T. The atomic chemical environment effect on the b decay probabilities: Relativistic calculation. *Herald of Kiev Nat. Univ. Ser.: Phys.-Math*. **2004**, N4, 427-432.
27. Bystryantseva, A., Khetselius, O.Yu., Dubrovskaya, Yu., Vitavetskaya, L.A., Berestenko, A.G. Relativistic theory of spectra of heavy pionic atomic systems with account of strong pion-nuclear interaction effects: ^{93}Nb,^{173}Yb,^{181}Ta, ^{197}Au. *Photoelectronics*. **2016**, *25*, 56-61.
28. Buyadzhi, V., Zaichko, P., Antoshkina, O., Kulakli, T., Prepelitsa, P., Ternovsky, V., Mansarliysky, V. Computing of radiation parameters for atoms and multicharged ions within relativistic energy approach: Advanced Code. *J. Phys.: Conf. Ser*. **2017**, *905*(1), 012003.
29. Khetselius, O.Yu., Lopatkin, Yu.M., Dubrovskaya, Yu.V, Svinarenko, A.A. Sensing hyperfine-structure, electroweak interaction and parity non-conservation effect in heavy atoms and nuclei: New nuclear-QED approach. *Sensor Electr. and Microsyst. Techn*. **2010,** 7(2), 11-19.
30. Danilov, V., Kruglyak, Y., Pechenaya, V. The electron density-bond order matrix and the spin density in the restricted CI method. *Theor. Chim. Act*. **1969**, *13*(4), 288-296.
31. Kruglyak, Yu. Configuration interaction in the second quantization representation: basics with application up to full CI. *Science Rise*. **2014**, *4*(2), 98-115.
32. Glushkov, A.V., Khetselius, O.Yu., Svinarenko, A., Buyadzhi, V. *Methods of computational mathematics and mathematical physics*. TES: Odessa, **2015**.
33. Ignatenko, A.V., Svinarenko, A.A., Prepelitsa, G.P., Perelygina, T.B. Optical bistability effect for multi-photon absorption in atomic ensembles in a strong laser field. *Photoelectronics*. **2009**, *18*, 103-105.

PACS 31.15.A-; 32.30.-r

E. A. Efimova, A. S. Chernyshev, V. V. Buyadzhi, L. V. Nikola

THEORETICAL AUGER SPECTROSCOPY OF THE NEON: TRANSITION ENERGIES AND WIDTHS

Summary. The combined relativistic energy approach and relativistic many-body perturbation theory with the zeroth order density functional approximation is applied to determination of the energy and spectral parameters of the resonant Auger decay for neon atomic system. The results are compared with reported experimental results as well as with those obtained by semiempirical and ab initio Hartree-Fock methods. The important point is linked with an accurate accounting for the complex exchange-correlation (polarization) effect contributions and using the optimized one-quasiparticle representation in the relativistic many-body perturbation theory zeroth order that significantly provides a physically reasonable agreement between theory and experiment.

Key words: relativistic theory, Auger spectroscopy, neon

PACS 31.15.A-; 32.30.-r

Е. А. Ефимова, А. С. Чернышев, В. В. Буяджи, Л. В. Никола

ТЕОРЕТИЧЕСКАЯ ОЖЕ-СПЕКТРОСКОПИЯ НЕОНА: ЭНЕРГИИ ПЕРЕХОДОВ И ШИРИНЫ

Резюме. Комбинированный релятивистский энергетический подход и релятивистская многочастичная теория возмущений с приближением функционала плотности нулевого порядка применяются для определения энергетических и спектральных параметров резонансного оже-распада для атомной системы неона. Результаты сравниваются с сообщенными экспериментальными результатами, а также с результатами, полученными полуэмпирическим и ab initio методами (типа Хартри-Фока). Важный момент связан с учетом вкладов сложных многочастичных обменных корреляционных ‘ффектов и использованием оптимизированного одноквазичастичного представления в нулевом приближении многочастичной теории возмущений, что определяет физически разумное согласие между теорией и экспериментом.

Ключевые слова: релятивистская теория, Оже-спектроскопия, неон

PACS 31.15.A-; 32.30.-r

Е. О. Єфімова, О. С. Чернишев, В. В. Буяджи, Л. В. Нікола

ТЕОРЕТИЧНА ОЖЕ-СПЕКТРОСКОПІЯ НЕОНУ: ЕНЕРГІЇ ПЕРЕХОДІВ ТА ШИРИНИ

Резюме. Комбінований релятивістський енергетичний підхід і релятивістська багаточастинкова теорія збурень з наближенням функціонала щільності нульового порядку застосовуються для визначення енергетичних і спектральних параметрів резонансного оже-розпаду для атомної системи неону. Результати порівнюються з повідомленими

експериментальними результатами, а також з результатами, отриманими напівемпіричними та ab initio методаи (типу Хартрі-Фока). Важливий момент пов'язаний з урахуванням вкладів складних багаточасткових обмінних кореляційних ефектів та з використанням оптимізованого одноквазічастічного уявлення в нульовому наближенні релятивістської багаточастинкової теорії збурень, що визначає фізично певну згоду між теорією і експериментом.

Ключові слова: релятивістська теорія, Оже-спектроскопія, неон

PACS 31.15.A-

A. A. Kuznetsova, A. V. Glushkov, E. S. Romanenko, E. K. Plisetskaya

National University "Odessa Maritime Academy", Didrikhson str. 8, Odessa, Ukraine
E-mail: kuznetsovaa232@gmail.com

SPECTROSCOPY OF MULTIELECTRON ATOM IN DC ELECTRIC FIELD: RELATIVISTIC OPERATOR PERTURBATION THEORY

We develop the theoretical basis of a new relativistic operator perturbation theory approach to multielectron atom in a DC electric field combined with a relativistic many-body perturbation theory formalism for a free multielectron atom. As illustration of application of the presented formalism, the results of energy and spectral parameters for a number of atoms are presented. The relativistic OPT method is tested for computing the Stark shifts of Rydberg states for a few the multielectron systems such as the sodium and rubidium. The approach allows an accurate and consistent treatment of a DC strong field Stark effect in multielectron atoms.

1. Introduction

An investigation of spectra, optical and spectral, radiative and autoionization characteristics for the rare-earth elements (isotopes) and corresponding ions in an external electric field is traditionally of a great interest for further development quantum optics and atomic spectroscopy and different applications in the plasma chemistry, astrophysics, laser physics, quantum and nano-electronics etc. (see Refs. [1–18]). At the present time it attracts a great interest especially for multielectron and Rydberg atoms that is stimulated by a whole range of interesting phenomena to be studied such as different processes in a laser plasma, astrophysical environments, quasi-discrete state mixing, a zoo of Landau- Zener anticrossings, autoionization in the multielectron atoms, the effects of potential barriers (shape resonances), new kinds of resonances above threshold etc [1-20]. There are many detailed reviews on the atomic Stark effect, including the DC strong field one (see, e g., [1-11]).

The calculation difficulties in description of the multielectron atoms in electromagnetic (electric) field inherent to the standard quantum mechanical approach are well known. Here one should mention the well-known Dyson phenomenon for a Strong Filed AC, DC Stark effect. Besides, in contrast to the hydrogen atom, the non-relativistic Schrödinger and relativistic Dirac equations for an electron moving in the field of the atomic core in many-electron atom and a uniform external electric field does not allow separation of variables in the parabolic coordinates. At the present time, the generalization of methods to account for the resonance interference, multielectron and relativistic effects is still an important problem, though here a definite progress has been reached too. Different calculational procedures are used in the Pade and then Borel summation of the divergent Rayleigh-Schrödinger perturbation theory series and in the sufficiently exact numerical solution of the difference equations following from expansion of the wave function over finite basis (see review in [2]). One should mention such approaches as a model potential method, quantum defect approximation, complex scaling plus B-spline methods (c.g., [1-19]) and effective operator perturbation theory (OPT) method [11-13]; the latter is taken as the basis for our approach.

In this paper we develop a new theoretical approach, namely, relativistic operator perturbation theory (ROPT) approach to multielectron atom in an electromagnetic field combined with a relativistic many-body perturbation theory (RMBPT) formalism for a free multielectron atom. The key advantage of such an approach that it can be applied to DC strong-field Stark effect problem for any multielectron system. As illustration here the approach is tested for the multielectron system such as rubidium Rb.

The relativistic density-functional approximation with the Kohn-Sham potential is taken as the zeroth approximation in the RMBPT formalism [20-29]. It allows to take into account the standard exchange-correlation corrections of the second order and dominated classes of the higher orders diagrams (polarization interaction, quasiparticles screening, etc.). The basis of our approach is an approach, developed in Refs. [17,18].

2. Relativistic operator perturbation theory for multielectron atoms in an electric field

As the principal ideas of the approach have been presented in Ref. [17,18], here we are limited to some key elements. As usually, we start from the Dirac Hamiltonian (in relativistic uni ts):

$$H = \alpha p + \beta - \alpha Z / r_i + \sqrt{\alpha} \cdot \varepsilon \cdot z\,, \quad (1)$$

Here a field strength intensity ε is expressed in the relativistic units (ε_{rel}= a$^{5/2}\varepsilon_{\text{at.un.}}$; a is the fine structure constant). One could see that a relativistic wave function in the Hilbert space is a bi-spinor. In order to further diagonalize the Hamiltonian (1), we need to choose the correct basis of relativistic functions, in particular, by choosing the following functions as in Ref, [1313]. The corresponding matrix elements of the total Hamiltonian will be no-zeroth only between the states with the same M_J. In fact this moment is a single limitation of the whole approach. Transformation of co-ordinates in the Pauli Hamiltonian (in comparison with the Schrodinger equation Hamiltonian it contents additional potential term of a magnetic dipole in an external field) can be performed by the standard way. However, procedure in this case is significantly simplified. They can be expressed through the set of one-dimensional integrals, described in details in Refs. [8,14]. To simplify the calculational procedure, the uniform electric field ε should be substitute by the function (c.g. [12]:

$$e\,(\mathrm{t}) = \frac{1}{t}\, e\left[(t-\tau)\frac{\tau^4}{\tau^4 + t^4} + \tau\right] \quad (2)$$

with sufficiently large t (t=1.5t_2). The motivation of a choice of the $\varepsilon(t)$ and some physical features of electron motion are presented in Refs. [56-58]. Here we only underline that the function $\varepsilon(t)$ practically coincides with the constant ε in the inner barrier motion region, i.e. $t < t_2$ and disappears at $t > t_2$. It is important that the final results do not depend on the parameter t. It is carefully checked in the numerical calculation. As usually (see [11-13]), the scattering states energy spectrum now spreads over the range $(-\varepsilon/2, +\infty)$, compared with $(-\infty, +\infty)$ in the uniform field. In contrast to the case of a free atom in scattering states in the presence of the uniform electric field remain quantified at any energy E, i.e. only definite values of β_1 are possible. The latter are determined by the confinement condition for the motion along the h-axis. The same is true in our case, but only for

$$E \subset \left(-\frac{1}{2}\varepsilon\tau, +\frac{1}{2}\varepsilon\tau\right).$$

Ultimately, such a procedure provides construction of realistic functions of the bound and scattering states. In a certain sense, this completely corresponds to the advantages of the distorted-wave approximation known in scattering theory [11].

The total Hamiltonian does not possess the bound stationary states. According to Ref. [12,13], one has to define the zero order Hamiltonian H_0, so that its spectrum reproduces qualitatively that of the initial one. To calculate the width G of the concrete quasistationary state in the lowest PT order one needs only two zeroth–order EF of H_0: bound state function $\Psi_Б$ and scattering state function Ψ_E. There can be solved a more general problem: a construction of the bound state function along with its complete orthogonal complementary of scattering functions Ψ_E with

$$\mathrm{E} \subset \left(-\frac{1}{2}\varepsilon\tau, +\infty\right).$$

The imaginary part of state energy (the resonance width) in the lowest PT order is determined by the standard way:

$$\mathrm{Im}E = \mathrm{G}/2 = p|\langle Y_{Eb}\,|H|\,Y_{Es}\rangle|^2 \quad (3)$$

with the total Hamiltonian H. The state functions $\Psi_{Б}$ and $\Psi_{Б}$ are assumed to be normalized to 1 and by the $\delta(k-k')$ condition, accordingly. The matrix elements $\langle\Psi_{Б}|H|\Psi_{E's}\rangle$ entering the high- order PT corrections can be determined in the same way. They can be expressed through the set of one-dimensional integrals, described in details in Refs. [2,12].

Further the ROPT scheme is combined with the RMBPT in spherical coordinates for a free atom. The details of this procedure can be found in the references [17,18]. The RMBPT formalism is constructed following to Refs. [2,23,26]. We will describe an atomic multielectron system by the relativistic Dirac Hamiltonian (the atomic units are used) as follows:

$$H = \sum_i \{\alpha c p_i - \beta c^2 - Z/r_i\} + \\ + \sum_{i>j} \exp(i\,|\,\omega\,|\,r_{ij})(1-\alpha_i\alpha_j)/r_{ij} \qquad (4)$$

where Z is a charge of nucleus, a_i, a_j are the Dirac matrices, w_{ij} is the transition frequency, c – the velocity of light. The interelectron interaction potential (second term in (4)) takes into account the retarding effect and magnetic interaction in the lowest order on parameter of the fine structure constant. In the PT zeroth approximation it is used ab initio mean-field potential:

$$V^{DKS}(r) = [V^D_{Coul}(r) + V_X(r) + V_C(r\,|\,a]\ , \quad (5)$$

with the standard Coulomb (or some model potential analog), exchange Kohn-Sham V_X and correlation Vc potentials (look details in Refs. [19,20]). An effective approach to accounting the multi-electron polarization contributions is described earlier and based on using the effective two-QP polarizable operator, which is included into the PT first order matrix elements.
In order to calculate the decay (transition) probabilities and widths an effective relativistic energy approach (version [19-21]) is used.
In particular, a width of the state, connected with an autoionization decay, is determined by a coupling with the continuum states and calculated as square of the matrix element [19]:

$$V_{\beta_1\beta_2;\beta_4\beta_3} = \sqrt{(2j_1+1)(2j_2+1)(2j_3+1)(2j_4+1)}\,(-1)^{j_1+j_2+j_3+j_4+m_1+m_2}\,\mathrm{x}$$

$$\mathrm{x}\sum_{a\mu}(-1)^{\mu}\begin{pmatrix} j_1 & j_3 & a \\ m_1 & -m_3 & \mu\end{pmatrix}\begin{pmatrix} j_2 & j_4 & a \\ m_2 & -m_4 & \mu\end{pmatrix}\times$$

$$\mathrm{x}Q_a\left(n_1l_1j_1n_2l_2j_2; n_4l_4j_4n_3l_3j_3\right) \qquad (6)$$

Here $Q_a = Q_a^{\mathrm{Qul}} + Q_a^{\mathrm{B}}$, where Q_a^{Qul}, and Q_a^{B} correspond to the Coulomb and Breit parts of the interelectron potential and express through Slater-like radial integrals and standard angle coefficients. Other details can be found in Refs. [2,23,26]. The most complicated problem of the relativistic PT computing the complex multielectron elements spectra is in an accurate, precise accounting for the multi-electron exchange-correlation effects (including polarization and screening effects, a continuum pressure etc), which can be treated as the effects of the PT second and higher orders.

The detailed description of the polarization diagrams and the corresponding analytical expressions for matrix elements of the polarization QPs interaction (through the polarizable core) potential is presented in Refs. [2,19,20,26].

3. Results and Conclusions

In the framework of the development of spectroscopy of the heavy atoms in the external field, a quantitative study of the electric field effect on the energy levels in the spectra of the some alkali atoms was performed.

In Table 1 we present the calculation results for the Stark resonance energies for some Rydberg states of the Na atom in an electric field with the strength 3.59 kV/cm.

Table 1.

The energies (in cm^{-1}) of the Stark resonances for Na atom (e=3.59 kV/cm).

State: (n_1n_2m)	Exp.	[4]	[7]	This work
26,0,0	15.5	15.5	15.5	15.4
25,0,1	21.1	21.1	21.1	20.9
25,0,0	35.5	35.5	35.5	35.3
24,0,1	41.1	40.4	41.0	40.9
24,1,0	50.5	50.3	50.5	50.4
24,0,0	56.5	57.0	56.5	56.3

23,0,1	61.2	60.7	61.1	61.0
23,0,0	79.3	80.3	79.4	79.2
22,0,1	84.1	83.1	83.9	83.5
22,1,1	75.0	74.9	75.1	74.9

For comparison, we also list the experimental data, the results of calculation within the 1/n-expansion and model PT version (c.g.[4,6,7, 10]). Agreement between both the theory and the experiment is quite satisfactory. Our results are obtained in the first PT order, i.e., the first PT order provides physically reasonable results. In Table 2 we present the calculation results for the Stark resonance energies for some Rydberg states of the Rb atom in an electric field with the strength 2.189 kV/cm. For comparison there are also presented the results of calculation in the framework of 1 / n-approximation (taking into account the permeability of the barrier), the method of summation of the PT series and experimental data (c.g.[4,6,7, 10]). There is physically reasonable agreement between theory and experiment.

Note that our results are obtained in the first PT order, i.e. already the first PT order

Table 2.

The energies (in cm^{-1}) of the Stark resonances for Rb atom (e=2.189 kV/cm).

$n_1 n_2 m$	Exp. [6]	1/n [4]	PT [7]	This work
23,0,0	133.1	132.8	132.9	133.0
22,0,0	157.0	157.1	157.2	157.1
21,1,0	161.1	159.5	160.6	160.9
20,2,0	163.9	163.2	163.7	163.9
21,0,0	185.2	184.2	184.8	185.1
20,1,0	186.3	185.4	185.8	186.2
20,0,0	217.2	214.6	214.9	216.9
18,1,0	248.4	247.2	247.3	248.2
16,2,0	284.7	284.0	284.1	285.5
18,0,0	289.5	288.6	289.0	289.3

provides the physically reasonable results. Naturally its accuracy can be increased by an account of the next PT order. The ROPT approach can be used in calculating the Stark resonance parameters in a case of the strong electric fields and it is of a great interest for many modern atomic, molecular, plasmas and semiconductors physics applications (see Refs. [31-39]).

References

1. Meng, H.-Y.; Zhang, Y.-X.; Kang, S.; Shi, T.-Y.; Zhan, M.-S. Theoretical complex Stark energies of lithium by a complex scaling plus the B-spline approach. *J. Phys. B: At. Mol. Opt. Phys*. **2008**, *41*, 155003.
2. Glushkov, A.V. *Relativistic Quantum theory. Quantum mechanics of atomic systems*. Astroprint: Odessa, **2008**.
3. Khetselius, O.Yu. *Quantum structure of electroweak interaction in heavy finite Fermi-systems*. Astroprint: Odessa, **2011**.
4. Mur, V. D. ; Popov, V.S.; Sergeev, A.V.; Shcheblykin, A.V. Stark resonances and scaling in Rydberg atoms. *JETP*. **1989,** *96*, 91-106.
5. Glushkov, A., Buyadzhi, V., Kvasikova, A., Ignatenko, A., Kuznetsova, A., Prepelitsa, G., Ternovsky, V. Non-Linear chaotic dynamics of quantum systems: Molecules in an electromagnetic field and laser systems. In*: Quantum Systems in Physics, Chemistry, and Biology.* Springer, Cham. **2017**, *30*, 169-180.
6. Harmin, D.A. Theory of the Stark effect. *Phys. Rev. A* **1982**, *26,* 2656.
7. Popov, V.; Mur, V.; Sergeev A.; Weinberg, V. Strong-field Stark effect: perturbation theory and 1/n expansion. *Phys. Lett. A* **1990**, *149(9),* 418-424.
8. Glushkov, A.V.; Ambrosov, S.V.; Ignatenko, A.V. Non-hydrogenic atoms and Wannier-Mott excitons in a DC electric field: Photoionization, Stark effect, Resonances in ionization continuum and stochasticity. *Photoelectr.* **2001,** *10*, 103-106.
9. Glushkov A.V.; Ivanov, L.N. DC strong-field Stark effect: consistent quantum-mechanical approach. *J. Phys. B: At. Mol. Opt. Phys.* **1993,** *26,* L379-386
10. Glushkov, A. *Atom in an electromagnetic field*. KNT: Kiev, **2005**.
11. Glushkov, A.V. Operator Perturbation Theory for Atomic Systems in a Strong DC

Electric Field. In: Hotokka M., Brändas E., Maruani J., Delgado-Barrio G. (eds) Advances in Quantum Methods and Applications in Chemistry, Physics, and Biology. Eds.; Springer: Cham. **2013**, *27*, 161–177.
12. Glushkov, A.V. Spectroscopy of atom and nucleus in a strong laser field: Stark effect and multiphoton resonances. *J. Phys.: Conf. Ser*. **2014**, *548*, 012020
13. Glushkov A. Spectroscopy of cooperative muon- gamma- nuclear processes: Energy and spectral parameters. *J. Phys.: Conf. Ser.* **2012,** *397,* 012011
14. Ignatenko, A.V. Probabilities of the radiative transitions between Stark sublevels in spectrum of atom in an DC electric field: New approach. *Photoelectronics,* **2007,** *16*, 71-74.
15. Glushkov, A.; Ambrosov, S.; Ignatenko, A. Non-hydrogenic atoms and Wannier-Mott excitons in a DC electric field: Photoionization, Stark effect, Resonances in ionization continuum and stochasticity. *Photoelectronics,* **2001,** *10*, 103-106.
16. Glushkov, A.V.; Ternovsky, V.B.; Buyadzhi, V.; Prepelitsa, G.P. Geometry of a Relativistic Quantum Chaos: New approach to dynamics of quantum systems in electromagnetic field and uniformity and charm of a chaos. *Proc. Intern. Geom. Center*. **2014**, *7(4)*, 60-71.
17. Kuznetsova, A.A.; Glushkov, A.V.; Ignatenko, A.V.; Svinarenko, A.A.; Ternovsky V.B. Spectroscopy of multielectron atomic systems in a DC electric field. *Adv. Quant. Chem*. (Elsevier) **2018**, *78*, 287-306.
18. Kuznetsova, A.; Buyadzhi, A.; Gurskaya, M.; Makarova, A. Spectroscopy of multi electron atom in a DC electric field: Modified operator perturbation theory approach to Stark resonances. *Photoelectronics***. 2018**, *27*, 94-102
19. Glushkov, A.V. *Relativistic and correlation effects in spectra of atomic systems;* Astroprint: Odessa, **2006.**
20. Khetselius, O.Yu. *Hyperfine structure of atomic spectra*. Astroprint: Odessa, **2008**
21. Glushkov, A.V. Advanced relativistic energy approach to radiative decay processes in multielectron atoms and multicharged ions. *In Quantum Systems in Chemistry and Physics: Progress in Methods and Applications.* Springer: Dordrecht, **2012**; Vol. 26, pp 231–252.
22. Svinarenko, A. A., Glushkov, A. V., Khetselius, O.Yu., Ternovsky,V.B., Dubrovskaya, Yu., Kuznetsova, A., Buyadzhi, V. Theoretical spectroscopy of rare-earth elements: spectra and autoionization resonances. *Rare Earth Element.* InTech, **2017**, pp 83-104.
23. Glushkov, A.V., Khetselius, O.Yu., Svinarenko, A.A., Buyadzhi, V.V., *Spectroscopy of autoionization states of heavy atoms and multiply charged ion*s. TEC: Odessa, **2015.**
24. Glushkov, A.V., Khetselius, O.Yu., Svinarenko, A., Buyadzhi, V. *Methods of computational mathematics and mathematical physics. P.1*. Odessa: **2015**.
25. Khetselius, O., Glushkov, A., Dubrovskaya, Yu., Chernyakova, Yu., Ignatenko, A.V., Serga, I., Vitavetskaya, L. Relativistic quantum chemistry and spectroscopy of exotic atomic systems with accounting for strong interaction effects. In: *Concepts, Methods and Applications of Quantum Systems in Chem. and Phys*. Springer, Cham, **2018,** 31, 71-91.
26. Glushkov, A.V., Khetselius, O.Yu., Svinarenko A.A., Buyadzhi, V.V., Ternovsky, V.B, Kuznetsova, A., Bashkarev, P Relativistic perturbation theory formalism to computing spectra and radiation characteristics: application to heavy element. *Recent Studies in Perturbation Theory*, ed. D. Uzunov (InTech) **2017**, 131-150.
27. Khetselius, O. Relativistic perturbation theory calculation of the hyperfine structure parameters for some heavy-element isotopes. *Int. Journ. Quant. Chem.* **2009,** *109,* 3330-3335.
28. Khetselius, O. Relativistic calculation of the hyperfine structure parameters for heavy elements and laser detection of the heavy isotopes. *Phys. Scr.* **2009,** *135,* 014023
29. Khetselius, O.Yu., Spectroscopy of cooperative electron-gamma-nuclear processes in heavy atoms: NEET effect. *J. Phys.: Conf. Ser*. **2012**, 3*97*, 012012.
30. Svinarenko, A. Study of spectra for lanthanides atoms with relativistic many- body

perturbation theory: Rydberg resonances. *J. Phys.: Conf. Ser.* **2014,** *548,* 012039.
31. Buyadzhi, V., Zaichko, P., Antoshkina, O., Kulakli, T., Prepelitsa, G., Ternovsky, V., Mansarliysky, V. Computing of radiation parameters for atoms and multicharged ions within relativistic energy approach: Advanced Code. *J. Phys.: Conf. Ser*. **2017**, *905*(1), 012003.
32. Buyadzhi, V.V., Glushkov, A.V., Mansarliysky, V.F., Ignatenko, A.V., Svinarenko, A.A. Spectroscopy of atoms in a strong laser field: new method to sensing ac stark effect, multiphoton resonances parameters and ionization cross-sections. *Sensor Electr. and Microsyst. Techn*. **2015**, *12*(4), 27-36
33. Ambrosov, S., Khetselius, O., Ignatenko, A. Wannier-Mott exciton and H, Rb atom in a DC electric field: Stark effect. *Photoelectronics*. **2008**, *17*, 84-87.
34. Ambrosov S., Ignatenko V., Korchevsky D., Kozlovskaya V. Sensing stochasticity of atomic systems in crossed electric and magnetic fields by analysis of level statistics for continuous energy spectra. *Sensor Electr. and Microsyst. Techn*. **2005**, Issue 2, 19-23.
35. Buyadzhi, V.V. Laser multiphoton spectroscopy of atom embedded in Debye plasmas: multiphoton resonances and transitions. *Photoelectrs.* **2015,** *24,* 128.
36. Buyadzhi, V.V.; Chernyakova, Yu.G.; Smirnov, A.V.; Tkach, T.B. Electron-collisional spectroscopy of atoms and ions in plasma: Be-like ions. *Photoelectronics*. **2016,** *25,* 97-101.
37. Buyadzhi, V.; Chernyakova, Yu.; Antoshkina, O.; Tkach, T. Spectroscopy of multicharged ions in plasmas: Oscillator strengths of Be-like ion Fe. *Photoelectronics*. **2017,** *26,* 94-102.
38. Chernyakova, Y.G., Ignatenko A.V., Vitavetskaya L.A. Sensing the tokamak plasma parameters by means high resolution x-ray theoretical spectroscopy method: new scheme. *Sensor Electr. and Microsyst. Techn*. **2004**, *1*, 20-24
39. Khetselius, O.Yu., Gurnitskaya, E.P., Loboda, A.V., Vitavetskaya, L.A. Consistent quantum approach to quarkony energy spectrum and semiconductor superatom and in external electric field. *Photoelectronics*. **2008**, *17*, 127-130.

PACS 31.15.A-

A. A. Kuznetsova, A. V. Glushkov, E. S. Romanenko, E. K. Plisetskaya

SPECTROSCOPY OF MULTIELECTRON ATOM IN DC ELECTRIC FIELD: RELATIVISTIC OPERATOR PERTURBATION THEORY

Summary. We develop the theoretical basis of a new relativistic operator perturbation theory approach to multielectron atom in a DC electric field combined with a relativistic many-body perturbation theory formalism for a free multielectron atom. As illustration of application of the presented formalism, the results of energy and spectral parameters for a number of atoms are presented. The relativistic OPT method is tested for computing the Stark shifts of Rydberg states for a few the multielectron systems such as the sodium and rubidium. The approach allows an accurate and consistent treatment of a DC strong field Stark effect in multielectron atoms.

Keywords: multielectron atom, electric field, relativistic operator perturbation theory, Rydberg states

PACS 31.15.A-

А. А. Кузнецова, А. В. Глушков, Э. С. Романенко, Е. К. Плисетская

СПЕКТРОСКОПИЯ МНОГОЭЛЕКТРОННОГО АТОМА В ЭЛЕКТРИЧЕСКОМ ПОЛЕ: РЕЛЯТИВИСТСКАЯ ОПЕРАТОРНАЯ ТЕОРИЯ ВОЗМУЩЕНИЙ

Резюме. Изложены теоретические основы нового аппарата релятивистской операторной теории возмущений в спектроскопии многоэлектронного атома в электрическом поле, объединенного с формализмом релятивистской многочастичной теории возмущений для свободного многоэлектронного атома. В качестве иллюстрации применения представленного формализма приведены результаты энергетических и спектральных параметров для ряда атомов. Релятивистский метод ОРТ тестируется для вычисления штарковских сдвигов ридберговских состояний для нескольких многоэлектронных систем, в частности, для натрия и рубидия. Новый подход разработан для последовательного описания эффекта Штарка в многоэлектронных атомах в сильном внешнем электрическом поле.

Ключевые слова: Многоэлектронные атом, электрическое поле, релятивистская операторная теория возмущений оператора, ридберговские состояния

PACS 31.15.A-

Г. О. Кузнецова, О. В. Глушков, Э. С. Романенко, Є. К. Плісетська

СПЕКТРОСКОПІЯ БАГАТОЕЛЕКТРОННОГО АТОМА В ЕЛЕКТРИЧНОМУ ПОЛІ: РЕЛЯТИВІСТСЬКА ОПЕРАТОРНА ТЕОРІЯ ЗБУРЕНЬ

Резюме. Викладено теоретичні основи нового апарату релятивістської операторної теорії збурень в спектроскопії багатоелектронного атома в електричному полі, об’єднаного з формалізмом релятивістської багаточастинкової теорії збурень для вільного багатоелектронного атома. В якості ілюстрації застосування представленого формалізму наведені результати обчислення енергетичних і спектральних параметрів для ряду атомів. Релятивістський метод ОРТ тестується для обчислення штарківських зсувів рідбергівських станів для декількох багатоелектронних систем, зокрема, для натрію і рубідію. Новий підхід розроблений для послідовного опису ефекту Штарка в багатоелектронних атомах в сильному зовнішньому електричному полі.

Ключові слова: багатоелектронний атом, електричне поле, релятивістська операторна теорія збурень оператора, рідбергівські стани

PACS 32.30.-r

V. B. Ternovsky

Odessa National Maritime Academy, Didrikhsona str. 4, Odessa, 65001
E-mail: ternovskyvb@gmail.com

THEORETICAL STUDYING RYDBERG STATES SPECTRUM OF THE URANIUM ATOM ON THE BASIS OF RELATIVISTIC MANY-BODY PERTURBATION THEORY

Theoretical studying spectrum of the Rydberg states for the uranium atom is carried out within the relativistic many-body perturbation theory with ab initio zeroth approximation and generalized relativistic energy approach. The zeroth approximation of the relativistic perturbation theory is provided by the optimized Dirac-Kohn-Sham ones. Optimization has been fulfilled by means of introduction of the parameter to the Kohn-Sham exchange potentials and further minimization of the gauge-non-invariant contributions into radiation width of atomic levels with using relativistic orbital set, generated by the corresponding zeroth approximation Hamiltonian.

1. Introduction

Development of new directions in the field of optics and spectroscopy, laser physics and quantum electronics, such as precision spectroscopy of heavy and ultra-heavy atoms and ions, newest astrospectroscopic studies, impulse heating methods in controlled thermonuclear synthesis spectrum, etc., necessitates the solution of urgent and important problems of atomic optics and laser spectroscopy at a fundamentally new level of theoretical sequence and fullness. In the last decade, spectroscopy of multiply charged ions, which covers the UV and X-ray bands of the spectrum, has been intensively developing. Significant progress in the development of experimental methods of research, in particular, a significant increase in the intensity and quality of laser radiation, the use of accelerators, colliders of heavy ions, sources of synchrotron radiation and, as a consequence, the possibility of precision study of increasingly energetic processes, stimulates the theories of new methods of theories calculation of their characteristics, in particular, radiation and autoionization ones. It is known that autoionization states play an essential role in various elementary atomic processes such as autoionization, selective photoionization, electron scattering at atoms, atomic and ionic atomic collisions, etc. The presence of autoionization states in ions significantly affects the nature of the spectrum of high-radiation astrophysical and laboratory plasma. Their radiation decay is accompanied by the formation of the most complex spectra of dielectronic satellites to resonant ion lines of subsequent ionization multiplicity, which contain information about the state of the plasma used for its diagnosis, as well as the study of the physical conditions in the solar corona and other astrophysical objects [1-25].

The multi-configuration Dirac-Fock method is the most reliable version of calculation for multielectron systems with a large nuclear charge. In these calculations the one- and two-particle relativistic and important exchange-correlation corrections are taken into account (see [9] and Refs. therein). However, one should remember about very complicated structure of spectra of the heavy atoms, including actinides, uranium, trans-uranium elements and others and necessity of correct accounting for the different correlation effects such as polarization interaction of the valent quasiparticles and their mutual screening, iterations of a mass operator etc.). One of the effective methods of studying the heavy atoms is the relativistic many-body perturbation theory (RMBPT), namely, [26-29]. It has been earlier effectively applied to computing spectra of low-lying states for some lanthanides atoms [25]

(see [26,27]). The aim of our present work is to use an analogous version of the relativistic many-body perturbation theory (PT) with an ab initio Dirac-Kohn-Sham approximation to study spectrum of autoionization states for the uranium. It is important to remind that isotope separation of atomic uranium using laser selective photoionization processes has attracted much attention now [3-6,9].

2. The relativistic many-body perturbation theory and energy approach

As the method of computing is earlier presented in detail, here we are limited only by the key topics [26-29]. Generally speaking, the majority of complex atomic systems possess a dense energy spectrum of interacting states with essentially relativistic properties. In the theory of the non-relativistic atom a convenient field procedure is known for calculating the energy shifts ΔE of degenerate states. This procedure is connected with the secular matrix M diagonalization [30-32]. In constructing M, the Gell-Mann and Low adiabatic formula for ΔE is used.

In contrast to the non-relativistic case, the secular matrix elements are already complex in the second order of the electrodynamical PT (first order of the interelectron interaction). Their imaginary part of ΔE is connected with the radiation decay (radiation) possibility. In this approach, the whole calculation of the energies and decay probabilities of a non-degenerate excited state is reduced to the calculation and diagonalization of the complex matrix M. In the papers of different authors, the $\mathrm{Re}\,\Delta E$ calculation procedure has been generalized for the case of nearly degenerate states, whose levels form a more or less compact group. One of these variants has been previously introduced: for a system with a dense energy spectrum, a group of nearly degenerate states is extracted and their matrix M is calculated and diagonalized. If the states are well separated in energy, the matrix M reduces to one term, equal to ΔE. The non-relativistic secular matrix elements are expanded in a PT series for the interelectron interaction. The complex secular matrix M is represented in the form [26,27]:

$$M = M^{(0)} + M^{(1)} + M^{(2)} + M^{(3)}. \quad (1)$$

where $M^{(0)}$ is the contribution of the vacuum diagrams of all order of PT, and $M^{(1)}$, $M^{(2)}$, $M^{(3)}$ those of the one-, two- and three-quasiparticle diagrams respectively. $M^{(0)}$ is a real matrix, proportional to the unit matrix. It determines only the general level shift. We have assumed $M^{(0)} = 0$. The diagonal matrix $M^{(1)}$ can be presented as a sum of the independent one-quasiparticle contributions. For simple systems (such as alkali atoms and ions) the one-quasiparticle energies can be taken from the experiment. Substituting these quantities into (1) one could have summarized all the contributions of the one -quasiparticle diagrams of all orders of the formally exact QED PT. However, the necessary experimental quantities are not often available.

The first two order corrections to $\mathrm{Re}\,M^{(2)}$ have been analyzed previously using Feynman diagrams (look Ref. in [2,3]). The contributions of the first-order diagrams have been completely calculated. In the second order, there are two kinds of diagrams: polarization and ladder ones. The polarization diagrams take into account the quasiparticle interaction through the polarizable core, and the ladder diagrams account for the immediate quasiparticle interaction [30-36]. Some of the ladder diagram contributions as well as some of the three-quasiparticle diagram contributions in all PT orders have the same angular symmetry as the two-quasiparticle diagram contributions of the first order. These contributions have been summarized by a modification of the central potential, which must now include the screening (anti-screening) of the core potential of each particle by the two others. The additional potential modifies the one-quasiparticle orbitals and energies.

Then the secular matrix is as follows:

$$M \to \tilde{M}^{(1)} + \tilde{M}^{(2)}, \quad (2)$$

where $\tilde{M}^{(1)}$ is the modified one-quasiparticle matrix (diagonal), and $\tilde{M}^{(2)}$ the modified two-quasiparticle one. $\tilde{M}^{(1)}$ is calculated by substituting the modified one-quasiparticle energies), and $\tilde{M}^{(2)}$ by means of the first PT order formulae for $M^{(2)}$, putting the modified radial functions of the one-quasiparticle states in the radial integrals..

Let us remind that in the QED theory, the photon propagator D(12) plays the role of this interaction. Naturally the analytical form of D(12) depends on the gauge, in which the electrodynamical potentials are written. Interelectron interaction operator with accounting for Breit interaction has been taken as follows:

$$V(r_i r_j) = exp(i\omega r_{ij}) \cdot \frac{(1 - \alpha_i \alpha_j)}{r_{ij}}, \qquad (3)$$

where, as usually, α_i are the Dirac matrices. In general, the results of all approximate calculations depended on the gauge. Naturally the correct result must be gauge-invariant. The gauge dependence of the amplitudes of the photoprocesses in the approximate calculations is a known fact and is investigated by Grant, Armstrong, Aymar and Luc-Koenig, Glushkov-Ivanov-Ivanova et al (see review in [9,32]). Grant has investigated the gauge connection with the limiting non-relativistic form of the transition operator and has formulated the conditions for approximate functions of the states, in which the amplitudes of the photo processes are gauge invariant (see review in [9]). These results remain true in the energy approach because the final formulae for the probabilities coincide in both approaches. Glushkov-Ivanov have developed a new relativistic gauge-conserved version of the energy approach [32]. In ref. [30,35-40] it has been developed its further generalization. Here we applied this approach for generating the optimized relativistic orbitals basis in the zeroth approximation of the many-body PT. Optimization has been fulfilled by means of introduction of the parameter to the Fock and Kohn-Sham exchange potentials and further minimization of the gauge-non-invariant contributions into radiation width of atomic levels with using relativistic orbital bases, generated by the corresponding zeroth approximation Hamiltonians [26]. Other details can be found in Refs. [9,27-29,41-47].

3. Some results and conclusion

In Table 1 we present the measured [3] and calculated energies (in cm^{-1}) of the levels of the lower members of the Rydberg series of uranium $5f^3 7s2np$, counted from the level of 33083.3 cm^{-1}; excitation sequence: 6056.81 + 6030.6 + (5943-5951) Å.

Table 1.

The measured and calculated energies (in cm^{-1}) of the levels of the lower members of the Rydberg series of uranium $5f^3 7s2np$, counted from the level of 33083.3 cm^{-1}; excitation sequence: 6056.81 + 6030.6 + (5943-5951) Å

E_{exp} [3]	E_{th} [3]	E_{th} This work	n_{calc}
49885.6	49885.9	49889.7	44
49889.4	49889.5	49891.9	45
49893.0	49892.8	49894.2	46
49896.3	49895.8	49896.6	47
49898.9	49898.8	49898.8	48
49901.4	49901.4	49901.3	49
49903.9	49903.9	49903.9	50
		49906.2	51
		49908.4	52
		49910.5	53

In Table 2 we present the measured [3] and calculated energies (in cm^{-1}) of the levels of the lower members of the Rydberg uranium series $5f^3 7s^2 nf$, counted from the level 32857.449cm^{-1} ($5f^3 6d7s8s\,^7L_5^0$); excitation sequence: 6056.81+6113.89+(5862-5914) Å.

Analysis shows that the correct account for the complex many-body exchange-correlation effects plays very critical role.

It should be noted too that the data on energies of the members of the Rydberg series should

be checked and correspond to so called the smoothness test.

Table 2.

The observed and calculated energies (in cm^{-1}) of the levels of the lower members of the Rydberg uranium series $5f^3 7s^2 nf$, counted from the level 32857.449 cm-1 ($5f^3 6d7s8s\ ^7L_5^0$); excitation sequence: 6056.81 + 6113.89 + (5862-5914) Å

E_{exp} [3]	E_{th} [3]	E_{th} This	$n^*_{\exp}$	$n_{calc.}$
49765.3	49767	49765.0	15.10	20
49830.7	49824	49829.1	16.23	21
49877.8	49871	49876.5	17.24	22
49917.0	49911	49916.2	18.23	23

The detailed analysis shows that some presented (in literature) values of the Rydberg states energies do not correspond to this test and as result, there is a possibility of a jump to another Rydberg series. More detailed data of this study are presented in Ref. [45].

References

1. Gubanova, E.R., Glushkov, A.V., Khetselius, O.Yu., Bunyakova, Yu.Ya., Buyadzhi, V., Pavlenko, E.P. *New methods in analysis and project management of environmental activity: Electronic and radioactive waste*. FOP: Kharkiv, **2017**.
2. Glushkov, A., Safranov, T., Khetselius, O., Ignatenko, A., Buyadzhi, V., Svinarenko, A. Analysis and forecast of the environmental radioactivity dynamics based on methods of chaos theory: General conceptions. *Environm. Problems.* **2016**, *1*(2), 115-120.
3. Solarz, R., May, C., Carlson, L., Worden, E., Johnson, S., Paisner, J., Radziemski, L. *Phys*. *Rev. A* **1976,** 14(3), 1129–1136.
4. Coste, A., Avril, R., Blancard, P., Chatelet, J., Lambert, D., Legre, S. Liberman and J. Pinard, New spectroscopic data on high-lying excited levels of atomic uranium. *J. Opt. Soc. Am*. **1982**, *72*(1), 103-109.
5. Khetselius, O.Yu. Relativistic perturbation theory calculation of the hyperfine structure parameters for some heavy-element isotopes. *Int. Journ. Quant.Chem.* **2009,** *109,* 3330-3335.
6. Khetselius, O. Relativistic calculation of the hyperfine structure parameters for heavy elements and laser detection of the heavy isotopes. *Phys.Scr.* **2009,** *T135,* 014023.
7. Khetselius, O.Yu. *Hyperfine structure of atomic spectra*. Astroprint: Odessa, **2008**.
8. Khetselius, O.Yu. Optimized relativistic many-body perturbation theory calculation of wavelengths and oscillator strengths for Li-like multicharged ions. Adv. Quant. Chem. **2019**, *78*, 223-251.
9. Glushkov, A.V. *Relativistic Quantum theory. Quantum mechanics of atomic systems*. Astroprint: Odessa, **2008**.
10. Glushkov, A.V., Khetselius, O.Yu., Svinarenko, A.A., Buyadzhi, V.V. *Spectroscopy of autoionization states of heavy atoms and multiply charged ion*s. TEC: Odessa, **2015**.
11. Dubrovskaya, Yu., Khetselius, O.Yu., Vitavetskaya, L., Ternovsky, V., Serga, I. Quantum chemistry and spectroscopy of pionic atomic systems with accounting for relativistic, radiative, and strong interaction effects. *Adv. in Quantum Chem.* **2019,** Vol.78, pp 193-222.
12. Bystryantseva, A., Khetselius, O.Yu., Dubrovskaya, Yu., Vitavetskaya, L.A., Berestenko, A.G. Relativistic theory of spectra of heavy pionic atomic systems with account of strong pion-nuclear interaction effects: ^{93}Nb, ^{173}Yb, ^{181}Ta, ^{197}Au. *Photoelectronics*. **2016**, *25*, 56-61.
13. Khetselius, O., Glushkov, A., Gurskaya, M., Kuznetsova, A., Dubrovskaya, Yu., Serga, I., Vitavetskaya, L. Computational modelling parity nonconservation and electroweak interaction effects in heavy atomic systems within the nuclear-relativistic many-body perturbation theory. *J. Phys.: Conf. Ser.* ***2017,*** *905*(1), 012029.
14. Khetselius, O.Yu., Glushkov, A.V., Dubrovskaya, Yu.V., Chernyakova, Yu., Ignatenko, A.V., Serga, I., Vitavetskaya, L. Relativistic quantum chemistry and spectroscopy of exotic atomic systems with accounting for strong interaction effects. In: Concepts,

Methods and Applications of Quantum Systems in Chemistry and Physics. Springer, Cham. **2018,** *31*, 71-91.
15. Svinarenko, A., Khetselius, O., Buyadzhi, V.V., Florko, T., Zaichko, P., Ponomarenko, E. Spectroscopy of Rydberg atoms in a Black-body radiation field: Relativistic theory of excitation and ionization. *J. Phys.: Conf. Ser*. **2014**, *548*, 012048.
16. Khetselius, O.Yu. *Quantum structure of electroweak interaction in heavy finite Fermi-systems.* Astroprint: Odessa, **2011**.
17. Khetselius, O.Y. Hyperfine structure of energy levels for isotopes ^{73}Ge, ^{75}As, ^{201} Hg. *Photoelectronics*. **2007,** *16*, 129-132.
18. Khetselius, O.Y., Gurnitskaya, E.P., Sensing the electric and magnetic moments of a nucleus in the N-like ion of Bi. *Sensor Electr. and Microsyst. Techn*. **2006**, *N3*, 35-39.
19. Khetselius, O.Yu., Lopatkin, Yu.M., Dubrovskaya, Yu.V, Svinarenko, A.A. Sensing hyperfine-structure, electroweak interaction and parity non-conservation effect in heavy atoms and nuclei: New nuclear-QED approach. *Sensor Electr. and Microsyst. Techn*. **2010,** 7(2), 11-19.
20. Florko, T.A., Tkach, T.B., Ambrosov, S.V., Svinarenko, A.A. Collisional shift of the heavy atoms hyperfine lines in an atmosphere of the inert gas. *J. Phys.: Conf. Ser*. **2012**, *397*, 012037.
21. Glushkov, A., Vitavetskaya, L. Accurate QED perturbation theory calculation of the structure of heavy and superheavy element atoms and multicharged ions with the account of nuclear size effect and QED corrections. *Herald of Uzhgorod Univ. Ser. Phys*. **2000**, *8*(2), 321-324.
22. Buyadzhi, V.V., Chernyakova, Yu.G., Smirnov, A.V., Tkach, T.B. Electron-collisional spectroscopy of atoms and ions in plasma: Be-like ions. *Photoelectronics*. **2016,** *25,* 97-101.
23. Buyadzhi, V.V., Chernyakova, Yu.G., Antoshkina, O., Tkach, T. Spectroscopy of multicharged ions in plasmas: Oscillator strengths of Be-like ion Fe. *Photoelectronics*. **2017,** *26,* 94-102
24. Glushkov, A.V., Malinovskaya, S.V., Dubrovskaya, Yu.V., Sensing the atomic chemical composition effect on the beta decay probabilities. Sensor Electr. and Microsyst. Techn. **2005**, *2*(1), 16-20.
25. Glushkov, A.V., Khetselius, O.Yu., Svinarenko A.A. Theoretical spectroscopy of autoionization resonances in spectra of lanthanides atoms. *Phys. Scripta*. **2013**, *T153*, 014029.
26. Svinarenko, A., Glushkov, A, Khetselius, O., Ternovsky, V., Dubrovskaya Y., Kuznetsova A., Buyadzhi V. Theoretical spectroscopy of rare-earth elements: spectra and autoionization resonances. *Rare Earth Element*, Ed. J. Orjuela (InTech). **2017**, pp 83-104.
27. Glushkov, A.V., Khetselius, O.Yu., Svinarenko A.A., Buyadzhi, V.V., Ternovsky, V.B, Kuznetsova, A., Bashkarev, P. Relativistic perturbation theory formalism to computing spectra and radiation characteristics: application to heavy element. *Recent Studies in Perturbation Theory*, ed. D. Uzunov (InTech). **2017**, 131-150.
28. Glushkov, A.V., Svinarenko, A.A., Ternovsky, V.B., Smirnov, A.V., Zaichko, P.A. Spectroscopy of the complex autoionization resonances in spectrum of helium: Test and new spectral data. *Photoelectronics*. **2015**, *24*, 94-102.
29. Glushkov, A.V., Ternovsky, V.B., Buyadzhi, V., Zaichko, P., Nikola, L. Advanced relativistic energy approach to radiation decay processes in atomic systems. *Photoelectr*. **2015**, *24*, 11-22.
30. Ivanov, L.N.; Ivanova, E.P. Method of Sturm orbitals in calculation of physical characteristics of radiation from atoms and ions. *JETP.* **1996,** *83,* 258-266.
31. Glushkov, A.V., Ivanov, L.N., Ivanova, E.P. Autoionization Phenomena in Atoms. *Moscow Univ. Press*, Moscow, **1986,** 58.
32. Glushkov, A.V., Ivanov, L.N. Radiation decay of atomic states: atomic residue polarization and gauge noninvariant contributions. *Phys. Lett. A* **1992,** *170,* 33.
33. Glushkov, A.V.; Ivanov, L.N. DC strong-field Stark effect: consistent quantum-mechanical approach. *J. Phys. B: At. Mol. Opt. Phys.* **1993,** *26,* L379-386.

34. Glushkov, A.V. *Relativistic and correlation effects in spectra of atomic systems*. Astroprint: Odessa, **2006**.
35. Glushkov, A.V. Multiphoton spectroscopy of atoms and nuclei in a laser field: Relativistic energy approach and radiation atomic lines moments method. *Adv. in Quantum Chem.* **2019**, *78*, 253-285.
36. Glushkov, A., Loboda, A., Gurnitskaya, E., Svinarenko, A. QED theory of radiation emission and absorption lines for atoms in a strong laser field. *Phys. Scripta.* **2009,** *T135,* 014022.
37. Glushkov, A. Spectroscopy of cooperative muon-gamma-nuclear processes: Energy and spectral parameters *J. Phys.: Conf. Ser.* **2012,** *397,* 012011.
38. Glushkov, A.V. Spectroscopy of atom and nucleus in a strong laser field: Stark effect and multiphoton resonances. *J. Phys.: Conf. Ser*. **2014**, *548*, 012020.
39. Glushkov, A.V., Ternovsky, V.B., Buyadzhi, V., Prepelitsa, G.P. Geometry of a Relativistic Quantum Chaos: New approach to dynamics of quantum systems in electromagnetic field and uniformity and charm of a chaos. *Proc. Int. Geom. Center*. **2014,** *7*(4), 60-71.
40. Glushkov, A., Buyadzhi, V., Kvasikova, A., Ignatenko, A., Kuznetsova, A., Prepelitsa, G., Ternovsky, V. Non-Linear chaotic dynamics of quantum systems: Molecules in an electromagnetic field and laser systems. In: *Quantum Systems in Physics, Chemistry, and Biology*. Springer, Cham. **2017**, *30*, 169-180.
41. Glushkov, A.V. Relativistic polarization potential of a many-electron atom. *Sov. Phys. Journal.* **1990**, *33(1)*, 1-4.
42. Glushkov, A., Svinarenko, A., Ignatenko, A. Spectroscopy of autoionization resonances in spectra of the lanthanides atoms. *Photoelectronics*. **2011**, *20*, 90-94.
43. Glushkov, A., Gurskaya, M., Ignatenko, A., Smirnov, A., Serga, I., Svinarenko, A., Ternovsky, E. Computational code in atomic and nuclear quantum optics: Advanced computing multiphoton resonance parameters for atoms in a strong laser field. *J. Phys.: Conf. Ser*. **2017**, *905*, 012004.
44. Glushkov, A.V., Khetselius, O.Yu., Svinarenko, A.A., Buyadzhi, V.V. *Methods of computational mathematics and mathematical physics*. *P.1*. TES: Odessa, **2015**.
45. Khetselius, O.Yu. Spectroscopy of cooperative electron-gamma-nuclear processes in heavy atoms: NEET effect. *J. Phys.: Conf. Ser*. **2012**, 3*97*, 012012.
46. Buyadzhi, V., Zaichko, P., Antoshkina, O., Kulakli, T., Prepelitsa, G., Ternovsky, V.B., Mansarliysky, V. Computing of radiation parameters for atoms and multicharged ions within relativistic energy approach: Advanced Code. *J. Phys.: Conf. Ser*. **2017**, *905*(1), 012003.
47. Ternovsky V. Theoretical study of the U spectrum. Preprint OSENU, **2019**, AM-1.

PACS 32.30.-r

V. B. Ternovsky

THEORETICAL STUDYING RYDBERG STATES SPECTRUM OF THE URANIUM ATOM ON THE BASIS OF RELATIVISTIC MANY-BODY PERTURBATION THEORY

Summary. Theoretical studying energies of the autoionization states for the uranium atom is carried out within the relativistic many-body perturbation theory with ab initio zeroth approximation and generalized relativistic energy approach. The zeroth approximation of the relativistic perturbation theory is provided by the optimized Dirac-Kohn-Sham ones. Optimization has been fulfilled by means of introduction of the parameter to the Kohn-Sham exchange potentials and further minimization of the gauge-non-invariant contributions into radiation width of atomic levels with using relativistic orbital set, generated by corresponding zeroth approximation Hamiltonian.

Keywords: Relativistic perturbation theory, optimized zeroth approximation, heavy atom, Rydberg states

PACS 32.30.-r

В. Б. Терновский

ТЕОРЕТИЧЕСКОЕ ИССЛЕДОВАНИЕ СПЕКТРА РИДБЕРГОВСКИХ СОСТОЯНИЙ АТОМА УРАНА НА ОСНОВЕ РЕЛЯТИВИСТСКОЙ МНОГОЧАСТИЧНОЙ ТЕОРИИ ВОЗМУЩЕНИЙ

Резюме. В рамках релятивистской многочастичной теории возмущений и обобщенного релятивистского энергетического подхода проведено теоретическое исследование спектра ридберговских состояний атома урана. В качестве нулевого приближения релятивистской теории возмущений выбрано оптимизированное приближение Дирака-Кона-Шэма. Оптимизация выполнена путем введения параметра в обменные потенциалы Фока и Кона-Шэма и дальнейшей минимизацией калибровочно-неинвариантных вкладов в радиационные ширины атомных уровней с использованием релятивистского базиса орбиталей, сгенерированного соответствующим гамильтонианом нулевого приближения.

Ключевые слова: Релятивистская теория возмущений, оптимизированное нулевое приближение, тяжелый атом, ридберговские состояния

PACS 32.30.-r

В. Б. Терновський,

ТЕОРЕТИЧНЕ ВИВЧЕННЯ СПЕКТРУ РІДБЕРГІВСЬКИХ СТАНІВ АТОМУ УРАНА НА ОСНОВІ РЕЛЯТИВІСТСЬКОЇ БАГАТОЧАСТКОВІ ТЕОРІЇ ЗБУРЕНЬ

Резюме. В рамках релятивістської багаточастинкової теорії збурень і узагальненого релятивістського енергетичного підходу проведено теоретичне дослідження спектра автоіонізаційних станів атома урану. В якості нульового наближення релятивістської теорії збурень обрано оптимізоване наближення Дірака-Кона-Шема. Оптимізація виконана шляхом введення параметра в обмінний потенціал Кона-Шема і подальшої мінімізації калібрувально-неінваріантних вкладів в радіаційні ширини атомних рівнів з використанням релятивістського базису орбіталей, згенерованого відповідним гамільтоніаном нульового наближення.

Ключові слова: Релятивістська теорія збурень, оптимізоване нульове наближення, важкий атом, рідбергівські стани

UDC 539.182

A. V. Tsudik, A. A. Kuznetsova, P. A. Zaichko, V. F. Mansarliysky

Odessa National Maritime Academy, Odessa, 4, Didrikhsona str., Odessa, Ukraine
e-mail: zaichkopa@gmail.com

RELATIVISTIC SPECTROSCOPY OF HEAVY RYDBERG ATOMIC SYSTEMS IN A BLACK-BODY RADIATION FIELD

We present the results of studying the spectroscopic characteristics of heavy Rydberg atomic systems in a black-body (thermal) radiation field. As theoretical approach we apply the combined generalized relativistic energy approach and relativistic many-body perturbation theory with ab initio Dirac zeroth approximation. There are presented the calculational data for the thermal black-body radiation ionization characteristics of the alkali Rydberg atoms, in particular, the sodium in Rydberg states with principal quantum number n=10-100 and ytterbium ion. Application of theory to computing the spectral parameters of studied atomic systems have demonstrated physically reasonable agreement between the theoretical and experimental data. The accuracy of the theoretical data is provided by a correctness of the corresponding relativistic wave functions and accounting for the exchange-correlation effects.

1. Introduction

At the present time, the study of Rydberg atoms (molecules) is definitely one of the most popular and very interesting directions of modern quantum physics and chemistry, atomic optics and spectroscopy. The huge relevance of the investigation of the energy and spectral properties of the Rydberg atoms (molecules) is, of course, due to the standard requirements for spectroscopic information of a number of applications and related physical disciplines, which include physics and chemistry of laboratory, astrophysical plasma, astrophysics and radioastronomy, atomic and molecular optics and spectroscopy, laser physics and quantum electronics and many others [1-94]). From the other side, the experiments with Rydberg atoms had very soon resulted in the discovery of an important ionization mechanism, provided by unique features of the Rydberg atoms.

Relatively new topic of the modern theory is connected with consistent treating the Rydberg atoms in a field of the Blackbody radiation (BBR). It should be noted that the BBR is one of the essential factors affecting the Rydberg states in atoms [1]. The account for the ac Stark shift, fast redistribution of the levels' population and photoionization provided by the environmental BBR became of a great importance for successfully handling atoms in their Rydberg states. The vast majority of existing papers on the description of Rydberg atoms in the thermal radiation field (c.g. [1-32]) are based on the Coulomb hydrogen-like approximation, different versions of the quantum defect method, classical and quasiclassical model approaches, the model and pseudo – potential methods. The authors of the papers [3-10] applied the Coulomb approximation, quantum defect formalism, different versions of the model and pseudo-potential method etc (as a rule, the non-relativistic versions are used) to determine the spectral and radiative properties of different Rydberg atoms and ions.

It should be noted separately the cycles of theoretical and experimental works by Ryabtsev-Beterov et al [2,3], as well as theoretical works of Dyachkov-Pankratov and others (c.g.[1-10]), in which the advanced versions of a quasi-classical approach to the calculation of radiation amplitudes, oscillator strengths, and cross-sections for the Rydberg atoms in the BBR radiation field were actually developed. In the papers [1-3,7-10] the authors present the calculational data on the ionization rates for Rydberg atoms of alkali elements (lithium, sodium, potassium, caesium) by a BBR radiation field. The calculations were carried out for the nS, nP, and nD states in the wide range of principal quantum numbers and temperatures. The above theoretical works and relevant models were substantially based on non-relativistic approximation.

At the same time one should note that for heavy Rydberg atoms (both in the free state and in an external electromagnetic field) it is fundamentally important to accurately account for both relativistic and exchange-correlation effects.

The quality and consistency of accounting for these effects also determine the accuracy of description of the energy and spectroscopic parameters of the heavy Rydberg atoms, including these atoms in a thermal radiation field.

Naturally, the standard methods of the theoretical atomic physics, including the Hartree-Fock and Dirac-Fock approximations should be used in order to determine the thermal ionization characteristics of neutral and Rydberg atoms [2].

One could note that the correct treating of the heavy Rydberg atoms parameters in an external electromagnetic field, including the BBR field, requires using strictly relativistic models. In a case of multielectron atomic systems it is necessary to account for thee exchange-correlation corrections.

Among the fundamentally important exchange-correlation effects for essentially many-electron systems, one should single out such effects as polarization interaction and screening, continuum pressure, the non-Coulomb grouping of levels in the heavy Rydberg atoms spectra etc. It should be noted that these effects are not correctly considered, for example, within simplified Coulomb approximation or quantum defect models (c.g.[11-20]). Their account requires using very consistent methods.

We present the results of studying the spectroscopic characteristics of heavy Rydberg atomic systems in a black-body (thermal) radiation field.

As theoretical approach we apply the combined generalized relativistic energy approach and relativistic many-body perturbation theory with ab anitio Dirac zeroth approximation.

2. Atom in a Black-body radiation field: Theoretical aspects

From the physical viewpoint, a qualitative picture of the BBR Rydberg atoms ionization is easily understandable. Even for temperatures of order T=10^4 K, the frequency of a greater part of the BBR photons ω does not exceed 0.1 a.u. Usually, it is enough to use a single- electron approximation for calculating the ionization cross section $\sigma_{nl}(\omega)$.

The latter appears in a product with the Planck's distribution for the thermal photon number density:

$$\rho(w,T)=\frac{\omega^2}{\pi^2 c^3[\exp(\omega/kT)-1]}, \qquad (1)$$

where k=3.1668×10^{-6} a.u., K^{-1} is the Boltzmann constant, c = 137.036 a.u. is the speed of light. Ionization rate of a bound state nl results in the integral over the Blackbody radiation frequencies:

$$P_{nl}(T)=c\int_{|E_{nl}|}^{\infty}\sigma_{nl}(\omega)\rho(\omega,T)d\omega. \qquad (2)$$

The ionization cross-section from a bound state with a principal quantum number n and orbital quantum number l by photons with frequency ω is as follows:

$$\sigma_{nl}(\omega)=\frac{4\pi^2\omega}{3c(2l+1)}[M^2_{nl\to E,l-1}+ \\ +(l+1)M^2_{nl\to E,l+1}], \qquad (3)$$

where the radial matrix element of the ionization transition from the bound state with the radial wave function $R_{nl}(r)$ to continuum state with the wave function $R_{El}(r)$ normalized to the delta function of energy.

The corresponding radial matrix elements are written by the standard way. Other details can be found in Refs. [9-16].

3. Relativistic perturbation theory and energy approach

We apply a generalized energy approach [9-20] and relativistic perturbation theory with the zeroth approximation [21-32] to computing the Rydberg atoms ionization parameters. According to Ref. [11,22], the RMBPT zeroth order Hamiltonian of the Rydberg atomic system is as follows:

$$H_0=\sum_i\{\alpha c p_i-\beta mc^2+[-Z/r_i+ \\ U_{MF}(r_i\,|\,b)+V_{XC}(r_i)] \qquad (4)$$

where c is the velocity of light, a_i, a_j – the Dirac matrices, w_{ij} –the transition frequency, Z is a charge of atomic nucleus. The general potential in (4) includes self-consistent Coulomb-like mean-field potential $U_{MF}(r_i \mid b)$, ab ibitio one-particle exchange-correlation (relativistic generalized exchange Kohn-Sham potential plus generalized correlation Lundqvist-Gunnarsson potential) $V_{XC}(r_i \mid b)$ with the gauge calibrated parameter b (it is determined within special relativistic procedure on the basis of relativistic energy approach; c.g. [21-32]).

The perturbation operator is as follows:

$$H^{PT} = \sum_{i>j} exp(i\omega_{ij} r_{ij}) \cdot \frac{(1 - \alpha_i \alpha_j)}{r_{ij}} - \sum_i [U_{MF}(r_i) + V_{XC}(r_i \mid b)] \quad (5)$$

The multielectron interelectron exchange-correlation effects (the core polarization and screening effects, continuum pressure etc) are taken into consideration as the RMBPT second and higher orders contributions. The details of calculation of the corresponding matrix elements of the polarization and screening interelectron interaction potentials are described in Refs. [9,22,33-38].

In relativistic theory radiation decay probability (ionization cross-section etc) is connected with the imaginary part of electron energy shift. The total energy shift of the state is usually presented in the form: DE = ReDE + i G/2, where G is interpreted as the level width, and a decay probability P = G. The imaginary part of electron energy shift is defined in the PT lowest order as:

$$\text{Im}\,\Delta E(B) = -\frac{e^2}{4\pi} \sum_{\substack{\alpha>n> \\ [\alpha<n\le f]}} V^{|\omega_{\alpha n}|}_{\alpha n \alpha n}, \quad (6)$$

where (a>n>f) for electron and (a<n<f) for vacancy. The matrix element is determined as follows:

$$V^{|\omega|}_{ijkl} = \iint dr_1 dr_2 \Psi^*_i(r_1) \Psi^*_j(r_2) \frac{\sin|\omega| r_{12}}{r_{12}} (1 - \alpha_1 \alpha_2) \Psi^*_k(r_2) \Psi^*_l(r_1) \quad (7)$$

Their detailed description of the matrix elements and procedure for their computing is presented in Refs. [16-20]. The relativistic wave functions are calculated by solution of the Dirac equation with the potential, which includes the Dirac-Fock consistent field potential and additionally polarization potential [22].

The total ionization rate of the Rydberg atomic system in the BBR radiation field is usually determined as the sum of direct BBR ionization rate of the initially excited state, the ionization (field ionization) rate of highly excited states, which are populated from the initial Rydberg state via absorption of the BBR photons, the rate of direct BBR-induced ionization of atoms from the neighbouring Rydberg states and the rate of field ionization of high-lying Rydberg states (with populating through so called two-step process via the BBR photons absorption).

The total width of the Rydberg state (naturally isolated from all external electromagnetic fields except BBR one) consists, apparently, of natural, spontaneous radiation width $\tilde{A}^{sp}_{nl}$ and BBR-induced (thermal) width $\tilde{A}^{BBR}_{nl}$:

$$\tilde{A}^{tot}_{nl} = \tilde{A}^{sp}_{nl} + \tilde{A}^{BBR}_{nl}(T). \quad (8)$$

Accordingly, the effective lifetime of the Rydberg state is inversely proportional to the total decay rate as a result of spontaneous transitions and transitions induced by the BBR radiation:

$$\frac{1}{\tau_{eff}} = \tilde{A}_0 + \tilde{A}_{BBR} = \frac{1}{\tau_0} + \frac{1}{\tau_{BBR}} \quad (9)$$

The detailed procedures of calculation of the radial and angular integrals (amplitudes) in the matrix elements are described in Refs. [9-20,22,38-41]. All calculations are performed on the basis of the numeral code Superatom-ISAN (version 93).

4. Results and conclusions

In Table 1 we present our theoretical data on the effective lifetime of the sodium nP, nD Rydberg states and for comparison some theoretical data by Beterov et al [2,3] for temperatures T=300, 600K. In Table 2 we present our theoretical data on the effective lifetime of the sodium nP, nD Rydberg states for temperatures T=300

and 600K. Obviously, the accuracy of the theoretical data is provided by a correctness of the corresponding relativistic wave functions and accounting for the exchange-correlation effects.

Table 1.

Effective lifetime (μs) of the nP Rydberg states in the sodium spectrum for the temperature T = 300: [2]- theory by Beterov et al and this work.

n	T= 300 K $P_{1/2}$ $P_{3/2}$ Ref. [2]	T= 300 K $P_{1/2}$ $P_{3/2}$ This work
10	4.80 4.76	4.84 4.81
20	20.99 20.89	21.06 20.96
30	48.71 48.56	48.84 48.70

Table 2.

Effective lifetime (μs) of the nP, nD Rydberg states in the sodium spectrum for the temperatures T = 300, 600K (this work).

n	T= 600 K $P_{1/2}$ $P_{3/2}$ This work	T= 300 K $D_{3/2}$ $D_{5/2}$ This work	T= 600 K $D_{3/2}$ $D_{5/2}$ This work
10	2.84 2.83	0.913 0.914	0.837 0.838
20	11.42 11.38	6.263 6.266	5.164 5.167
30	26.03 25.97	18.602 18.609	14.281 14.285

In conclusion we also present our result of computing the relative blackbody radiative shift (in 10^{-14}) for singly ionized Yb: β=--0.097. The similar β values are obtained using third-order relativistic many-body calculations [4] β=−0.0983 and *ab initio* method [5]: β=−0.094. In these calculations different methods are used to compute matrix elements and different orbital basises are used. The details of this problem will be presented in a separate paper.

References

1. Beloy K., Safronova U., Derevianko, A. High-accuracy calculation of the blackbody radiation shift in the 133Cs primary frequency standard. *Phys. Rev. Lett*. **2006**, 97, 040801.
2. Beterov, I.I., Ryabtsev, I., Tretyakov D., Entin, V. Quasiclassical calculations of blackbody-radiation-induce depopulation rates and effective lifetimes of Rydberg *nS*, *nP*, and *nD* alkali-metal atoms with *n*~80. *Phys Rev A*. **2009,** 79, 052504.
3. Beterov I.I., Ionization of Rydberg atoms by blackbody radiation/ Beterov I.I., TretyakovD.V., Ryabtsev I.I., Entin V.M., Ekers A., Bezuglov N.N.//New J. Phys.-2009.-Vol.11.-P.013052
4. Safronova U., Safronova M. Third-order relativistic many-body calculations of energies, transition rates, hyperfine constants, blackbody radiation shift in $^{171}Yb^{+}$. *Phys. Rev. A*. **2009**, *79*, 022512.
5. Angstmann, E., Dzuba, V., Flambaum, V. Frequency shift of hyperfine transitions due to blackbody radiation. *Phys. Rev. A*. **2006**, *74*, 023405.
6. Gallagher T.F., Cooke W.E. Interactions of Blackbody Radiation with atoms. *Phys. Rev. Let*t. **1979**, *42*, 835–839.
7. Lehman G. W. Rate of ionization of H and Na Rydberg atoms by black-body radiation. *J. Phys. B: At. Mol. Phys*. **1983**, *16*, 2145-2156.
8. D'yachkov L., Pankratov P. On the use of the semiclassical approximation for the calculation of oscillator strengths and photoionization cross sections. *J. Phys. B: At. Mol. Opt. Phys*. **1994**, *27*, 461-468.
9. Svinarenko A.A., Khetselius O.Yu., Buyadzhi V.V., Florko T.A., Zaichko P.A., Ponomarenko E.L., Spectroscopy of Rydberg

atoms in a Black-body radiation field: Relativistic theory of excitation and ionization. *J. Phys.: Conf. Ser*. **2014**, *548,* 012048.
10. Svinarenko A.A., Khetselius O.Yu., Buyadzhi V., Kvasikova A., Zaichko P. Spectroscopy of Rydberg atoms in a Black-body radiation field: Relativistic theory of excitation and ionization. *Photoelectronics*. **2014**, *23*, 147-151.
11. Glushkov, A.V., Ternovsky, V.B., Buyadzhi, V., Tsudik, A., Zaichko, P. Relativistic approach to calcuation of ionization characteristics for rydberg alkali atom in a black-body radiation field. *Sensor Electr. and Microsyst. Techn*. **2019**, *16*(3), 69-77.
12. Glushkov, A.V. *Relativistic Quantum theory. Quantum mechanics of atomic systems*. Astroprint: Odessa, **2008**.
13. Glushkov, A.V., Khetselius, O.Yu., Svinarenko, A.A., Buyadzhi, V.V., *Spectroscopy of autoionization states of heavy atoms and multiply charged ion*s. TEC: Odessa, **2015**.
14. Glushkov, A.V., Svinarenko, A.A., Ternovsky, V.B., Smirnov, A.V. , Zaichko, P.A., Spectroscopy of the complex autoionization resonances in spectrum of helium: Test and new spectral data. *Photoelectronics*. **2015**, *24*, 94-102.
15. Glushkov A.V., Ternovsky V.B., Buyadzhi V., Zaichko P., Nikola L. Advanced relativistic energy approach to radiation decay processes in atomic systems. *Photoelectr*. **2015**, *24*, 11-22.
16. Ivanov, L.N.; Ivanova, E.P. Method of Sturm orbitals in calculation of physical characteristics of radiation from atoms and ions. *JETP.* **1996,** *83,* 258-266.
17. Glushkov, A.; Ivanov, L.; Ivanova, E.P. Autoionization Phenomena in Atoms. *Moscow Univ. Press*, Moscow, **1986,** 58.
18. Glushkov, A.; Ivanov, L. Radiation decay of atomic states: atomic residue polarization and gauge noninvariant contributions. *Phys. Lett.A* **1992,** *170,* 33.
19. Glushkov A.V.; Ivanov, L.N. DC strong-field Stark effect: consistent quantum-mechanical approach. *J. Phys. B: At. Mol. Opt. Phys.* **1993,** *26,* L379-386.
20. Glushkov A.V., Multiphoton spectroscopy of atoms and nuclei in a laser field: Relativistic energy approach and radiation atomic lines moments method. *Adv. in Quantum Chem.* **2019**, *78*, 253-285.
21. Glushkov, A.V.; Khetselius, O.Yu.; Svinarenko A. Theoretical spectroscopy of autoionization resonances in spectra of lanthanides atoms. *Phys. Scripta*. **2013**, *T153*, 014029.
22. Glushkov, A.V. *Relativistic and correlation effects in spectra of atomic systems*. Astroprint: Odessa, **2006**.
23. Khetselius, O.Yu. *Hyperfine structure of atomic spectra*. Astroprint: Odessa, **2008**.
24. Khetselius, O.Yu. Relativistic perturbation theory calculation of the hyperfine structure parameters for some heavy-element isotopes. *Int. Journ. Quant.Chem.* **2009,** *109,* 3330-3335.
25. Khetselius, O. Relativistic calculation of the hyperfine structure parameters for heavy elements and laser detection of the heavy isotopes. *Phys.Scr.* **2009,** *T135,* 014023
26. Khetselius, O.Yu. Optimized relativistic many-body perturbation theory calculation of wavelengths and oscillator strengths for Li-like multicharged ions. Adv. Quant. Chem. **2019**, *78*, 223-251.
27. Khetselius, O.Yu., Glushkov, A.V., Dubrovskaya, Yu.V., Chernyakova, Yu., Ignatenko, A.V., Serga, I., Vitavetskaya, L. Relativistic quantum chemistry and spectroscopy of exotic atomic systems with accounting for strong interaction effects. In: Concepts, *Methods and Applications of Quantum Systems in Chemistry and Physics*. Springer, Cham, **2018,** *31*, 71-91.
28. Khetselius, O.Yu. *Quantum structure of electroweak interaction in heavy finite Fermi-systems.* Astroprint: Odessa, **2011**.
29. Glushkov, A., Vitavetskaya, L. Accurate QED perturbation theory calculation of the structure of heavy and superheavy element atoms and multicharged ions with the account of nuclear size effect and QED corrections. *Herald of Uzhgorod Univ.* **2000**, *8*(2), 321-324.
30. Svinarenko, A., Glushkov, A, Khetselius, O., Ternovsky, V., Dubrovskaya Y., Kuznetsova

A., Buyadzhi V. Theoretical spectroscopy of rare-earth elements: spectra and autoionization resonances. *Rare Earth Element*, Ed. J. Orjuela (InTech) **2017**, pp 83-104.
31. Glushkov, A.V., Khetselius, O.Yu., Svinarenko A.A., Buyadzhi, V.V., Ternovsky, V.B, Kuznetsova, A., Bashkarev, P Relativistic perturbation theory formalism to computing spectra and radiation characteristics: application to heavy element. *Recent Studies in Perturbation Theory*, ed. D. Uzunov (InTech) **2017**, 131-150.
32. Glushkov A.V., Khetselius O.Yu., Svinarenko A.A., Buyadzhi V.V., *Methods of computational mathematics and mathematical physics*. *P.1*. TES: Odessa, **2015**.
33. Dubrovskaya, Yu., Khetselius, O.Yu., Vitavetskaya, L., Ternovsky, V., Serga, I. Quantum chemistry and spectroscopy of pionic atomic systems with accounting for relativistic, radiative, and strong interaction effects. *Adv. in Quantum Chem.* **2019,** Vol.78, pp 193-222.
34. Bystryantseva A., Khetselius O.Yu., Dubrovskaya Yu., Vitavetskaya L.A., Berestenko A.G. Relativistic theory of spectra of heavy pionic atomic systems with account of strong pion-nuclear interaction effects: ^{93}Nb, ^{173}Yb, ^{181}Ta , ^{197}Au. *Photoelectronics*. **2016**, *25*, 56-61.
35. Khetselius, O., Glushkov, A., Gurskaya, M., Kuznetsova, A., Dubrovskaya Yu., Serga I., Vitavetskaya L. Computational modelling parity nonconservation and electroweak interaction effects in heavy atomic systems within the nuclear-relativistic many-body perturbation theory. *J. Phys.: Conf. Ser.* ***2017,*** *905*(1), 012029.
36. Khetselius O., Gurnitskaya E. Sensing the electric and magnetic moments of a nucleus in the N-like ion of Bi. *Sensor Electr. and Microsyst. Tech*. **2006**, *N3*, 35
37. Khetselius, O.Yu., Lopatkin Yu.M., Dubrovskaya, Yu.V, Svinarenko A.A. Sensing hyperfine-structure, electroweak interaction and parity non-conservation effect in heavy atoms and nuclei: New nuclear-QED approach. *Sensor Electr. and Microsyst. Techn*. **2010,** 7(2), 11-19.
38. Glushkov A.V., Malinovskaya S.V., Dubrovskaya Yu.V., Sensing the atomic chemical composition effect on the beta decay probabilities. Sensor Electr. and Microsyst. Techn. **2005**, *2*(1), 16-20.
39. Florko, T.A.; Tkach, T.B.; Ambrosov, S.V.; Svinarenko, A.A. Collisional shift of the heavy atoms hyperfine lines in an atmosphere of the inert gas. *J. Phys.: Conf. Ser*. **2012**, *397*, 012037.
40. Buyadzhi V.; Chernyakova Yu.; Smirnov A; Tkach T. Electron-collisional spectroscopy of atoms and ions in plasma: Be-like ions. *Photoelectronics*. **2016,** *25,* 97-101
41. Buyadzhi, V.V.; Chernyakova, Yu.G.; Antoshkina, O.; Tkach, T. Spectroscopy of multicharged ions in plasmas: Oscillator strengths of Be-like ion Fe. *Photoelectronics*. **2017,** *26,* 94-102.

PACS: 31.15.ac, 31.15.ag, 31.15.aj

A. V. Tsudik, A. A. Kuznetsova, P. A. Zaichko, V. F. Mansarliysky

RELATIVISTIC SPECTROSCOPY OF HEAVY RYDBERG ATOMIC SYSTEMS IN A BLACK-BODY RADIATION FIELD

Summary. We present the results of studying the spectroscopic characteristics of heavy Rydberg atomic systems in a black-body (thermal) radiation field. As theoretical approach we apply the combined generalized relativistic energy approach and relativistic many-body perturbation theory with ab initio Dirac zeroth approximation. There are presented the calculational data for the thermal black-body radiation ionization characteristics of the alkali Rydberg atoms, in particular, the sodium in Rydberg states with principal quantum number n=10-100 and ytterbium ion. Application of theory to computing the spectral parameters of studied atomic systems have demonstrated physically reasonable agreement between the theoretical and experimental data. The accuracy of the theoretical data is provided by a correctness of the corresponding relativistic wave functions and accounting for the exchange-correlation effects.

Key words: Rydberg heavy atoms, relativistic theory, black-body radiation field.

PACS: 31.15.ac, 31.15.ag, 31.15.aj

А. В. Цудик, А. А. Кузнецова, П. А. Заичко, В. Ф. Мансарлийский

РЕЛЯТИВИСТСКАЯ СПЕКТРОСКОПИЯ ТЯЖЕЛЫХ РИДБЕРГОВСКИХ АТОМНЫХ СИСТЕМ В ПОЛЕ ИЗЛУЧЕНИЯ ЧЕРНОГО ТЕЛА

Резюме. Представлены результаты изучения спектроскопических характеристик тяжелых ридберговских атомных систем в поле чернотел(теплового) излучения. В качестве теоретического подхода мы применяем комбинированный релятивистский энергетический подход и релятивистскую многочастичную теорию возмущений с оптимизированныи дираковским нулевым приближением. Представлены результаты расчета спектроскопических характеристик щелочных ридберговских атомов в поле теплового излучения черного тела, в частности, натрия в ридберговских состояниях с главным квантовым числом n=20-100 и иона иттербия. Применение теории к вычислению спектральных параметров исследуемых атомных систем продемонстрировало физически разумное согласие между теоретическими и экспериментальными данными. Точность теоретических данных обеспечивается корректностью вычисления соответствующих релятивистских волновых функций и полнотой учета обменно-корреляционных эффектов.

Ключевые слова: ридберговские тяжелые атомы, релятивистская теория, тепловое излучение.

PACS: 31.15.ac, 31.15.ag, 31.15.aj

А. В. Цудік, Г. О. Кузнецова, П. А. Заічко, В. Ф. Мансарлійський

РЕЛЯТИВІСТСЬКА СПЕКТРОСКОПІЯ ВАЖКИХ РІДБЕРГІВСЬКИХ АТОМНИХ СИСТЕМ В ПОЛІ ВИПРОМІНЮВАННЯ ЧОРНОГО ТІЛА

Резюме. Представлені результати вивчення спектроскопічних характеристик важких рідбергівських атомних систем в полі чорнотільного (теплового) випромінювання. В якості теоретичного підходу ми застосовуємо комбінований релятивістський енергетичний підхід і ре-

лятивістську багаточастинкову теорію збурень з оптимізованим дираківським нульовим наближенням. Представлені результати розрахунку спектроскопічних характеристик лужних рідбергівських атомів в полі теплового випромінювання, зокрема, натрію в рідбергівських станах з головним квантовим числом n = 20-100 та іону ітербію. Застосування теорії до обчислення спектральних параметрів досліджуваних атомних систем продемонструвало фізично розумну згоду між теоретичними і експериментальними даними. Точність теоретичних даних забезпечується коректністю обчислення відповідних релятивістських хвильових функцій і повнотою обліку обмінно-кореляційних ефектів.

Ключові слова: рідбергівські важкі атоми, релятивістська теорія, теплове випромінювання.

PACS 31.30.Gs

O. A. Antoshkina, M. P. Makushkina, O. Yu. Khetselius, T. B. Tkach

Odessa State Environmental University, L'vovskaya str.15, Odessa-9, 65016, Ukraine
E-mail: tkachtb@gmail.com

RELATIVISTIC CALCULATION OF THE HYPERFINE STRUCTURE PARAMETERS FOR COMPLEX ATOMS WITHIN MANY-BODY PERTURBATION THEORY

Abstract. The hyperfine structure parameters and electric quadrupole moment of the ^{201}Hg mercury isotope the Mn atom are estimated within the relativistic many-body perturbation theory formalism with a correct and effective taking into account the exchange-correlation, relativistic, nuclear and radiative corrections. Analysis of the data shows that an account of the interelectron correlation effects is crucial in the calculation of the hyperfine structure parameters. The fundamental reason of physically reasonable agreement between theory and experiment is connected with the correct taking into account the inter-electron correlation effects, nuclear (due to the finite size of a nucleus), relativistic and radiative corrections. The key difference between the results of the relativistic Hartree-Fock Dirac-Fock and many-body perturbation theory methods calculations is explained by using the different schemes of taking into account the inter-electron correlations as well as nuclear and radiative ones.

1. Introduction

The research on the hyperfine structure (HFS) characteristics of the heavy neutral and highly ionized atoms is of a great fundamental importance in many fields of atomic physics (spectroscopy, spectral lines theory), astrophysics, plasma physics, laser physics and so on (see, for example, refs. [1-37]). The experiments on the definition of hyperfine splitting also enable to refine the deduction of nuclear magnetic moments of different isotopes and to check an accuracy of the various calculational models employed for the theoretical description of the nuclear effects. In recent years, due to significant progress in experimental studies, interest in studying the spectra of elements with empty d, f shells has sharply increased (see [1-10]). The multi-configuration relativistic Hartree-Fock (RHF) , Dirac-Fock (DF), ulriconfiguration DF (MCDF) approaches (see, for example, refs. [1-9]) are the most reliable versions of calculation for multi-electron systems with a large nuclear charge. Usually, in these calculations the one- and two-body relativistic effects are taken into account practically precisely. It should be given the special attention to three very general and important computer systems for relativistic and QED calculations of atomic and molecular properties such as "GRASP", "Dirac"; "BERTHA", "QED", "Dirac" etc. (see refs. [1-9] and refs. there).

In this paper we present the calculational results for the HFS structure parameters for the Mn atom and electric quadrupole moment of the isotope ^{201}Hg, using the optimized method of the relativistic many-body perturbation theory with the Dirac-Kohn-Sham zeroth approximation and a correct and effective taking into account the exchange-correlation, relativistic, nuclear and radiative corrections [9-30]. Analysis of the data shows that an account of the interelectron correlation effects is crucial in the calculation of the hyperfine structure parameters.

2. Relativistic method to computing hyperfine structure parameters of atoms and ions

Let us describe the key moments of the approach (more details can be found in refs. [19-30]). The electron wave functions (the PT zeroth basis) are found from solution of the relativistic Dirac equation with potential, which includes ab initio mean-field potential, electric, polarization potentials of a nucleus. The charge

distribution in the Li-like ion is modelled within the Gauss model. The nuclear model used for the Cs isotope is the independent particle model with the Woods-Saxon and spin-orbit potentials (see refa. [20]). Let us consider in details more simple case of the Li-like ion. We set the charge distribution in the Li-like ion nucleus $\rho(r)$ by the Gaussian function:

$$\rho(r|R) = \left(4\gamma^{3/2}/\sqrt{\pi}\right)\exp\left(-\gamma r^2\right) \qquad (1)$$

where $\gamma=4/\pi R^2$ and R is the effective nucleus radius. The Coulomb potential for the spherically symmetric density $\rho(r)$ is:

$$V_{nucl}(r|R) = -\left((1/r)\int_0^r dr' r'^2 \rho\left(r'\middle|R\right) + \int_r^\infty dr' r' \rho\left(r'\middle|R\right)\right) \qquad (2)$$

Consider the DF type equations. Formally they fall into one-electron Dirac equations for the orbitals with the potential $V(r|R)$ which includes the electrical and the polarization potentials of the nucleus; the components of the Hartree potential (in the Coulomb units):

$$V(r|i) = \frac{1}{Z}\int d\vec{r}'\rho(r|i)/|\vec{r}-\vec{r}'| \qquad (4)$$

Here $\rho(r|i)$ is the distribution of the electron density in the state $|i>$, V_{ex} is the exchange inter-electron interaction. The main exchange and correlation effects will be taken into account in the first two orders of the PT by the total inter-electron interaction [21,22].

A procedure of taking into account the radiative QED corrections is in details given in the refs. [19,20].

Regarding the vacuum polarization effect let us note that this effect is usually taken into consideration in the first PT theory order by means of the Uehling-Serber potential. This potential is usually written as follows:

$$U(r) = -\frac{2\alpha}{3\pi r}\int_1^\infty dt\ \exp(-2tr/\alpha Z)\left(1+1/2t^2\right)\frac{\sqrt{t^2-1}}{t^2} \equiv$$

$$\equiv -\frac{2\alpha}{3\pi r}C(g), \qquad (5)$$

where $g=r/(\alpha Z)$. In our calculation we use more exact approach [20]. The Uehling potential, determined as a quadrature (5), may be approximated with high precision by a simple analytical function. The use of new approximation of the Uehling potential permits one to decrease the calculation errors for this term down to 0.5 – 1%.

A method for calculation of the self-energy part of the Lamb shift is based on the methods [19-24]. The radiative shift and the relativistic part of energy in an atomic system are, in principle, defined by one and the same physical field. One could suppose that there exists some universal function that connects the self-energy correction and the relativistic energy.

Its form and properties are in details analyzed in Refs.[19-24,30-35]. Unlike usual purely electronic atoms, the Lamb shift self-energy part in the case of a pionic atom is not significant and much inferior to the main vacuum-polarization effect.

The energies of electric quadruple and magnetic dipole interactions are defined by a standard way with the hyperfine structure constants, usually expressed through the standard radial integrals:

$$A=\{[(4,32587)10^{-4}Z^2\chi g_I]/(4\chi^2-1)\}(RA)_{-2},$$

$$B=\{7.2878\ 10^{-7}\ Z^3Q/[(4\chi^2-1)I(I-1)\}\ (RA)_{-3}, \qquad (7)$$

Here g_I is the Lande factor, Q is a quadruple momentum of nucleus (in Barn); $(RA)_{-2}$, $(RA)_{-3}$ are the radial integrals usually defined as follows:

$$(RA)_{-2} = \int_0^\infty dr r^2 F(r)G(r)U(1/r^2, R)$$

$$(RA)_{-3} = \int_0^\infty dr r^2 [F^2(r)+G^2(r)U(1/r^2, R)\cdot \qquad (8)$$

The radial parts F and G of the Dirac function two components for electron, which moves in

the potential *V(r,R)+U(r,R),* are determined by solution of the Dirac equations.

The key elements of the numerical approach to computing the corresponding matrix elements are presented in [19-36]. All calculations are performed on the basis of the numeral code Superatom-ISAN (version 93).

3. Results and Conclusions

In this subsection we present experimental data and the results of the calculation of the HFS parameters for some complex atoms. It should be noted that the Mn element has one stable isotope with a mass number of 55, a nuclear spin of 5/2, a magnetic dipole moment of 3.46871668 $m_я$ and an electric quadrupole moment of Q = 0.33 (1) barn. Basic electronic configuration: $3d^54s^2$ ($^6S_{5/2}$).

Given the complexity of the spectrum, theoretical study of the HFS should be based on a full multi-electron calculation. An useful review and detailed analysis of the studies of the HFS of the Mn atom was given, for example, in [6].

In table 1 we present the available experimental (A_{exp}, B_{exp}) and theoretical (our calculation) values of the energy levels and the HFS parameters for the Mn configuration $3d^54s^2$,3d64s. The reasonable agreement between theoretical and measured data can be reached by way of using the optimized wave functions basises and complete, correct accounting for the exchange-correlation corrections.

Further we present the results of calculating the HFS constants and the electric quadrupole moment for the ^{201}Hg isotope. The mercury atom has an external valent configuration $6s^2$ and can be considered within the many-body paerturbation theory as the two-quasipartial system. Mercury has one stable isotope ^{201}Hg (I = 3/2) with a relative prevalence of 13.2%.

The ^{199}Hg isotope with a relative distribution of 16.9% has two quadrupole excited states with energies of 158 and 208 keV. The values of quadrupole moment for a few radioactive isotopes with masses from 185 to 203 are presented by the group Ulm and others (see, for example, [4,5]).

Table 1.

Experimental (A_{exp}, E_{exp}) and theoretical (our calculation) values of the energy levels (cm^{-1}) and HFS constants (MHz) for the Mn configuration $3d^54s^2$

Level	Term	E_{exp}	E_{th}
$3d^54s^2$	$a^6S_{5/2}$	0.0	0.0
$3d^64s$	$a^6D_{9/2}$	17052.29	17001.38
$3d^64s$	$a^6D_{7/2}$	17282.00	17209.34
$3d^64s$	$a^6D_{5/2}$	17451.52	17394.91
$3d^64s$	$a^6D_{3/2}$	-	17500.12
$3d^64s$	$a^6D_{1/2}$	-	17565.24
$3d^54s^2$	$a^4G_{11/2}$	25265.74	25201.43
$3d^54s^2$	$a^4G_{5/2}$	25281.04	25219.45
$3d^54s^2$	$a^4G_{9/2}$	25285.43	25221.36
$3d^54s^2$	$a^4G_{7/2}$	25287.74	25224.16
$3d^54s^2$	$b^4D_{5/2}$	30419.61	30382.46
$3d^54s^2$	$b^4D_{3/2}$	-	30374.97
Level	Term	A_{exp}	A_{th}
$3d^54s^2$	$a^6S_{5/2}$	-72.4	-73
$3d^64s$	$a^6D_{9/2}$	503(8)	504
$3d^64s$	$a^6D_{7/2}$	457(3)	457
$3d^64s$	$a^6D_{5/2}$	434(4)	434
$3d^64s$	$a^6D_{3/2}$	467(6)	466
$3d^64s$	$a^6D_{1/2}$	892(16)	891
$3d^54s^2$	$a^4G_{11/2}$	405.3(9)	405.4
$3d^54s^2$	$a^4G_{5/2}$	596.2(9)	596.0
$3d^54s^2$	$a^4G_{9/2}$	395.2(3)	395.1
$3d^54s^2$	$a^4G_{7/2}$	437,1	437.4
$3d^54s^2$	$b^4D_{5/2}$	288(5)	290
$3d^54s^2$	$b^4D_{3/2}$	456	453
Level	Term	B_{exp}	B_{th}
$3d^54s^2$	$a^6S_{5/2}$	0.019	0.016
$3d^54s^2$	$b^4D_{5/2}$	130(5)	129
$3d^54s^2$	$b^4D_{3/2}$	-	-36

A reasonable compilation of the values of quadrupole moments for isotopes in the mass range 185–206 is presented in the well-known Raghavan table. Currently available experimental values of the quadrupole moment Q (201Hg) are given in table 2. The muon "muonic 3d" value of 386 (49) mb was used in the recent final report "year-2001" on the nuclear quadrupole moments [6].

Table 2.

The values of the electric quadrupole moment Q (mb) for isotope of ^{201}Hg

Q (mb)	Method	Ref.	Year
383	Atomic	This work	2018
381	Atomic	Khetselius	2006
387 (6)	Atomic	Pyykko et al	2005
347(43)	Nuclear	Fornal et al	2001
385 (40)	Atomic[a]	Ulm et al	1988
485 (68)	Muonic[b]	Gunther et	1983
386 (49)	Muonic	al	1979
267 (37)	3d[c]	Hahn et al	1979
390 (20)	Muonic 2p[c]	Hahn et al Edelstein-	1975
455 (40)	Solid[d]	Pound McDermott-	1960
420	Atomic	Lichten	1959
500 (50)	$^3P_2$	Murakawa Blaise-	1957
600	Atomic	Chantrel	1954
500	Atomic[e]	Dehmelt et al	1935
	Solid[e]	Schuler-Schmidt	
	Atomic[e]		

Note: a- standard Raghavan value; the value of ^{199}Hg (I = 5/2) is consistent with the ratio 201/199; c - direct muon experiment for ^{201}Hg; d- solid state $HgCl_2$ plus compiled value ^{199}Hg;

In table 3 we list the experimental and calculated values of the nuclear electric quadrupole moment Q (mb) for ^{201}Hg and the HFS constants (MHz) for the $^3\mathbf{P}_1$ state of the ^{201}Hg neutral mercury. The calculations were performed within the uncorrelated DF method, multi-configuration DF (MCDF) approximation with accounting for the Breit-QED corrections [6], the N-QED theory with an accounting for the Breit-QED corrections [20], and the present method (RMBPT) with the Gaussian model for a nuclear density distribution). The value of Q obtained by us is in the best agreement with the data obtained by the group Ulm. Comparison of our calculational results and data by the DF method (single-configuration and multi-configuration approximations taking into account the Breit and QED corrections) shows that our values of the constant A are in

Table 3.

Experimental and calculated values of the nuclear electric quadrupole moment Q (mb) for ^{201}Hg and the values of the HFS constants (MHz) for the $^3\mathbf{P}_1$ state of a neutral mercury atom ^{201}Hg states (see text)

Method	*Q* (mb)
DF	478.13
MCDF (+Breit_QED)	386.626
N-QED	380. 518
This work (e-Corr)	-90.824
This work (Breit+QED)	-2.420
This work (Total)	380. 518
Exp.	Look Table 2
Method	A (MHz)
DF	-4368.266
MCDF (+Breit_QED)	-5470.810
N-QED	-5460.324
This work (e-Corr)	-1162
This work (Breit+QED)	-20.868
This work (Total)	-5460,.324
Exp.	-5454.569 (0.003)
Method	B (MHz)
DF	---
MCDF (+Breit_QED)	---

N-QED	-286.512
This work (e-Corr)	-60.974
This work (Breit+QED)	-1.099
This work (Total)	-286.512
Exp.	-280.107 (0,005)

reasonable agreement with the experiment. The analysis shows that the contribution due to the electron – electron correlations t o the values of the HFS constants is ~ 100–500 MHz for various states. This circumstance explains the low degree of consistency in accuracy of the data provided, obtained in the framework of different versions of the DF method. The key difference between the results of the calculation in the framework of our approach and the MCDF is due to different methods of taking into account the electron-electron correlations.

The contributions of higher-order QED TV corrections and corrections for the finite core size can reach 1–2 tens of MHz, and it seems obviously important to consider them more correctly. In addition, it is necessary to take direct account of nuclear polarization contributions, which can be done within the framework of solving the corresponding nuclear problem, for example, using the shell model with Woods-Saxon and spin-orbit potentials. Such an approach is outlined in Refs [20,33]. These topics require the separated accurate treatment.

References

1. Grant I. *Relativistic Quantum Theory of Atoms and Molecules.* Oxford, **2007**.
2. Glushkov, A; Khetselius, O; Svinarenko, A; Buyadzhi, V. *Spectroscopy of autoionization states of heavy atoms and multiply charged ions*. Odessa: **2015**.
3. Khetselius, O.Yu. *Hyperfine structure of atomic spectra*. Astroprint: **2008**.
4. Pyykko, P. Year2008 nuclear quadrupole moments. *Mol. Phys.* **2008,** *106*, 16.
5. Bieron J., Pyykkő P., Jonsson P. Nuclear quadrupole moment of ^{201}Hg. Phys.Rev. A. **2005**, *71*, 012502.
6. Basar Gu., Basar Go., Acar G., Ozturk I.K., Kroger S. Hyperfine structure investigations of MnI: Experimental and theoretical studies of the hyperfine structure in the even configurations. Phys.Scr. **2003**, *67*, 476-484.
7. Gubanova E., Glushkov A., Khetselius O., Bunyakova Yu., Buyadzhi V., Pavlenko E. New methods in analysis and project management of environmental activity: Electronic and radioactive waste. FOP: Kharkiv, **2017.**
8. Florko, T.A.; Tkach, T.B.; Ambrosov, S.V.; Svinarenko, A.A. Collisional shift of the heavy atoms hyperfine lines in an atmosphere of the inert gas. *J. Phys.: Conf. Ser*. **2012**, *397*, 012037.
9. Khetselius, O.Yu., Lopatkin Yu.M., Dubrovskaya, Yu.V, Svinarenko A.A. Sensing hyperfine-structure, electroweak interaction and parity non-conservation effect in heavy atoms and nuclei: New nuclear-QED approach. *Sensor Electr. and Microsyst. Techn*. 2010, 7(2), 11-19
10. Glushkov, A.V. *Relativistic Quantum theory. Quantum mechanics of atomic systems*. Astroprint: Odessa, **2008**.
11. Khetselius, O.Yu. Atomic parity non-conservation effect in heavy atoms and observing P and PT violation using NMR shift in a laser beam: To precise theory. *J. Phys.: Conf. Ser.* **2009,** *194,* 022009
12. Khetselius, O.Yu. Hyperfine structure of radium. *Photoelectronics*. **2005,** *14,* 83.
13. Khetselius, O.. Relativistic perturbation theory calculation of the hyperfine structure parameters for some heavy-element isotopes. *Int. Journ. Quant. Chem.* **2009,** *109,* 3330-3335.
14. Khetselius, O.Yu. Relativistic calculation of the hyperfine structure parameters for heavy elements and laser detection of the heavy isotopes. *Phys.Scripta.* **2009,** *135,* 014023.
15. Khetselius, O.Yu. Relativistic Hyperfine Structure Spectral Lines and Atomic Parity Non-conservation Effect in Heavy Atomic Systems within QED Theory. *AIP Conf. Proc.* **2010,** *1290(1),* 29-33.
16. Khetselius O.Yu.; Gurnitskaya, E.P. Sensing the hyperfine structure and nuclear quadrupole moment for radium. *Sensor Electr. and*

Microsyst. Techn. **2006,** *2,* 25-29.
17. Khetselius, O.Yu.; Gurnitskaya, E.P. Sensing the electric and magnetic moments of a nucleus in the N-like ion of Bi. *Sensor Electr. and Microsyst. Techn.* **2006,** *3,* 35-39.
18. Khetselius, O.Yu. Relativistic calculating the spectral lines hyperfine structure parameters for heavy ions. *AIP Conf. Proc.* **2008,** *1058,* 363-365.
19. Glushkov, A.V. *Relativistic and correlation effects in spectra of atomic systems*. Astroprint: Odessa, **2006**.
20. Khetselius, O.Yu. *Quantum structure of electroweak interaction in heavy finite Fermi-systems.* Astroprint: Odessa, **2011**.
21. Svinarenko, A.A. Study of spectra for lanthanides atoms with relativistic many- body perturbation theory: Rydberg resonances. *J. Phys.: Conf. Ser.* **2014,** *548,* 012039.
22. Svinarenko, A. A., Glushkov, A. V., Khetselius, O.Yu., Ternovsky,V.B., Dubrovskaya, Yu., Kuznetsova, A., Buyadzhi, V. Theoretical spectroscopy of rare-earth elements: spectra and autoionization resonances. *Rare Earth Element*, Ed. J. Orjuela (InTech) **2017**, pp 83-104.
23. Khetselius, O.Yu. Optimized relativistic many-body perturbation theory calculation of wavelengths and oscillator strengths for Li-like multicharged ions. Adv. Quant. Chem. **2019**, *78*, 223-251.
24. Khetselius, O. Optimized perturbation theory for calculating the hyperfine line shift and broadening of heavy atoms in a buffer gas. *In Frontiers in Quantum Methods and Applications in Chemistry and Physics*, Springer: Cham, **2015;** Vol. 29, pp. 55-76
25. Glushkov, A.V., Khetselius, O.Yu., Svinarenko A.A., Buyadzhi, V.V., Ternovsky, V.B, Kuznetsova, A., Bashkarev, P Relativistic perturbation theory formalism to computing spectra and radiation characteristics: application to heavy element. *Recent Studies in Perturbation Theory*, ed. D. Uzunov (InTech) **2017**, 131-150.
26. Glushkov A., Lovett L., Khetselius O., Gurnitskaya E., Dubrovskaya Y., Loboda A. Generalized multiconfiguration model of decay of multipole giant resonances applied to analysis of reaction (μ-n) on the nucleus ^{40}Ca. *Int. J. Mod. Phys. A*. **2009**, *24*(2-3), 611-615
27. Dubrovskaya, Yu., Khetselius, O.Yu., Vitavetskaya, L., Ternovsky, V., Serga, I. Quantum chemistry and spectroscopy of pionic atomic systems with accounting for relativistic, radiative, and strong interaction effects. *Adv. in Quantum Chem.* **2019,** Vol.78, pp 193-222.
28. Bystryantseva A., Khetselius O.Yu., Dubrovskaya Yu., Vitavetskaya L.A., Berestenko A.G. Relativistic theory of spectra of heavy pionic atomic systems with account of strong pion-nuclear interaction effects: ^{93}Nb, ^{173}Yb, ^{181}Ta , ^{197}Au. *Photoelectronics*. **2016**, *25*, 56-61.
29. Khetselius, O., Glushkov, A., Gurskaya M., Kuznetsova, A., Dubrovskaya, Yu., Serga I., Vitavetskaya, L. Computational modelling parity nonconservation and electroweak interaction effects in heavy atomic systems within the nuclear-relativistic many-body perturbation theory. *J. Phys.: Conf. Ser.* ***2017,*** *905*(1), 012029.
30. Khetselius, O.Yu., Glushkov, A.V., Dubrovskaya, Yu.V., Chernyakova, Yu., Ignatenko, A.V., Serga, I., Vitavetskaya, L. Relativistic quantum chemistry and spectroscopy of exotic atomic systems with accounting for strong interaction effects. In: Concepts, *Methods and Applications of Quantum Systems in Chemistry and Physics*. Springer, Cham, **2018,** *31*, 71-91.
31. Svinarenko A., Khetselius O., Buyadzhi V., Florko T., Zaichko P., Ponomarenko E. Spectroscopy of Rydberg atoms in a Blackbody radiation field: Relativistic theory of excitation and ionization. *J. Phys.: Conf. Ser*. **2014**, *548*, 012048.
32. Svinarenko, A.; Ignatenko, A.; Ternovsky, V.B.; Nikola, L.; Seredenko, S.S.; Tkach, T.B. Advanced relativistic model potential approach to calculation of radiation transition parameters in spectra of multicharged ions. *J. Phys.: Conf. Ser.* **2014,** *548,* 012047.
33. Glushkov A Spectroscopy of cooperative muon-gamma-nuclear processes: Energy and spectral parameters *J. Phys.: Conf. Ser.*

2012, *397,* 012011.
34. Glushkov, A.V. Spectroscopy of atom and nucleus in a strong laser field: Stark effect and multiphoton resonances. *J. Phys.: Conf. Ser*. **2014**, *548*, 012020
35. Glushkov A.V.; Ivanov, L.N. DC strong-field Stark effect: consistent quantum-mechanical approach. *J. Phys. B: At. Mol. Opt. Phys.* **1993,** *26,* L379-386.
36. Glushkov A.V., Khetselius O.Yu., Svinarenko A.A., Buyadzhi V.V., *Methods of computational mathematics and mathematical physics*. *P.1*. TES: Odessa, **2015**.

PACS 31.30.Gs

О. О. Антошкіна, М. П. Макушкіна, О. Ю. Хецеліус, Т. Б. Ткач

РЕЛЯТИВІСТСЬКИЙ РОЗРАХУНОК ПАРАМЕТРІВ НАДТОНКОЇ СТРУКТУРИ СКЛАДНИХ АТОМІВ В РАМКАХ БАГАТОЧАСТИНКОВОЇ ТЕОРІЇ ЗБУРЕНЬ

Резюме. Параметри надтонкою структури і електричний квадрупольний момент ізотопу ртуті ^{201}Hg і атома Mn розраховані на основі релятивістської багаточастинкової теорії збурень з ефективним акуратним урахуванням обмінно-кореляційних, релятивістських, ядерних і радіаційних поправок. Аналіз даних показує, що урахування ефектів міжелектронної кореляції має критичне значення при обчисленні параметрів надтонкої структури. Фізично розумне узгодження теорії і прецизійного експерименту може бути забезпечено завдяки повному послідовному обліку міжелектронних кореляційних ефектів, ядерних, релятивістських та радіаційних поправок. Ключова відмінність між результатами розрахунків в наближеннях Дірака-Фока, різних версіях формалізму теорії збурень в основному пов'язано з використанням різних схем обліку міжелектронних кореляцій, а також врахування ядерних і радіаційних поправок.

Ключові слова: Надтонка структура, важкий атом, релятивістська теорія збурень, кореляційні, ядерні, радіаційні поправки

PACS 31.30.Gs

O. A. Antoshkina, M. P. Makushkina, O. Yu. Khetselius, T. B. Tkach

RELATIVISTIC CALCULATION OF THE HYPERFINE STRUCTURE PARAMETERS FOR COMPLEX ATOMS WITHIN MANY-BODY PERTURBATION THEORY

Summary. The hyperfine structure parameters and electric quadrupole moment of the ^{201}Hg mercury isotope the Mn atom are estimated within the relativistic many-body perturbation theory formalism with a correct and effective taking into account the exchange-correlation, relativistic, nuclear and radiative corrections. Analysis of the data shows that an account of the interelectron correlation effects is crucial in the calculation of the hyperfine structure parameters. The fundamental reason of physically reasonable agreement between theory and experiment is connected with the correct taking into account the inter-electron correlation effects, nuclear (due to the finite size of a nucleus), relativistic and radiative corrections. The key difference between the results of the

relativistic Hartree-Fock Dirac-Fock and many-body perturbation theory methods calculations is explained by using the different schemes of taking into account the inter-electron correlations as well as nuclear and radiative ones.

Keywords: Hyperfine structure, Heavy atoms, Relativistic perturbation theory, correlation, nuclear, radiative corrections

PACS 31.30.Gs

О. А. Антошкина, М. П. Макушкина, О. Ю. Хецелиус, Т. Б. Ткач

РЕЛЯТИВИСТСКИЙ РАСЧЕТ ПАРАМЕТРОВ СВЕРХТОНКОЙ СТРУКТУРЫ СЛОЖНЫХ АТОМОВ В РАМКАХ МНОГОЧАСТИЧНОЙ ТЕОРИИ ВОЗМУЩЕНИЙ

Резюме. Параметры сверхтонкой структуры и электрический квадрупольный момент изотопа ртути ^{201}Hg и атома Mn рассчитаны на основе релятивистской многочастичной теории возмущений с эффективным аккуратным учетом обменно-корреляционных, релятивистских, ядерных и радиационных поправок. Анализ данных показывает, что учет эффектов межэлектронной корреляции имеет критическое значение при вычислении параметров сверхтонкой структуры. Физически разумное согласие теории и прецизионного эксперимента может быть обеспечено благодаря полному последовательному учету межэлектронных корреляционных эффектов, ядерных, релятивистских и радиационных поправок. Ключевое различие между результатами расчетов в приближениях Дирака-Фока, различных версиях формализма теории возмущений в основном связано с использованием различных схем учета межэлектронных корреляций, а также учета ядерных и радиационных поправок.

Ключевые слова: Сверхтонкая структура, тяжелый атом, релятивистская теория возмущений, корреляционные, ядерные, радиационные поправки

PACS 31.15.-p

V. V. Buyadzhi

Odessa State Environmental University, 15, Lvovskaya str., Odessa-16, 65016, Ukraine
E-mail: buyadzhivv@gmail.com

ELECTRON-COLLISIONAL SPECTROSCOPY OF ATOMS AND IONS: ADVANCED ENERGY APPROACH

An advanced relativistic energy approach combined with a scattering theory is used to calculate the electron-collision excitation cross-sections, collision strengths for a number of multicharged ions. The relativistic many-body perturbation theory is used alongside the gauge-invariant scheme to generate an optimal Dirac-Kohn-Sham- Debye-Hückel one-electron representation. The results of relativistic calculation (taking into account the exchange and correlation corrections) of the electron collision cross-sections (strengths) of excitation of the transition between the fine-structure levels ($2P_{3/2}$- $2P_{1/2}$) of the ground state of F-like ions with Z = 19-26 and of the [$2s^2\ ^1S$ -($2s2p\ ^1P$)] transition in the B-like O^{4+} are presented and analysed.

1. Introduction

Electron-collisional spectroscopy of atoms and multicharged ions is one of the most fast developing branches of modern atomic spectroscopy. The properties of laboratory and astrophysical plasmas have drawn considerable attention over the last decades [1-15]. It is known that multicharged ions play an important role in the diagnostics of a wide variety of plasmas. Similar interest is also stimulated by importance of this information for correct determination of the characteristics for plasma in thermonuclear (tokamak) reactors, searching new mediums for X-ray range lasers.

In the case of solving collision problems involving multi-electron atomic systems, as well as low-energy processes, etc., the structure of atomic systems should be described on the basis of rigorous methods of quantum theory. As a rule, the Hartree-Fock (HF) or Hartree-Fock-Slater (HFS) models implemented in the tight-binding approximation were used to describe the wave functions of the bound states of atoms and ions. Another direction is the models of the central potential (model potential, pseudopotential) implemented in the distorted wave approximation (DWA). It should be mentioned the currently widespread and widely used R-matrix method and its various promising modifications, as well as a generalization of the well-known Dirac-Fock method to the case of taking into account multipolarity in the corresponding operators (see, e.g. , [1-7]). It should be noted that, depending on the perturbation theory (PT) basis used, different versions of the R-matrix method received the corresponding names. For example, in specific calculations such versions as R-MATR-CI3-5R and R-MATR-41 R-matrix method were used using respectively wave functions in the multiconfiguration approximation, in particular, 5- and 41- configuration wave functions. As numerous applications of the R-matrix method have shown, it has certain advantages in terms of accuracy and consistency over such popular approaches as the first-order PT method, as well as the distorted wave approximation taking into account configuration interaction (CI-DWBA); --- approximation of distorted waves using the HF basis (HF-DWBA), finally, the relativistic approximation of distorted waves with a 1-configuration and multi-configuration wave function of the ground state (SCGS-RDWA, MCGS-RDWA, etc.). Improved models have also appeared in theories of the coupled-channel (VC) type VCDWA (Variational Continuum Distorted Wave), for example, a modification of the Vraun-Scroters type and others (see [1-5]). Various cluster methods have also been widely used (see in more details [1-3,14,15]).

In this paper, we present and use an advanced relativistic energy approach to calculate the electron-ion collision strengths, effective

collision strengths and the associated cross sections. The relativistic many-body PT is utilised alongside the gauge-invariant scheme to generate an optimal one-electron representation. The calculated effective collision strengths of the Ne-like krypton excitation are listed.

2. Advanced energy approach to electron collision strengths for atomic systems

The detailed description of our approach was earlier presented (see, for example, Refs. [7-9,13]). Therefore, below we are limited only by the key points. The generalized relativistic energy approach combined with the RMBPT has been in details described in Refs. [6,14-18]. It generalizes earlier developed energy approach [6,16].

The key idea is in calculating the energy shifts D*E* of degenerate states that is connected with the secular matrix *M* diagonalization [6,16]. To construct *M*, one should use the Gell-Mann and Low adiabatic formula for D*E*. The secular matrix elements are already complex in the PT second order. The whole calculation is reduced to calculation and diagonalization of the complex matrix *M* .and definition of matrix of the coefficients with eigen state vectors $B^K_{i,v}$ [6,8,9].

To calculate all necessary matrix elements one must use the basis's of the 1QP relativistic functions. Within an energy approach the total energy shift of the state is usually presented as [6,16]:

$$\Delta E = \mathrm{Re}\Delta E + i\,\Gamma/2 \qquad (1)$$

where Γ is interpreted as the level width and decay possibility $P = \Gamma$. The imaginary part of electron energy of the system, which is defined in the lowest PT order as [6]:

$$\mathrm{Im}\,\Delta E(B) = -\frac{e^2}{4\pi} \sum_{\substack{\alpha>n>f \\ [\alpha<n\le f]}} V^{|\omega_{\alpha n}|}_{\alpha n \alpha n}, \qquad (2)$$

where $\sum_{\alpha>n>f}$ for electron and for vacancy.

The separated terms of the sum in (3) represent the contributions of different channels. It is known that their adequate description requires using the optimized basis's of wave functions. In [6] it has been proposed "ab initio" optimization principle for construction of cited basis's. It uses a minimization of the gauge dependent multielectron contribution of the lowest QED PT corrections to the radiation widths of atomic levels. This contribution describes collective effects and it is dependent upon the electromagnetic potentials gauge (the gauge non-invariant contribution δE_{ninv}). The minimization of ImδE_{ninv} leads to integral differential equation, that is numerically solved. In result one can get the optimal one-electron basis of the PT [14,16,17]. It is worth to note that this approach was used under solving of multiple problems of modern atomic , nuclear and molecular physics (see [14-25]). The scattered part of ImE appears first in the second order of the atomic PT. The collisional de-excitation cross section is defined as follows [6,8,9]:

$$\sigma(K \to 0) = 2\pi \sum_{j_{in}, j_{\varepsilon}} (2j_{\varepsilon} + 1) * \qquad (1)$$

$$* \{ \sum_{j_{ie}, j_{iv}} < 0 \,|\, j_{in}, j_{\varepsilon} \,|\, j_{ie}, j_{iv}, J_i > B^K_{ie,iv} \}^2 ,$$

$$< 0 \,|\, j_{in}, j_{\varepsilon} \,|\, j_{ie}, j_{iv}, J_i \rangle =$$

$$\sqrt{(2j_{ie}+1)(2j_{iv}+1)}(-1)^{j_{ie}+1/2} \times \sum_{\lambda} (-1)^{\lambda + J_i} \times$$

$$\times \{ \delta_{\lambda, J_i} (2J_i + 1) Q_{\lambda}(\varepsilon, ie; iv, in) + , \qquad (2)$$

$$\begin{bmatrix} j_{in} \ldots j_{\varepsilon} \ldots J_i \\ j_{ie} \ldots j_{iv} \ldots \lambda \end{bmatrix} Q_{\lambda}(ie; in; iv, \varepsilon) \}$$

where $Q_{\square}$ is the sum of the known Coulomb and Breit matrix elements [6,14,16]. The effective collision strength $\Omega(I \to F)$ is associated with a collisional cross section σ as follows (in the Coulomb units):

$$\sigma(I \to F) = \Omega(I \to F) \cdot \pi / \qquad (3)$$

$$/\{(2J_i + 1)\varepsilon_{in} [\alpha Z)^2 \varepsilon_{in} + 2\}$$

where Z is the nucleus charge and α is the fine structure constant, ε_{in} is the incident energy. Further let us firstly consider the Debye shielding model according to Refs. [7-9].

It is known in the classical theory of plasmas developed by Debye-Hückel, the interaction potential between two charged particles is

modelled by the Yukawa-type potential, which contains the shielding parameter μ. The parameter μ is connected with the plasma parameters such as the temperature *T* and the charge density n as follows: $\mu \sim \sqrt{e^2 n / k_B T}$. Here, as usually, e is the electron charge and κ_B is the Boltzman constant.

The density *n* is given as a sum of the electron density N_e and ion density N_k of the k-th ion species having the nuclear charge

$$q_k : n = N_e + \sum_k q_k^2 N_k \,. \qquad (4)$$

It should be noted that indeed the Debye screening for the atomic electrons in the Coulomb field of nuclear charge is well understood due to the presence of the surrounding plasma electrons with high mobility. On the other hand, the contribution due to the Debye screening between electrons would be of smaller magnitude orders.

Majority of the previous works on the spectroscopy study have considered the screening effect only in the electron-nucleus potential where the electron-electron interaction potential is truncated at its first term of the standard exponential expansion for its dominant contribution [3-69]. However, it is also important to take into account the screening in the electron-electron interactions for large plasma strengths to achieve more realistic results in the search for stability of the atomic structure in the plasma environment.

By introducing the Yukawa-type e-N and e-e interaction potentials, an electronic Hamiltonian for N-electron ion in a plasma is in atomic units as follows [7]:

$$H = \sum_i [\alpha cp - \beta mc^2 - Z \exp(-\mu r_i) / r_i] + \\ + \sum_{i>j} \frac{\left(1 - \alpha_i \alpha_j\right)}{r_{ij}} \exp(-\mu r_{ij}) \qquad (5)$$

To generate the wave functions basis we use the optimized Dirac-Kohn-Sham potential with one parameter [14,15], which calibrated within the special ab initio procedure within the relativistic energy approach [16,17]. All calculations are performed on the basis of the code Superatom-ISAN (version 93).

3. Results and conclusion

In Table 1 we present the results of our relativistic calculation (taking into account the exchange and correlation corrections) of the electron collision strengths of excitation the transition between the fine-structure levels ($2P_{3/2}$- $2P_{1/2}$) of the ground state of F-like ions with Z = 19-26.

The energy of the incident electron is e_{in} = 0.1294×Z^2 eV, T = z^2 keV (z is the core charge), $N_e = 10^{18}$ cm^{-3}. For comparison, in Table 1 there are also listed the calculation results based on the most advanced versions of the R-matrix method, nonrelativistic calculation data in the framework of the energy approach, and also the available experimental data [1-3].

The analysis shows that the presented data are in physically reasonable agreement, however, some difference can be explained by using different relativistic orbital basises and different models for accounting of the plasma screening effect. This circumstance is mainly associated with the correct accounting of relativistic and exchange-correlation effects, using the optimized basis of relativistic orbitals ($2s^2$ $2p^5$; 2s $2p^6$ $2s^2$ $2p^4$ 3l, l=0-2)

Table 1.

The electron collision strengths of excitation the transition between the fine-structure levels ($2P_{3/2}$- $2P_{1/2}$) of the ground state of F-like ions with Z = 19-26

Ion	ICFT R-matrix	LS+JAJOM R-matrix
Ar X	0.582	0.420
Ca XII	0.162	0.160
Ti XIV	0.225	0.220
Cr XVI	0.112	0.100
Fe XVIII	0.132	0.110
Ion	Our data	Exp. [6]
Ar X	0.492	0.49
Ca XII	0.159	-
Ti XIV	0.252	-
Cr XVI	0.142	-
Fe XVIII	0.148	0.15

and, to a lesser extent, taking into account the effect of the plasma environment.

The electron-ion collision characteristics for Be-like ions are of great interest for applications such as the diagnosis of astrophysical, laboratory, and thermonuclear plasmas, as well as EBIT plasmas (see, for example, [4,5]). In the latter case, the characteristic values of electron density turn out to be significantly (several orders of magnitude) less than those considered above (10^{15}-10^{17}). In particular, the so-called MEIBEL (the merged electron-ion beams energy-loss) experiment (1999), the results of which for a Be-like oxygen ion are presented in Fig. 1. In this figure there also listed the cross section (10^{-16} cm^3) of the electron-collision excitation of the [$2s^2\ ^1S$ -($2s2p\ ^1P$)] transition in the spectra of Be-like oxygen together with the data from an alternative 3-configuration R-matrix calculation [4]. At energies below 20eV there is the reasonable agreement between the theoretical and experimental, but, above 20eV there is a discrepancy, which is due to different degrees of allowance for correlation effects (interaction of configurations) due to the difference in the bases used.

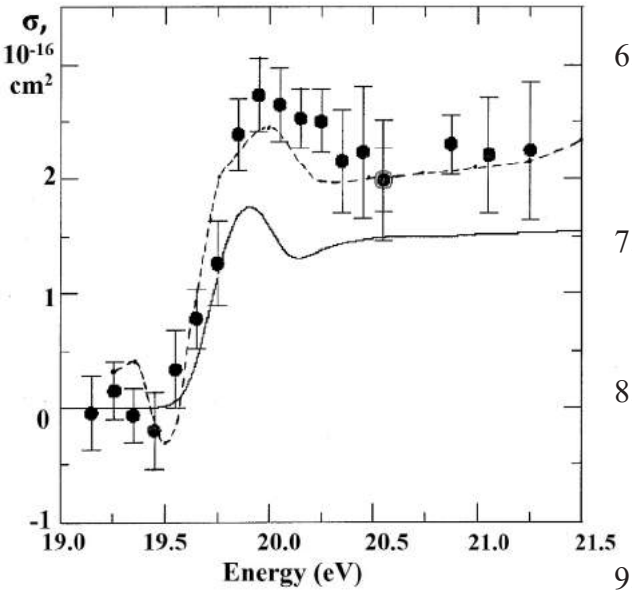

Fig.1. Cross section for electron-collision excitation of the [$2s^2\ ^1S$ -($2s2p\ ^1P$)] transition in the spectra of B-like O^{4+}: Experiment MEIBEL - points; Theory: R-matrix – solid line; our theory - dashed line.

References

1. Badnell, N.R. Calculations for electron-ion collisions and photoionization processes for plasma modeling. *J. Phys.: Conf. Ser*. **2007**, *88*, 012070.
2. Griffin, D.C., Balance, C., Mitnik, D., Berengut, J.C. Dirac *R*-matrix calculations of electron-impact excitation of neon-like krypton. *J. Phys. B: At. Mol. Opt. Phys*. **2008**, *41*, 215201.
3. Yongqiang, Li; Jianhua, Wu; Yong, Hou, Jianmin Yuan. Influence of hot and dense plasmas on energy levels and oscillator strengths of ions: Be-like ions for *Z* = 26–36, *J. Phys. B: At. Mol. Opt. Phys.* **2008,** *41,* 145002.
4. Bannister, M. E., Djurić, N., Woitke, O., Dunn, G., Chung, Y. -S, Smith, A. C. H., Wallbank, B., Berrington, K. A. Absolute cross-sections for near–threshold electron-impact excitation of Be-like C^{2+}, N^{3+}, O^{4+}. *Int. J. Mass Spectr*. **1999**, *192*, 39-48.
5. Smith, A. C. H., Bannister, M. E., Chung, Y. -S, Djuri,ć N., Dunn, G. H., Wallbank, B., Woitke, O. Near-threshold Electron-impact Excitation of Multiply-charged Be-like Ions. *Phys.Scr*. 1999, T80, 283-287.
6. Ivanov, L.N.; Ivanova, E.P.; Knight, L. Energy approach to consistent QED theory for calculation of electron-collision strengths: Ne-like ions. *Phys. Rev. A.* **1993,** *48,* 4365-4374.
7. Buyadzhi, V.V. Laser multiphoton spectroscopy of atom embedded in Debye plasmas: multiphoton resonances and transitions. *Photoelectronics.* **2015,** *24,* 128-133.
8. Buyadzhi, V.V.; Chernyakova, Yu.G.; Smirnov, A.V.; Tkach, T.B. Electron-collisional spectroscopy of atoms and ions in plasma: Be-like ions. *Photoelectronics*. **2016,** *25,* 97-101.
9. Buyadzhi, V.; Chernyakova, Yu.; Antoshkina, O.; Tkach, T. Spectroscopy of multicharged ions in plasmas: Oscillator strengths of Be-like ion Fe. *Photoelectronics*. **2017,** *26,* 94-102.
10. Glushkov, A.V.; Malinovskaya, S.V.; Prepelitsa, G.P.; Ignatenko, V. Manifestation of the new laser-electron nuclear spectral effects in the thermalized plasma: QED theory

of co-operative laser-electron-nuclear processes. *J. Phys.: Conf. Ser.* **2005,** *11,* 199-206.
11. Glushkov, A.V.; Malinovskaya, S.V.; Chernyakova Y.G.; Svinarenko, A.A. Co-operative laser-electron-nuclear processes: QED calculation of electron satellites spectra for multi-charged ion in laser field. *Int. Journ. Quant. Chem.* **2004,** *99,* 889-893.
12. Glushkov, A.V.; Malinovskaya, S.V.; Loboda, A.V.; Shpinareva, I.M.; Gurnitskaya, E.P.; Korchevsky, D.A. Diagnostics of the collisionally pumped plasma and search of the optimal plasma parameters of x-ray lasing: calculation of electron-collision strengths and rate coefficients for Ne-like plasma. *J. Phys.: Conf. Ser.* **2005,** *11,* 188-198.
13. Glushkov, A.V.; Ambrosov, S.V.; Loboda, A.V.; Gurnitskaya, E.P.; Prepelitsa, G.P. Consistent QED approach to calculation of electron-collision excitation cross sections and strengths: Ne-like ions. *Int. J. Quantum Chem.* **2005,** *104,* 562-569.
14. Glushkov, A.V. *Relativistic Quantum theory. Quantum mechanics of atomic systems;* Astroprint: Odessa, **2008**.
15. Khetselius, O.Yu. *Hyperfine structure of atomic spectra*. Astroprint: Odessa, **2008**.
16. Glushkov, A.V.; Ivanov, L.N.; Ivanova, E.P. Autoionization Phenomena in Atoms. *Moscow Univ. Press*, **1986,** 58-160
17. Glushkov, A.; Ivanov, L. Radiation decay of atomic states: atomic residue polarization and gauge noninvariant contributions. *Phys. Lett. A* **1992,** *170,* 33.
18. Glushkov, A.V. Spectroscopy of atom and nucleus in a strong laser field: Stark effect and multiphoton resonances. *J. Phys.: Conf. Ser*. **2014**, *548*, 012020
19. Khetselius, O.Yu. Spectroscopy of cooperative electron-gamma-nuclear processes in heavy atoms: NEET effect. *J. Phys.: Conf. Ser.* **2012,** *397,* 012012.
20. Glushkov A.V.; Ivanov, L.N. DC strong-field Stark effect: consistent quantum-mechanical approach. *J. Phys. B: At. Mol. Opt. Phys.* **1993,** *26,* L379-386.
21. Ignatenko, A.V. Probabilities of the radiative transitions between Stark sublevels in spectrum of atom in an DC electric field: New approach. *Photoelectronics,* **2007,** *16*, 71-74.
22. Glushkov, A.V.; Ambrosov, S.V.; Ignatenko, A.V. Non-hydrogenic atoms and Wannier-Mott excitons in a DC electric field: Photoionization, Stark effect, Resonances in ionization continuum and stochasticity. *Photoelectronics,* **2001,** *10*, 103-106.
23. Glushkov A., Ternovsky V., Buyadzhi V., Prepelitsa G., Geometry of a relativistic quantum chaos: New approach to dynamics of quantum systems in electromagnetic field and uniformity and charm of a chaos. *Proc. Intern. Geom. Center*. **2014,** *7*(4), 60-71.
24. Khetselius, O.Yu. Relativistic perturbation theory calculation of the hyperfine structure parameters for some heavy-element isotopes. *Int. Journ.Quant.Chem.* **2009,** *109,* 3330-3335.
25. Khetselius, O. Hyperfine structure of radium. *Photoelectronic*. **2005,** *14,* 83-85.

PACS 31.15.-p

V. V. Buyadzhi

ELECTRON-COLLISIONAL SPECTROSCOPY OF ATOMS AND IONS: ADVANCED ENERGY APPROACH

Summary. An advanced relativistic energy approach combined with a scattering theory is used to calculate the electron-collision excitation cross-sections, collision strengths for a number of multicharged ions. The relativistic many-body perturbation theory is used alongside the gauge-invariant scheme to generate an optimal Dirac-Kohn-Sham- Debye-Hückel one-electron representation. The results of relativistic calculation (taking into account the exchange and correlation corrections) of the electron-collision cross-sections (strengths) of excitation of the transition between the fine-structure levels ($2P_{3/2}$- $2P_{1/2}$) of the ground state of F-like ions with Z = 19-26 and of the [$2s^2\,{}^1S$ -($2s2p\,{}^1P$)] transition in the B-like O^{4+} are presented and analysed

Key words: spectroscopy of ions, relativistic energy approach, collision cross-sections

PACS 31.15.-p

В. В. Буяджи

ЭЛЕКТРОН-СТОЛКНОВИТЕЛЬНАЯ СПЕКТРОСКОПИЯ АТОМОВ И ИОНОВ: РЕЛЯТИВИСТСКИЙ ЭНЕРГЕТИЧЕСКИЙ ПОДХОД

Резюме. Эффективный релятивистский энергетический подход в сочетании с теорией столкновений используется для расчета сечений электрон-столкновительного возбуждения, сил столкновений для ряда многозарядных ионов. Релятивистская теория многочастичная теория возмущений наряду с эффективной калибровочно-инвариантной схемой используется для генерации оптимального одноэлектронного представления Дирака-Кона-Шама-Дебая-Хюккеля. Представлены и анализируются результаты расчета (с учетом обменных и корреляционных поправок) сечений столкновительного возбуждения перехода между уровнями тонкой структуры ($2P_{3/2}$- $2P_{1/2}$) F-подобных ионов и возбуждения перехода [$2s^2\,{}^1S$ -($2s2p\,{}^1P$)] в Be-подобном O^{4+}.

Ключевые слова: спектроскопия ионов, энергетический подход, сечения столкновений

PACS 31.15.-p

В. В. Буяджи

СПЕКТРОСКОПІЯ ЗА РАХУНОК ЕЛЕКТРОННИХ ЗІТКНЕНЬ АТОМІВ І ИОНОВ: РЕЛЯТИВІСТСЬКИЙ ЕНЕРГЕТИЧНИЙ ПІДХІД

Резюме. Ефективний релятивістський енергетичний підхід в поєднанні з теорією зіткнень використовується для розрахунку перетинів електрон-зіткнень збудження, сил зіткнень для ряду багатозарядних іонів. Релятивістська теорія багаточастинкових теорія збурень використовується для генерації оптимального одноелектронного уявлення Дірака-Кона-Шама-Дебая-Хюккеля. Представлені і аналізуються результати розрахунку (з урахуванням обмінних і кореляційних поправок) перерізів збудження за рахунок зіткнення переходу між рівнями тонкої структури ($2P_{3/2}$- $2P_{1/2}$) F-подібних іонів і збудження переходу [$2s^2\,{}^1S$ -($2s2p\,{}^1P$)] в Be-подібному O^{4+}.

Ключові слова: спектроскопія іонів, енергетичний підхід, перерізи зіткнень

PACS 36.10.-k

Yu. V. Dubrovskaya, I. N. Serga, Yu. G. Chernyakova, L. A. Vitavetskaya

Odessa State Environmental University, L'vovskaya str., 15, Odessa, 65016, Ukraine
E-mail: dubrovskayayv@gmail.com

RELATIVISTIC THEORY OF SPECTRA OF PIONIC AND KAONIC ATOMS: HYPERFINE STRUCTURE, TRANSITION PROBABILITIES FOR NITROGEN

A new theoretical approach to energy and spectral parameters of the hadronic (pionic and kaonic) atoms in the excited states with precise accounting for the relativistic, radiation and nuclear effects is applied to the study of radiation parameters of transitions between hyperfine structure components of the pionic and kaonic nitrogen. The advanced data on the probabilities of radiation transitions between components of the hyperfine structure transitions 5g-4f, 5f-4d in the spectrum of pionic nitrogen and 8k-7i, 8i-7h in the spectrum of kaonic nitrogen are presented and compared with alternative theoretical data.

1. Introduction

Our work is devoted to the further application of earlier developed new theoretical approach [1-8] to the description of spectra and different spectral parameters, in particular, radiative transitions probabilities for hadronic (pionic and kaonic) atoms in the excited states with precise accounting for the relativistic, nuclear and radiative effects. As it was indicated earlier [7-12] nowadays investigation of the pionic, kaonic and at whole the exotic hadronic atomic systems represents a great interest as from the viewpoint of the further development of atomic and nuclear spectral theories as creating new tools for sensing the nuclear structure and fundamental hadron-nucleus strong interactions [6-14]. Spectroscopy of hadronic atoms already in the electromagnetic sector is extremely valuable area of research that provide unique data for different areas of physics, including nuclear, atomic, molecular physics, physics of particles, sensor electronic etc. It should be emphasized that the theory of pion spectra of atoms are highly excited, even in the electromagnetic sector (ie short-range strong pion-N interaction neglects little) is extremely complex and at present, despite the known progress remains very poorly developed. It is about the fundamental theoretical problems describing relativistic atoms considering nuclear, radiation effects, and a completely insufficient spectral data for pion atoms. While determining the properties of pion atoms in theory is very simple as a series of H such models and more sophisticated methods such combination chiral perturbation theory (TC), adequate quantitative description of the spectral properties of atoms in the electromagnetic pion sector (not to mention even the strong interaction sector) requires the development of High-precision approaches, which allow you to accurately describe the role of relativistic, nuclear, radiation QED (primarily polarization electron-positron vacuum, etc.). pion effects in the spectroscopy of atoms.

The most popular theoretical models for pionic and kaonic atoms are naturally based on the using the Klein-Gordon-Fock equation, but there are many important problems connected with accurate accounting for as pion-kaon-nuclear strong interaction effects as QED radiative corrections (firstly, the vacuum polarization effect etc.). This topic has been a subject of intensive theoretical and experimental interest (see [1-16]). The perturbation theory expansion on the physical; parameter aZ is usually used to take into account the radiative QED corrections, first of all, effect of the polarization of electron-positron vacuum etc. This approximation is sufficiently correct and comprehensive in a case of the light pionic atoms, however it becomes incorrect in a case of the heavy atoms with large charge of a nucleus Z.

The more correct accounting of the QED, finite nuclear size and electron-screening effects

for pionic atoms is also very serious and actual problem to be solved more consistently in comparison with available theoretical models and schemes. At last, a development of the comprehensive theory of hyperfine structure and computing radiative transitions probabilities between its components is of a great interest and importance in a modern theory of the hadronic atom spectra [1-39].

2. Theory

The basic topics of our theoretical approach have been earlier presented [3-8,27,28], so here we are limited only by the key elements. The relativistic dynamic of a spinless boson (pion) particle is described by the Klein-Gordon-Fock (KGF) equation. As usually, an electromagnetic interaction between a negatively charged pion and the atomic nucleus can be taken into account introducing the nuclear potential A_ν in the KG equation via the minimal coupling $p_\nu \rightarrow p_\nu - qA_\nu$. Generally speaking, the Klein-Gordon-Fock equation can be rewritten as the corresponding two-component equation :

$$[-(\sigma_3 + i\sigma_2)\frac{\nabla^4}{2\mu} + \sigma_3\mu + (\sigma_3 + i\sigma_2)V_{opt}^{(0)} + V_C^{(0)}]\Psi_i = E_i\Psi_i, \quad (1)$$

where s_i are the Pauli spin matrices and

$$\Psi_i = \frac{1}{2}\begin{pmatrix} (1 + (E - V_C^{(0)})/\mu)\phi_i \\ (1 - (E - V_C^{(0)})/\mu)\phi_i \end{pmatrix}. \quad (2)$$

This equation is equivalent to the stationary Klein-Gordon-Fock equation. The corresponding non-stationary Klein-Gordon-Fock equation can be written as follows:

$$\mu^2 c^2 \Psi(x) = \{\frac{1}{c^2}[i\hbar\partial_t + eV_0(r)]^2 + \hbar^2\nabla^2\}\Psi(x) \quad (3)$$

where c is the speed of light, *h* is the Planck constant, *m* is the reduced mass of the pion-nuclear system, and $\Psi_0(x)$ is the scalar wave function of the space-temporal coordinates. Usually one considers the central potential $[V_0(r), 0]$ approximation with the stationary solution:

$$\Psi(x) = \exp(-iEt/\hbar)\phi(x), \quad (4)$$

where $\phi(x)$ is the solution of the equation:

$$\{\frac{1}{c^2}[E + eV_0(r)]^2 + \hbar^2\nabla^2 - \mu^2 c^2\}\phi(x) = 0 \quad (5)$$

Here *E* is the total energy of the system (sum of the mass energy mc^2 and binding energy e_0). In principle, the central potential V_0 is the sum of the following potentials: the electric potential of a nucleus, vacuum-polarization potential. The strong interaction potential can be added below. Generally speaking, an energy of the pionic atomic system can be represented as the following sum:

$$E \approx E_{KG} + E_{FS} + E_{QED} + E_N, \quad (6)$$

where E_{KG} is the energy of a pion in a nucleus (Z, A) with the point-like charge, E_{FS} is the contribution due to the nucleus finite size effect, E_{VP} is the radiation QED correction, E_N is the energy shift due to the strong (pion- or kaon- nuclear) interaction V_N. In principle, the central potential V_0 should include the central Coulomb potential, the radiative (in particular, vacuum-polarization) potential as well as the electron-screening potential in the atomic-optical (electromagnetic) sector. Surely, the full solution of the pionic atom energy especially for the low-excited state requires an inclusion the hadron-nuclear strong potential.

The next step is accounting the nuclear finite size effect or the Breit-Rosenthal-Crawford-Schawlow one. In order to do it we use the widespread Gaussian model for nuclear charge distribution. The advantages of this model in comparison with usually used models such as for example an uniformly charged sphere model and others had been analysed in Ref. [3]. Usually the Gauss model is determined as follows:

$$\rho(r|R) = (4\gamma^{3/2}/\sqrt{\pi})\exp(-\gamma r^2), \quad (7)$$

where $\gamma = 4\pi/R^2$, R is an effective radius of a nucleus.

In order to take into account very important radiation QED effects we use the radiative potential from the Flambaum-Ginges theory [15]. In includes the standard Ueling-Serber

potential and electric and magnetic form-factors plus potentials for accounting of the high order QED corrections such as:

$$\Phi_{rad}(r) = \Phi_U(r) + \Phi_g(r) + \Phi_f(r) + .$$

$$+ \Phi_l(r) + \frac{2}{3}\Phi_U^{high-order}(r) \qquad (8)$$

where

$$\Phi_U^{high-order}(r) = -\frac{2\alpha}{3\pi}\Phi(r)\frac{0.092Z^2\alpha^2}{1+(1.62r/r_C)^4}.$$

$$\Phi_l(r) = -\frac{B(Z)}{e}Z^4\alpha^5 mc^2 e^{-Zr/a_B} \qquad (9)$$

Here e – a proton charge and universal function $B(Z)$ is defined by expression: $B(Z)$=0.074+0.35Za.

At last to take into account the electron screening effect we use the standard procedure, based on addition of the total interaction potential SCF potential of the electrons, which can be determined within the Dirac-Fock method by solution of the standard relativistic Dirac equations. It should be noted however, that contribution of theses corrections is practically zeroth for the pionic nitrogen, however it can be very important in transition to many-electron as a rule heavy hadronic atoms.

Further in order to calculate probabilities of the radiative transitions between energy level of the pionic atoms we have used the well-known relativistic energy approach (c. g.[16-28]). Other details are in Refs. [4,7,8].

3. Results and conclusions

As example of application of the presented approach, in table 1 we present the data on radiative transition probabilities (in s^{-1}) for hyperfine transitions 5g-4f in the spectrum of the pion nitrogen): Th1- data by Trassinelli-Indelicato; Th2- our data.

Table 1.

The radiative transition probabilities (in s^{-1}) for hyperfine transitions 5g-4f in the spectrum of the pion nitrogen: Th1- data by Trassinelli-Indelicato; Th2- our data

F-F’	T.I : P (5g-4f)	T.II : P (5g-4f)
5-4	7.13×10^{13}	7.04×10^{13}
4-3	5.47×10^{13}	5.41×10^{13}
4-4	5.27×10^{13}	5.23×10^{13}
3-2	4.17×10^{13}	4.12×10^{13}
3-3	0.36×10^{13}	0.34×10^{13}
3-4	0.01×10^{13}	0.009×10^{13}

In theory by Trassinelli-Indelicato (look, for example, [6]) it has been used the standard atomic spectroscopy amplitude scheme when the transitions energies and probabilities are calculated in the known degree separately. At the same time this computing within the relativistic energy approach is performed more correctly and self-consistently (look details in [4,9] and Refs. therein).

In table 2 we present our data for radiative transition probabilities (in s^{-1}) for hyperfine transitions 5f-4d in the spectrum of the pionic nitrogen: our data.

In table 3 we present the data on radiative transition probabilities (in s^{-1}) for the hyperfine transitions 8k-7i in the spectrum of the kaonic nitrogen atom: Th1- the data by Trassinelli-Indelicato; Th2 - our data.

Table 2.

Radiative transition probabilities (s^{-1}) for hyperfine transitions 5f-4d in the spectrum of the pioniv nitrogen: our data

F-F’	Our data (5f-4d)
4-3	4.57×10^{13}
3-2	3.16×10^{13}
3-3	2.98×10^{13}
2-1	2.13×10^{13}
2-2	2.25×10^{13}
2-3	0.01×10^{13}

Table 3.

The radiative transition probabilities (in s^{-1}) for the 8k-7i transition in the k-N atom: Th1- Trassinelli-Indelicato; Th2- our data

F-F'	TI, P	T.II: our data
8-7	1.54×10^{13}	1.51×10^{13}
7-6	1.33×10^{13}	1.32×10^{13}
7-7	1.31×10^{13}	1.29×10^{13}
6-5	1.15×10^{13}	1.12×10^{13}
6-6	0.03×10^{13}	0.02×10^{13}
6-7	0.00×10^{13}	0.004×10^{13}

In table 4 we present our data for radiative transition probabilities (in s^{-1}) for hyperfine transitions 8i-7h in the spectrum of the kaonic nitrogen: our data. In whole, the computed radiative transition probabilities values for considered transitions between hyperfine structure components in the spectrum of the pion within theory by Trassinelli-Indelicato and ours demonstrate physically reasonable agreement, however our values are a little lower.

This circumstance fact can be reasonably explained by difference in the computing schemes and different level of accounting for nuclear finite size, QED and other effects (c.g. [1-3,20,21]). In any case the data obtained can be considered as sufficiently accurate ones and used in the corresponding applications, indicated in the introduction.

Table 4.

Radiative transition probabilities (in s^{-1}) for hyperfine transitions 8i-7h in spectrum of the kaonic nitrogen: our data

F-F'	Our data (8i-7h)
7-6	1.16×10^{13}
6-5	0.99×10^{13}
6-6	0.96×10^{13}
5-4	0.81×10^{13}
5-5	0.02×10^{13}
5-6	0.005×10^{13}

References

1. Khetselius, O.Yu. Relativistic perturbation theory calculation of the hyperfine structure parameters for some heavy-element isotopes. *Int. J. Quant. Chem.* **2009,** *109,* 3330–3335.
2. Khetselius, O. Relativistic calculation of the hyperfine structure parameters for heavy elements and laser detection of the heavy isotopes. *Phys. Scripta* **2009,** *135,* 014023.
3. Khetselius, O. *Hyperfine structure of atomic spectra*; Astroprint: Odessa, **2008**.
4. Dubrovskaya, Yu., Khetselius, O.Yu., Vitavetskaya, L., Ternovsky, V., Serga, I. Quantum chemistry and spectroscopy of pionic atomic systems with accounting for relativistic, radiative, and strong interaction effects. *Adv. in Quantum Chem.* **2019,** *78,* 193-222.
5. Khetselius, O.Yu., Glushkov, A.V., Dubrovskaya, Yu.V., Chernyakova, Yu.G., Ignatenko, A.V., Serga, I.N., Vitavetskaya, L. Relativistic quantum chemistry and spectroscopy of exotic atomic systems with accounting for strong interaction effects. In: Wang YA, Thachuk M, Krems R, Maruani J (eds) Concepts, Methods and Applications of Quantum Systems in Chemistry and Physics. Springer, Cham, **2018**; Vol. 31, pp. 71-91.
6. Serga, I.N.; Dubrovskaya, Yu.V.; Kvasikova, A.S.; Shakhman, A.N; Sukharev, D.E. Spectroscopy of hadronic atoms: Energy shifts. *J. Phys.: Conf. Ser*. **2012,** *397***,** 012013.
7. Serga, I.N.; Khetselius, O.Yu.; Vitavetskaya, L.A.; Bystryantseva A.N. Relativistic theory of spectra of pionic atomic systems ^{208}Pb with account of strong pion-nuclear interaction effects. *Photoelectronics*. **2017**, *26*, 68-77.
8. Sukharev, D.E.; Khetselius, O.Yu.; Dubrovskaya, Yu.V. Sensing strong interaction effects in spectroscopy of hadronic atoms. *Sensor Electr. and Microsyst. Techn*. **2009**, *N3*, 16-21.
9. Khetselius, O.Yu. *Quantum structure of electroweak interaction in heavy finite Fermi-systems*. Astroprint: Odessa, **2011**.
10. Khetselius, O.Y.., Glushkov, A.V., Gurskaya, M.Y., Kuznetsova, A.A., Dubrovs-

kaya, Yu.V., Serga, I.N., Vitavetskaya, L.A. Computational modelling parity nonconservation and electroweak interaction effects in heavy atomic systems within the nuclear-relativistic many-body perturbation theory. *J. Phys.: Conf. Ser.* **2017,** *905*(1), 012029.
11. Batty, C.; Eckhause, M.; Gall, K. et al. Strong interaction effects in high-Z K^- atoms. *Phys. Rev. C.* **1989,** *40,* 2154.
12. Erikcson, M.; Ericson, T. Optical Properties of Low Energy Pions in Nuclei. *Ann. Phys.* **1966,** *36,* 323.
13. Batty, C J.; Friedman, E.; Gal, A. Saturation effects in pionic atoms and the π−-nucleus optical potential. *Nucl. Phys. A.* **1983,** *402,* 411-428.
14. Indelicato, P. Relativistic effects in few-electron heavy ions. Ab initio evaluation of levels energy and transitions probabilities. *Phys. Scripta* **1996,** *65,* 57.
15. Flambaum, V.; Ginges J. Radiative potential and calculation of QED radiative corrections to energy levels and electromagnetic amplitudes in many-electron atoms. *Phys. Rev.A*. **2005**, *72*, 052115.
16. Glushkov A.V., Malinovskaya S.V., Svinarenko A.A., Vitavetskaya L.A., Sensing spectral hierarchy, quantum chaos, chaotic diffusion and dynamical stabilisation effects in a multi- photon atomic dynamics with intense laser field. *Sensor Electr. and Microsyst. Techn*. **2005**, *2*(2), 29-35.
17. Mohr, P.J. Quantum Electrodynamics Calculations in few-Electron Systems. *Phys. Scripta*. **1993,** *46,* 44.
18. Rusov V., Glushkov A., Vaschenko V., Korchevsky D., Ignatenko A. Stochastic dynamics of the atomic systems in the crossed electric and magnetic field: the rubidium atom recurrence spectra. *Bull.of Kiev Nat. Univ.:Ser.Phys.-Math*. **2004**, N4, 433.
19. Glushkov, A.V. Spectroscopy of cooperative muon-gamma-nuclear processes: Energy and spectral parameters. *J. Phys.: Conf. Ser*. **2012,** *397,* 012011.
20. Gubanova, E.R., Glushkov, A.V., Khetselius, O.Yu., Bunyakova, Yu., Buyadzhi, V., Pavlenko, E. *New methods in analysis and project management of environmental activity: Electronic and radioactive waste*. Kharkiv, FOP**, 2017.**.
21. Khetselius, O.Yu., Lopatkin Yu.M., Dubrovskaya, Yu.V, Svinarenko A.A. Sensing hyperfine-structure, electroweak interaction and parity non-conservation effect in heavy atoms and nuclei: New nuclear-QED approach. *Sensor Electr. and Microsyst. Techn*. **2010,** *7*(2), 11-19.
22. Bystryantseva A., Khetselius O.Yu., Dubrovskaya Yu., Vitavetskaya L.A., Berestenko A.G. Relativistic theory of spectra of heavy pionic atomic systems with account of strong pion-nuclear interaction effects: ^{93}Nb, ^{173}Yb, ^{181}Ta , ^{197}Au. *Photoelectronics*. **2016**, *25*, 56-61.
23. Glushkov, A.V. *Relativistic Quantum theory. Quantum mechanics of atomic systems*; Astroprint: Odessa, **2008**.
24. Kuznetsova A.A., Vitavetskaya L.A., Chernyakova Yu.G., Korchevsky D., Calculating the radiative vacuum polarization contribution to the energy shift of 2p-3s transition in pionic deuterium. *Photoelectronics.* **2013**, *22*, 108-111.
25. Glushkov, A.V.; Khetselius, O.Yu.; Svinarenko, A.A.; Buyadzhi, V.V. *Spectroscopy of autoionization states of heavy atoms and multiply charged ions*. Odessa: TEC**, 2015**.
26. Glushkov, A.V. Spectroscopy of atom and nucleus in a strong laser field: Stark effect and multiphoton Resonances. *J. Phys.: Conf. Ser*. **2014**, 548, 012020.
27. Khetselius, O.Yu. Atomic parity non-conservation effect in heavy atoms and observing P and PT violation using NMR shift in a laser beam: To precise theory. *J. Phys.: Conf. Ser.* **2009,** *194,* 022009.
28. Khetselius, O. Relativistic hyperfine structure spectral lines and atomic parity nonconservation effect in heavy atomic systems within QED theory. *AIP Conf. Proc.* **2010,** *1290,* 29–33.
29. Chernyakova, Y.G., Vitavetskaya L., Bashkaryov, P., Serga I., Berestenko, A. The radiative vacuum polarization contribution to the energy shift of some levels of the pionic hydrogen. *Photoelectronic*s **2015**, *24,*

122-127.
30. Glushkov, A., Gurskaya, M., Ignatenko, A., Smirnov, A., Serga, I., Svinarenko, A., Ternovsky, E. Computational code in atomic and nuclear quantum optics: Advanced computing multiphoton resonance parameters for atoms in a strong laser field. *J. Phys.: Conf. Ser*. **2017**, *905*(1), 012004.
31. Ambrosov S., Ignatenko V., Korchevsky D., Kozlovskaya V. Sensing stochasticity of atomic systems in crossed electric and magnetic fields by analysis of level statistics for continuous energy spectra. *Sensor Electr. and Microsyst. Techn*. **2005**, Issue 2, 19-23.
32. Glushkov, A.V. *Relativistic and correlation effects in spectra of atomic systems;* Astroprint: **2006.**
33. Chernyakova, Y.G., Ignatenko A.V., Vitavetskaya L.A., Sensing the tokamak plasma parameters by means high resolution x-ray theoretical spectroscopy method: new scheme. *Sensor Electr. and Microsyst. Techn*. **2004**, *1*, 20-24.
34. Glushkov, A.V., Malinovskaya, S.V., Dubrovskaya, Yu.V., Sensing the atomic chemical composition effect on the beta decay probabilities. *Sensor Electr. and Microsyst. Techn*. **2005**, *2*(1), 16-20.
35. Glushkov, A.V., Khetselius, O.Yu., Svinarenko, A.A., Buyadzhi, V.V. *Methods of computational mathematics and mathematical physics. P.1*. Odessa: TES, **2015**.
36. Svinarenko,A.A.,Glushkov,A.V.,Khetselius, O.Yu., Ternovsky,V.B., Dubrovskaya, Yu., Kuznetsova, A., Buyadzhi, V. Theoretical spectroscopy of rare-earth elements: spectra and autoionization resonances. *Rare Earth Element*, Ed. J. Orjuela (InTech) **2017**, pp 83-104
37. Glushkov, A.V., Khetselius, O.Yu., Svinarenko A.A., Buyadzhi, V.V., Ternovsky, V.B, Kuznetsova, A., Bashkarev, P Relativistic perturbation theory formalism to computing spectra and radiation characteristics: application to heavy element. *Recent Studies in Perturbation Theory*, ed. D. Uzunov (InTech) **2017**, 131-150.
38. Danilov, V., Kruglyak, Y., Pechenaya, V. Electron density-bond order matrix and the spin density in the restricted CI method. *Theor. Chim Acta*. **1969**, *13*(4), 288-296.
39. Glushkov, A.V., Safranov, T.A., Khetselius, O.Yu., Ignatenko, A.V., Buyadzhi, V.V., Svinarenko, A.A. Analysis and forecast of the environmental radioactivity dynamics based on methods of chaos theory: General conceptions. *Environm. Problems*. **2016**, *1*(2), 115-120.

PACS 36.10.-k

Yu. V. Dubrovskaya, I. N. Serga, Yu. G. Chernyakova, L. A. Vitavetskaya

RELATIVISTIC THEORY OF SPECTRA OF PIONIC AND KAONIC ATOMS: HYPERFINE STRUCTURE, TRANSITION PROBABILITIES FOR NITROGEN

Summary. A new theoretical approach to energy and spectral parameters of the hadronic (pionic and kaonic) atoms in the excited states with precise accounting for the relativistic, radiation and nuclear effects is applied to the study of radiation parameters of transitions between hyperfine structure components of the pionic and kaonic nitrogen. The advanced data on the probabilities of radiation transitions between components of the hyperfine structure transitions 5g-4f, 5f-4d in the spectrum of pionic nitrogen and 8k-7i, 8i-7h in the spectrum of kaonic nitrogen are presented and compared with alternative theoretical data**.**

Keywords: relativistic theory, hyperfine structure, hadronic atoms

PACS 36.10.-k

Ю. В. Дубровская, И. Н. Серга, Ю. Г. Чернякова, Л. А. Витавецкая

РЕЛЯТИВИСТСКАЯ ТЕОРИЯ СПЕКТРОВ ПИОННЫХ И КАОННЫХ АТОМОВ СВЕРХТОНКАЯ СТРУКТУРА, ВЕРОЯТНОСТИ ПЕРЕХОДОВ ДЛЯ АЗОТА

Резюме. Новый теоретический подход к описанию энергетических и спектральных параметров адронного (пионного и каонного) атомов в возбужденных состояниях с аккуратным учетом релятивистских, радиационных и ядерных эффектов применяется к изучению характеристик радиационных переходов между компонентами сверхтонкой структуры пионного и каонного атомов азота. Представлены уточненные данные о вероятностях радиационных переходов между компонентами сверхтонких структурных переходов 5g-4f, 5f-4d в спектре пионного азота и 8k-7i, 8i-7h в спектре каонного азота, некоторые из которых сравниваются с альтернативными теоретическими данными.

Ключевые слова: релятивистская теория, сверхтонкая структура, адронные атомы

PACS 36.10.-k

Ю. В. Дубровська, І. М. Сєрга, Ю. Г. Чернякова, Л. А. Вітавецька

РЕЛЯТИВІСТСЬКА ТЕОРІЯ СПЕКТРІВ ПІОННИХ ТА КАОННИХ АТОМІВ: НАДТОНКА СТРУКТУРА, ЙМОВІРНОСТІ ПЕРЕХОДІВ ДЛЯ АЗОТА

Резюме. Новий теоретичний підхід до опису енергетичних і спектральних параметрів адронних (піонних і каонних) атомів в збуджених станах з акуратним урахуванням релятивістських, радіаційних і ядерних ефектів застосовується до вивчення характеристик радіаційних переходів між компонентами надтонкої структури піонного і каонов атомів азоту. Представлені уточнені дані про ймовірності радіаційних переходів між компонентами надтонкої структури, зокрема, переходів 5g-4f, 5f-4d в спектрі піонного азоту і 8k-7i, 8i-7h в спектрі каонного азоту, деякі з яких порівнюються з альтернативними теоретичними даними.

Ключові слова: релятивістська теорія, надтонка структура, адронні атоми

PACS 32.30.-r

A. V. Glushkov, I. S. Cherkasova, V. B. Ternovsky, A. A. Svinarenko

Odessa State Environmental University, L'vovskaya str.15, Odessa, 65016
E-mail: svinarenkoaa@gmail.com

THEORETICAL STUDYING SPECTRAL CHARACTERISTICS OF Ne-LIKE IONS ON THE BASIS OF OPTIMIZED RELATIVISTIC MANY-BODY PERTURBATION THEORY

Theoretical studying spectroscopic characteristics of the Ne-like multicharged ions is carried out within the relativistic many-body perturbation theory and generalized relativistic energy approach. The zeroth approximation of the relativistic perturbation theory is provided by the optimized Dirac-Kohn-Sham ones. Optimization has been fulfilled by means of introduction of the parameter to the Kohn-Sham exchange potentials and further minimization of the gauge-non-invariant contributions into radiation width of atomic levels with using relativistic orbital set, generated by the corresponding zeroth approximation Hamiltonian.

1. Introduction

It is well known that the correct data about different radiation, energetic and spectroscopic characteristics of the multielectron atoms and multicharged ions, namely, radiative decay widths, probabilities and oscillator strengths of atomic transitions, excitation and ionization cross-sections are needed in astrophysics and laboratory, thermonuclear plasma diagnostics and in fusion research. In this light, studying the spectral characteristics of the alkali elements attracts a special interest. There have been sufficiently many reports of calculations and compilation of energies and oscillator strengths for these atoms and corresponding ions (see, for example, [1–28]). In many papers the standard Hartree-Fock, Dirac-Fock methods, model potential approach, quantum defect approximation etc in the different realizations have been used for calculating energies and oscillator strengths. However, it should be stated that for the heavy alkali atoms (such as caesium and francium and corresponding ions) and particularly for their high-excited (Rydberg) states, there is not enough precise information available in literature. The multi-configuration Dirac-Fock method is the most reliable version of calculation for multielectron systems with a large nuclear charge. In these calculations the one- and two-particle relativistic and important exchange-correlation corrections are taken into account (see Refs. [1] and Refs. therein). However, one should remember about very complicated structure of spectra of the lanthanides atoms and necessity of correct accounting for different correlation effects such as polarization interaction of the valent quasiparticles and their mutual screening, iterations of a mass operator etc.).The known method of the model relativistic many-body perturbation theory (RMBPT) has been earlier effectively applied to computing spectra of low-lying states for some lanthanides atoms [5-11] (see also [12-22]). We use an analogous version of the perturbation theory (PT) to study spectroscopic characteristics of some Ne-like ions.

2. Advanced relativistic many-body perturbation theory and energy approach

As the method of computing is earlier presented in detail, here we are limited only by the key topics [5-15]. Generally speaking, the majority of complex atomic systems possess a dense energy spectrum of interacting states with essentially relativistic properties. In the theory of the non-relativistic atom a convenient field procedure is known for calculating the energy shifts ΔE of degenerate states. This procedure is connected with the secular matrix M diagonalization [12-22]. In constructing M, the Gell-Mann and Low adiabatic formula for ΔE

is used. In contrast to the non-relativistic case, the secular matrix elements are already complex in the second order of the electrodynamical PT (first order of the interelectron interaction). Their imaginary part of ΔE is connected with the radiation decay (radiation) possibility. In this approach, the whole calculation of the energies and decay probabilities of a non-degenerate excited state is reduced to the calculation and diagonalization of the complex matrix *M*. In the papers of different authors, the $\mathrm{Re}\,\Delta E$ calculation procedure has been generalized for the case of nearly degenerate states, whose levels form a more or less compact group. One of these variants has been previously introduced: for a system with a dense energy spectrum, a group of nearly degenerate states is extracted and their matrix *M* is calculated and diagonalized. If the states are well separated in energy, the matrix *M* reduces to one term, equal to ΔE. The non-relativistic secular matrix elements are expanded in a PT series for the interelectron interaction. The complex secular matrix *M* is represented in the form [12-14]:

$$M = M^{(0)} + M^{(1)} + M^{(2)} + M^{(3)}. \qquad (1)$$

where $M^{(0)}$ is the contribution of the vacuum diagrams of all order of PT, and $M^{(1)}$, $M^{(2)}$, $M^{(3)}$ those of the one-, two- and three-quasiparticle diagrams respectively. $M^{(0)}$ is a real matrix, proportional to the unit matrix. It determines only the general level shift. We have assumed $M^{(0)} = 0$. The diagonal matrix $M^{(1)}$ can be presented as a sum of the independent one-quasiparticle contributions. For simple systems (such as alkali atoms and ions) the one-quasiparticle energies can be taken from the experiment. Substituting these quantities into (1) one could have summarized all the contributions of the one -quasiparticle diagrams of all orders of the formally exact QED PT. However, the necessary experimental quantities are not often available. The first two order corrections to $\mathrm{Re}\,M^{(2)}$ have been analyzed previously using Feynman diagrams (look Ref. in [1,2]). The contributions of the first-order diagrams have been completely calculated. In the second order, there are two kinds of diagrams: polarization and ladder ones. The polarization diagrams take into account the quasiparticle interaction through the polarizable core, and the ladder diagrams take into account the immediate quasiparticle interaction [11-20]. Some of the ladder diagram contributions as well as some of the three-quasiparticle diagram contributions in all PT orders have the same angular symmetry as the two-quasiparticle diagram contributions of the first order. These contributions have been summarized by a modification of the central potential, which must now include the screening (anti-screening) of the core potential of each particle by the two others. The additional potential modifies the one-quasiparticle orbitals and energies. Then the secular matrix is as follows [1,2]:

$$M \to \tilde{M}^{(1)} + \tilde{M}^{(2)}, \qquad (2)$$

where $\tilde{M}^{(1)}$ is the modified one-quasiparticle matrix (diagonal), and $\tilde{M}^{(2)}$ is the modified two-quasiparticle one. $\tilde{M}^{(1)}$ is calculated by substituting the modified one-quasiparticle energies), and $\tilde{M}^{(2)}$ by means of the first PT order formulae for $M^{(2)}$, putting the modified radial functions of the one-quasiparticle states in the radial integrals..

Let us remind that in the QED theory, the photon propagator D(12) plays the role of this interaction. Naturally the analytical form of D(12) depends on the gauge, in which the electrodynamical potentials are written. Interelectron interaction operator with accounting for the Breit interaction has been taken as follows:

$$V(r_i r_j) = exp(i\omega r_{ij}) \cdot \frac{(1 - \alpha_i \alpha_j)}{r_{ij}}, \qquad (3)$$

where, as usually, α_i are the Dirac matrices. In general, the results of all approximate calculations depended on the gauge. Naturally

the correct result must be gauge-invariant. The gauge dependence of the amplitudes of the photo processes in the approximate calculations is a well known fact and is in details investigated by Grant, Armstrong, Aymar and Luc-Koenig, Glushkov-Ivanov et al (see reviews in [5-7] and Refs. therein). Grant has investigated the gauge connection with the limiting non-relativistic form of the transition operator and has formulated the conditions for approximate functions of the states, in which the amplitudes of the photo processes are gauge invariant [3]. Glushkov-Ivanov have developed a new relativistic gauge-conserved version of the energy approach [14]. In ref. [25, 29-35] it has been developed its further generalization. Here we applied this approach for generating the optimized relativistic orbitals basis in the zeroth approximation of the many-body PT. Optimization has been fulfilled by means of introduction of the parameter to the Fock and Kohn-Sham exchange potentials and further minimization of the gauge-non-invariant contributions into radiation width of atomic levels with using relativistic orbital bases, generated by the corresponding zeroth approximation Hamiltonians. Other details can be found in Refs. [1-5,36-44].

3. Some results and conclusion

In tables 1 and 2 we present the values of probabilities of the transitions between levels of the configurations $2s^22p^53s,3d,4s,4d$ and $2s2p^63p,4p$ in the Ne-like ions of the Ni XIX, Br XXVI (in s^{-1}; total angle moment J=1): a – the MCDF method; b- relativistic PT with the empirical zeroth approximation (RPTMP); c1 – REA-PT data (without correlation corrections); c2 – REA-PT data (with an account for the correlation); exp.- experimental data (look [1-6] and Refs therein); This work -our data.

Table 1.

Probabilities of radiation transitions between levels of the configurations $2s^22p^53s,3d,4s,4d$ and $2s2p^63p,4p$ in the Ne-like ion of Ni XIX (in s^{-1}; total angle moment J=1): a – the MCDF method; b- relativistic PT with the empirical zeroth approximation (RPTMP); c1, c2 – REA PT data (without and with account for correlation effects); exp. - experiment; this work-our data (see text)

Level J=1	Exp.	a-MCDF	b-RPTMP
$2p_{3/2}3s_{1/2}$	7.6+11	9.5+11	1.3+12
$2p_{1/2}3s_{1/2}$	6.0+11	1.8+12	1.0+12
$2p_{3/2}3d_{3/2}$	1.4+11	2.2+11	1.5+11
$2p_{3/2}3d_{5/2}$	1.2+13	2.1+13	1.2+13
$2p_{1/2}3d_{3/2}$	3.2+13	4.8+13	3.6+13
$2s_{1/2}\ 3p_{1/2}$			8.5+11
$2s_{1/2}\ 3p_{3/2}$			5.1+12
$2p_{3/2}4s_{1/2}$	3.3+11		3.6+11
$2p_{1/2}4s_{1/2}$	2.0+11		3.0+11
$2p_{3/2}4d_{3/2}$	4.5+10		5.2+10
$2p_{3/2}4d_{5/2}$	8.3+12		8.3+12
$2p_{1/2}4d_{3/2}$	8.1+12		7.9+12
Level J=1	c1- REA PT	c2- REA PT	This work
$2p_{3/2}3s_{1/2}$	9.7+11	8.1+11	7.9+11
$2p_{1/2}3s_{1/2}$	7.6+11	6.2+11	6.1+11
$2p_{3/2}3d_{3/2}$	1.7+11	1.4+11	1.3+11
$2p_{3/2}3d_{5/2}$	1.5+13	1.2+13	1.1+13
$2p_{1/2}3d_{3/2}$	4.0+13	3.3+13	3.2+13
$2s_{1/2}\ 3p_{1/2}$	9.5+11	8.1+11	8.0+11
$2s_{1/2}\ 3p_{3/2}$	5.6+12	4.7+12	4.6+12
$2p_{3/2}4s_{1/2}$	4.1+11	3.4+11	3.3+11
$2p_{1/2}4s_{1/2}$	3.1+11	2.4+11	2.2+11
$2p_{3/2}4d_{3/2}$	5.4+10	4.8+10	4.6+10
$2p_{3/2}4d_{5/2}$	9.2+12	8.2+12	8.1+12
$2p_{1/2}4d_{3/2}$	8.9+12	8.0+12	8.0+12
$2s_{1/2}4p_{1/2}$	6.3+11	5.7+11	5.6+11
$2s_{1/2}4p_{3/2}$	2.7+12	2.4+12	2.3+12

Analysis of the data shows that the computational method used provides a

physically reasonable agreement between the theoretical and experimental data.

Table 2.

Probabilities of radiation transitions between levels of the configurations $2s^2 2p^5 3s,3d,4s,4d$ and $2s2p^6 3p,4p$ in the Ne-like ion of Br XXVI (in s^{-1}; total angle moment J=1): a – the DF method; b- RPTMP; c1,2 – REA PT data (without and with account for correlation effects); exp. - experiment; this -our data

Level J=1	Exp.	a-MCDF	b-RPTMP
$2p_{3/2}3s_{1/2}$	4.5+12	6.2+12	4.4+12
$2p_{1/2}3s_{1/2}$	3.1+12	4.8+12	2.8+12
$2p_{3/2}3d_{3/2}$	2.8+11	3.9+11	2.9+11
$2p_{3/2}3d_{5/2}$	6.1+13	8.0+13	6.3+13
$2p_{1/2}3d_{3/2}$	8.6+13	9.5+13	8.7+13
$2s_{1/2}\ 3p_{1/2}$	3.9+12		4.2+12
$2s_{1/2}\ 3p_{3/2}$	1.4+13		1.5+13
$2p_{3/2}4s_{1/2}$	1.1+12		1.2+12
$2p_{1/2}4s_{1/2}$	2.1+12		2.5+12
$2p_{3/2}4d_{3/2}$	2.8+10		7.3+10
$2p_{3/2}4d_{5/2}$			2.8+13
$2p_{1/2}4d_{3/2}$	2.0+13		2.2+13
$2s_{1/2}4p_{1/2}$	2.5+12		
$2s_{1/2}4p_{3/2}$	7.1+12		
Level J=1	c1-QED PT	c2-QED PT	This work
$2p_{3/2}3s_{1/2}$	5.5+12	4.4+12	4.3+12
$2p_{1/2}3s_{1/2}$	3.6+12	2.7+12	2.6+12
$2p_{3/2}3d_{3/2}$	3.5+11	2.8+11	2.7+11
$2p_{3/2}3d_{5/2}$	7.5+13	6.1+13	6.1+13
$2p_{1/2}3d_{3/2}$	9.9+13	8.6+13	8.5+13
$2s_{1/2}\ 3p_{1/2}$	4.7+12	4.0+12	3.9+12
$2s_{1/2}\ 3p_{3/2}$	1.8+13	1.4+13	1.3+13
$2p_{3/2}4s_{1/2}$	1.5+12	1.1+12	1.1+12
$2p_{1/2}4s_{1/2}$	2.8+12	2.3+12	2.2+12
$2p_{3/2}4d_{3/2}$	6.9+10	6.3+10	6.0+10
$2p_{3/2}4d_{5/2}$	2.7+13	2.3+13	2.2+13
$2p_{1/2}4d_{3/2}$	2.3+13	2.0+13	1.9+13
$2s_{1/2}4p_{1/2}$	2.9+12	2.6+12	2.5+12
$2s_{1/2}4p_{3/2}$	8.9+12	8.0+12	7.8+12

Let us note that the transition probabilities values in the different photon propagator gauges are practically equal. Besides, an account of the inter particle (electron) correlation effects is of a great importance.

References

1. Ivanova, E., Glushkov, A. Theoretical investigation of spectra of multicharged ions of F-like and Ne-like isoelectronic sequences. J. Quant. Spectr. and Rad. Tr. **1986**, *36*(2), 127-145.
2. Ivanova, E.P., Ivanov, L.N., Glushkov, A., Kramida, A. High order corrections in the relativistic perturbation theory with the model zeroth approximation, Mg-Like and Ne-Like Ions. *Phys. Scripta* **1985**, *32,* 513-522.
3. Safronova, U., Cowan, T., Safronova, M. Relativistic many-body calculations of electric-dipole lifetimes, transition rates and oscillator strengths for 2l−13l′ states in Ne-like ions. *J. Phys. B: At., Mol. and Opt. Phys*. **2005**, *38*(15), 2741–2763.
4. Glushkov, A.V., Khetselius, O.Yu., Svinarenko, A.A., Buyadzhi, V.V., *Spectroscopy of autoionization states of heavy atoms and multiply charged ions*. TEC: Odessa, **2015**.
5. Glushkov, A.V. *Relativistic Quantum theory. Quantum mechanics of atomic systems*. Astroprint: Odessa, **2008**.
6. Khetselius, O.Yu. *Hyperfine structure of atomic spectra*. Astroprint: **2008**.
7. Khetselius, O.Yu. *Quantum structure of electroweak interaction in heavy finite Fermi-systems*. Astroprint: Odessa, **2011**.
8. Glushkov, A.V. Operator Perturbation Theory for Atomic Systems in a Strong DC Electric Field. In Advances in Quantum Methods and Applications in Chemistry, Physics, and Biology. Springer: Cham, **2013,** 27, 161–177.
9. Buyadzhi, V., Zaichko P., Antoshkina, O., Kulakli T., Prepelitsa, P., Ternovsky, V., Mansarliysky V. Computing of radiation parameters for atoms and multicharged ions within relativistic energy approach:

Advanced Code. *J. Phys.: Conf. Ser*. **2017**, *905*(1), 012003.
10. Glushkov, A.V., Gurskaya, M.Yu., Ignatenko, A., Smirnov, A., Serga, I.N., Svinarenko, A., Ternovsky, E. Computational code in atomic and nuclear quantum optics: Advanced computing multiphoton resonance parameters for atoms in a strong laser field. *J. Phys: C Ser*. **2017**, *905*, 012004.
11. Svinarenko, A.A., Ternovsky, V.B., Cherkasova I., Mironenko D. Theoretical studying spectra of ytterbium atom on the basis of relativistic many-body perturbation theory: doubly excited states. *Photoelectr.* **2018**, 27, 113-120**.**
12. Ivanov, L.N., Ivanova, E.P., Knight, L. Energy approach to consistent QED theory for calculation of electron-collision strengths: Ne-like ions. *Phys. Rev. A.* **1993,** *48,* 4365-4374.
13. Glushkov, A., Ivanov, L., Ivanova, E.P. Autoionization Phenomena in Atoms. *Moscow Univ. Press*, Moscow, **1986,** 58.
14. Glushkov, A., Ivanov, L. Radiation decay of atomic states: atomic residue polarization and gauge noninvariant contributions. *Phys. Lett.A.***1992,** *170,* 33.
15. Glushkov A.V., Ivanov, L.N. DC strong-field Stark effect: consistent quantum-mechanical approach. *J. Phys. B: At. Mol. Opt. Phys.* **1993,** *26,* L379-386.
16. Glushkov, A.V. *Relativistic and Correlation Effects in Spectra of Atomic Systems*. Astroprint: **2006**.
17. Glushkov, A.V. Relativistic polarization potential of a many-electron atom. *Sov. Phys. Journal.* **1990**, *33(1)*, 1-4.
18. Glushkov, A.V. Advanced relativistic energy approach to radiative decay processes in multielectron atoms and multicharged ions. In *Quantum Systems in Chemistry and Physics*: *Progress in Methods and Applications.* Springer: Dordrecht, **2012,** 26, 231–252.
19. Glushkov, A.V. Energy approach to resonance states of compound superheavy nucleus and EPPP in heavy nuclei collisions. In Low Energy Antiproton Physics. AIP: New York, *AIP Conf. Proc*. **2005**, *796*, 206-210.
20. Glushkov, A. Spectroscopy of coope-rative muon-gamma-nuclear processes: Energy and spectral parameters *J. Phys.: Conf. Ser.* **2012,** *397,* 012011.
21. Khetselius O. Spectroscopy of cooperative electron-gamma-nuclear processes in heavy atoms: NEET effect *J. Phys.: Conf. Ser.* **2012,** *397,* 012012.
22. Glushkov, A.V. Spectroscopy of atom and nucleus in a strong laser field: Stark effect and multiphoton resonances. *J. Phys.: Conf. Ser*. **2014**, *548*, 012020
23. Glushkov, A., Svinarenko, A., Ternovsky, V., Smirnov, A., Zaichko, P. Spectroscopy of the complex auto ionization resonances in spectrum of helium. *Photoelectr*. **2015**, *24*, 94-102.
24. Glushkov, A. Multiphoton spectroscopy of atoms and nuclei in a laser field: Relativistic energy approach and radiate-on atomic lines moments method. *Adv. in Quantum Chem.* **2019**, *78*, 253-285.
25. Khetselius, O.Yu. Optimized relativistic many-body perturbation theory calculation of wavelengths and oscillator strengths for Li-like multicharged ions. Adv. Quant. Chem. **2019**, *78*, 223-251
26. Glushkov, A., Loboda, A., Gurnitskaya, E., Svinarenko, A. QED theory of radiation emission and absorption lines for atoms in a strong laser field. *Phys. Scripta.* **2009,** *T135,* 014022.
27. Florko, T.A., Tkach, T.B., Ambrosov, S.V., Svinarenko, A.A. Collisional shift of the heavy atoms hyperfine lines in an atmosphere of the inert gas. *J. Phys.: Conf. Ser*. **2012**, *397*, 012037.
28. Buyadzhi, V. Laser multiphoton spectro scopy of atom embedded in Debye plasmas: multiphoton resonances and transitions. *Photoelectr*. **2015,** *24,* 128.
29. Buyadzhi, V.V., Chernyakova, Yu.G., Smirnov, A.V., Tkach, T.B. Electron-collisional spectroscopy of atoms and ions in plasma: Be-like ions. *Photoelectronics*.

2016, *25,* 97-101.
30. Buyadzhi, V.V., Chernyakova, Yu.G., Antoshkina, O., Tkach, T. Spectroscopy of multicharged ions in plasmas: Oscillator strengths of Be-like ion Fe. *Photoelectronics*. **2017,** *26,* 94-102.
31. Khetselius, O.Yu. Relativistic Energy Approach to Cooperative Electron-γ-Nuclear Processes: NEET Effect. In Quantum Systems in Chem. and Phys., Springer: Dordrecht, **2012,** *26,* 217-229.
32. Svinarenko, A. Study of spectra for lanthanides atoms with relativistic many-body perturbation theory: Rydberg resonances. *J. Phys.: Conf. Ser.* **2014,** *548,* 012039.
33. Khetselius, O.Yu. Relativistic perturbation theory calculation of the hyperfine structure parameters for some heavy-element isotopes. *Int. Journ. Quant. Chem.* **2009,** *109,* 3330-3335.
34. Khetselius, O.Yu. Relativistic calculation of the hyperfine structure parameters for heavy elements and laser detection of the heavy isotopes. *Phys.Scripta.* **2009,** *135,* 014023.
35. Khetselius, O. Optimized perturbation theory for calculating the hyperfine line shift and broadening of heavy atoms in a buffer gas. In *Frontiers in Quantum Methods and Applications in Chemistry and Physics*. Springer, **2015,** 29, 55-76.
36. Svinarenko, A. A., Glushkov, A. V., Khetselius, O.Yu., Ternovsky, V.B., Dubrovskaya, Yu., Kuznetsova, A., Buyadzhi, V. Theoretical spectroscopy of rare-earth elements: spectra and autoionization resonances. *Rare Earth Element* (InTech). **2017**, pp 83-104.
37. Glushkov, A.V., Khetselius, O.Yu., Svinarenko, A.A., Buyadzhi, V.V., Ternovsky, V., Kuznetsova, A.A., Bashkarev P. Relativistic perturbation theory formalism to computing spectra and radiation characteristics: application to heavy element. *Recent Studies in Perturbation Theory.* InTech. **2017**, 131.
38. Glushkov A., Svinarenko, A., Ignatenko, A.V. Spectroscopy of autoionization resonances in spectra of the lanthanides atoms. *Photoelectr*. **2011**, *20*, 90-94.
39. Dubrovskaya, Yu., Khetselius, O.Yu., Vitavetskaya, L., Ternovsky, V., Serga, I. Quantum chemistry and spectroscopy of pionic atomic systems with accounting for relativistic, radiative, and strong interaction effects. *Adv. Quantum Chem.* **2019,** *78*, 193-222.
40. Khetselius, O.Yu., Glushkov, A.V., Dubrovskaya, Yu.V., Chernyakova, Yu., Ignatenko, A., Serga, I., Vitavetskaya, L. Relativistic quantum chemistry and spectroscopy of exotic atomic systems with accounting for strong interaction effects. In *Concepts, Methods and Applications of Quantum Systems in Chem. and Phys*. Springer, **2018,** *31*, 71.
41. Ambrosov S., Ignatenko V., Korchevsky D., Kozlovskaya V. Sensing stochasticity of atomic systems in crossed electric and magnetic fields by analysis of level statistics for continuous energy spectra. *Sensor Electr. and Microsyst. Techn*. **2005**, Issue 2, 19-23.
42. Glushkov, A., Buyadzhi, V., Kvasikova, A., Ignatenko, A., Kuznetsova, A., Prepelitsa, G., Ternovsky, V. Non-linear chaotic dynamics of quantum systems: Molecules in an electromagnetic field and laser systems. In: *Quantum Systems in Phys., Chem. and Biology*. Springer, Cham. **2017**, *30*, 169-180.
43. Glushkov A., Khetselius, O., Svinarenko A. Theoretical spectroscopy of auto ionization resonances in spectra of lanthanides atoms. *Phys. Scripta*. **2013**, *T153*, 014029.
44. Glushkov A., Khetselius O., Svinarenko A, Buyadzhi V, *Methods of computational mathematics and mathematical physics. P1.* TES: Odessa, **2015.**

PACS 32.30.-r

A. V. Glushkov, I. S. Cherkasova, V. B. Ternovsky, A. A. Svinarenko

THEORETICAL STUDYING SPECTRAL CHARACTERISTICS OF Ne-LIKE IONS ON THE BASIS OF OPTIMIZED RELATIVISTIC MANY-BODY PERTURBATION THEORY

Summary. Theoretical studying spectroscopic characteristics of the Ne-like multicharged ions is carried out within the relativistic many-body perturbation theory and generalized relativistic energy approach.The zeroth approximation of the relativistic perturbation theory is provided by the optimized Dirac-Kohn-Sham ones. Optimization has been fulfilled by means of introduction of the parameter to the Fock and Kohn-Sham exchange potentials and further minimization of the gauge-non-invariant contributions into radiation width of atomic levels with using relativistic orbital sets, generated by the corresponding zeroth approximation Hamiltonian.

Keywords: Relativistic perturbation theory, optimized zeroth approximation, Ne-like multicharged ions

PACS 32.30.-r

А. В. Глушков, И. С. Черкасова, В. Б. Терновский, А. А. Свинаренко

ТЕОРЕТИЧЕСКОЕ ИЗУЧЕНИЕ СПЕКТРАЛЬНЫХ ХАРАКТЕРИСТИК Ne-ПОДОБНЫХ ИОНОВ НА ОСНОВЕ ОПТИМИЗИРОВАННОЙ РЕЛЯТИВИСТСКОЙ МНОГОЧАСТИЧНОЙ ТЕОРИИ ВОЗМУЩЕНИЙ

Резюме. В рамках релятивистской многочастичной теории возмущений и обобщенного релятивистского энергетического подхода проведено теоретическое изучение спектроскопических характеристик ряда Ne-подобных многозарядных ионов. В качестве нулевого приближения релятивистской теории возмущений выбрано оптимизированное приближение Дирака-Кона-Шэма. Оптимизация выполнена путем введения параметра в обменные потенциалы Фока и Кона-Шэма и дальнейшей минимизацией калибровочно-неинвариантных вкладов в радиационные ширины атомных уровней с использованием релятивистского базиса орбиталей, сгенерированного соответствующим гамильтонианом нулевого приближения.

Ключевые слова: Релятивистская теория возмущений, оптимизированное нулевое приближение, Ne-подобные многозарядные ионы

PACS 32.30.-r

О. В. Глушков, І. С. Черкасова, В. Б. Терновський, А. А. Свинаренко

ТЕОРЕТИЧНЕ ВИВЧЕННЯ СПЕКТРАЛЬНИХ ХАРАКТЕРИСТИК Ne-ПОДІБНИХ ИОНОВ НА ОСНОВІ ОПТИМІЗОВАНОЇ РЕЛЯТИВІСТСЬКОЇ БАГАТОЧАСТКОВІ ТЕОРІЇ ЗБУРЕНЬ

Резюме. В рамках релятивістської багаточастинкової теорії збурень і узагальненого релятивістського енергетичного підходу проведено теоретичне вивчення спектроскопічних

характеристик ряду Ne-подібних багатозарядних іонів. В якості нульового наближення релятивістської теорії збурень обрано оптимізоване наближення Дірака-Кона-Шема. Оптимізація виконана шляхом введення параметра в обмінний потенціал Кона-Шема і подальшої мінімізації калібрувально-неінваріантних вкладів в радіаційні ширини атомних рівнів з використанням релятивістського базису орбіталей, згенерованого відповідним гамільтоніаном нульового наближення.

Ключові слова: Релятивістська теорія збурень, оптимізоване нульове наближення, Ne-подібні багатозарядні іони

PACS 33.20.-t

A. V. Ignatenko, A. P. Lavrenko

Odessa State Environmental University, 15, Lvovskaya str., Odessa, 65016
E-mail: ignatenkoav13@gmail.com

SPECTROSCOPIC FACTORS OF DIATOMIC MOLECULES: OPTIMIZED GREEN'S FUNCTIONS AND DENSITY FUNCTIONAL METHOD

It is presented an advanced approach to computing the spectroscopic factors of the diatomic molecules, which is based on the hybrid combined density functional theory (DFT) and the Green's-functions (GF) approach. The Fermi-liquid quasiparticle version of the density functional theory is modified and used. The density of states, which describe the vibrational structure in photoelectron spectra, is defined with the use of combined DFT-GF approach and is well approximated by using only the first order coupling constants in the optimized one-quasiparticle approximation. Using the combined DFT-GF approach to computing the spectroscopic factors of diatomic molecules leads to significant simplification of the calculation procedure and increasing an accuracy of theoretical prediction.

1. Introduction

In this paper we study the problem of calculating the important spectroscopic characteristics of multielectron systems (atoms and molecules), namely, the spectroscopic factor. The spectroscopic factor is one of the most important characteristics of atomic and molecular systems and the precise information about it is very important for many applications [1-38]. The theoretical determination of spectroscopic factor for multielectron atomic and molecular systems is a rather complicated task, since in the framework of traditional a priori methods it is reduced to a calculation of corrections of perturbation theory of the type:

$$\sum_{i} \left|\mathrm{Vij}\right|^2 /(\varepsilon_i - \varepsilon_j)$$

with summation over a large number of intermediate states. The spectroscopic factor is usually experimentally determined using inelastic scattering of fast electrons, as well as photoelectron spectroscopy (see [1]). In this case, as a rule, there is a discrepancy between the results of measurements of spectroscopic factors in these experiments caused by the influence of many electronic correlations in the initial state of the multielectron system

In this paper we present an advanced approach to computing the spectroscopic factors of the diatomic molecules within the hybrid combined density functional theory (DFT) in the Fermi-liquid formulation and the Green's-functions (GF) approach to quantitative determination of the spectroscopic factors for some molecular systems. The approach is based on the Green's function method (Cederbaum-Domske version) [1,2] and Fermi-liquid DFT formalism [3-7] and using the novel effective density functionals (see also [11-22]). It is important that the calculational procedure is significantly simplified with using the quasiparticle DFT formalism.

As usually (see details in refs. [1,4,7]), the quantity which contains the information about the ionization potentials (I.P.) and molecular vibrational structure due to quick ionization is the density of occupied states:

$$N_k(\epsilon) = (1/2\pi\hbar)\int dt e^{i\hbar^{-1}\epsilon t}\langle\psi_0|\mathrm{a}_k^t(0)a_k(t)|\psi_0\rangle\,, \quad (1)$$

where $|\Psi_0\rangle$ is the exact ground state wave function of the reference molecule and $a_k(t)$ is an electron destruction operator, both in the Heisenberg picture.

2. Theory: Density of states in one-body and many-body solution

As usually, introducing a field operator $\Psi(R,\theta,x)=\sum_i \phi_i(x,R,\theta)a_i(R,\theta)$ with the Hartree-Fock (HF) one–particle functions ϕ_i ($\epsilon_i(R)$ are the one-particle HF energies and f denotes the set of orbitals occupied in the HF ground state; R_0 is the equilibrium geometry on the HF level) and dimensionless normal coordinates Q_s one can write the standard Hamiltonian as follows [2,7]:

$$H = H_E + H_N + H_{BN}^{(1)} + H_{BN}^{(2)}, \qquad (3)$$

$$H_E = \sum_i \epsilon_i(R_0)a_i^t a_i + \frac{1}{2}\sum V_{ijkl}(R_0)a_i^t a_j^t a_l a_k - \\ - \sum_{i,j}\sum_{k\in f}[V_{ikjk}(R_0) - V_{ikkj}(R_0)]\, a_i^t a_j$$

$$H_N = \hbar\sum_{s=1}^{M}\omega_s\left(b_s^t b_s + \frac{1}{2}\right)$$

$$H_{BN}^{(1)} = 2^{-1/2}\sum_{s=1}^{M}\left(\frac{\partial \epsilon_i}{\partial Q_s}\right)_0 (b_s + b_s^t)[a_i^t a_i - n_i] + \\ + \frac{1}{4}\sum_i\sum_{s,s'=1}^{M}\left(\frac{\partial^2 \epsilon_i}{\partial Q_s \partial Q_{s'}}\right)_0 (b_s + b_s^t)(b_{s'} + b_{s'}^t)[a_i^t a_i - n_i]$$

$$H_{BN}^{(2)} = 2^{-3/2}\sum\sum_{s=1}^{M}\left(\frac{\partial V_{ijkl}}{\partial Q_s}\right)_0 (b_s + b_s^t)[\delta v_1 a_i^t a_j^t a_k a_l + \\ + \delta v_2 a_l a_k a_i^t a_j^t + 2\delta v_3 a_j^t a_k a_l a_i^t] + \\ + \frac{1}{8}\sum\sum_{s,s'=1}^{M}\left(\frac{\partial^2 V_{ijkl}}{\partial Q_s \partial Q_{s''}}\right)_0 (b_s + b_s^t)(b_{s'} + b_{s'}^t)\cdot \\ [\delta v_1 a_i^t a_j^t a_k a_l + \delta v_2 a_l a_k a_i^t a_j^t + 2\delta v_3 a_j^t a_k a_l a_i^t]$$

with n_i=1 (0), $i\in f$ ($i\notin f$), $\delta\sigma_f$=1 (0) , $(ijkl)\in\sigma_f$, where the index set v_1 means that at least ϕ_k and ϕ_l or ϕ_i and ϕ_j are unoccupied, v_2 that at most one of the orbitals is unoccupied, and v_3 that ϕ_k and ϕ_j or ϕ_l and ϕ_j are unoccupied. The ω_s are the HF frequencies; b_s, b_s^t are destruction and creation operators for vibrational quanta as

$$Q_s = (1/\sqrt{2})(b_s + b_s^t) \\ \partial/\partial Q_s = (1/\sqrt{2})(b_s - b_s^t). \qquad (4)$$

The interpretation of the above Hamiltonian and an exact solution of the one-body HF problem is given in refs. [1,-7]. The usual way is to define the HF-single-particle component H_0 of the Hamiltonian (4) is as in Refs. [1,4]. Correspondingly in the one-particle picture the density of occupied states is given by

$$N_k^0(\epsilon) = \frac{1}{2\pi\hbar}\int_{-\infty}^{\infty} dt e^{i\hbar^{-1}(\epsilon-\epsilon_k)t}\langle 0|\ e^{\pm i\hbar^{-1}\tilde{H}_{0'}t}\ |0\rangle, \qquad (5)$$

$$\tilde{H}_0 = \sum_{s=1}^{M}\hbar\omega_s b_s^t b_s + \sum_{s=1}^{M} g_s^k(b_s + b_s^t) + \\ + \sum_{s,s'=1}^{M}\gamma_{ss'}^k(b_s + b_s^t)(b_{s'} + b_{s'}^t) \qquad (6)$$

$$g_s^i = \pm\frac{1}{\sqrt{2}}\left(\frac{\partial \epsilon_i}{\partial Q_s}\right)_0, \quad \gamma_{s'}^i = \pm\frac{1}{4}\left(\frac{\partial^2 \epsilon_i}{\partial Q_s \partial Q_{s'}}\right)_0. \qquad (7)$$

To get function $N_k(\epsilon)$ one calculates the GF $G_{kk'}(\epsilon)$ (see details in Refs. [1-7,31-35]:

$$G_{kk'}(\epsilon) = -i\hbar^{-1}\int_{-\infty}^{\infty} dt e^{i\hbar^{-1}\eta}\langle\psi_0|\ \hat{O}\{\ a_k(t)a_{k'}^t(0)\ \}\ |\psi_0\rangle \qquad (8)$$

Choosing the unperturbed H_0 to be $H_0 = \sum \epsilon_i a_i^t a_i + H_N$ one could define GF as

$$G_{kk'}^{0}(t) = \pm\delta_{kk'} i\exp\left[-i\hbar^{-1}(\varepsilon_k \mp \Delta\varepsilon)t\right]\cdot \\ \cdot\sum_n\left|\langle\hat{n}_k|U_k|0\rangle\right|^2\exp(\pm i\hbar^{-1}\cdot\hat{\omega}_k t) \qquad (9)$$

The direct method for calculation of $N_k(\epsilon)$ as the imaginary part of the GF includes a definition of the vertical I.P. (V.I.P.s) of the reference molecule and then of $N_k(\epsilon)$.

The zeros of the functions:

$$D_k(\epsilon) = \epsilon - [\epsilon^0 + \Sigma(\epsilon)]_k, \qquad (10)$$

where $(\epsilon^0 + \Sigma)_k$ denotes the k-th eigenvalue

of the diagonal matrix of the one-particle energies added to matrix of the self-energy part, are the negative V. I. P. 's for a given geometry. One can write [2,4]:

$$(V.I.P.)_k = -(\epsilon_k + F_k) \quad ,$$

$$F_k = \Sigma_k\left(-(V.I.P.)_k\right) \approx \frac{1}{1-\partial\Sigma_k(\epsilon_k)/\partial_\epsilon}\Sigma_k(\epsilon_k) \quad (11)$$

.

Expanding the ionic energy E_k^{N-1} about the equilibrium geometry of the reference molecule in a power series of the normal coordinates leads to a set of linear equations for the unknown normal coordinate shifts δQ_S, and new coupling constants:

$$g_1 = \pm\left(1/\sqrt{2}\right)\left[\partial(\epsilon_k + F_k)/\partial Q_l\right]_0 \quad (12)$$

$$\gamma_{ll'} = \pm\left(\frac{1}{4}\right)\left[\partial^2(\epsilon_k + F_k)/\partial Q_l/\partial Q_{l'}\right]_0$$

The coupling constants g_l, $y_{ll'}$ are calculated by the well-known perturbation expansion of the self-energy part. One could write:

$$\sum_k^{(2)}(\epsilon) = \sum_{\substack{i,j \\ s\notin F}} \frac{(V_{ksij} - V_{ksji})V_{ksij}}{\epsilon + \epsilon_s - \epsilon_i - \epsilon_j} + \sum_{\substack{i,j \\ s\notin F}} \frac{(V_{ksij} - V_{ksji})V_{ksij}}{\epsilon + \epsilon_s - \epsilon_i - \epsilon_j} \quad (13)$$

and the coupling constant g_l, are as [17]:

$$g_l \approx \pm\frac{1}{\sqrt{2}}\frac{\partial\epsilon_k}{\partial Q_l}\frac{1 + q_k(\partial/\partial\epsilon)\sum_k\left[-(V.I.P.)_k\right]}{1-(\partial/\partial\epsilon)\sum_k\left[-(V.I.P.)_k\right]} \quad (14)$$

The pole strength of the corresponding GF:

$$\rho_k = \left\{1 - \frac{\partial}{\partial\epsilon}\sum_k\left[-(V.I.P)_k\right]\right\}^{-1}; 1 \geq \rho_k \geq 0,$$

$$g_l \approx g_l^0[\rho_k + q_k(\rho_k - 1)],$$

$$g_l^0 = \pm 2^{-1/2}\partial\epsilon_k/\partial Q_l \quad (15)$$

3. Fermi-liquid quasiparticle density functional theory

The quasiparticle Fermi-liquid version of the DFT [3-8,31,36] is used to determine the coupling constants etc. The master equations can be obtained on the basis of variational principle, if we start from a Lagrangian of a molecule L_q. It should be defined as a functional of quasiparticle densities:

$$\nu_0(r) = \sum_\lambda n_\lambda |\Phi_\lambda(r)|^2,$$

$$\nu_1(r) = \sum_\lambda n_\lambda |\nabla\Phi_\lambda(r)|^2, \quad (16)$$

$$\nu_2(r) = \sum_\lambda n_\lambda[\Phi_\lambda^*\Phi_\lambda - \Phi_\lambda^*\Phi_\lambda]$$

The densities υ_0 and υ_1 are similar to the HF electron density and kinetical energy density correspondingly; the density υ_2 has no an analog in the HF or DFT theory and appears as result of account for the energy dependence of the mass operator Σ. A Lagrangian L_q can be written as a sum of a free Lagrangian and Lagrangian of interaction: $L_q = L_q^0 + L_q^{int}$, where the interaction Lagrangian is defined in the form, which is characteristic for a standard DFT (as a sum of the Coulomb and exchange-correlation terms), but, it takes into account for a mass operator energy dependence of Σ :

$$L_q^{\text{int}} = L_K - \frac{1}{2}\sum_{i,k=0}^{2}\int\beta_{ik}F(r_1,r_2)\nu_i(r_1)\nu_k(r_2)dr_1dr_2 \quad (17)$$

where F is an effective exchange-correlation interaction potential. The constants β_{ik} are defined in Refs. [3-5]. The constant β_{02} can be calculated by analytical way, but it is very useful to keep in mind its connection with a spectroscopic factor F_{sp} [4,5]:

$$F_{sp} = \left\{1 - \frac{\partial}{\partial\epsilon}\sum_k\left[-(V.I.P)_k\right]\right\} \quad (18)$$

The new element is linked with using the DFT correlation Gunnarsson-Lundqvist, Lee-Yang-Parrr functionals (c.g.[12-16]).

4. Results and conclusions

Below we present the results of calculation of the spectroscopic factors for a number of diatomic molecules, in particular, C_2, N_2, O_2, F_2 in the ground state, as well as dimers of noble gases A_2^*, K_2^*, Kr_2^* in the lowest excited state. As the input data, the data obtained in the HF approximation [2,40] are used. For the C_2, N_2, O_2, F_2 the following spectroscopic factors

were obtained for core (F_{sp}^{c}) and valence (F_{sp}^{V}) shells:

$$C_2 - F_{sp}^{c} = 0.49, F_{sp}^{v} = 0.80,$$
$$N_2 - F_{sp}^{c} = 0.46, F_{sp}^{v} = 0.77,$$
$$O_2 - F_{sp}^{c} = 0.43, F_{sp}^{v} = 0.74,$$
$$F_2 - F_{sp}^{c} = 0.39, F_{sp}^{v} = 0.71.$$

The obtained values of spectroscopic factors make it possible to assess to a certain extent the role of various types of correlations, in particular, intra-core and intra-valent, in these molecules. Since the spectroscopic factor, by its definition, is related to the dependence of the MSS on energy not taken into account in the HF approximation (always in this approximation: $F_{sp} = 1$), the difference F_{sp} from 1 indicates the corresponding role of various correlation effects. In particular, for these molecules, the contribution of intra-core correlations is somewhat more significant than that of intra-valent ones, which is also confirmed in ab initio calculations (c.f., [40]). For noble gas dimers ($n\,^{2}_{g}$ outer shells) F_{sp}^{n} are calculated:

$$Ar_2^{*} - F_{sp}^{4} = 0{,}58 - (R_e = 7.1\text{a.u.}),$$
$$Kr_2^{*} - F_{sp}^{7} = 0.37 - (R_e = 7.6\text{a.u.}),$$
$$Xe_2^{*} - F_{sp}^{10} = 0.26 - (R_e = 8.2\text{a.u.})$$

An analysis of the data indicates presence of strong correlation effects for the molecules, a number of features in the photoionization cross section of the $n\delta^2$ shells, namely, the possible collectivization of the $n\delta^2{}_g$ shells, the presence of "shadow" states in the molecules with which strong mixing takes place and to which the strength of the initial level $(1 - F_{sp})$ is transmitted. Note that such effects are known in the theory of atomic photoelectric effect, namely, for noble gas atoms (Ar and others) [6,41]).

References

1. Köppel, H., Domcke, W., Cederbaum, L.S., Green's function method in quantum chemistry. *Adv. Chem. Phys*. **1984**, *57*, 59-132
2. Cederbaum, L., Domcke, W., On vibrational structure of photoelectron spectra by the Green's functions method. *J.Chem. Phys*. **1984**, *60*, 2878-2896.
3. Glushkov, A. An universal quasiparticle energy functional in a density functional theory for relativistic atom. *Opt. and Spectr*. **1989**, *66*(1), 31-36.
4. Glushkov, A.V. New approach to theoretical definition of ionization potentials for molecules on the basis of Green's function method. *J. Phys. Chem*. **1992**, 66, 2671-2677.
5. Glushkov, A.V. *Relativistic and correlation effects in spectra of atomic systems*. Astroprint: Odessa, **2006**.
6. Glushkov, A.V. *Relativistic Quantum theory. Quantum mechanics of atomic systems.* Astroprint: Odessa, **2008**.
7. Ignatenko, A.V., Glushkov, A.V., Lepikh, Ya.I., Kvasikova, A.S. Photoelectron spectroscopy of diatomic molecules:optimized Green's functions and density functional approach**.** *Photoelectronics*. **2018**, *27*, 44-51.
8. Glushkov A., Khetselius O., Svinarenko A., Buyadzhi V. *Spectroscopy of autoionization states of heavy atoms and multiply charged ion*s. TEC, **2015**.
9. Ponomarenko, E.L., Kuznetsova, A.A., Dubrovskaya, Yu.V., Bakunina, E.V. Energy and spectroscopic parameters of diatomics within generalized equation of motion method. *Photoelectronics*. **2016**, *25*, 114-118.
10. Svinarenko, A.A., Glushkov, A. V., Khetselius, O.Yu., Ternovsky,V.B., Dubrovskaya, Yu., Kuznetsova, A., Buyadzhi, V. Theoretical spectroscopy of rare-earth elements: spectra and autoionization resonances. *Rare Earth Element*, Ed. J. Orjuela (InTech) **2017**, pp 83-104
11. Glushkov, A.V., Khetselius, O.Yu., Svinarenko A.A., Buyadzhi, V.V., Ternovsky, V.B, Kuznetsova, A., Bashkarev, P Relativistic perturbation theory formalism to computing spectra and radiation characteristics: application to heavy element. *Recent Studies in Perturbation Theory*, ed. D. Uzunov (InTech) **2017**, 131-150.
12. Kobayashi, K., Kurita, N., Kumahora, H.,

Kuzatami, T. Bond-energy calculations of Cu, Ag, CuAg with the generalized gradient approximation. *Phys.Rev.A*. **1991**, *43*, 5810
13. Lagowscki, J., Vosko, S. Analysis of local and gradient-correction correlation energy functionals using electron removal energies. *J. Phys.B: At. Mol. Opt. Phys*. **1988**, *21*(1), 203-208.
14. Guo, Y., Whitehead, M. Effect of the correlation correction on the ionization potential and electron affinity in atoms. *Phys.Rev.A.* **1989**, *39*(1), 28-34.
15. Khetselius, O.Yu., Lopatkin Yu.M., Dubrovskaya, Yu.V, Svinarenko A.A. Sensing hyperfine-structure, electroweak interaction and parity non-conservation effect in heavy atoms and nuclei: New nuclear-QED approach. *Sensor Electr. And Microsyst. Techn*. **2010,** 7(2), 11-19.
16. Florko, T., Ambrosov, S., Svinarenko A., Tkach, T. Collisional shift of the heavy atoms hyperfine lines in an atmosphere of the inert gas. *J. Phys: Conf. Ser*. **2012**, *397*(1), 012037.
17. Khetselius, O. Relativistic perturbation theory calculation of the hyperfine structure parameters for some heavy-element isotopes. *Int. J. Quant. Chem.* **2009,** *109,* 3330–3335.
18. Khetselius, O. Relativistic calculation of the hyperfine structure parameters for heavy elements and laser detection of the heavy isotopes. *Phys. Scr.* **2009,** *135,* 014023.
19. Glushkov A.V., *Atom in electromagnetic field*. KNT: Kiev, **2005**.
20. Khetselius, O. Yu. *Hyperfine structure of atomic spectra*; Astroprint: Odessa, **2008**.
21. Khetselius, O.Yu. *Quantum structure of electroweak interaction in heavy finite Fermi-systems*. Astroprint: Odessa, **2011**.
22. Khetselius, O.Y.., Glushkov, A.V., Gurskaya, M.Y., Kuznetsova, A.A., Dubrovskaya, Yu.V., Serga, I.N., Vitavetskaya, L.A. Computational modelling parity nonconservation and electroweak interaction effects in heavy atomic systems within the nuclear-relativistic many-body perturbation theory. *J. Phys.: Conf. Ser.* **2017,** *905*(1), 012029.
23. Glushkov, A., Gurskaya, M., Ignatenko, A., Smirnov, A., Serga, I., Svinarenko, A., Ternovsky, E. Computational code in atomic and nuclear quantum optics: Advanced computing multiphoton resonance parameters for atoms in a strong laser field. *J. Phys.: Conf. Ser*. **2017**, *905*(1), 012004.
24. Ambrosov S., Ignatenko V., Korchevsky D., Kozlovskaya V. Sensing stochasticity of atomic systems in crossed electric and magnetic fields by analysis of level statistics for continuous energy spectra. *Sensor Electr. and Microsyst. Techn*. **2005**, Issue 2, 19-23.
25. Buyadzhi, V.V., Glushkov, A.V., Mansarliysky, V.F., Ignatenko, A.V., Svinarenko, A. Spectroscopy of atoms in a strong laser field: new method to sensing ac stark effect, multiphoton resonances parameters and ionization cross-sections. *Sensor Electr. and Microsyst. Techn*. **2015**, *12*(4), 27-36.
26. Svinarenko A.A., Mischenko E., Loboda A., Dubrovskaya Yu. Quantum measure of frequency and sensing the collisional shift of the ytterbium hyperfine lines in medium of helium gas. *Sensor Electr. and Microsyst. Techn*. **2009**, 1, 25-29.
27. Malinovskaya S.V., Dubrovskaya Yu.V., Zelentzova T.N. The atomic chemical environment effect on the b decay probabilities: Relativistic calculation. *Herald of Kiev Nat. Univ. Ser.: Phys.-Math*. **2004**, N4, 427-432.
28. Glushkov A., Khetselius O., Svinarenko A., Prepelitsa G., Mischenko E., The Green's functions and density functional approach to vibrational structure in the photoelectron spectra for molecules. *AIP Conf. Proc*. **2010**, *1290*, 263-268.
29. Khetselius O., Florko T., Svinarenko A., Tkach T. Radiative and collisional spectroscopy of hyperfine lines of the Li-like heavy ions and Tl atom in an atmosphere of inert gas. *Phys.Scripta*. **2013**, *T153*, 014037.
30. Glushkov, A.V., Kivganov, A.F., Khokhlov, V.N., Buyadzhi, T.V., Vitavetskaya, L.A., Borovskaya, G.A., Polishchuk, V.N. Calculation of the spectroscopic characteristics of diatomic van der Waals molecules and ions: Inert gas atom—halogen-type inert gas ion in the ground state. *Russian Phys. Journ*. **1998**, *41*(3), 223-226
31. Glushkov, A., Malinovskii, A., Efimov, V.,

Kivganov, A., Khokhlov, V., Vitavetskaya, L., Borovskaya, G., Calculation of alkaline metal dimers in terms of model perturbation theory. *J. Struct. Chem*. **1998**, *39*(2), 179-185.
32. Khetselius, O.Yu. Hyperfine structure of radium. *Photoelectron*. **2005**, *14*, 83-85
33. Khetselius O.Yu., Quantum Geometry: New approach to quantization of the quasistationary states of Dirac equation for super heavy ion and calculating hyper fine structure parameters. *Proc. Int. Geometry Center*. **2012**, *5*(3-4), 39-45.
34. Dubrovskaya, Yu., Khetselius, O.Yu., Vitavetskaya, L., Ternovsky, V., Serga, I. Quantum chemistry and spectroscopy of pionic atomic systems with accounting for relativistic, radiative, and strong interaction effects. *Adv. in Quantum Chem.* **2019,** Vol.78, pp 193-222.
35. Khetselius, O.Yu., Glushkov, A.V., Dubrovskaya, Yu.V., Chernyakova, Yu.G., Ignatenko, A.V., Serga, I.N., Vitavetskaya, L. Relativistic quantum chemistry and spectroscopy of exotic atomic systems with accounting for strong interaction effects. In: Wang YA, Thachuk M, Krems R, Maruani J (eds) *Concepts, Methods and Applications of Quantum Systems in Chemistry and Physics*. Springer, Cham, **2018**; Vol. 31, pp. 71-91.
36. Glushkov, A., Ivanov, L. DC strong-field Stark effect: consistent quantum-mechanical approach. *J. Phys.B: At. Mol. Opt. Phys*. **1993**, *26*(14), L379 –386.
37. Glushkov, A.V., Khetselius, O.Yu., Svinarenko, A.A., Buyadzhi, V. *Methods of computational mathematics and mathematical physics*. *P.1*. TES: Odessa, **2015.**
38. Glushkov, A.V., Safranov, T.A., Khetselius, O.Yu., Ignatenko, A.V., Buyadzhi, V.V., Svinarenko, A.A. Analysis and forecast of the environmental radioactivity dynamics based on methods of chaos theory: General conceptions. *Environm. Problems*. **2016**, *1*(2), 115-120.
39. Glushkov, A., Buyadzhi, V., Kvasikova, A., Ignatenko, A., Kuznetsova, A., Prepelitsa, G., Ternovsky, V. Non-Linear chaotic dynamics of quantum systems: Molecules in an electromagnetic field and laser systems. In: Tadjer A, Pavlov R, Maruani J etal, (eds) *Quantum Systems in Physics, Chemistry, and Biology*. Springer, Cham. **2017**, *30*, 169
40. Robert, C., Morrison, R., Liu, G., Extended Koopmans theorem: approximate ionization energies from MCSCF Wave Functions. *J. Comp. Chem*. **1992**, *13*, 1004-1010.
41. Svinarenko, A. Spectroscopy of autoionization resonancesin spectra of barium. *Photoelectronics*. *2014*, *23*, 86-90.

PACS 33.20.-t

A. V. Ignatenko, A. P. Lavrenko

SPECTROSCOPIC FACTORS OF DIATOMIC MOLECULES: OPTIMIZED GREEN'S FUNCTIONS AND DENSITY FUNCTIONAL METHOD

Summary. It is presented an advanced approach to computing the spectroscopic factors of the diatomic molecules, which is based on the hybrid combined density functional theory (DFT) and the Green's-functions (GF) approach. The Fermi-liquid quasiparticle DFT version is modified and used. The density of states, which describe the vibrational structure in photoelectron spectra, is defined with the use of combined DFT-GF approach and is well approximated by using only the first order coupling constants in the optimized one-quasiparticle approximation. Using the combined DFT-GF approach leads to significant simplification of calculation procedure and increasing an accuracy of theoretical prediction.

Key words: diatomic molecules, Green's functions, density functional

PACS 33.20.-t

А. В. Игнатенко, А. П. Лавренко

СПЕКТРОСКОПИЧЕСКИЕ ФАКТОРЫ ДЛЯ ДВУХАТОМНЫХ МОЛЕКУЛ: ОПТИМИЗИРОВАННЫЙ МЕТОД ФУНКЦИЙ ГРИНА И ФУНКЦИОНАЛА ПЛОТНОСТИ

Резюме. Представлен усовершенствованный подход к вычислению спектроскопических факторов двухатомных молекул, базирующийся на гибридной комбинированной теории функционала плотности (ТФП) и методе функций Грина (ФГ). Используется модель ферми-жидкостная квазичастичная версия ТФП. Плотность состояний, которая описывает колебательную структуру в фотоэлектронных спектрах, определяется с использованием комбинированного подхода ТФП - ФГ. Использование комбинированного ТФП-ФГ подхода приводит к значительному упрощению процедуры расчета и повышению точности теоретического прогнозирования.

Ключевые слова: двухатомные молекулы, функция Грина, функционал плотности

PACS 33.20.-t

Г. В. Ігнатенко, О. П. Лавренко

СПЕКТРОСКОПІЧНІ ФАКТОРИ ДВОАТОМНИХ МОЛЕКУЛ: ОПТИМІЗОВАНИЙ МЕТОД ФУНКЦІЙ ГРІНА І ФУНКЦІОНАЛУ ГУСТИНИ

Резюме. Представлений вдосконалений метод обчислення спектроскопічних факторів 2-атомних молекул, що базується на гібридній теорії функціонала щільності (ТФП) і методі функцій Гріна (ФГ). Використано фермі-рідинну квазічастинкову версію ТФП. Густина станів, які описує коливальну структуру фотоелектронного спектру, визначається в межах ТФП-ФГ методу. Використання комбінованого ТФП-ФГ методу призводить до спрощення процедури обчислень, підвищення точності прогнозу.

Ключові слова: двоатомні молекули, функція Гріна, функціонал густини

PACS 31.15.A-; 32.30.-r

A. S. Chernyshev, O. L. Mykhailov, A. V. Tsudik, I. S. Cherkasova

Odessa State Environmental University, L'vovskaya str.15, Odessa-16, 65016, Ukraine
E-mail: veronevonor@gmail.com

RELATIVISTIC THEORY OF CALCULATION OF E1 TRANSITION AMPLITUDES, AND GAUGE INVARIANCE PRINCIPLE

The combined relativistic energy approach and relativistic many-body perturbation theory with the zeroth order Dirac-Kohn-Sham one-particle approximation are used for estimating the energies and the E1 radiative transitions amplitudes (oscillator strengths) for the low-excited states of the francium. The comparison with available theoretical and experimental (compilated) data is performed. The important point is linked with an accurate accounting for the complex exchange-correlation (polarization) effect contributions and using the optimized one-quasiparticle representation in the relativistic many-body perturbation theory zeroth order that significantly provides a physically reasonable agreement between theory and precise experiment.

1. Introduction

The development of new directions in the field of laser, atomic physics, quantum electronics, etc., such as pulsed heating methods in research on controlled thermonuclear fusion, new laser schemes in VUV, X-ray spectral regions, astrophysical studies, etc., necessitates the solution of new classes of problems of atomic and laser physics at a fundamentally new level of theoretical consistency and accuracy. Significant progress in the development of experimental research methods, in particular, a significant increase in the intensity and quality of laser radiation, the use of accelerators, heavy ion colliders, sources of synchrotron radiation and, as a result, the possibility of studying more and more energy processes, stimulates the development of new theoretical methods in the theory of heavy atoms calculation of their characteristics, in particular, radiation and autoionization ones [1-10].

However, a study of the spectral characteristics of heavy atoms and ions in the Rydberg states has to be more complicated as it requires a necessary accounting for the relativistic, exchange-correlations effects and possibly the QED corrections for superheavy atomic systems. The simultaneous correct accounting of relativistic, quantum electrodynamic (QED), and many-particle correlation effects is essential [1–10]. The results of calculating the characteristics of atomic processes based on modern theoretical methods often differ several times.

The difference in the values of the transition amplitudes, the oscillator strengths, and the radiation widths for heavy atoms using various expressions for the photon propagator reaches 5–30% (we are essentially talking about the non-fulfillment of the principle of gauge invariance when calculating physical quantities) [11-18]. From the point of view of applications for the majority of the most important atomic systems, there is very often partially or completely missing information on their energy, radiation or/ and autoionization characteristics (heavy atoms, atoms of alkaline-earth elements, lanthanides and actinides).

In this paper the combined relativistic energy approach and relativistic many-body perturbation theory with the zeroth order Dirac-Kohn-Sham 1-particle approximation [2,19] are used for are used for estimating the energies and the E1 radiative transitions amplitudes (oscillator strengths) for some low-excited states of the francium atom and studying an effect of the gauge invariance on the transition amplitude values for heavy atoms on example of the francium.

2. The theoretical method

In Refs. [2,18-22] the fundamentals of the relativistic many-body PT formalism have been in detail presented, so further we are limited only by the novel elements. Let us remind that the majority of complex atomic systems possess a dense energy spectrum of interacting states. In Refs. [10-12] there is realized a field procedure for calculating the energy shifts ΔE of degenerate states, which is connected with the secular matrix M diagonalization. The whole calculation of the energies and decay probabilities of a non-degenerate excited state is reduced to the calculation and diagonalization of the M. The complex secular matrix M is represented in the form:

$$M = M^{(0)} + M^{(1)} + M^{(2)} + M^{(3)}. \qquad (1)$$

where $M^{(0)}$ is the contribution of the vacuum diagrams of all order of PT, and $M^{(1)}$, $M^{(2)}, M^{(3)}$ those of the one-, two- and three-QP diagrams respectively. The diagonal matrix $M^{(1)}$ can be presented as a sum of the independent 1QP contributions. The optimized 1-QP representation is the best one to determine the zeroth approximation. In the relativistic energy approach, which has received a great application during solving numerous problems of atomic, molecular and nuclear physics (e.g., see Refs. [21-27]), the imaginary part of electron energy shift of an atom is directly connected with the radiation decay possibility (transition probability). An approach, using the Gell-Mann and Low formula with the QED scattering matrix, is used in treating the relativistic atom. The total energy shift of the state is usually presented in the form:

$$\Delta E = \mathrm{Re}\Delta E + i\,\Gamma/2 \qquad (2)$$

where Γ is interpreted as the level width, and the decay possibility P = Γ. The imaginary part of electron energy of the system, which is defined in the lowest order of perturbation theory as [10,11]:

$$\mathrm{Im}\,\Delta E(B) = -\frac{e^2}{4\pi} \sum_{\substack{\alpha>n>f \\ [\alpha<n\le f]}} V^{|\omega_{\alpha n}|}_{\alpha n \alpha n}, \qquad (3)$$

where (α>n>f) for electron and (α<n<f) for vacancy. The matrix element is determined as follows:

$$V^{|\omega|}_{ijkl} = \iint dr_1 dr_2 \Psi^*_i(r_1)\Psi^*_j(r_2)\frac{\sin|\omega|r_{12}}{r_{12}}(1-\alpha_1\alpha_2)\Psi^*_k(r_2)\Psi^*_l(r_1) \qquad (4)$$

where ω_{ij} is the transition frequency; α_i ,α_j are the Dirac matrices. The separated terms of the sum in (1) represent the contributions of different channels and a probability of the dipole transition

Naturally, the physical values should not depend on the calibration of the photonic propagator. In general form, it can be written as

$$D = D_T + C \cdot D_L,$$
$$D_T = \frac{\delta_{\mu\nu}}{k_0^2 - k^2},$$
$$D_L = \frac{k_\mu k_\nu}{k_0^2 - k^2} \qquad (5)$$

where the term D_T is corresponding to exchange by transverse photons, D_L — longitudinal ones, C is the gauge constant. contribution of the main exchange-correlation (the second and higher orders of the atomic perturbation theory or fourth etc of the QED perturbation theory) diagrams to imaginary part of an electron energy shift looks like [11]:

$$\mathrm{Im}\,E_{ninv}(\alpha - s \mid A_d) = -C\frac{e^2}{4\pi}\iiint dr_1 dr_2 dr_3 dr_4$$

$$\sum\left(\frac{1}{\omega_{mn}+\omega_{\alpha_s}} + \frac{1}{\omega_{mn}-\omega_{\alpha_s}}\right)\Psi^+_\alpha(r_1)\Psi^+_m(r_2)\Psi^+_s(r_3)\cdot$$

$$\cdot\,\Psi^+_n(r_4)(1-\alpha_1\alpha_2)/r_{12}\cdot\{[(\alpha_3\alpha_4 - (\alpha_3 n_{34})(\alpha_4 n_{34}))/r_{34}\cdot$$
$$\sin[\omega_{\alpha_n}(r_{12}+r_{34})] + \omega_{\alpha_n}\cdot\cos[\omega_{\alpha_n}(r_{12}+r_{34})](1+(\alpha_3 n_{34})$$
$$(\alpha_4 n_{34}))]\}\Psi_m(r_3)\Psi_\alpha(r_4)\Psi_n(r_2)\Psi_s(r_1) \qquad (6)$$

Expression (6) can be represented as an a sum:

$$\sum\langle \alpha m \mid W_1 \mid s\rangle\langle s \mid W_2 \mid m\alpha\rangle/(\omega_m \pm \omega_{\alpha s}) \qquad (7)$$

with (4) different operator combinations W_1, W_2. The sum over n can be calculated by the

method of differential equations. The index m numbers a finite number of states occupied in the core and the state of the real continuum. The continuum-related part describes the vacuum polarization of the electron field and leads to divergent integrals in the non-renormalizable theory. Its contribution to the main contribution has an additional order of smallness (aZ^2). The minimization of the density functional ImdE leads to the integral differential equation for the r_c, that can be numerically solved. This step allows to determine the optimization parameter b. In Ref. [11] the authors elaborated a simplified computational procedure.

The contribution of the main exchange-correlation (the second and higher orders of the atomic perturbation theory or fourth etc ones of the QED perturbation theory) to imaginary part of an electron energy shift is determined by the polarizability of an atomic core, which is related to the electronic core density r_c. The expression (6) can be represented an a functional of the density r_c.

Under calculating the matrix elements (2) one should use the expansion for potential $\sin|w|r_{12}/r_{12}$ on spherical functions as follows [10,11]:

$$\frac{\sin|\omega|r_{12}}{r_{12}} = \frac{\pi}{2\sqrt{r_1 r_2}} \sum_{\lambda=0}^{\infty} (\lambda) J_{\lambda+1/2}(|\omega|r_1) J_{\lambda+1/2}(|\omega|r_2) P_\lambda(\cos \widehat{r_1 r_2}) \quad (8)$$

where J is the Bessel function of first kind and (l)= 2l + 1. Substitution of the expansion (5) to matrix element of interaction gives as follows [14]:

$$V_{1234}^{\omega} = [(j_1)(j_2)(j_3)(j_4)]^{1/2} \sum_{\mu} (-1)^{\mu} \begin{pmatrix} j_1 j_3 & \lambda \\ m_1 - m_3 & \mu \end{pmatrix} \times$$

$$\times \mathrm{Im}\{Q_\lambda^{Qul}(1234) + Q_\lambda^{B}(1234)\}, \quad (9)$$

where j_i is the total single electron momentums, m_i – the projections; Q^{Qul} is the Coulomb part of interaction, Q^{Br} - the Breit part. Their detailed definitions are presented in Refs. [10-11,18,19]. The relativistic wave functions are calculated by solution of the Dirac equation with the potential, which includes the "outer electron- ionic core" potential and exchange-polarization potential [20]. In fact, we realize the procedure of optimization of relativistic orbitals base. The main idea is based on using ab initio optimization procedure, which is reduced to minimization of the gauge dependent multielectron contribution ImDE_{ninv} of the lowest QED PT corrections to the radiation widths of atomic levels. According to [11, 18], "in the fourth order of QED PT (the second order of the atomic PT) there appear the diagrams, whose contribution to the ImDE_{ninv} accounts for correlation effects and this contribution is determined by the electromagnetic potential gauge (the gauge dependent contribution)". The accurate procedure for minimization of the functional ImdE_{ninv} leads to the Dirac-Kohn-Sham-like equations for the electron density that are numerically solved by the Runge-Cutta standard method It is very important to know that the regular realization of the total scheme allows to get an optimal set of the 1QP functions and more correct results in comparison with so called simplified one, which has been used in Refs. [11-13] and reduced to the functional minimization using the variation of the correlation potential parameter b. Other details can be found in Refs. [11,18,19,29].

The adequate, precise computation of radiative parameters of the heavy Rydberg alkali-metal atoms within relativistic perturbation theory requires an accurate accounting for the multielectron exchange-correlation effects (including polarization and screening effects, a continuum pressure etc). These effects within our approach are treated as the effects of the perturbation theory second and higher orders. Using the standard Feynman diagrammatic technique one should consider two kinds of diagrams (the polarization and ladder ones), which describe the polarization and screening exchange-correlation effects. The detailed description of the polarization diagrams and the corresponding analytical expressions for matrix elements of the polarization interelectron interaction (through the polarizable core of an alkali atom) potential is presented in Refs. [2,18,19,29].

An effective approach to accounting for the polarization diagrams contributions is in adding the effective two-quasiparticle polarizable operator into the perturbation theory first order matrix elements. In Ref. [10] the corresponding non-relativistic polarization functional has been derived. More correct relativistic expression has

been presented in the Refs. [2,18] and used in our theory.

The corresponding two-quasiparticle polarization potential looks as follows: (10a)

$$V^{d}_{pol}(r_1 r_2) = X\left\{\int \frac{dr'\left(\rho_c^{(0)}(r')\right)^{1/3}\theta(r')}{|r_1 - r'|\cdot|r' - r_2|} - \right.$$
$$\left. - \int \frac{dr'\left(\rho_c^{(0)}(r')\right)^{1/3}\theta(r')}{|r_1 - r'|}\int \frac{dr''\left(\rho_c^{(0)}(r'')\right)^{1/3}\theta(r'')}{|r'' - r_2|} \Big/ \left\langle \left(\rho_c^{(0)}\right)^{1/3}\right\rangle\right\} \quad (10a)$$

$$\left\langle \left(\rho_c^{(0)}\right)^{1/3}\right\rangle = \int dr\left(\rho_c^{(0)}(r)\right)^{1/3}\theta(r), \quad (10b)$$

$$\theta(r) = \left\{1 + \left[3\pi^2 \cdot \rho_c^{(0)}(r)\right]^{2/3} / c^2\right\}^{1/2}, \quad (10c)$$

where ρ_c^0 is the core electron density (without account for the quasiparticle), X is numerical coefficient, c is the light velocity. The contribution of the ladder diagrams (these diagrams describe the immediate interparticle interaction) is summarized by a modification of the perturbation theory zeroth approximation mean-field central potential (look [2,18]), which includes the screening (anti-screening) of the core potential of each particle by the two others. All computing was performed with using the modified PC code "Superatom-ISAN" (version 93).

3. Results and conclusion

We applied the above described approach to compute the oscillator strengths (reduced dipole matrix elements) for a number of transitions in spectra of the heavy alkali atoms and corresponding ions.

As an illustration we present below the data for francium. In Table 1 there are listed the theoretical reduced dipole matrix elements for a number of transitions, computed within: i) relativistic Hartree-Fock (RHF) method [6], ii) the empirical relativistic model potential method (ERMP) [7], iii) the relativistic single-double (SD) method in which single and double excitations of the Dirac-Hartree-Fock (DHF) wave function are included to all orders of perturbation theory [8] and iv) our data.

Let us note that the precise experimental data for the francium $7p_{1/2,3/2}$-7s transition are as follows: $7p_{1/2}$-7s=4.277 and $7p_{3/2}$-7s=5.898 [8]. The important features of the approach used are using the optimized one-particle representation and an effective taking into account the exchange-correlation (including the core polarization) effects (see Refs. [2,18-20,30]).

Really, as it is indicated in Ref. [8], the semiempirical values agree with the ab initio SD calculations to better than 1% with the exceptions of the 7s-8p and 7s-9p transitions, where contributions from correlation corrections are very large. The most important conclusions relate to an effect of the gauge invariance on the transition amplitude values.

An estimate of the gauge-non-invariant contributions (the difference between the oscillator strengths values calculated with using the transition operator in the form of "length" G1 and "velocity" G2) is about 0.1%. The theoretical data, obtained with using the different photon propagator gauges (Coulomb and Babushkin ones) are practically equal.

Table 1.

Theoretical reduced dipole matrix elements for a set of Fr transitions

Transition	i: RHF	ii: ERMP
$7p_{1/2}$-$7s_{1/2}$	4.279 4.304	-
$8p_{1/2}$-$7s_{1/2}$	0.291 0.301	0.304
$9p_{1/2}$-$7s_{1/2}$	-	0.096
$7p_{3/2}$-$7s_{1/2}$	5.894 5.927	-
$8p_{3/2}$-$7s_{1/2}$	0.924	0.908
$9p_{3/2}$-$7s_{1/2}$	-	0.420
Transition	iii: SD-DHF	iv: Our data
$7p_{1/2}$-$7s_{1/2}$	4.256	4.275 (G1) 4.277 (G2)

$8p_{1/2}$-$7s_{1/2}$	0.327 0.306	0.339
$9p_{1/2}$-$7s_{1/2}$	0.110	0.092
$7p_{3/2}$-$7s_{1/2}$	5.851	5.891
$8p_{3/2}$-$7s_{1/2}$	0.934 0.909	0.918
$9p_{3/2}$-$7s_{1/2}$	0.436	0.426

References

1. Grant, I. Relativistic Quantum Theory of Atoms and Molecules. Oxford, 2007.
2. Glushkov, A., Khetselius, O., Svinaren-ko, A., Buyadzhi, V. Spectroscopy of autoionization states of heavy atoms and multiply charged ions. Odessa: 2015.
3. Buyadzhi, V. Laser multiphoton spectroscopy of atom embedded in Debye plasmas: multiphoton resonances and transitions. Photoelectronics. 2015, 24, 128-133.
4. Khetselius, O.Yu. Relativistic perturbation theory calculation of the hyperfine structure parameters for some heavy-element isotopes. Int. J. Quant. Chem. 2009, 109, 3330–3335.
5. Chernyakova, Y., Ignatenko, A., Vitavetskaya, L.A. Sensing the tokamak plasma parameters by means high resolution x-ray theoretical spectroscopy method: new scheme. Sensor Electr. and Microsyst. Techn. 2004, 1, 20-24.
6. Dzuba, V.A., Flambaum, V.V., Sushkov, O.P. Calculation of energy levels, E1 transition amplitudes, and parity violation in Fr Phys. Rev. A. 1995, 51, 3454.
7. Marinescu, M., Vrinceanu, D., Sadeghpour, H. Radiative transitions and van der Waals coefficients for francium. Phys. Rev. A. 1998, 58, R4259.
8. Safronova, U., Johnson, W., Derevianko, A. Relativistic many-body calculations of energy levels, hyperfine constants, electric-dipole matrix elements, and static polarizabilities for alkali-metal atoms. Phys. Rev. A. 1999, 60, 4476.
9. Ivanov, L.N., Ivanova, E.P., Aglitsky, E. Modern trends in the spectroscopy of multicharged ions. Phys. Rep. 1988, 166.
10. Svinarenko, A., Khetselius, O., Buyadzhi, V., Florko, T., Zaichko,P., Ponomarenko, E. Spectroscopy of Rydberg atoms in a Blackbody radiation field: Relativistic theory of excitation and ionization. J. Phys.: Conf. Ser. 2014, 548, 012048.
11. Glushkov, A.V., Ivanov, L.N. Radiation decay of atomic states: atomic residue polarization and gauge noninvariant contributions. Phys. Lett. A 1992, 170, 33-36.
12. Glushkov A.V., Ivanov, L.N. DC strong-field Stark effect: consistent quantum-mechanical approach. J. Phys. B: At. Mol. Opt. Phys. 1993, 26, L379-386.
13. Glushkov, A. Spectroscopy of atom and nucleus in a strong laser field: Stark effect and multiphoton resonances. J. Phys.: Conf. Ser. 2014, 548, 012020
14. Glushkov, A. Spectroscopy of coope-rative muon-gamma-nuclear processes: Energy and spectral parameters J. Phys.: Conf. Ser. 2012, 397, 012011.
15. Khetselius, O.Yu. Quantum Geometry: New approach to quantization of quasistationary states of Dirac equation for superheavy ion and calculating hyperfine structure parameters. Proc. Int. Geometry Center. 2012, 5(3-4), 39-45.
16. Danilov, V., Kruglyak, Y., Pechenaya, V. The electron density-bond order matrix and the spin density in the restricted CI method. Theor. Chim. Act. 1969, 13(4), 288-296.
17. Kruglyak, Yu. Configuration interaction in the second quantization representation: basics with application up to full CI. ScienceRise. 2014, 4(2), 98-115.
18. Glushkov, A.V. Relativistic and correlation effects in spectra of atomic systems. Astroprint: Odessa, 2006.
19. Khetselius, O.Yu. Hyperfine structure of atomic spectra.- Odessa: Astroprint, 2008
20. Glushkov, A., Buyadzhi, V., Svinarenko, A., Ternovsky, E. Advanced relativistic energy approach in electron-collisional spectroscopy of multicharged ions in plasma. Concepts, Methods, Applications of Quantum

Systems in Chemistry and Physics (Springer). 2018, 31, 55-69.
21. Dubrovskaya, Yu., Khetselius, O.Yu., Vitavetskaya, L., Ternovsky, V., Serga, I. Quantum chemistry and spectroscopy of pionic atomic systems with accounting for relativistic, radiative, and strong interaction effects. Adv. Quantum Chem. 2019, 78, 193-222.
22. Khetselius, O.Yu., Glushkov, A.V., Dubrovskaya, Yu., Chernyakova, Yu., Ignatenko, A., Serga, I., Vitavetskaya, L. Relativistic quantum chemistry and spectroscopy of exotic atomic systems with accounting for strong interaction effects. In Concepts, Methods and Applications of Quantum Systems in Chem. and Phys. Springer. 2018, 31, 71.
23. Buyadzhi, V.V., Chernyakova, Yu.G., Antoshkina, O., Tkach, T. Spectroscopy of multicharged ions in plasmas: Oscillator strengths of Be-like ion Fe. Photoelectronics. 2017, 26, 94-102.
24. Malinovskaya, S.V., Dubrovskaya, Yu.V., Zelentzova, T.N. The atomic chemical environment effect on the b decay probabilities: Relativistic calculation. Herald of Kiev Nat. Univ. Ser.: Phys.-Math. 2004, N4, 427-432.
25. Bystryantseva, A., Khetselius, O.Yu., Dubrovskaya, Yu., Vitavetskaya, L.A., Berestenk, A.G. Relativistic theory of spectra of heavy pionic atomic systems with account of strong pion-nuclear interaction effects: ^{93}Nb, ^{173}Yb, ^{181}Ta, ^{197}Au. Photoelectronics. 2016, 25, 56-61.
26. Buyadzhi, V., Zaichko, P., Antoshkina, O., Kulakli, T., Prepelitsa, P., Ternovsky, V., Mansarliysky, V. Computing of radiation parameters for atoms and multicharged ions within relativistic energy approach: Advanced Code. J. Phys.: Conf. Ser. 2017, 905(1), 012003.
27. Buyadzhi, V., Kuznetsova, A., Buyadzhi, A., Ternovsky, E.V., Tkach, T.B. Advanced quantum approach in radiative and collisional spectroscopy of multicharged ions in plasmas. Adv. in Quant. Chem. 2019, 78, 171-191.
28. Khetselius, O.Yu., Lopatkin, Yu.M., Dubrovskaya, Yu.V, Svinarenko, A.A. Sensing hyperfine-structure, electroweak interaction and parity non-conservation effect in heavy atoms and nuclei: New nuclear-QED approach. Sensor Electr. and Microsyst. Techn. 2010, 7(2), 11-19.
29. Glushkov, A.V., Khetselius, O.Yu., Svinarenko, A., Buyadzhi, V. Methods of computational mathematics and mathematical physics TES: Odessa, 2015
30. Ignatenko, A.V., Svinarenko, A.A., Prepelitsa, G.P., Perelygina, T.B. Optical bi-stability effect for multi-photon absorption in atomic ensembles in a strong laser field. Photoelectronics. 2009, 18, 103-105.

PACS 31.15.A-; 32.30.-r

A. S. Chernyshev, O. L. Mykhailov, A. V. Tsudik, I. S. Cherkasova

RELATIVISTIC THEORY OF CALCULATION OF E1 TRANSITION AMPLITUDES, AND GAUGE INVARIANCE PRINCIPLE

Summary. The combined relativistic energy approach and relativistic many-body perturbation theory with the zeroth order Dirac-Kohn-Sham one-particle approximation are used for estimating the energies and the E1 radiative transitions amplitudes (oscillator strengths) for the low-excited states of the francium. The comparison with available theoretical and experimental (compillated) data is performed. The important point is linked with an accurate accounting for the complex exchange-correlation (polarization) effect contributions and using the optimized one-quasiparticle

representation in the relativistic many-body perturbation theory zeroth order that significantly provides a physically reasonable agreement between theory and precise experiment.

Key words: relativistic theory, radiative transitions, francium

PACS 31.15.A-; 32.30.-r

А. С. Чернышов, А. Л. Михайлов, А. В. Цудик, И. С. Черкасова

РЕЛЯТИВИСТСКАЯ ТЕОРИЯ РАСЧЕТА ПЕРЕХОДНЫХ АМПЛИТУД E1 ПЕРЕХОДОВ И ПРИНЦИП КАЛИБРОВОЧНОЙ ИНВАРИАНТНОСТИ

Резюме. Комбинированный релятивистский энергетический подход и релятивистская многочастичная теория возмущений с дирак-кон-шэмовским одночастичным нулевым приближением используются для для вычисления энергий и амплитуд E1 радиационных переходов (сил осцилляторов) для низко возбужденных состояний франция. Проведено сравнение с имеющимися теоретическими и экспериментальными данными. Важный момент связан с аккуратным учетом вкладов сложных многочастичных обменных корреляционных (поляризационных) эффектов и с использованием оптимизированного одноквазичастичного представления в нулевом приближении релятивистской многочастичной теории возмущений, что определяет определенное согласие теории и эксперимента.

Ключевые слова: релятивистская теория, радиационные переходы, франций

PACS 31.15.A-; 32.30.-r

О. С. Чернишов, О. Л. Михайлов, А. В. Цудік, І. С. Черкасова

РЕЛЯТИВІСТСЬКА ТЕОРІЯ РОЗРАХУНКУ АМПЛІТУД E1 ПЕРЕХОДІВ І ПРИНЦИП КАЛІБРУВАЛЬНОЇ ІНВАРІАНТНОСТІ

Резюме. Комбінований релятивістський енергетичний підхід і релятивістська багаточастинкова теорія збурень з дірак-кон-шемівським одночастинковим наближенням нульового порядку використовуються для обчислення енергій та амплітуд E1 радіаційних переходів (сил осцилляторов) для низько збуджених станів францію. Проведено порівняння з наявними теоретичними і експериментальними даними. Важливий момент пов'язаний з акуратним урахуванням вкладів складних багаточасткових обмінних кореляційних (поляризаційних) ефектів і з використанням оптимізованого одноквазічастічного уявлення в нульовому наближенні релятивістської багаточастинкової теорії збурень, що визначає певну згоду теорії та експерименту.

Ключові слова: релятивістська теорія, радіаційні переходи, франций

PACS 64.60.A+82.70.R

O. Yu. Khetselius, A. V. Glushkov, S. N. Stepanenko, A. A. Svinarenko, Yu. Ya. Bunyakova, E. T. Vitovskaya

Odessa State Environmental University, L'vovskaya str.15, Odessa-9, 65016, Ukraine
E-mail: okhetsel@gmail.com

ADVANCED PHOTOCHEMICAL BOX AND QUANTUM-KINETIC MODELS FOR SENSING ENERGY, RADIATION EXCHANGE IN ATMOSPHERIC GASES MIXTURES AND LASER- MOLECULES INTERACTION

Abstract. The aim of the work is to develop a set of optimal photochemical models with the inclusion of a submodel of the boundary layer using complex plane field methods and spectral algorithms and optimized blocks describing nonlinear radiation transfer and chemical conversion mechanisms, quantum-kinetic and photoelectronic models for describing nonlinear optical effects due to the interaction of infrared laser radiation with the gas atmosphere of an industrial city. An obvious consequence of the resonant interaction (in particular, absorption) of electromagnetic radiation by atmospheric molecular gases is a quantitative redistribution of molecules by energy levels of internal degrees of freedom, which quantitatively changes the so-called gas absorption coefficient. A change in the population levels of the gas mixture causes a violation of the thermodynamic equilibrium between the vibrations of the molecules and their translational motion and causes a new nonlinear effect of the photokinetic cooling of the atmospheric environment.

1. Introduction

At the present time laser systems for monitoring the environmental state of atmosphere have become widespread. The classical laser sensing methods is mainly based on the processes of linear interaction of radiation with the atmospheric gases and aerosol components of the atmosphere [1-10]. However, as it was shown in multiple investigations (c.g., [1-5,9]), there are a number of important problems and tasks, where the linear methods of sensing are ineffective both due to technical difficulties arising due to small interaction cross sections and because of fundamental physical limitations when these effects do not contain information about the desired medium parameters. First of all, speech is about such tasks as remote elemental analysis of condensed matter of aerosols and underlying surface, determination of heavy metals and inert gas atoms content, detection of ultra-low concentrations of gas impurities and substance vapors with selective absorption coefficients cm^{-1}, and a number of other problems related, in particular, to diagnostics industrial pollution etc [1]. It is very important to remember about some fundamental aspects of the interaction of electromagnetic radiation with atoms and molecules of the atmospheric environment , especially in a case of the intense external field. Here it should be noted a nonlinear response of atoms and molecules . The obvious consequence of resonant interaction (in particular, absorption) of electromagnetic radiation (hereinafter, as a rule, will be coherent, that is, laser radiation) by molecular gases of the atmosphere is the quantitative redistribution of molecules by the energy levels of internal degrees of freedom. In turn, this will change the so-called gas absorption coefficient. Changing the population levels of the mixture of gases causes a disturbance of thermodynamic equilibrium between the vibrations of molecules and their translational motion, resulting in kinetic cooling of the environment.

According to [4], the industrial city's air quality and the formation of photochemical oxidants (of which ozone is a major component) involves the interaction of source emissions and a series of different quite complex physical and chemical processes. Ozone is formed in the atmosphere as a result of a complex series of thermal and photochemical reactions involving nitrogen oxides and reactive hydrocarbons. The known photochemical box model (PBM) by Jin-Schere-Demerjian [4] includes three main blocks: (1) a boundary-layer submodel, (2) a revised radiative transfer and photolytic rate constant calculation routine, and (3) two chemical

mechanisms of different complexity. In Refs. [7,11] it is presented an advanced quantum-kinetic model to describe the nonlinear-optical (spectroscopic) effect caused by the interaction of infrared laser radiation with a gas atmosphere. The quantitative features of energy exchange in a mixture of CO_2-N_2-H_20 atmospheric gases of atmospheric gases were determined and can be used in development of new technologies for observing a state of atmosphere. The results of computing the relative absorption coefficient (normalized to linear absorption coefficient) are presented. In Refs. [11,12] it is presented a new generalized approach, including an improved theory of atmospheric circulation in combination with the hydrodynamic model (he Arakawa-Schubert method of calculation of cloud convection and theory of a complex geophysical field is applied to the simulation of heat and air transfer in atmosphere of industrial region. In this paper we present a set of advanced photochemical box models (APBM) with the inclusion of a submodel of the boundary layer using complex plane field methods [2,13-16]) and spectral algorithms with optimized blocks describing nonlinear radiation transfer and chemical conversion mechanisms [11,12], quantum-kinetic and photoelectronic models for describing nonlinear optical effects due to the interaction of infrared laser radiation with the gas atmosphere of an industrial city..

2. An advanced photochemical model

The APBM is based on the principle of an energy and mass conservation. As in the original version [4], we assume too that (1) the box volume is well mixed at all times and no spatial variations of concentration occur within it; (2) emission sources are homogeneously distributed across the bottom surface of the box; (3) entrainment of outside air occurs laterally by advective transport and vertically by the growth in mixed layer height. Under these assumptions, the chemical species conservation equation becomes:

$$\frac{\partial C_i}{\partial t} = -u\frac{\partial C_i}{\partial x} - \frac{dl}{dt}\frac{\partial C_i}{\partial z} - \frac{Q_i}{z} + R_i(C_1,...,C_n) + F(x,z,t) \quad (1)$$

where C_i is the mean concentration of species "I" within the definite domain, u the mean advection speed, Q_i the source emissions flux of species i in the domain, and R_i the rate of production and/or destruction of species i due to chemical reactions. The original model by Jin-Schere-Demerjian [4] has a horizontal extension of 20 km and a vertical extension of the mixed-layer height. Our APBM model has a horizontal extension of 40 km and less significantly lower resolution (grid scale). A schematic illustration and flowchart of our APBM with the incorporated blocks is shown at Figure 1. The physical features of air ventilation predetermine the necessary modification of the well-known Arakawa-Schubert model. The model includes the budget equations for mass, moist static energy, total water content plus the equations of motion [2,13]:

$$E - D - \frac{\partial M_c}{\partial z} = 0; \quad (2a)$$

$$E\tilde{s} - Ds_c - \frac{\partial M_c s_c}{\partial z} + pLc = 0; \quad (2b)$$

$$E\tilde{q} - Dq_c - \frac{\partial M_c q_c}{\partial z} + pc = 0; \quad (2c)$$

where E is an inflow, D is an outflow, $M_c = \sum pw_i\sigma_i = pw_c\sigma$ - vertical mass flow of air in the cloud; w_i is an average (on the cross-section) speed in the i-th cloud, c - horizontal cross-section square for the i-th cloud; $w_c, s_c = c_pT + gz$, q_c is weighted

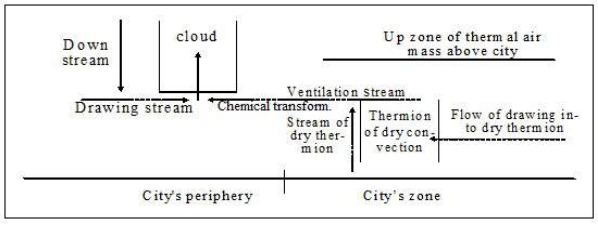

Fig. 1. Flowchart of the APBM with the incorporated blocks

verage values of vertical speed, statistical energy and the ratio of the mixture of water vapor; $\tilde{s}, \tilde{q}$ - average statistical energy and the ratio of the mixture of water vapor in the ambient air, p - air density; c is an amount of the condensed moisture. If e is an amount of evaporated moisture, L - specific heat of phase transitions, then the equation of heat and moisture influx will be as follows [2,13]:

$$\frac{\partial\overline{ps}}{\partial t} + v\overline{ps\vec{v}} + \frac{\partial\overline{(pws)}}{\partial z} + pL(c-e) - \frac{\partial\overline{(pw)'s'}}{\partial z}; \quad (3a)$$

$$\frac{\partial\overline{pq}}{\partial t} + v\overline{pq\vec{v}} + \frac{\partial\overline{(pwq)}}{\partial z} + p(c-e) - \frac{\partial\overline{(pw)'q'}}{\partial z}; \quad (3b)$$

Spectral representations in ensemble of clouds are:

$$E(z) = \int \varepsilon(z,\lambda) m_B(\lambda) d\lambda \quad (4a)$$

$$D(z) = \int d(z,\lambda) m_B(\lambda) d\lambda \quad (4b)$$

If A is a work of the convective cloud then it consists of convection work and work of down falling streams in the neighbourhood of a cloud:

$$dA/dt = dA/dt_{conv} + dA/dt_{downstr}, \quad (5a)$$

$$dA/dt_{downstr} = \int_0^{\lambda_{\max}} m_B(\lambda') K(\lambda,\lambda') d\lambda', \quad (5b)$$

Here λ is a speed of involvement, $m_B(\lambda)$ is an air mass flux, $K(\lambda, \lambda')$ is the Arakawa-Schubert integral equation kernel [3], which determines the dynamical interaction between the neighbours clouds. In the case of air ventilation emergence, mass balance equation in the convective thermals is [13]:

$$m_B(\lambda) = F(\lambda) + \beta \int_0^{\lambda_{\max}} m_B(\lambda') K(\lambda,\lambda') d\lambda' \quad (6)$$

Here β is parameter which determines disbalance of cloud work due to the return of part of the cloud energy to the organization of a wind field in their vicinity, and balance regulating its contribution to the synoptic processes. The solution of the Eqs. (3)(-4) with accounting for air stream superposition of synoptic processes is given by a resolvent:

$$m_B(\lambda) = F(\lambda) + \beta \int_0^{\lambda_{\max}} F(s)\Gamma(\lambda,s;\beta) ds, \quad (7)$$

$$\Gamma(\lambda,s;\beta) = \sum_{i=1}^{\infty} \beta^{i-1} \cdot K_i(\lambda,s) \quad (8)$$

The key idea [2,13] is to determine the resolvent as an expansion to the Laurent series in a complex plane ζ. Its centre coincides with the centre of the city's "heating" island and the internal cycle with the city's periphery. The external cycle can be moved beyond limits of the urban recreation zone. The Laurent representation for resolvent is provided by the standard expansion:

$$\Gamma = \sum_{n=\infty}^{\infty} c_n (\zeta - a)^n, \quad (9)$$

$$c_n = \frac{1}{2\pi i} \oint_{|\zeta|=1} \frac{\Gamma(\zeta) d\zeta}{(\zeta - a)^{n+1}} = \frac{1}{2\pi i} \int_0^{2\pi} \Gamma(e^{it}) e^{-int} dt, \quad (10)$$

where a is center of the Laurent series convergence ring. The method for calculating a turbulence spectra inside the urban zone should be based on solving the system of equations for the Reynolds tensions, moments of connection of the speed pulsations with entropy ones and the corresponding closure equations [2,13-17]. The important parameter of the turbulent processes is the kinetic energy of turbulent vortices $b^2 = \overline{u'_k u'_k}$, which can be found from the equation [13]. The speed components, say, u_x, u_y, of an air flux can be determined in an approximation of "shallow water" [2]. In contrast to the standard difference methods of solution, here we use the spectral expansion algorithms [16]. The necessary solution, for example, for the v_x-iv_y component for the city's heat island has the form of expansion into series on the Bessel functions. From the other side, a air flux speed over a city's periphery in a case of convective instability can be found by method of plane complex field theory (in analogy with the Karman vortices chain model) [2,13-16].

3. Advanced quantum-kinetic model

The interaction of laser radiation with a mixture of atmospheric gases, leads to relatively complex processes of resonant excitation transfer, in particular, from CO_2 molecules to nitrogen molecules. As a result, the complex dielectric constant of the atmospheric medium will change, which will lead to a significant transformation of the energy of laser pulses in the gas atmosphere [1,3]. The dielectric constant depends on the intensity of the electromagnetic wave *I*:

$$\varepsilon = \varepsilon(I) = \bar{\varepsilon}_0 + \varepsilon_N(I) \qquad (11)$$

$$I = \frac{c\sqrt{\varepsilon_0}}{8\pi}\left|\vec{E}\right|^2 \qquad (12)$$

where *c* is the speed of light, *E* is the electric field strength of the wave. When laser radiation interacts with atoms and molecules of atmospheric gases, there is also the so-called Kerr electronic effect, which arises due to the deformation of the electron density distributed by the field, almost immediately following the change of field, as well as the orientation effect of Kerr [3]. The relaxation time of this effect for atmospheric air under normal conditions is 10^{-13} s. This effect leads to the dependence of the dielectric constant on the field of the electromagnetic wave in the formula (11) of the form

$$\varepsilon_N = \varepsilon_2 \left|E\right|^2. \qquad (13)$$

For Gaussian beams and plateau beams, the Kerr effect leads to the self-focusing of light, described in detail, for example, in [3,8,9, 11]. If the length of the nonlinear interaction (self-focusing) is a Gaussian beam with radius R_0

$$L_N = \frac{R_0}{\sqrt{\varepsilon_2\left|E\right|^2}} = R_0\left(\frac{8\pi\varepsilon_2}{c\sqrt{\varepsilon_0}}I\right)^{-1/2}, \qquad (14)$$

then the realization of the effect on distance $L_{\|}$ is possible if the threshold intensity is defined [3]:

$$I_{\text{ïîð}} \geq \frac{c\sqrt{\varepsilon_0}}{8\pi}\frac{R_0^2}{\varepsilon_2 L_{\|}^2}. \qquad (15)$$

I_{THR}~10^{10} $\text{W}\cdot\text{cm}^{-2}$ for R_0=*0.1* and $L_{\|} = 10^3$ m. If $L_{\|} = 10^5$ m, then I_{THR}~10^8 $\text{W}\cdot\text{cm}^{-2}$. For infrared laser wavelength λ=10.6 μm, the critical autofocus ($L_{\|} = L_d$) power is:

$$P_{êð} = \pi R_0^2 I_{\text{ïîð}} = \frac{c\sqrt{\varepsilon_0}}{8k^2\varepsilon_2} = 1,7\cdot 10^{11} \qquad (16)$$

One finds $P_{êð} = 1,7\cdot 10^9$ W for λ=1,06 μm.

Further let us present an advanced quantum-kinetic model to describe the nonlinear-optical (spectroscopic) effect caused by the interaction of infrared laser radiation with a gas atmosphere and consider the quantitative features of energy exchange in a mixture of CO_2-N_2-H_20 atmospheric gases of atmospheric gases. The original version was presented in Refs. [11,12].

Typically, for the quantitative description of energy exchange and the corresponding relaxation processes in a mixture of CO_2-N_2-H_20 gases in the laser radiation field, one should first consider the kinetics of three levels: 10°0, 00°1 (CO_2) i v = 1 (N_2). The system of differential equations of balance for relative populations is written in the following form:

$$\begin{aligned}
&\frac{dx_1}{dt} = -\beta(\omega + 2gP_{10})x_1 + \beta\omega x_2 + \\
&+ 2\beta g P_{10})x_1^0 + F_N(x_1) \\
&\frac{dx_2}{dt} = \omega x_1 - (\omega + Q + P_{20})x_2 + \\
&+ Qx_3 + P_{20}x_2^0 + F_N(x_2), \\
&\frac{dx_3}{dt} = \delta Q x_2 - (\delta Q + P_{30})x_3 + \\
&P_{30}x_3^0 + F_N(x_3)
\end{aligned} \qquad (17)$$

Here, $x_1 = N_{100}/N_{CO_2}$, $x_2 = N_{001}/N_{CO_2}$, $x_3 = \delta N_{N_2} / N_{CO_2}$; N_{100}, N_{001} are the level populations 10°0, 00°1 (CO_2); N_{CO_2} is concentration of CO_2 molecules; N_{N_2} is the level

population v=1(N_2); Q is the probability (s^{-1}) of resonant transfer in the reaction $CO_2 \rightarrow N_2$,ω is a probability (s^{-1}) of CO_2 light excitation, $g = 3$ is statistical weight of level 02°0, β=(1+g)$^{-1}$= ¼; δ is ratio of common concentrations of CO_2 and N_2 in atmosphere (δ = 3.85×10^{-4}); $F_N(x)$ – additional nonlinear term; x_1^0, x_2^0 and x_3^0 are the equilibrium relative values of populations under gas temperature T:

$$x_1^0 = \exp(-E_1/T), \qquad (18)$$

$$x_2^0 = x_3^0 = \exp(E_2/T) \qquad (19)$$

Values E_1 and E_2 in (1) are the energies (K) of levels 10°0, 00°1 (consider the energy of quantum N_2 equal to E_2); P_{10}, P_{20} and P_{30} are the probabilities (s^{-1}) of the collisional deactivation of levels 10°0, 00°1 (CO_2) and v = 1 (N_2).

Note that having obtained the solution of the differential equation system (17), one can further calculate the absorption coefficient of radiation by CO_2 molecules:

$$\alpha_{CO_2} = \sigma(x_1 - x_2)N_{CO_2}. \qquad (20)$$

The σ in Eq. (20) is dependent upon the thermodynamical medium parameters according to [1]. The different estimates (c.g., [3,11]) show that for emission of the CO_2-laser the absorption coefficient:

$$\alpha_g = \alpha_{CO_2} + \alpha_{H_2O}. \qquad (21)$$

is equal in conditions, which are typical for summer mid-latitudes $\alpha_g[H=0]=(1.1\text{-}2.6)\cdot 10^6$ cm^{-1}, from which $0.8\cdot 10^6$ cm^{-1} accounts for CO_2 and the rest – for water vapour (data are from ref. [3]) . The resonance absorption by the molecules of the atmospheric mixture of laser radiation is determined by the change in the population of the low-lying level 10°0 (CO_2), the population of the level 00°1 and vibration-translational relaxation (VT-relaxation), as well as intergenerational vibration relaxation (VV'-relaxation). For the wavelength of infrared laser radiation (eg, CO_2 laser of 10.6μm), the duration of the corresponding pulse will satisfy the inequality $t_R \ll t_i <$ t_{VT},, where t_R , t_{VT} are the values of time, respectively, of rotational and oscillatory relaxation. In Ref. [12] there are presented the results of an accurate numerical calculations with using the accurately determined probabilities of P_{10}, P_{20} , P_{30} of deactivation due to the levels of 10°0, 00°1 (CO_2) and v = 1 (N_2), the probability of Q resonance energy transfer $CO_2 \rightarrow N_2$, the excitation probability ω pulse of CO_2 laser and other constants. The results of computing the relative absorption coefficient $\overline{\alpha}_{O_2}$ (normalized to linear absorption coefficient) based on the solutions of the system (17) have been presented for the distribution of pressure altitude and temperature within the model of atmosphere of the middle latitudes (Odessa) [2,13]. It is clear that the time dependence of the relative resonance absorption coefficient of laser radiation by CO2 molecules for different laser pulses differs. Using these data we determine that the effect of kinetic cooling of the CO_2 is determined by the condition (for Odessa region):

$$\alpha_{H_2O}^0 < (E_1/(E_2 - E_1))\alpha_{CO_2}^0 = 1.51\alpha_{CO_2}^0 \qquad (22)$$

Note that Eq. (22) is sufficiently significantly different from early qualitative estimates [3,11]. The numerical parameters obtained allow us to further quantify the effects of the kinetic cooling of CO_2, depending on the parameters of the model of the atmosphere and the parameters of laser radiation [3].

4. Conclusions

To conclude, we presented an advanced photochemical box model with the incorporation of a boundary-layer complex plane field submodel [2,13-17], advanced quantum-kinetic and photoelectronic models to describe the nonlinear-optical (spectroscopic) effect caused by the interaction of infrared laser radiation with a gas atmosphere, and an advanced nonlinear radiative transfer and chemical mechanisms blocks. From physical viewpoint, it is clear that because of the resonant interaction (in particular, absorption) of electromagnetic radiation with atmo-

spheric molecular gases there is the quantitative redistribution of molecules by the energy levels of internal degrees of freedom. The radiative and energy flux that causes the gas to be heated through the absorption by the water vapour, is proportional to the intensity of the laser radiation. When the critical value is reached, the heating of the steam will prevail over its cooling for any moment of time. In such a physical situation, the effect of kinetic cooling will cease to exist. The quantitative manifestation of the kinetic effect may vary for different atmospheric conditions, laser radiation parameters, and different values of atomic-molecular parameters.

References

1. Gubanova E.R., Glushkov A.V., Khetselius O.Yu., Bunyakova Yu.Ya., Buyadzhi V.V., Pavlenko E.P., *New methods in analysis and project management of environmental activity: Electronic and radioactive waste*. FOP: Kharkiv, **2017**.
2. Bunyakova, Yu.Ya.; Glushkov, A.V. *Analysis and forecast of the impact of anthropogenic factors on air basein of an industrial city*. Ecology: Odessa, **2010.**
3. Zuev V., Zemlyanov A., Kopytin Y., Kuzikovsky A *The laser radiation in atmospheric aerosol*. Novosybirsk, **1984**
4. Jin, S., Demerjian, K. A photochemical box model for urban air quality study. *Atm. Envir.B. Urban Atm*. **1993**, *27*, 371
5. Glushkov, A., Safranov, T., Khetselius, O., Ignatenko, A., Buyadzhi, V., Svinarenko, A. Analysis and forecast of the environmental radioactivity dynamics based on methods of chaos theory: General conceptions. *Environm. Problems*. **2016**, *1*(2), 115-120.
6. Khetselius, O. Optimized perturbation theory for calculating the hyperfine line shift and broadening of heavy atoms in a buffer gas. *Frontiers in quantum methods and applications in Chem. and Phys.*; Cham: Springer, **2015**, *29*, 55-76.
7. Glushkov, A., Buyadzhi, V., Kvasikova, A., Ignatenko, A., Kuznetsova, A., Prepelitsa G., Ternovsky, V. Non-linear chaotic dynamics of quantum systems: Molecules in an electromagnetic field and laser systems. In: *Quantum Systems in Physics, Chemistry, and Biology*. Springer, Cham. **2017**, *30*, 169-180
8. Gordiets B., Osipov A.I., Kokhlov R. About cooling gas under powerful CO_2 laser radiation passing in atmosphere. *J. Tech. Phys*. **1974**, *14*, 1063-1066.
9. Geints Y., Zemlyanov A. Near- and mid-IR ultrashort laser pulse filamentation in a molecular atmosphere: a comparative analysis. *Appl. Opt*. **2017**, *56*, 1397.
10. Wei, P.-S., Hsieh, Y.-C., Chiu, H.-H., Yen, D.-L., Lee, C., Tsai, Y.-C., & Ting, T.-C. Absorption coefficient of carbon dioxide across atmospheric troposphere layer. *Heliyon*. **2018**, 4(10), e00785.
11. Glushkov A.V., Serbov N.G., Bunyakova Yu.Ya., Prepelitsa G.P., Svinarenko A.A. Sensing the kinetical features of energy exchange in mixture CO_2-N_2-$H_2$0 of atmospheric gases under interacting with laser radiation. *Sensor Electr. and Microsyst. Techn*. **2006**. N4. P.20-22.
12. Bunyakova, Yu.Ya., Glushkov, A.V., Khetselius, O.Yu., Svinarenko, A.A., Ignatenko, A.V., Bykowszczenko, N. Modeling of nonlinear optical effects in the interaction of laser radiation with atmosphere and sensing for energy exchange in a mixture atmospheric gases. *Sensor Electr. and Microsyst. Techn*. **2019**, *16*(3), 42-50.
13. Sofronkov A, Khetselius O, Glushkov A, Buyadzhi V, Romanova A., Ignatenko A. New geophysical complex-field approach to modelling dynamics of heat-mass-transfer and ventilation in atmosphere of the industrial region. *Phys. Aerodisp. Syst*. **2018**, *55*, 104-111
14. Glushkov, A.V., Svinarenko, A.A., Khetselius, O., Serbov, N. The sea and ocean 3D acoustic waveguide: rays dynamics and chaos phenomena. *J. Acoust. Soc. America*. **2008**, *123*, 3625.
15. Serbov N.G., Svinarenko A.A. Wavelet and multifractal analysis of oscillations in system of couled autogenerators in chaotic regime. *Photoelectr*. **2006**, *15*, 27

16. Glushkov A.V., Khetselius O.Yu., Svinarenko A.A., Buyadzhi V.V., *Methods of computational mathematics and mathematical physics. P.1*. TES: Odessa, 2015.

17. Khetselius, O. Forecasting evolutionary dynamics of chaotic systems using advanced non-linear prediction method. *Dynamical Systems Applications*; Lodz Univ.: Lodz. **2013**, *T2*, 145-152.

PACS 64.60.A+82.70.R

O. Yu. Khetselius, A. V. Glushkov, S. N. Stepanenko, A. A. Svinarenko, Yu. Ya. Bunyakova, E. T. Vitovskaya

ADVANCED PHOTOCHEMICAL BOX AND QUANTUM-KINETIC MODELS FOR SENSING ENERGY, RADIATION EXCHANGE IN ATMOSPHERIC GASES MIXTURES AND LASER- MOLECULES INTERACTION

Summary. The aim of the work is to develop a set of optimal photochemical models with the inclusion of a submodel of the boundary layer using complex plane field methods and spectral algorithms and optimized blocks describing nonlinear radiation transfer and chemical conversion mechanisms, quantum-kinetic and photoelectronic models for describing nonlinear optical effects due to the interaction of infrared laser radiation with the gas atmosphere of industrial city. The resonant interaction of electromagnetic radiation with molecular gases leads to redistribution of molecules by energy levels of freedom internal degrees, which changes the gas absorption coefficient. A change in the population levels causes a violation of thermodynamic equilibrium between the vibrations of molecules and their translational motion, providing a new nonlinear effect of the photokinetic cooling of atmosphere.

Key words: energy exchange kinetics, atmospheric gases, laser radiation, photochemical model, quantum kinetic model

PACS 64.60.A+82.70.R

О. Хецелиус, А. Глушков, С. Степаненко, А. Свинаренко, Ю. Бунякова, Е. Витовская

ОПТИМАЛЬНЫЕ ФОТОХИМИЧЕСКАЯ И КВАНТОВО-КИНЕТИЧЕСКАЯ МОДЕЛИ ДЛЯ ДЕТЕКТИРОВАНИЯ ЭНЕРГО-РАДИАЦИОННО-ОБМЕННЫХ ПРОЦЕССОВ В СМЕСИ АТМОСФЕРНЫХ ГАЗОВ И ВЗАИМОДЕЙСТВИЯ ЛАЗЕРНОГО ИЗЛУЧЕНИЯ С АТМОСФЕРНЫМИ МОЛЕКУЛАМИ

Резюме. Цель работы состоит в разработке комплекса оптимальной фотохимической модели (с включением субмодели пограничного слоя и использованием методов комплексного плоского поля) и спектральных моделей с оптимизированными блоками, описывающими нелинейный перенос излучения и химические преобразовательные механизмы, квантово-кинетической и фотоэлектронной моделей для описания нелинейно-оптических эффектов, обусловленных взаимодействием инфракрасного лазерного излучения с газовой атмосферой промышленного города. Резонансное взаимодействия электромагнитного излучения с молекулярными газами атмосферы приводит к количественному перераспределению молекул по энергетическим уровням внутренних степеней свободы, что изменяет называемый коэффициент поглощения газа. Изменение уровней заселенности смеси газов вызывает нарушение

термодинамического равновесия между колебаниями молекул и их поступательным движением и обуславливает новый нелинейный эффект фотокинетического охлаждения атмосферной среды.

Ключевые слова: кинетика энергообмена, атмосферные газы, лазерное излучение, фотохимическая модель, квантово-кинетическая модель

PACS 64.60.A+82.70.R

О. Хецеліус, О. Глушков, С. Степаненко, А. Свинаренко, Ю. Бунякова, О. Вітовська

ОПТИМАЛЬНІ ФОТОХІМІЧНА І КВАНТОВО-КІНЕТИЧНА МОДЕЛІ ДЛЯ ДЕТЕКТУВАННЯ ЕНЕРГО-РАДІАЦІЙНО-ОБМІННИХ ПРОЦЕСІВ В СУМІШІ АТМОСФЕРНИХ ГАЗІВ І ВЗАЄМОДІЇ ЛАЗЕРНОГО ВИПРОМІНЮВАННЯ З АТМОСФЕРНИМИ МОЛЕКУЛАМИ

Резюме. Мета роботи полягає в розробці комплексу оптимальної фотохімічної моделі (з включенням субмоделі прикордонного шару і використанням методів комплексного плоского поля) і спектральних моделей з оптимізованими блоками, що описують нелінійний перенос випромінювання і хімічні перетворюючі механізми, квантово-кінетичної і фотоелектронної моделей для опису нелінійно-оптичних ефектів, обумовлених взаємодією інфрачервоного лазерного випромінювання з газової атмосферою промислового міста. Резонансна взаємодія електромагнітного випромінювання з молекулярними газами атмосфери веде до кількісного перерозподілу молекул по енергетичним рівням внутрішніх ступенів свободи, що змінює званий коефіцієнт поглинання газу. Зміна рівнів заселеності суміші газів викликає порушення термодинамічної рівноваги між коливаннями молекул і їх поступальним рухом і обумовлює новий нелінійний ефект фотокінетичного охолодження атмосферного середовища.

Ключові слова: кінетика енергообміну, атмосферні гази, лазерне випромінювання, фотохімічна модель, квантово-кінетична модель

PACS 31.15.-p

E. V. Ternovsky

Odessa State Environmental University, 15, Lvovskaya str., Odessa-16, 65016, Ukraine
E-mail: ternovskyev@gmail.com

RELATIVISTIC SPECTROSCOPY OF MULTICHARGED IONS IN PLASMAS: Li-LIKE IONS

The transition probabilities and lifetimes for different excited states in spectrum of the Li-like calcium are computed within the consistent relativistic many-body approach for different values of the plasmas screening parameter (correspondingly, electron density and temperature) and compared with available alternative data. The approach is based on the generalized relativistic energy approach combined with the optimized relativistic many-body perturbation theory with the Dirac-Debye shielding model as zeroth approximation, adapted for application to study of the spectral parameters of ions in plasmas. An electronic Hamiltonian for N-electron ion in plasmas is added by the Yukawa-type electron-electron and nuclear interaction potential.

1. Introduction

The properties of laboratory, thermonuclear (tokamak), laser-produced, astrophysical plasmas have drawn considerable attention over the last decades [1-14]. It is known that multicharged ions play an important role in the diagnostics of a wide variety of plasmas [1-10]. Electron-ion collisions involving multiply charged ions, as well as various radiation and radiation-collisional processes, predetermine the quantitative characteristics of the energy balance of the plasmas [1-6,15-20]. For this reason, the plasmas modelers and diagnosticians require absolute cross sections for these processes. The cross sections for electron-impact excitation of ions are needed to interpret spectroscopic measurements and for simulations of plasmas using collisional-radiative models. The electron-ion collisions play a major role in the energy balance of plasmas. ([1-6]). Different theoretical methods were employed along with the Debye screening to study plasma medium. Earlier we have developed a new version of a relativistic energy approach combined with the many-body perturbation theory (RMBPT) for multi-quasiparticle (QP) systems to study spectra of plasma of the multicharged ions, electron-ion collisional parameters [15-20]. The method is based on the Debye shielding model and energy approach [21-23]. A new element of this paper is in using the effective optimized Dirac-Kohn-Sham method in general relativistic energy approach to collision processes in the Debye plasmas.

In this paper, which goes on our work [15-20], we present the results of computing the transition probabilities and lifetimes for different excited states in spectrum of the Li-like calcium for different values of the plasmas screening (Debye) parameter (respectively, electron density, temperature) and compared with available alternative spectroscopic data. The approach used is based on the generalized relativistic energy approach combined with the optimized RMBPT with the Dirac-Debye shielding model as zeroth approximation, adapted for application to study the spectral parameters of ions in plasmas. An electronic Hamiltonian for N-electron ion in plasmas is added by the Yukawa-type electron-electron and nuclear interaction potential.

2. Optimized relativistic perturbation theory formalism for ions in plasmas

The detailed description of our approach was earlier presented (see, for example, Refs. [15-20]). Therefore, below we are limited only by the key points. The generalized relativistic energy approach combined with the RMBPT has been in detail described in Refs. [6,24-29]. It

generalizes earlier developed energy approach. The key idea is in calculating the energy shifts ΔE of degenerate states that is connected with the secular matrix M diagonalization [6,24,25]. To construct M, one should use the Gell-Mann and Low adiabatic formula for ΔE. The secular matrix elements are already complex in the PT second order. The whole calculation is reduced to calculation and diagonalization of the complex matrix M and definition of matrix of the coefficients with eigen state vectors $B^K_{k,i}$ [6,25]. To calculate all necessary matrix elements one must use the bases of the 1QP relativistic functions. Within an energy approach the total energy shift of the state is usually presented as [24]:

$$\Delta E = \mathrm{Re}\Delta E + i\,\Gamma/2 \qquad (1)$$

where Γ is interpreted as the level width and decay (transition) possibility $P = \Gamma$. The imaginary part of electron energy of the system, which is defined in the lowest PT order as [6]:

$$\mathrm{Im}\,\Delta E(B) = -\frac{e^2}{4\pi} \sum_{\substack{\alpha>n>f \\ [\alpha<n\le f]}} V^{|\omega_{\alpha n}|}_{\alpha n \alpha n}, \qquad (2)$$

$$V^{|\omega|}_{ijkl} = \iint dr_1 dr_2 \Psi^*_i(r_1)\Psi^*_j(r_2)\frac{\sin|\omega| r_{12}}{r_{12}}(1-\alpha_1\alpha_2)\Psi^*_k(r_2)\Psi^*_l(r_1) \qquad (3)$$

where $\sum$ for electron and $\sum$ for vacancy. The separated terms of the sum in (2) represent the contributions of different channels.

According to the definition, a lifetime of some excited state f is defined as follows (included all possible transition channels):

$$\tau_f = 1/\sum_{A,i} P^A_{f-i} \qquad (4)$$

for the transition rate P^A_{f-i} due to a radiative operator A. The transition rates via various multipole channels are determined as follows:

$$P^{E1}_{f-i} = \frac{2.02613\cdot 10^{18}}{\lambda^3 (2J_f+1)} S^{E1}_{f-i} \qquad (5a)$$

$$P^{M1}_{f-i} = \frac{2.69735\cdot 10^{13}}{\lambda^3 (2J_f+1)} S^{M1}_{f-i} \qquad (5b)$$

$$P^{E2}_{f-i} = \frac{1.11995\cdot 10^{18}}{\lambda^5 (2J_f+1)} S^{E2}_{f-i} \qquad (5c)$$

where λ is the wavelength (Å), J_f is the total angular momentum of the f state, $S^A_{f-i} \sim \mathrm{Im}\Delta E$ is a line strength due to the corresponding transition operator A (the decay channels E1, M1 and E2 represent the electric dipole, magnetic dipole, and electric quadrupole transition channels respectively). It is known [3,4,25] that the matrix elements computed with using the length gauge expressions converge faster than the velocity ones with respect to the configuration space of the orbital bases; the authors [3] considered the length gauge expressions for evaluating the foregoing transition properties.

This fact is directly linked with correct accounting for the correlation effects and using the optimized basis of wave functions. In [25] it has been proposed "ab initio" optimization principle for construction of cited basis. It uses a minimization of the gauge dependent multielectron contribution of the lowest QED PT corrections to the radiation widths of atomic levels. This contribution describes collective effects and it is dependent upon the electromagnetic potentials gauge (the gauge non-invariant contribution δE_{ninv}). The minimization of $\mathrm{Im}\delta E_{ninv}$ leads to integral differential equation, that is numerically solved. In result one can get the optimal one-electron basis of the PT [24-26]. It is worth to note that this approach was used while solving multiple problems of modern atomic, nuclear and molecular physics (see [30-38]).

Further let us firstly consider the Debye shielding model according to Refs. [15,16]. What is known from the classical theory of plasmas developed by Debye-Hückel, the interaction potential between two charged particles is modeled by the Yukawa-type potential, which contains the shielding parameter μ. The parameter μ is connected with the plasma parameters such as

the temperature T and the charge density n as follows: $\mu \sim \sqrt{e^2(1+Z)n_e / k_B T_e}$. Here, as usually, e is the electron charge and κ_B is the Boltzman constant. The density n is given as a sum of the electron density N_e and ion density N_k of the k-th ion species having the nuclear charge

$$q_k : n = N_e + \sum_k q_k^2 N_k . \qquad (6)$$

It is very useful to remind the simple estimates for the shielding parameter. For example, under typical laser plasmas conditions of T~ 1keV and n~ 10^{22} cm^{-3} the parameter μ is of the order of 0.1 in atomic units; in the EBIT plasmas T~ 0.05keV, n~10^{18} cm^{-3} and μ~10^{-3}. We are interested in studying the spectral parameters of ions in plasmas with the temperature T~ 0.1-1keV (10^6-10^7K) and n~10^{14}-10^{26} cm^{-3} (μ~10^{-5}-10^0). It should be noted that indeed the Debye screening for the atomic electrons in the Coulomb field of nuclear charge is well understood due to the presence of the surrounding plasma electrons with high mobility. On the other hand, the contribution due to the Debye screening between electrons would be of smaller magnitude orders. Majority of the previous works on the spectroscopy study have considered the screening effect only in the electron-nucleus potential where the electron-electron interaction potential is truncated at its first term of the standard exponential expansion for its dominant contribution [3]. However, it is also important to take into account the screening in the electron- electron interactions for large plasma strengths to achieve more realistic results in the search for stability of the atomic structure in the plasma environment.

By introducing the Yukawa-type e-N and e-e interaction potentials, an electronic Hamiltonian for N-electron ion in a plasma is in atomic units as follows [15,16]:

$$H = \sum_i [\alpha cp - \beta mc^2 - Z\exp(-\mu r_i)/r_i] + \sum_{i>j} \frac{(1-\alpha_i\alpha_j)}{r_{ij}} \exp(-\mu r_{ij}) \qquad (7)$$

To generate the wave functions basis we use the optimized Dirac-Kohn-Sham potential with one parameter [15], which is calibrated within the special ab initio procedure within the relativistic energy approach [24]. The modified PC numerical code 'Superatom" is used in all calculations. Other details can be found in Refs. [15-20,22,23,38].

3. Results and conclusion

Firstly, we present our results on the transition probabilities and lifetimes for some excited states of the Li-like ion of calcium. The spectroscopic properties for plasma-isolated ion with μ=0 have been considered. In Tables 1 and 2 there are listed probabilities values for transitions (E1, M1, and E2 channels) from the excited states to the low-lying states of Ca XVIII. Using these values, one could calculate the corresponding lifetimes of the excited states.

Table 1.

The transition probabilities (P) for some transitions in spectrum of Ca XVIII: RCC - relativistic coupled-cluster (RCC) method [3]; This - this work

Transition	$P_{f\to i}$	$P_{f\to i}$
f-i	RCC	This
$2p_{1/2}$-(E1)-$2s_{1/2}$	1.31[9]	1.33[9]
$2p_{3/2}$-(E1)-$2s_{1/2}$	2.00[9]	2.02[9]
-(M1)-$2p_{1/2}$	7.00[2]	7.03[2]
-(E2)-$2p_{1/2}$	2.54[-2]	2.57[-2]
$3s_{1/2}$- M1 -$2s_{1/2}$	2.04[4]	2.06[4]
-(E1)-$2p_{1/2}$	3.01[11]	3.02[11]
-(E1)-$2p_{3/2}$	6.22[11]	6.24[11]

The analysis shows that the presented data are in physically reasonable agreement with the NIST experimental data and theoretical

Table 2.

The transition probabilities (P) for some transitions in spectrum of Ca XVIII (our data)

Transition	$P_{f\to i}$
f-i	This
$3p_{1/2}$ - E1-$2s_{1/2}$	2.37[12]
- M1-$2p_{1/2}$	1.48[3]
- M1-$2p_{3/2}$	6.78[4]
- E2-$2p_{3/2}$	8.45[8]
- E1-$3s_{1/2}$	1.72[8]
$3p_{3/2}$ - E1-$2s_{1/2}$	2.32[12]
- M1-$2p_{1/2}$	1.24[4]
- E2-$2p_{3/2}$	4.25[8]
- M1-$2p_{3/2}$	2.78[4]
- E2-$2p_{3/2}$	4.22[8]
- E1-$3s_{1/2}$	2.66[8]
- M1-$3p_{1/2}$	1.83[1]
- E2-$3p_{1/2}$	2.13[-3]

results by relativistic coupled-cluster (RCC) method calculation [3]. However, some difference between the corresponding results can be explained by using different relativistic orbital bases and by difference in the model of accounting for the screening effect as well as some numerical differences. In Tables 3 and 4 we list the numerical variations in the lifetimes of the $2p_{1/2}$, $3s_{1/2}$, $3p_{1/2}$, $3d_{3/2}$, and $4s_{1/2}$ states in Ca XVIII for different μ values. It is worth to note that our computing oscillator strengths within energy

Table 3.

The dependence of the lifetimes (ps) of the $2p_{1/2}$ state in the Ca XVIII spectrum upon the screening parameter μ: RCC - relativistic coupled-cluster (RCC) method [3]; This - this work

μ	$2p_{1/2}$	$2p_{1/2}$
	RCC	This
0.133	741	738
0.667	494	492
1.000	334	332
1.250	242	241
1.429	192	190
0.60	140	138

Table 4.

The dependence of the lifetimes (ps) of the 3lj,4lj states in the Ca XVIII spectrum upon the parameter μ (this work)

μ	$3s_{1/2}$	$3p_{1/2}$	$3d_{3/2}$	$4s_{1/2}$
0.133	1.07	0.428	0.143	1.62
0.667	1.26	0.518	0.688	2.54
1.000	1.53	0.658	0.206	4.81
1.250	1.85	0.849	0.262	12.48
1.429	2.20	1.072	0.336	82.77

approach with different forms of transition operator (i.e. using the photon propagators in the form of Coulomb, Feynman or Babushkin) gives very close results.

References

1. Yongqiang, Li Y., Wu, J., Hou, Y., Yuan, J. Influence of hot and dense plasmas on energy levels and oscillator strengths of ions: Be-like ions for Z = 26–36, *J. Phys. B: At. Mol. Opt. Phys.* **2008,** *41,* 145002.
2. Saha B., Fritzsche S. Influence of dense plasma on the low-lying transitions in Be-like ions: relativistic multiconfiguration Dirac–Fock calculation. *J. Phys. B: At. Mol. Opt. Phys.* **2007,** *40,* 259-270.
3. Madhulita Das, Sahoo B. K., Sourav Pal. Relativistic spectroscopy of plasma embedded Li-like systems with screening effects in two-body Debye potentials. *J. Phys. B: At. Mol. Opt. Phys.* **2014,** *47*, 175701.
4. Han, Y.-C., Madsen, L.B. Comparison between length and velocity gauges in quantum simulations of high-order harmonic

generation *Phys. Rev. A*. **2010**, *81*, 06343.
5. Glushkov, A.V., Khetselius, O.Yu., Svinarenko, A.A., Buyadzhi, V.V., *Spectroscopy of autoionization states of heavy atoms and multiply charged ion*s. TEC: Odessa, **2015**.
6. Ivanov, L.N., Ivanova, E.P., Aglitsky, E. Modern trends in the spectroscopy of multicharged ions. *Phys. Rep.* **1988,** *166.*
7. Bandrauk, A.D., Fillion-Gourdeau, F., Lorin, E. Atoms and molecules in intense laser fields: gauge invariance of theory and models *J. Phys. B: At. Mol. Opt. Phys*. **2013**, *46*, 153001
8. Glushkov, A.V., Malinovskaya, S.V., Prepelitsa, G.P., Ignatenko, V. Manifestation of the new laser-electron nuclear spectral effects in the thermalized plasma: QED theory of co-operative laser-electron-nuclear processes. *J. Phys.: Conf. Ser.* **2005,** *11,* 199-206.
9. Gubanova, E., Glushkov, A.V., Khetselius, O.Yu., Bunyakova, Yu.Ya., Buyadzhi, V.V., Pavlenko, E.P. New methods in analysis and project management of environmental activity: Electronic and radioactive waste. FOP: Kharkiv, **2017**.
10. Glushkov, A.V., Malinovskaya, S.V., Chernyakova Y.G., Svinarenko, A.A. Co-operative laser-electron-nuclear processes: QED calculation of electron satellites spectra for multi-charged ion in laser field. *I. J. Quant. Ch.* **2004,** *99,* 889.
11. Glushkov, A., Malinovskaya, S., Loboda, A., Shpinareva, I., Gurnitskaya, E., Korchevsky, D. Diagnostics of the collisionally pumped plasma and search of the optimal plasma parameters of x-ray lasing: calculation of electron-collision strengths and rate coefficients for Ne-like plasma. *J. Phys.: Conf. Ser.* **2005,** *11,* 188-198.
12. Glushkov, A., Ambrosov, S., Loboda, A., Gurnitskaya, E., Prepelitsa, G. Consistent QED approach to calculation of electron-collision excitation cross sections and strengths: Ne-like ions. *Int. J. Quant. Chem.* **2005,** *104,* 562-569.
13. Ignatenko, A.V. Probabilities of the radiative transitions between Stark sublevels in spectrum of atom in an DC electric field: New approach. *Photoelectronics,* **2007,** *16*, 71-74.
14. Glushkov, A.V., Ambrosov, S.V., Ignatenko, A. Non-hydrogenic atoms and Wannier-Mott excitons in a DC electric field: Photoionization, Stark effect, Resonances in ionization continuum and stochasticity. *Photoelect.,* **2001,** *10*, 103.
15. Buyadzhi, V., Kuznetsova, A., Buyadzhi, A., Ternovsky, E.V., Tkach, T.B. Advanced quantum approach in radiative and collisional spectroscopy of multicharged ions in plasmas. Adv. in Quant. Chem. (Elsevier). **2019**, *78*, 171-191,
16. Glushkov, A., Buyadzhi, V., Svinarenko, A., Ternovsky, E. Advanced relativistic energy approach in electron-collisional spectroscopy of multicharged ions in plasma. *Concepts, Methods, Applications of Quantum Systems in Chemistry and Physics* (Springer). **2018**, *31*, 55-69.
17. Buyadzhi, V.V., Chernyakova, Yu.G., Smirnov, A.V., Tkach, T.B. Electron-collisional spectroscopy of atoms and ions in plasma: Be-like ions. *Photoelectronics*. **2016,** *25,* 97-101.
18. Buyadzhi, V.V., Chernyakova, Yu.G., Antoshkina, O.A., Tkach, T.B. Spectroscopy of multicharged ions in plasmas: Oscillator strengths of Be-like ion Fe. *Photoelectronics.* **2017,** *26,* 94..
19. Buyadzhi, V. Laser multiphoton spectroscopy of atom embedded in Debye plasmas: multiphoton resonances and transitions. *Photoelectronics.* **2015,** *24,* 128-133.
20. Buyadzhi, V., Zaichko, P., Antoshkina, O., Kulakli T., Prepelitsa P., Ternovsky V., Mansarliysky, V. Computing of radiation parameters for atoms and multicharged ions within relativistic energy approach: Advanced Code. *J. Phys.: Conf. Ser*. **2017**, *905*(1), 012003.
21. Glushkov, A., Svinarenko, A., Ignatenko, A. Spectroscopy of autoionization resonances in spectra of the lanthanides atoms. *Photoelectronics*. **2011**, *20*, 90-94.
22. Glushkov, A.V. *Relativistic Quantum theory. Quantum mechanics of atomic systems;* Astroprint: Odessa, **2008**.

23. Khetselius, O.Yu. *Hyperfine structure of atomic spectra*. Astroprint: Odessa, **2008**.
24. Glushkov, A., Ivanov, L., Ivanova, E.P. Autoionization Phenomena in Atoms. *Moscow Univ. Press*, Moscow, **1986,** 58.
25. Glushkov, A.V., Ivanov, L.N. Radiation decay of atomic states: atomic residue polarization and gauge noninvariant contributions. *Phys. Lett.A.* **1992,** *170,* 33.
26. Glushkov, A.V. Spectroscopy of atom and nucleus in a strong laser field: Stark effect and multiphoton resonances. *J. Phys.: Conf. Ser*. **2014**, *548*, 012020.
27. Glushkov, A., Svinarenko, A., Ternovsky, V., Smirnov, A., Zaichko, P. Spectroscopy of the complex autoionization resonances in spectrum of helium: Test and new spectral data. *Photoelectr*. **2015**, *24*, 94.
28. Glushkov A.V.; Ivanov, L.N. DC strong-field Stark effect: consistent quantum-mechanical approach. *J. Phys. B: At. Mol. Opt. Phys.* **1993,** *26,* L379-386.
29. Khetselius, O.Yu. *Quantum structure of electroweak interaction in heavy finite Fermi-systems*. Astroprint: Odessa, **2011**.
30. Khetselius, O.Yu., Lopatkin, Yu.M., Dubrovskaya, Yu.V, Svinarenko, A.A. Sensing hyperfine-structure, electroweak interaction and parity non-conservation effect in heavy atoms and nuclei: New nuclear-QED approach. *Sensor Electr. and Microsyst. Techn*. **2010,** 7(2), 11-19.
31. Khetselius, O.Yu. Relativistic perturbation theory calculation of the hyperfine structure parameters for some heavy-element isotopes. *Int. J. Quant. Chem.* **2009,** *109,* 3330–3335.
32. Khetselius, O. Relativistic calculation of the hyperfine structure parameters for heavy elements and laser detection of heavy isotope. *Phys. Scr.* **2009,** *135,*01402
33. Svinarenko, A.A., Glushkov, A.V., Khetselius, O.Yu., Ternovsky, V.B., Dubrovskaya, Yu., Kuznetsova, A., Buyadzhi, V. Theoretical spectroscopy of rare-earth elements: spectra and autoionization resonances. *Rare Earth Element*, Ed. J.Orjuela (InTech). **2017**, 83.
34. Glushkov, A.V., Khetselius, O.Yu., Svinarenko, A.A., Buyadzhi, V.V., Ternovsky, V.B, Kuznetsova, A., Bashkarev, P Relativistic perturbation theory formalism to computing spectra and radiation characteristics: application to heavy element. *Recent Studies in Perturbation Theory*, InTech. **2017**, 131.
35. Dubrovskaya, Yu., Khetselius, O.Yu., Vitavetskaya, L., Ternovsky, V., Serga, I. Quantum chemistry and spectroscopy of pionic atomic systems with accounting for relativistic, radiative, and strong interaction effects. *Adv. Quantum Chem.* **2019,** *78*, 193-222.
36. Khetselius, O.Yu., Glushkov, A.V., Dubrovskaya, Yu.V., Chernyakova, Yu.G., Ignatenko, A.V., Serga, I.N., Vitavetskaya, L. Relativistic quantum chemistry and spectroscopy of exotic atomic systems with accounting for strong interaction effects. In *Concepts, Methods and Applications of Quantum Systems in Chem. and Phys.* Springer. **2018,** *31*, 71.
37. Glushkov, A., Buyadzhi, V., Kvasikova, A., Ignatenko, A., Kuznetsova, A., Prepelitsa, G., Ternovsky, V. Non-Linear chaotic dynamics of quantum systems: Molecules in an electromagnetic field and laser systems. In: Tadjer A, Pavlov R, Maruani J, Brändas E, Delgado-Barrio G (eds) Quantum Systems in Physics, Chemistry, and Biology. Springer, Cham. **2017**, *30*, 169-180.
38. Glushkov, A.V., Khetselius, O.Yu., Svinarenko, A.A., Buyadzhi, V.V., *Methods of computational mathematics and mathematical physics*. *P.1*.TES: **2015**.

PACS 31.15.-p

E. V. Ternovsky

RELATIVISTIC SPECTROSCOPY OF MULTICHARGED IONS IN PLASMAS: Li-LIKE IONS

Summary. The transition probabilities and lifetimes for different excited states in spectrum of the Li-like calcium are computed within the consistent relativistic many-body approach for different values of the plasmas screening parameter (correspondingly, electron density and temperature) and compared with available alternative data. The approach is based on the generalized relativistic energy approach combined with the optimized relativistic many-body perturbation theory with the Dirac-Debye shielding model as zeroth approximation, adapted for application to study of the spectral parameters of ions in plasmas. An electronic Hamiltonian for N-electron ion in plasmas is added by the Yukawa-type electron-electron and nuclear interaction potential.

Key words: spectroscopy of ions in plasmas, relativistic energy approach, radiative transition probabilities

PACS 31.15.-p

Е. В. Терновский

РЕЛЯТИВИСТСКАЯ СПЕКТРОСКОПИЯ МНОГОЗАРЯДНЫХ ИОНОВ В ПЛАЗМЕ: Li-ПОДОБНЫЕ ИОНЫ

Резюме. Вероятности переходов и времена жизни для различных возбужденных состояний в спектре Li-подобного кальция вычисляются в рамках последовательного релятивистского многочастичного подхода для различных значений параметра экранирования плазмы (соответственно, электронной плотности и температуры) и сравниваются с имеющимися альтернативными данными. Подход основан на обобщенном релятивистском энергетическом подходе, совмещенном с формализмом оптимизированной релятивистской многочастичной теории возмущений с приближением Дирака-Дебая в качестве нулевого приближения, адаптированной для применения при изучении спектральных параметров ионов в плазме. Электронный гамильтониан для иона N-электронов в плазме добавляется потенциалом электрон-электронного и ядерного взаимодействия типа Юкавы.

Ключевые слова: спектроскопия ионов в плазме, энергетический подход, вероятности радиационных переходов

PACS 31.15.-p

Є В. Терновський

РЕЛЯТИВІСТСЬКА СПЕКТРОСКОПІЯ БАГАТОЗАРЯДНИХ ІОНІВ В ПЛАЗМІ: Li-ПОДІБНІ ІОНИ

Резюме. Ймовірності переходів і часи життя для різних збуджених станів в спектрі Li-подібного кальцію обчислюються в рамках послідовного релятивістського багаточастинко-

вого підходу для різних значень параметра екранування плазми (відповідно, електронної щільності і температури) і порівнюються з наявними альтернативними даними. Підхід ґрунтується на узагальненому релятивістському енергетичному підході, поєднаному з формалізмом оптимізованої релятивістської багаточастинкової теорії збурень з наближенням Дірака-Дебая в якості нульового наближення, адаптованого для застосування при вивченні спектральних параметрів іонів у плазмі. Електронний гамільтоніан для іона N-електронів в плазмі додається потенціалом електрон-електронного та ядерного взаємодії типу Юкави.

Ключові слова: спектроскопія іонів в плазмі, енергетичний підхід, ймовірності радіаційних переходів

PACS 31.15.A-;32.30.-r

O. L. Mykhailov, E. A. Efimova, E. V. Ternovsky, R. E. Serga

Odessa State Environmental University, L'vovskaya str.15, Odessa-9, 65016, Ukraine
E-mail: mykhailovol94@gmail.com

HYPERFINE STRUCTURE PARAMETERS FOR Li-LIKE MULTICHARGED IONS WITHIN RELATIVISTIC MANY-BODY PERTURBATION THEORY

Abstract. The relativistic many-body perturbation theory with the optimized Dirac-Kohn-Sham zeroth approximation is applied to calculation of the hyperfine structure parameters for some Li-like multicharged ions. The relativistic, exchange-correlation and other corrections are accurately taken into account. The optimized relativistic orbital basis set is generated in the optimal many-body perturbation theory approximation with fulfilment of the gauge invariance principle. The obtained data on the hyperfine structure parameters of the Li-like multicharged ions are analyzed and compared with alternative theoretical and experimental results.

1. Introduction

In last years a studying the spectra of heavy and superheavy elements atoms and ions is of a great interest for further development as atomic and nuclear theories (c.f.[1-12]). Theoretical methods used to calculate the spectroscopic characteristics of heavy and superheavy ions may be divided into three main groups: a) the multi-configuration Hartree-Fock method, in which relativistic effects are taken into account in the Pauli approximation, gives a rather rough approximation, which makes it possible to get only a qualitative idea on the spectra of heavy ions. b) The multi-configuration Dirac-Fock (MCDF) approximation (the Desclaux program, Dirac package) [1-4] is, within the last few years, the most reliable version of calculation for multielectron systems with a large nuclear charge; in these calculations one- and two-particle relativistic effects are taken into account practically precisely.

The calculation program of Desclaux is compiled with proper account of the finiteness of the nucleus size; however, a detailed description of the method of their investigation of the role of the nucleus size is lacking.

In the region of small Z (Z is a charge of the nucleus) the calculation error in the MCDF approximation is connected mainly with incomplete inclusion of the correlation and exchange effects which are only weakly dependent on Z; c) In the study of lower states for ions with $Z \leq 40$ an expansion into double series of the PT on the parameters 1/Z, aZ (a is the fine structure constant) turned out to be quite useful. It permits evaluation of relative contributions of the different expansion terms: non-relativistic, relativistic, QED contributions as the functions of Z.

Nevertheless, the serious problems in calculation of the heavy elements spectra are connected with developing new, high exact methods of account for the QED effects, in particular, the Lamb shift (LS), self-energy (SE) part of the Lamb shift, vacuum polarization (VP) contribution, correction on the nuclear finite size for superheavy elements and its account for different spectral properties of these systems, including calculating the energies and constants of the hyperfine structure, deriviatives of the one-electron characteristics on nuclear radius, nuclear electric quadrupole, magnetic dipole moments etc (c.f.[1-10]).

In this paper the relativistic many-body perturbation theory with the optimized Dirac-Kohn-Sham zeroth approximation [11-19] is applied to calculation of the hyperfine structure parameters for Li-like multicharged ions. The relativistic, exchange-correlation and nuclear effects corrections are accurately taken into account with using the consistent and high precise procedures (c.g. [11-17]).

2. Relativistic many-body perturbation theory with optimized zeroth approximation and energy approach

The theoretical basis of the RMBPT with the Dirac-Kohn-Sham zeroth approximation was widely discussed [11-17], and here we will only present the essential features. As usually, we use the charge distribution in atomic (ionic) nucleus *r(r)* in the Gaussian approximation:

$$\rho(r|R) = \left(4\gamma^{3/2}/\sqrt{\pi}\right)\exp\left(-\gamma r^2\right) \qquad (1)$$

where $\gamma=4/pR^2$ and R is the effective nucleus radius. The Coulomb potential for the spherically symmetric density $r(r)$ is:

$$V_{nucl}(r|R) = -\left((1/r)\int_0^r dr' r'^2 \rho\left(r'\middle|R\right) + \int_r^\infty dr' r' \rho\left(r'\middle|R\right)\right) \qquad (2)$$

Further consider the Dirac-like type equations for the radial functions F and G (components of the Dirac spinor) for a three-electron system $1s^2nlj$. Formally a potential $V(r|R)$ in these equations includes electric and polarization potentials of the nucleus, V_X is the exchange inter-electron interaction (in the zeroth approximation). The standard Kohn-Sham (KS) exchange potential is [13]:

$$V_X^{KS}(r) = -(1/\pi)[3\pi^2\rho(r)]^{1/3}. \qquad (3)$$

In the local density approximation the relativistic potential is [33]:

$$V_X[\rho(r), r] = \frac{\delta E_X[\rho(r)]}{\delta\rho(r)}, \qquad (4)$$

where $E_X[\rho(r)]$ is the exchange energy of the multielectron system corresponding to the homogeneous density $\rho(r)$, which is obtained from a Hamiltonian having a transverse vector potential describing the photons. In this theory the exchange potential is [3,4]:

$$V_X[\rho(r), r] = V_X^{KS}(r)\cdot\left\{\frac{3}{2}\ln\frac{[\beta+(\beta^2+1)^{1/2}]}{\beta(\beta^2+1)^{1/2}} - \frac{1}{2}\right\}, \qquad (5)$$

where $\beta = [3\pi^2\rho(r)]^{1/3}/c$, c is the velocity of light. The corresponding one-quasiparticle correlation potential

$$V_C[\rho(r), r] = -0.0333\cdot b\cdot\ln[1+18.3768\cdot\rho(r)^{1/3}], \qquad (6)$$

(here b is the optimization parameter; see below).

The perturbation operator contains the relativistic potential of the interelectron interaction of the form:

$$V_{e-e}^{rel}(r_i, r_j) = \frac{\left(1-\alpha_i\alpha_j\right)}{r_{ij}}\exp(i\omega_{ij}r_{ij}), \qquad (7)$$

(here a_i ,a_j are the Dirac matrices, w_{ij} is the transition frequency) with the subsequent subtraction of the exchange and correlation potentials. The rest of the exchange and correlation effects is taken into account in the first two orders of the PT (c.g.[3-5].

In Refs. [20-29] it was presented the effective relativistic formalism with ab initio optimization principle for construction of the optimal relativistic orbital basis set. The minimization condition of the gauge dependent multielectron contribution of the lowest QED PT corrections to the radiation widths of the atomic levels is used. The alternative versions are proposed in refs. [30-37].

The general scheme of treatment of the spectra for Li-like ion is as follows. Consider the Dirac-type equations for a three-electron system $1s^2nlj$. Formally they fall into one-electron Dirac equations for the orbitals $1s$ 1s and nlj with the potential:

$$V(r) = 2V(r|1s) + V(r|nlj) + V_x(r) + V(r|R) \qquad (8)$$

$V(r|R)$ includes the electrical and the polarization potentials of the nucleus; the components of the self-consistent Hartree-like potential, V_{ex} is the exchange inter-electron interaction (look below). The main exchange effect will be taken into account if in the equation for the $1s$ orbital we assume

$$V(r) = V(r|1s) + V(r|nlj) \qquad (9)$$

and in the equation for the nlj orbital

$$V(r) = 2V(r|1s) \qquad (10)$$

The rest of the exchange and correlation effects will be taken into account in the first two orders of the PT by the total inter-electron interaction [13-17].

The used expression for $\rho(r|1s)$ coincides with the precise one for a one-electron relativistic atom with a point nucleus. The finiteness of the nucleus and the presence of the second 1*s* electron are included effectively into the energy E_{1s}.

Actually, for determination of the properties of the outer *nlj* electron one iteration is sufficient. Refinement resulting from second iteration (by evaluations) does not exceed correlation corrections of the higher orders omitted in the present calculation.

The relativistic potential of core (the "screening" potential) $2V^{(1)}(r|1s) = V_{scr}$ has correct asymptotic at zero and in the infinity. The procedures for accounting of the nuclear, radiative QED corrections are in details presented in Refs. [3-5,14, 39-42].

3. Results and Conclusions

Energies of the quadruple (W_q) and magnetic dipole (W_m) interactions, which define a hyperfine structure, are calculated as follows [4]:

$$W_q = [D+C(C+1)]B,$$

$$W_m = 0{,}5\,AC,$$

$$D = -(4/3)(4c-1)(I+1)/[i(I-1)(2I-1)],$$

$$C = F(F+1)-J(J+1)-I(I+1). \qquad (16)$$

Here I is a spin of nucleus, F is a full momentum of system, J is a full electron momentum. Constants of the hyperfine splitting are expressed through the standard radial integrals:

$$A = \{[(4{,}32587)10^{-4}Z^2cg_I]/(4c^2-1)\}(RA)_{-2}, \qquad (17)$$

$$B = \{7.2878\ 10^{-7}\ Z^3Q/[(4c^2-1)I(I-1)\}\ (RA)_{-3},$$

Here g_I is the Lande factor, Q is a quadruple momentum of nucleus (in Barn); radial integrals are defined as follows:

$$(RA)_{-2} = \int_0^\infty drr^2F(r)G(r)U(1/r^2,R),$$

$$(RA)_{-3} = \int_0^\infty drr^2[F^2(r)+G^2(r)]U(1/r^3,R) \qquad (18)$$

and calculated in the Coulomb units (=3,57 $10^{20}Z^2m^{-2}$; = 6,174 $10^{30}Z^3m^{-3}$ for valuables of the corresponding dimension). The radial parts F and G of two components of the Dirac function for electron, which moves in the potential $V(r,R)+U(r,R)$, are determined by solution of the Dirac equations (look above).

We have carried out the calculation of constants of the hyperfine interaction: the electric quadruple constant B, the magnetic dipole constant A with inclusion of nuclear finiteness and the Uehling potential for Li-like ions (c.g. [3-5]).

In table 4 the calculation results for the constants of the hyperfine splitting for the lowest excited states of Li-like ions are presented.

Analogous data for other states have been presented earlier (see ref. [5,20]). Our calculation showed also that a variation of the nuclear radius on several persents could lead to to changing the transition energies on dozens of thousands 10^3cm^{-1}.

Table 1.

Constants of the hyperfine electron-nuclear interaction: $A=Z^3g_I\ \overline{A}$ cm^{-1}, $B=\dfrac{Z^3Q}{I(2I-1)}\overline{B}$ cm^{-1}

nlj	*Z*	69	79	92
2s	$\overline{A}$	176 -02	215 -02	314 -02
3s	$\overline{A}$	51 –03	63 –03	90 –03
4s	$\overline{A}$	19 –03	24 –03	36 –03

$2p_{1/2}$	$\overline{A}$	56 –03	71 –03	105 –02
$3p_{1/2}$	$\overline{A}$	16 –03	20 –03	31 –03
$4p_{1/2}$	$\overline{A}$	72 –04	91 –04	11 –03
$2p_{3/2}$	$\overline{A}$	67 –04	71 –04	72 –04
	$\overline{B}$	13 –04	15 –04	17 –04
$3p_{3/2}$	$\overline{A}$	19 –04	21 –04	22 –04
	$\overline{B}$	51 –05	55–05	62 –05
$4p_{3/2}$	$\overline{A}$	89 –05	92 –05	8 –04
	$\overline{B}$	20 –05	22 –05	26 –05
$3d_{3/2}$	$\overline{A}$	10 –04	11 –04	12 –04
	$\overline{B}$	9 –05	10 –05	11 –05
$4d_{3/2}$	$\overline{A}$	51 –05	55 –05	58 –05
	$\overline{B}$	44 –06	50 –06	56 –06
$3d_{5/2}$	$\overline{A}$	48 –05	50 –05	52 –05
	$\overline{B}$	38 –06	39 –06	40 –06
$4d_{5/2}$	$\overline{A}$	19 –05	20 –05	21 –05
	$\overline{B}$	15 –06	16 –06	17 –06

References

1. Grant I. *Relativistic Quantum Theory of Atoms and Molecules.* Oxford, **2007**.
2. Glushkov, A; Khetselius, O; Svinarenko, A; Buyadzhi, V. *Spectroscopy of autoionization states of heavy atoms and multiply charged ions*. Odessa: **2015**.
3. Glushkov, A.V. *Relativistic and correlation effects in spectra of atomic systems*. Astroprint: Odessa, **2006**.
4. Khetselius, O.Yu. *Hyperfine structure of atomic spectra*. Astroprint: Odessa, **2008**.
5. Glushkov, A.V. *Relativistic Quantum theory. Quantum mechanics of atomic systems*. Astroprint: Odessa, **2008**.
6. Khetselius, O.Yu. Atomic parity non-conservation effect in heavy atoms and observing P and PT violation using NMR shift in a laser beam: To precise theory. *J. Phys.: Conf. Ser.* **2009,** *194,* 022009
7. Khetselius, O.Yu. Hyperfine structure of radium. *Photoelectronics*. **2005,** *14,* 83.
8. Khetselius, O.. Relativistic perturbation theory calculation of the hyperfine structure parameters for some heavy-element isotopes. *Int. Journ. Quant. Chem.* **2009,** *109,* 3330-3335.
9. Khetselius, O.Yu. Relativistic calculation of the hyperfine structure parameters for heavy elements and laser detection of the heavy isotopes. *Phys.Scripta.* **2009,** *135,* 014023.
10. Khetselius, O.Yu. Relativistic Hyperfine Structure Spectral Lines and Atomic Parity Non-conservation Effect in Heavy Atomic Systems within QED Theory. *AIP Conf. Proc.* **2010,** *1290(1),* 29-33.
11. Khetselius, O. Relativistic Calculating the Spectral Lines Hyperfine Structure Parameters for Heavy Ions. *AIP Conf. Proc.* **2008,** *1058,* 363-365.
12. Khetselius O.Yu.; Gurnitskaya, E.P. Sensing the hyperfine structure and nuclear quadrupole moment for radium. *Sensor Electr. and Microsyst. Techn.* **2006,** *2,* 25-29.
13. Khetselius, O.Yu.; Gurnitskaya, E.P. Sensing the electric and magnetic moments of a nucleus in the N-like ion of Bi. *Sensor Electr. and Microsyst. Techn.* **2006,** *3,* 35-39.
14. Khetselius, O.Yu. *Quantum structure of electroweak interaction in heavy finite Fermi-systems.* Astroprint: Odessa, **2011**.
15. Svinarenko, A.A. Study of spectra for lanthanides atoms with relativistic many- body perturbation theory: Rydberg resonances. *J. Phys.: Conf. Ser.* **2014,** *548,* 012039.
16. Svinarenko, A.A. Study of spectra for lanthanides atoms with relativistic many- body perturbation theory: Rydberg resonances. *J. Phys.: Conf. Ser.* **2014,** *548,* 012039.
17. Svinarenko, A.A.; Ignatenko, A.V.; Ternovsky, V.B.; Nikola, L.V.; Seredenko, S.S.; Tkach, T.B. Advanced relativistic model potential approach to calculation of radiation

transition parameters in spectra of multicharged ions. *J. Phys.: Conf. Ser.* **2014,** *548,* 012047.
18. Florko, T.A.; Tkach, T.B.; Ambrosov, S.V.; Svinarenko, A.A. Collisional shift of the heavy atoms hyperfine lines in an atmosphere of the inert gas. *J. Phys.: Conf. Ser*. **2012**, *397*, 012037.
19. Ivanova, E.P.; Ivanov, L.N.; Glushkov, A.V.; Kramida, A.E. High order corrections in the relativistic perturbation theory with the model zeroth approximation, Mg-Like and Ne-Like Ions. *Phys. Scripta* 1985, *32,* 513-522.
20. Ivanov, L. N.; Ivanova, E. P.; Aglitsky, E. V. Modern Trends in the Spectroscopy of Multicharged Ions. *Phys. Rep*. **1988**, *166,* 315-390.
21. Glushkov, A.V.; Ivanov, L.N.; Ivanova, E.P. Autoionization Phenomena in Atoms. *Moscow University Press*, Moscow, **1986,** 58-160
22. Glushkov, A.V.; Ivanov, L.N. Radiation decay of atomic states: atomic residue polarization and gauge noninvariant contributions. *Phys. Lett. A* **1992,** *170,* 33-36.
23. Glushkov A.V.; Ivanov, L.N. DC strong-field Stark effect: consistent quantum-mechanical approach. *J. Phys. B: At. Mol. Opt. Phys.* **1993,** *26,* L379-386.
24. Glushkov, A.V. Spectroscopy of atom and nucleus in a strong laser field: Stark effect and multiphoton resonances. *J. Phys.: Conf. Ser*. **2014**, *548*, 012020
25. Glushkov, A.V. Spectroscopy of cooperative muon-gamma-nuclear processes: Energy and spectral parameters *J. Phys.: Conf. Ser.* **2012,** *397,* 012011
26. Glushkov, A.V. Advanced Relativistic Energy Approach to Radiative Decay Processes in Multielectron Atoms and Multicharged Ions. *In Quantum Systems in Chemistry and Physics: Progress in Methods and Applications, Series: Progress in Theoretical Chemistry and Physics*; Nishikawa, K., Maruani, J., Brandas, E., Delgado-Barrio, G., Piecuch, P., Eds.; Springer: Dordrecht, **2012**; Vol. 26, pp 231–252.
27. Glushkov, A. Multiphoton spectroscopy of atoms and nuclei in a laser field: relativistic energy approach and radiation atomic lines moments method// Adv. Quant.Chem. (Elsevier), **2018**, *7*8, doi.org/10.1016/bs.aiq.2018.06.004
28. Khetselius, O.Yu. Relativistic Energy Approach to Cooperative Electron-γ-Nuclear Processes: NEET Effect *In Quantum Systems in Chemistry and Physics, Series: Progress in Theoretical Chemistry and Physics;* Nishikawa, K., Maruani, J., Brändas, E., Delgado-Barrio, G., Piecuch, P., Eds.; Springer: Dordrecht, **2012;** Vol. 26, pp 217-229.
29. Khetselius, O.Yu. Optimized Perturbation Theory for Calculating the Hyperfine Line Shift and Broadening of Heavy Atoms in a Buffer Gas. *In Frontiers in Quantum Methods and Applications in Chemistry and Physics*, *Series: Progress in Theoretical Chemistry and Physics;* Springer: Cham, **2015;** Vol. 29, pp. 55-76.
30. Khetselius, O.Yu. Optimized relativistic many-body perturbation theory calculation of wavelengths and oscillator strengths for Li-like multicharged ions. Adv. Quant. Chem. **2019**, *78*, 223-251.
31. Khetselius, O.Yu. *Quantum structure of electroweak interaction in heavy finite Fermi-systems.* Astroprint: Odessa, **2011**.
32. Svinarenko, A. A., Glushkov, A. V., Khetselius, O.Yu., Ternovsky,V.B., Dubrovskaya, Yu., Kuznetsova, A., Buyadzhi, V. Theoretical spectroscopy of rare-earth elements: spectra and autoionization resonances. *Rare Earth Element*, InTech. **2017**, pp 83-104.
33. Glushkov, A.V., Khetselius, O.Yu., Svinarenko A.A., Buyadzhi, V.V., Ternovsky, V.B, Kuznetsova, A., Bashkarev, P Relativistic perturbation theory formalism to computing spectra and radiation characteristics: application to heavy element. *Recent Studies in Perturbation Theory*, ed. D. Uzunov (InTech) **2017**, 131-150.
34. Glushkov A., Lovett L., Khetselius O., Gurnitskaya E., Dubrovskaya Y., Loboda A. Generalized multiconfiguration model of decay of multipole giant resonances applied to analysis of reaction (m-n) on the nucleus

^{40}Ca. *Int. J. Mod. Phys. A*. **2009**, *24*(2-3), 611-615
35. Glushkov, A.V.; Malinovskaya S.V. Co-operative laser nuclear processes: border lines effects *In New Projects and New Lines of Research in Nuclear Physics.* World Sci.: Singapore, **2003**, 242-250.
36. Buyadzhi, V.V.; Chernyakova, Yu.G.; Smirnov, A.V.; Tkach, T.B. Electron-collisional spectroscopy of atoms and ions in plasma: Be-like ions. *Photoelectronics*. **2016,** *25,* 97-101.
37. Buyadzhi, V.V.; Chernyakova, Yu.G.; Antoshkina, O.; Tkach, T. Spectroscopy of multicharged ions in plasmas: Oscillator strengths of Be-like ion Fe. *Photoelectronics*. **2017,** *26,* 94-102.
38. Glushkov, A.V.; Ambrosov, S.V.; Ignatenko, A.V. Non-hydrogenic atoms and Wannier-Mott excitons in a DC electric field: Photoionization, Stark effect, Resonances in ionization continuum and stochasticity. *Photoelectronics,* **2001,** *10*, 103-106.
39. Khetselius, O., Glushkov, A., Gurskaya M., Kuznetsova, A., Dubrovskaya, Yu., Serga I., Vitavetskaya, L. Computational modelling parity nonconservation and electroweak interaction effects in heavy atomic systems within the nuclear-relativistic many-body perturbation theory. *J. Phys.: Conf. Ser.* ***2017,*** *905*(1), 012029.
40. Glushkov, A.V.; Gurskaya, M.Yu.; Ignatenko, A.V.; Smirnov, A.V.; Serga, I.N.; Svinarenko, A.A.; Ternovsky, E.V. Computational code in atomic and nuclear quantum optics: Advanced computing multiphoton resonance parameters for atoms in a strong laser field. *J. Phys.: Conf. Ser*. **2017**, *905*, 012004.
41. Svinarenko A., Khetselius O., Buyadzhi V., Florko T., Zaichko P., Ponomarenko E. Spectroscopy of Rydberg atoms in a Blackbody radiation field: Relativistic theory of excitation and ionization. *J. Phys.: Conf. Ser*. **2014**, *548*, 012048.
42. Glushkov A.V., Khetselius O.Yu., Svinarenko A.A., Buyadzhi V.V., *Methods of computational mathematics and mathematical physics*. *P.1*. TES: Odessa, **2015**

PACS 31.15.A-;32.30.-r

O. L. Mykhailov, E. A. Efimova, E. V. Ternovsky, R. E. Serga

HYPERFINE STRUCTURE PARAMETERS FOR Li-LIKE MULTICHARGED IONS WITHIN RELATIVISTIC MANY-BODY PERTURBATION THEORY

Summary. The relativistic many-body perturbation theory with the optimized Dirac-Kohn-Sham zeroth approximation is applied to calculation of the hyperfine structure parameters for some Li-like multicharged ions. The relativistic, exchange-correlation and other corrections are accurately taken into account. The optimized relativistic orbital basis set is generated in the optimal many-body perturbation theory approximation with fulfilment of the gauge invariance principle. The obtained data on the hyperfine structure parameters of the Li-like multicharged ions are analyzed and compared with alternative theoretical and experimental results.

Keywords: Relativistic many-body perturbation theory – Optimal one-quasiparticle representation – Oscillator strengths –Energy approach – Correlation corrections

PACS 31.15.A-;32.30.-r

А. Михайлов, Э. А. Ефимова, Е. В. Терновский, Р. Э. Серга

ПАРАМЕТРЫ СВЕРХТОНКОЙ СТРУКТУРЫ ДЛЯ Li-ПОДОБНЫХ МНОГОЗАРЯДНЫХ ИОНОВ В РАМКАХ РЕЛЯТИВИСТСКОЙ МНОГОЧАСТИЧНОЙ ТЕОРИИ ВОЗМУЩЕНИЙ

Резюме. Релятивистская многочастичная теория возмущений с оптимизированным нулевым приближением Дирака-Кона-Шэма применена для расчета параметров сверхтонкой структуры Li-подобных многозарядных ионов. Релятивистские, обменно-корреляционные и другие поправки учитываются в рамках последовательных процедур. Оптимизированный базис релятивистских орбиталей генерируется в последовательном нулевом приближении релятивистской многочастичной теории возмущений, исходя из условия выполнения принципа калибровочной инвариантности. Полученные данные для параметров сверхтонкой структуры для Li-подобных многозарядных ионов анализируются и сравниваются с альтернативными теоретическими и экспериментальными результатами.

Ключевые слова: Релятивистская многочастичная теория возмущений., сверхтонкая структура, литий-подобные ионы

PACS 31.15.A-;32.30.-r

О. Л. Михайлов, Е. О. Ефімова, Є. В. Терновський, Р. Е. Сєрга

ПАРАМЕТРИ НАДТОНКОЇ СТРУКТУРИ ДЛЯ Li-ПОДІБНИХ БАГАТОЗАРЯДНИХ ІОНІВ В РАМКАХ РЕЛЯТИВІСТСЬКОЇ БАГАТОЧАСТИНКОВОЇ ТЕОРІЇ ЗБУРЕНЬ

Резюме. Релятивістська багаточастинкова теорія збурень з оптимізованим нульовим наближенням Дірака-Кона-Шема застосована для розрахунку параметрів надтонкої структури для Li-подібних багатозарядних іонів. Релятивістські, обмінно-кореляційні та інші поправки

враховуються в рамках послідовних процедур. Оптимізований базис релятивістських орбіталей генерується в послідовному нульовому наближенні релятивістської багаточастинкової теорії збурень, виходячи з умови виконання принципу калібрувальної інваріантності. Отримані дані параметрів надтонкої структури для Li-подібних багатозарядних іонів порівнюються з альтернативними теоретичними і експериментальними результатами.

Ключові слова: Релятивістська багаточастинкова теорія збурень, надтонка структура, літій-подібні іони

PACS 31.15.-p; 33.20.-t

E. V. Pavlov, A. V. Ignatenko, S. V. Kirianov, A. A. Mashkantsev

Odessa State Environmental University, 15, L'vovskaya str., Odessa, 65016
E-mail: kirianovserg@gmail.com

DYNAMICAL AND TOPOLOGICAL INVARIANTS OF PbO DYNAMICS IN A RESONANT ELECTROMAGNETIC FIELD

Nonlinear chaotic dynamics of the PbO molecule interacting with a resonant linearly polarized electromagnetic field is computed within the quantum model, based on the numerical solution of the Schrödinger equation and model potential method. To calculate the system dynamics in a chaotic regime the known chaos theory and non-linear analysis methods such as a correlation integral algorithm, the Lyapunov's exponents and Kolmogorov entropy analysis are used. There are listed the data of computing dynamical and topological invariants such as the correlation, embedding and Kaplan-Yorke dimensions, Lyapunov's exponents, Kolmogorov entropy etc..

1. Introduction

At present time theoretical and experimental studying regular and chaotic dynamics of nonlinear processes in the different classes of quantum systems (in particular, atomic and molecular systems in an external electromagnetic field) attracts a great interest that is of a significant importance for multiple scientific and technical applications etc [1-9].

Some of the beauty of quantum chaos is that it has developed a set of tools which have found applications in a large variety of different physical contexts, ranging from atomic, molecular and nuclear physics optical) or resonators and mesoscopic physics and others (see [1-16]). According to Refs. [1-3], under the definite conditions, such systems are described by the corresponding model, when Hamiltonians are possessing only a few degrees of freedom. For the low-dimensional chaotic case the corresponding conditions of transition to deterministic chaos in the system dynamics are quite well understood at the classical level [1-4].

Under quantum treatment of the problem, the similar systems (in particular, the diatomic molecules in a resonant electromagnetic field) are studied with using the known quasiclassical approach [2]. At the theoretical level, the majority of studies, devoted to chaos phenomena in molecular dynamics, is carried out with the using simple tools of dynamical systems theory and qualitative theory of differential equations. New field of investigations of the quantum and other systems has been provided by the known progress in a development of a nonlinear analysis and chaos theory methods [1-12,17-30].

In Refs. [11,27-33] the authors applied different approaches to quantitative studying regular and chaotic dynamics of atomic and molecular systems interacting with a strong electromagnetic field and laser systems. The most popular approach includes the combined using the advanced non-linear analysis and a chaos theory methods such as the autocorrelation function method, multi-fractal formalism, mutual information approach, correlation integral analysis, false nearest neighbour algorithm, Lyapunov exponent's analysis, surrogate data method, stochastic propagators method, memory and Green's functions approaches etc (see details in Refs. [17-24]).

In Ref. [1-3,5-7] the authors performed a study of deterministic chaos in a number of diatomic molecules (GeO, ZrO etc) using as the quasiclassical method as quantum ones.

In this paper we present the corresponding results of computing the characteristic dynamical and topological invariants of the chaotic dynamics of the PbO molecule interacting with a linearly polarized resonant electromagnetic field.

2. Quantum-dynamical and chaos-geometric approach

As the main ideas of the quantum-dynamic approach to diatomic molecule in an electromagnetic field are in details presented in the Refs. [5-7], here we will restrict yourself only by some key elements. The quantum-dynamic approach to a diatomic molecule in an electromagnetic field is based on the solution of the time-dependent Schrödinger equation, optimized operator perturbation theory and realistic model potential (density functional) method (see more details in Ref. [5]).

The problem of dynamics of diatomic molecules in an infrared field is reduced to solving the Schrödinger equation:

$$i\partial\Psi/\partial t = [H_0 + U(x) - d(x)E_M\varepsilon(t)\cos(\omega_L t]\ \Psi \quad (1)$$

where E_M - the maximum field strength, $\varepsilon(t)=E_0 cos(\omega t)$ corresponds the pulse envelope (chosen equal to one at the maximum value of electric field).

A molecule in the field gets the induced polarization and its high-frequency component can be defined as [3,5]. It is important to remind that in the regular case of molecular dynamics, a spectrum will consist of a small number of the well resolved lines. In the case of chaotic dynamics of molecule in a field situation changes essentially. The corresponding energy of interaction with the field is much higher than anharmonicity constant $W > xh\Omega$. It is obvious that a spectrum in this case become more complicated [5,6].

The main output data of the quantum-dynamical approach application are the corresponding theoretical temporal dependence of polarization of a molecule in a resonant electromagnetic field the field in a chaotic regime.

In order to perform the detailed analysis of the chaotic regime polarization time series, further a total dynamics of the quantum system in an electromagnetic field and to calculate the fundamental topological and dynamical invariants of the system in a chaotic regime we used the universal chaos-geometric approach, presented earlier (see, c.g., [5-7,19-20]).

Generally speaking, the approach includes a set of such non-linear analysis and a chaos theory methods as the correlation integral approach, multi-fractal and wavelet analysis, average mutual information, surrogate data, Lyapunov's exponents and Kolmogorov entropy approach, spectral methods, nonlinear prediction (predicted trajectories, neural network etc) algorithms.

One of the important tasks here is to determine the corresponding embedding dimension and to reconstruct a Euclidean space R^d large enough so that the set of points d_A can be unfolded without ambiguity. In accordance with the embedding theorem, the embedding dimension, d_E, must be greater, or at least equal, than a dimension of attractor, d_A, i.e. $d_E > d_A$.

Usually one should use several standard approaches to reconstruction of the attractor dimension (see, e.g., [17-20]). The correlation integral analysis is one of the widely used techniques to investigate the signatures of chaos in a time series. The analysis uses the correlation integral, $C(r)$, to distinguish between chaotic and stochastic systems.

To compute the correlation integral, the algorithm of Grassberger and Procaccia is the most commonly used approach. According to this algorithm, the correlation integral is

$$C(r) = \lim_{N\to\infty} \frac{2}{N(n-1)} \sum_{\substack{i,j \\ (1\le i<j\le N)}} H\left(r - |\ \mathbf{y}_i - \mathbf{y}_j\ |\right) \quad (2)$$

where H is the Heaviside step function with $H(u) = 1$ for $u > 0$ and $H(u) = 0$ for $u \le 0$, r is the radius of sphere centered on $\mathbf{y}_i$ or $\mathbf{y}_j$, and N is the number of data measurements.

In order to perform the verification of the results obtained by means of the correlation integral analysis, one could use so called known surrogate data method. This approach makes use of the substitute data generated in accordance to the probabilistic structure underlying the original data.

The important dynamical invariants of a chaotic system are the Lyapunov's exponents

(see, c.g., [17-20]). These characteristics can be defined as asymptotic average rates, they are independent of the initial conditions, and therefore they do comprise an invariant measure of attractor. Saying simply, the Lyapunov's exponents are the parameters to detect whether the system is chaotic or not.

Another important characteristics, namely, the Kolmogorov entropy K_{ent} measures the average rate at which information about the state is lost with time. According to the definition, the Kolmogorov entropy can be determined as the sum of the positive Lyapunov's exponents.

The estimate of the dimension of the attractor is provided by the Kaplan and York conjecture:

$$d_L = j + \frac{\sum_{\alpha=1}^{j} \lambda_\alpha}{|\lambda_{j+1}|}, \qquad (3)$$

where j is such that $\sum_{\alpha=1}^{j} \lambda_\alpha > 0$ and $\sum_{\alpha=1}^{j+1} \lambda_\alpha < 0$, and the Lyapunov's exponents λ_α are taken in descending order.

There are a few approaches to computing the Lyapunov's exponents. One of them computes the whole spectrum and is based on the Jacobi matrix of system. In this work we use an advanced algorithm with fitted map with higher order polynomials. To calculate the spectrum of the Lyapunov's exponents, one could determine the time delay τ and embed the data in the four-dimensional space. In this point it is very important to determine the Kaplan-York dimension and compare it with the correlation dimension, defined by the Grassberger-Procaccia algorithm].

As a rule, the calculational results of the state-space reconstruction are highly sensitive to the length of data set (i.e. it must be sufficiently large) as well as to the time lag and embedding dimension correctly determined.

Indeed, there are limitations on the applicability of chaos theory for observed (finite) dynamical variable series arising from the basic assumptions that these series must be infinite. A finite and small data set may probably result in an underestimation of the actual dimension of the process. The details of the procedures and algorithms used are presented in Refs. [5,7,19-26].

3. Some results and conclusions

Here we present the results of numerical simulation of the time dynamics for diatomic molecule PbO in the electromagnetic field. The parameter W of interaction of an electromagnetic radiation with a molecule is as follows:

$$W[cm^{-1}] = 120.3(d_0 / r_0)(S / M\omega_e)^{1/2} \qquad (4)$$

where, as usually, an electromagnetic field caan be characterized by the following parameter: S = $cE/8\pi$ (c is the velocity of light and E is a field strength), an interatomic distance r_0 in Å, dipole moment d_o in D, ω_e in cm^{-1}, M in a.u.m., and the field parameter S in GW/cm^2. The set of the PbO molecular constants and electromagnetic field parameters is listed in Table 1 [27]. The corresponding Chirikov parameter in this case is as:

$$\delta n = 2(Ed/B)^{\frac{1}{2}} \gg 1. \qquad (5)$$

The typical theoretical time dependence of polarization for PbO molecule in the field in a chaotic regime is presented in Ref. [5]. The concrete step is an analysis of the corresponding time series with the n=7.6×10^3 and Δt=5×10^{-14}s.

In Table 2 we present the calculational values of the correlation dimension d_2, the Kaplan-York attractor dimension (d_L), the Lyapunov's exponents (λ_i), Kolmogorov entropy (K_{entr}),

Table 1.

Set of the PbO molecular constants and electromagnetic field parameters

Parameters	PbO
$\omega_e = \hbar\Omega$ (cm^{-1})	721.0
$\omega_e x_e = x\hbar\Omega$ (cm^{-1})	3.54
B_e (cm^{-1})	0.3073
D_e (cm^{-1})	2.23×10^{-7}

d_0 (D)	4.65
r_0 (Å)	1.92
M (a.u.m)	14.86
W (cm^{-1})	4.45-14.08

the Gottwald-Melbourne parameter. It is very important to declare that the dynamics of the PbO molecule in a resonant linearly polarized electromagnetic field has the elements of a deterministic chaos (the strange attractor).

Table 2.

Correlation dimension d_2, Lyapunov's exponents (λ_i, i=1,2), Kaplan-York attractor dimension (d_L), Kolmogorov entropy (K_{entr}), Gottwald-Melbourne parameter K_{GW}

d_2	λ_1	λ_2
2.87	0.151	0.0184
d_L	K_{entr}	K_{GW}
2.64	0.169	0.84

From one side, this conclusion is entirely agreed with the results of modelling for other diatomic molecules [3,7-11]. From the other side, one should fix the increasing of the spectral chaos in the molecule studied in comparison with other diatomics such as GeO and similar ones. To conclude, the values of the dynamical and topological invariants (the correlation, Kaplan-York dimensions, the Lyapunov's exponents etc) for the PbO molecule interacting with the resonant linearly polarized electromagnetic field are computed. In particular, the first two Lyapunov's exponents are positive. These data indicate on emerging dynamical chaos elements (indeed the low-dimensional attractor) in behaviour of diatomic molecule interacting with electromagnetic field.

References

1. Zhang C.; Katsouleas T.; Joshi C. Harmonic frequency generation & chaos in laser driven molecular vibrations. *In Proc. of Short-wavelength Physics with Intense Laser Pulses*, San-Diego. **1993**.
2. Berman, G.; Bulgakov, E.; Holm, D. Nonlinear resonance and dynamical chaos in diatomic molecule driven by a resonant IR field. *Phys. Rev. A* **1995,** *52*, 3074
3. López, G.; Mercado, A. classical chaos on double nonlinear resonances in diatomic molecules. *J. Mod. Phys*. **2015**, *6*, 496-509.
4. Glushkov, A.V. Spectroscopy of atom and nucleus in a strong laser field: Stark effect and multiphoton resonances. *J. Phys.: Conf. Ser*. **2014**, *548*, 012020.
5. Ignatenko A., Buyadzhi A., Buyadzhi V., Kuznetsova, A.A., Mashkantsev, A.A., Ternovsky E. Nonlinear chaotic dynamics of quantum systems: molecules in an electromagnetic field. *Adv. Quant Chem.* **2019**, *78*, 149-170.
6. Glushkov, A., Buyadzhi, V., Kvasikova, A., Ignatenko, A., Kuznetsova, A., Prepelitsa, G., Ternovsky, V. Non-Linear chaotic dynamics of quantum systems: Molecules in an electromagnetic field and laser systems. In: *Quantum Systems in Physics, Chemistry, and Biology*. Springer, Cham. **2017**, *30*, 169-180
7. Mashkantsev, A. A. ; Ignatenko, A.V. ; Kirianov, S.V. ; Pavlov, E.V. Chaotic dynamics of diatomic molecules in an electromagneic field**.** *Photoelectronics.* **2018,** *27*, 103-112**.**
8. Glushkov A., Ternovsky V., Buyadzhi V, Prepelitsa G. Geometry of a relativistic quantum chaos: New approach to dynamics of quantum systems in electromagnetic field and uniformity and charm of a chaos. *Proc. Int. Geom. Center*. **2014,** *7*(4), 60-71.
9. Glushkov A.V.; Ivanov, L.N. DC strong-field Stark effect: consistent quantum-mechanical approach. *J. Phys. B: At. Mol. Opt. Phys.* **1993,** *26,* L379-386.
10. Glushkov, A.; Lovett, L.; Khetselius, O.; Gurnitskaya E.; Dubrovskaya, Y.; Loboda A. Generalized multiconfiguration model of decay of multipole giant resonances applied to analysis of reaction (μ - n) on the nucleus ^{40}Ca. *Int. J. Mod. Phys. A.* **2009,** *24(2-3),* 611-615.

11. Serbov N., Svinarenko A. Wavelet and multifractal analysis of oscillations in system of couled autogenerators in chaotic regime. *Photoelectr*. **2006**, *15*, 27.
12. Serbov, N., Svinarenko, A. Wavelet and multifractal analysis of oscillations in a grid of couled autogenerators. *Photoelectr*. **2007**, *16*, 53-56.
13. Glushkov, A.V.; Khetselius, O.Yu.; Svinarenko, A.A.; Serbov, N.G. The sea and ocean 3D acoustic waveguide: rays dynamics and chaos phenomena, *J. Acoust. Soc. Amer*. **2008**, *123(5)*, 3625.
14. Glushkov A.V., Serbov N.G., Bunyakova Yu.Ya., Prepelitsa G.P., Svinarenko A.A. Sensing the kinetical features of energy exchange in mixture CO2-N2-H20 of atmospheric gases under interacting with laser radiation. *Sensor Electr. and Microsyst. Techn*. **2006**. N4. P.20-22.
15. Danilov, V., Kruglyak, Y., Pechenaya, V. Electron density-bond order matrix and the spin density in the restricted CI method. *Theor. Chim Acta*. **1969**, *13*(4), 288-296.
16. Danilov, V., Kruglyak, Y., Kuprievich, V., Ogloblin, V. Electronic aspects of photodimerization of the pyrimidine bases and of their derivatives. *Theor. Chim.Acta*. **1969**, *14*(3), 242-249.
17. Abarbanel, H.; Brown, R.; Sidorowich, J; Tsimring, L. The analysis of observed chaotic data in physical systems. *Rev. Mod. Phys*. **1993**, *65,* 1331- 1392.
18. Kennel, M.; Brown, R.; Abarbanel, H. Determining embedding dimension for phase-space reconstruction using geometrical construction. *Phys. Rev. A*. **1992**, *45,* 3403-3412.
19. Glushkov, A.V. *Methods of a Chaos Theory.* Astroprint: Odessa, **2012**.
20. Khetselius, O. Forecasting evolutionary dynamics of chaotic systems using advanced non-linear prediction method *In Dynamical Systems Applications;* Łódz, **2013**; Vol T2, pp 145-152.
21. Glushkov A., Khetselius O., Bunyakova Yu., Prepelitsa G., Solyanikova E., Serga E. Non-linear prediction method in short-range forecast of atmospheric pollutants: low-dimensional chaos. In: *Dynamical Systems - Theory and Applications*. Lodz Univ. **2011**, LIF111
22. Glushkov A., Khetselius O., Kuzakon V., Prepelitsa G., Solyanikova E., Svinarenko A. Modeling of interaction of the non-linear vibrational systems on the basis of temporal series analyses (application to semiconductor quantum generators*). Dynamical Systems - Theory and Applications*. Lodz. **2011**, BIF110.
23. Glushkov, A.., Safranov, T., Khetselius, O., Ignatenko, A., Buyadzhi, V., Svinarenko, A. Analysis and forecast of the environmental radioactivity dynamics based on methods of chaos theory: General conceptions. *Environm. Probl.*. **2016**, *1*(2), 115-120.
24. Glushkov, A., Khetselius, O., Serbov, N., Svinarenko, A., Buyadzhi, V. Dynamics of multi-layers neural networks on bais of photon echo: Effects of chaos and stochastic resonance. *Proc. of Int.. Conf. on Statistical Phys.* Crete. **2008**, 26
25. Bunyakova Yu.; Glushkov, A.; Fedchuk A; Serbov N.; Svinarenko A.; Tsenenko, I. Sensing non-linear chaotic features in dynamics of system of coupled auto generators: multifractal analysis, *Sensor Electr.& Microsyst. Techn*. **2007,** *1,*14-17
26. Glushkov, A.V.; Buyadzhi, V.V.; Ponomarenko, E.L. Geometry of Chaos: Advanced approach to treating chaotic dynamics in some nature systems. *Proc. Int. Geom. Center***. 2014** *7(1)*,24-30.
27. Oolg, M.; Nicklass, A.; Stoll, H. On the dipole moment of PbO. *J. Chem. Phys*. **1993**, *99* (5), 3614.

PACS 31.15.-p; 33.20.-t

E. V. Pavlov, A. V. Ignatenko, S. V. Kirianov, A. A. Mashkantsev

DYNAMICAL AND TOPOLOGICAL INVARIANTS OF PbO DYNAMICS IN A RESONANT ELECTROMAGNETIC FIELD

Summary. Nonlinear chaotic dynamics of the PbO molecule interacting with a resonant linearly polarized electromagnetic field is computed within the quantum model, based on the numerical solution of the Schrödinger equation and model potential method. To calculate the system dynamics in a chaotic regime the known chaos theory and non-linear analysis methods such as a correlation integral algorithm, the Lyapunov's exponents and Kolmogorov entropy analysis are used. There are listed the data of computing dynamical and topological invariants such as correlation, embedding, Kaplan-Yorke dimensions, Lyapunov's exponents etc.

Key words: Chaotic dynamics, diatomic molecule, electromagnetic field

PACS 31.15.-p; 33.20.-t

Е. В. Павлов, А. В. Игнатенко, С. В. Кирьянов, А. А. Машканцев

ДИНАМИЧЕСКИЕ И ТОПОЛОГИЧЕСКИЕ ИНВАРИАНТЫ ДИНАМИКИ МОЛЕКУЛЫ PbO В РЕЗОНАНСНОМ ЭЛЕКТРОМАГНИТНОМ ПОЛЕ

Резюме. Нелинейная хаотическая динамика молекулы PbO в резонансном линейно поляризованным электромагнитным поле рассчитывается в рамках квантовой модели, базирующейся на численном решении уравнения Шредингера и методе модельного потенциала. Для моделирования динамики в хаотическом режиме используются известные методы нелинейного анализа и теории хаоса, в т.ч., метод корреляционного интеграла, анализ на основе показателей Ляпунова, энтропии Колмогорова и др. Представлены данные вычисления динамических и топологических инвариантов, в т.ч., размерностей вложения, корреляционной, Каплана-Йорка, показателей Ляпунова, др.

Ключевые слова: хаотическая динамика, 2-атомная молекула, электрическое поле

PACS 31.15.-p; 33.20.-t

Є. В. Павлов, Г. В. Ігнатенко, С. В. Кір'янов, О. А. Машканцев,

ДИНАМІЧНІ І ТОПОЛОГІЧНІ ІНВАРІАНТИ ДИНАМИКИ МОЛЕКУЛИ PbO У РЕЗОНАНСНОМУ ЕЛЕКТРОМАГНІТНОМУ ПОЛІ

Резюме. Нелінійна хаотична динаміка молекули PbO, взаємодіючей з резонансним лінійно-поляризованим електромагнітним полем, розраховується в рамках квантової моделі на основі рішення рівняння Шредінгера і методу модельного потенціалу. Для аналізу динаміки системи в хаотичному режимі використані методи нелінійного аналізу та теорії хаосу, у т.ч., метод кореляційного інтеграла, аналіз на основі показників Ляпунова, ентропії Колмогорова т.і. Надані дані обчислення динамічних і топологічних інваріантів: розмірностей кореляційної, вкладення, Каплана-Йорка, показників Ляпунова, та інших.

Ключові слова: хаотична динаміка, 2-атомна молекула, електромагнітне поле

UDC 550.93

L. N. Vilinskaya[1], G. M. Burlak[1], V. A. Borschak[2], M. I. Kutalova[2], N. P. Zatovskaya[2]

[1]Odessa State Academy of Civil Engineering and Architecture, 4 Didrikhson str., Odessa 65029
[2]Odessa I. I. Mechnikov National University, 2, Dvorianskaya str., Odessa, 650026,
E-mail: vilsem56@gmail.com

FEATURES OF APPLICATION OF THE THERMOLUMINESCENT METHOD FOR DATING

To determine the age of geological rocks, we studied the thermoluminescence of the natural light sum stored as a result of uncontrolled radioactive radiation, as well as after annealing and exposure to a controlled irradiation dose. The magnitude of the stored light sum was determined from the area under the curve of thermoluminescence. It is shown that the thermoluminescent method allows to accurately determine the age of geological objects and can find practical application for creating sensors of dating.

1. INTRODUCTION

Thermally stimulated luminescence (TSL) is used in radiation dosimetry to determine the age of archaeological ceramics and geological rocks [1-3]. Since the luminescence is very sensitive to the defects in a solid, it can also be used in material research. The TSL method of dating ceramics and geological objects is based on the fact that, under the action of radioactive radiation of a number of elements in the earth's crust, the light sum is accumulated by the objects under study. The process of storing non-equilibrium charge carriers occurs at local capture levels in dielectrics under the action of ionizing radiation from natural radionuclides contained in the dating object [1,4]. During heat treatment of ceramics (880–980 K), quartz contained in it loses all its previously accumulated light sum, the accumulation of which occurred since the formation of quartz as a mineral. Thus, when dating by the thermoluminescent method, a zero-moment is realized, which is undoubtedly the main advantage of this method.

After storing the light sum with the subsequent heating, this energy is released in the form of TSL. The magnitude of the stored light sum is determined by the properties of the samples investigated: porosity, the content of quartz in them, and the dose power received by them. The content of quartz is fundamentally important, therefore, the application of this method is limited only to those periods, the geological history of which is inherent to quartz-stone. The technique and interpretation of the results of the thermoluminescent method differ for different groups of researchers, that is, they are under development, so the research topic is very relevant.

2. THERMOLUMINESCENCE EXCITED BY INTERACTION WITH WATER VAPOR

The use of the TSL method is based on the assumption that the accumulation of the light sum occurs only as a result of the exposure of the test samples to the elements of the geological environment by radiation of the natural radiation background. However, as is well known, the accumulation of a light sum by a number of solids can occur without exposure to ionizing radiation as a result of their interaction with water [5–7]. In this case, the accumulation of the light sum occurs near the surface of a solid. The value of the stored light sum is determined by the value of its specific surface, its state and the nature of the substance itself.

The storage process of the light sum is due to the formation of radical ions, in particular, during the dissociation of water, and their adsorption on the catalytically active centers of the solid surface [7]. Radical ions can come to the

surface from the environment, or form on the catalytically active surface of a solid as a result of dissociation of the adsorbent. The amount of stored light sum is determined mainly by the number of centers on the surface of a solid on which radical ions can adsorb, creating complexes of adsorption nature that perform the functions of traps filled with electrons.

The process of storing the light sum often ends within a few days, but sometimes it takes much longer to complete. The light sum stored in this way is determined only by the properties and state of the solid surface, while the light sum accumulated under the action of radioactive radiation is due to the processes occurring in its bulk and is determined by the presence of both emission centers and electron traps in the substance under study. Therefore, "surface" luminescence can also manifest itself in the case when the usual "bulk" thermoluminescence is absent. Obviously, the existence of both types of thermoluminescence is also possible. The ratio of their intensities is determined by the nature of the substance, the impurities in it, the value of the specific surface and its properties, the conditions of its keeping, the magnitude of the radiation dose received and its nature.

The presence of such a "surface" thermoluminescence should lead to overestimated values of the rock age, however, it is not taken into account in any way when dating geological objects. It is precisely because of the presence of "surface" thermoluminescence that, apparently, the age of rocks, determined by the authors in the work by the thermoluminescent method [8], is often $1,5 \div 2$ times their age, determined by the radiocarbon method. It is the "surface" component of thermoluminescence that is apparently due to the course of "natural" thermoluminescence of granite in [9], the position of the maximum of which on the temperature scale differs significantly from the position of the maxima of "artificial" thermoluminescence stimulated by X-rays and irradiation in a nuclear reactor. This difference was interpreted by the author in favor of assuming that thermoluminescent dating is not applicable in this case. In our opinion, this fact is a manifestation of the influence of various types of centers (surface and bulk) on TSL.

Obviously, the presence of "surface" thermoluminescence is largely due to the large difference observed in [10] in the intensities of the "natural" thermoluminescence peaks of apatite within the same array. Indeed, the intensity of "surface" thermoluminescence is determined by the state of the surface, which, in turn, depends significantly on the conditions of the sample, which, of course, within the same array in different parts of it. It is precisely the accumulation of the light sum by the surface of the samples that apparently caused the spontaneous recovery observed in the same work with the thermoluminescence time of the samples after their calcination.

Thermoluminescent dating method is also used in archeology to determine the age of ceramics [1,2,10,11]. The method is based on the application for dating quartz, extracted from or contained in ceramics. As with dating in geology, it is believed that the light sum is stored only as a result of irradiation of samples with radioactive radiation. However, usually on quartz, as well as on ceramics, the surface is very strongly developed. The specific surface is often tens and hundreds of square meters per 1 g of substance. Since there are usually 10^{13} centers per 1 cm^2 of the surface of a solid, capable of performing the functions of traps filled with electrons (complexes of adsorption nature), there will be 10^{19} in 1g of such centers. Provided that impurities capable of performing the functions of deep electron traps in the bulk of a solid body are ~ 10^{-2}, we find that the number of such centers per gram of substance is 10^{19}.

Thus, the numbers of both types of centers can be commensurate, and in some cases the number of surface centers can significantly exceed the number of bulk centers. Accordingly, the intensity of the "surface" luminescence is commensurate with the intensity of the "bulk". Since the use of the thermoluminescent method assumes the presence of only "bulk" thermoluminescence, while the total is recorded, it is obvious that a significant error is possible when dating in this way, and therefore, just like when dating geological objects, it is necessary to take

into account the "surface" component of luminescence.

The given examples testify to the manifestation of the "surface" component of thermoluminescence in a number of geological objects and indicate the need to take it into account when dating by the thermoluminescent method. The spectral composition of the luminescence that arises when the light sum stored as a result of exposure to water is determined by the luminescence centers located near the surface of the samples. These centers can also be largely associated with the adsorption of water. The spectral composition of the luminescence arising from the thermoluminescence of the light sum stored during radioactive irradiation is determined mainly by the luminescence centers located in the sample volume. Such centers can be impurities of a number of metals, lattice structure defects, etc.

Thus, since the nature of the centers responsible for the emission of "surface" and "volume" luminescence may be different, the spectra of these two types of luminescence may also differ. The aim of the work was to study the spectral composition of "natural" thermoluminescence induced by radioactive radiation and thermoluminescence excited when interacting with water. Such information may provide additional information for determining the age of geological rocks.

3. EXPERIMENTAL

Taking into account the above considerations on the role of water and the surface component of luminescence, the method [8–14] of thermoluminescent dating can be somewhat changed. At the first stage, the curve of thermoluminescence of a prepared archaeological or mineralogical object should be removed. The area under the curve of thermoluminescence gives the value of the natural light sum, accumulated as a result of uncontrolled radioactive radiation.

At the second stage, the previously highlighted sample is heated at a temperature of 970-1070 K to erase the remnants of the progenetic amount, which could remain unreleased as a result of the previous measurement. Since thermostimulated luminescence associated with surface states is strongly influenced by the products of the dissociation of water and some other inorganic substances, such a measurement should be carried out in a vacuum, atmosphere of dry air or inert gases. At the third stage, the sample is exposed to a controlled dose of radiation, after which thermoluminescence is again performed. All studies known to us at this stage were carried out without isolating the samples from moisture, as a result of which the latter, together with the irradiation, stored the light sum. It gave the overestimated value of the total light sum and, as a result, the overestimated age of the rocks. Comparing the light sum, obtained under the action of natural uncontrolled irradiation and controlled dose, you can determine the age of the sample.

It is known that the intensity of thermoluminescence is proportional to the radiation dose [15]:

$$I_{nat} = CP_1t_1$$

P_1 – natural dose power (natural background), t_1 - age of geological rocks, C - constant, independent of the power and time of exposure. Similarly, the intensity of the TSL, which is observed as a result of irradiation with a controlled dose of radiation, is induced by the TSL:

$$I_{ind} = CP_2t_2$$

where P_2 is the dose power control, t_2 is the exposure time C – constant, which does not depend on the power and time of exposure. Hence the age of the rocks:

$$t_1 = \frac{I_{nat}P_2t_2}{P_1I_{ind}}$$

The accuracy of dating is determined by both the accuracy of the method and the possibility of the temporary separation of various geological rocks. The accuracy of the TSL method is quite high [16]. The possibility of temporary separation of various rocks is determined by geological laws and is not less than 200-300 years.

We carried out thermoluminescent dating of quartz samples. Quartz was chosen for the reason that, being a mineral, it is also present in archaeological samples and, moreover, as can be seen from the previous one, due to the presence of quartz, the thermally stimulated dating of archaeological rocks is possible.

By the method of wet sieve analysis, fractions of 100–140 μm in size were determined from quartz rock sediments previously identified by radiocarbon analysis with different periods of the quaternary period. Quartz was extracted by mineral separation in heavy liquids (bromoform). Degree of purity is 98-99%. Surface cleaning from contamination was carried out by processing in a 10% $HF + HCl$ solution for 10 minutes. The obtained samples were pressed into tablets with a diameter of 12 mm and a thickness of 2 mm.

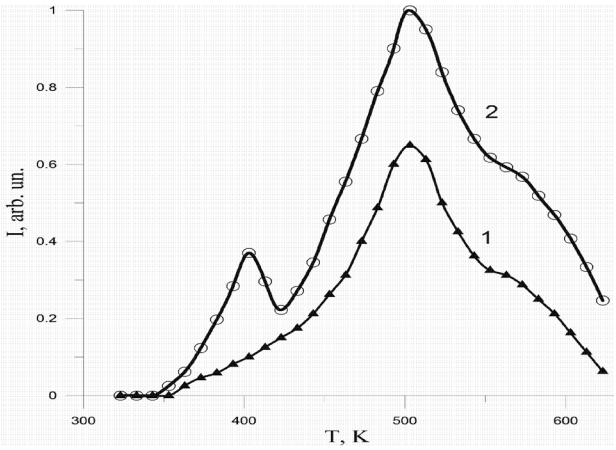

Fig.1. Curves of thermoluminescence of samples: 1) the intensity of the natural light sum stored as a result of uncontrolled radioactive radiation; 2) the intensity of the light sum after heating at a temperature of 970-1070 K and the effects of a controlled dose of radiation.

For measurements, a standard thermoluminescent installation was used in the integral sensitivity mode (the signal was amplified by an IMT-005 direct current meter and fed to one of the coordinates of the recording device). The temperature was measured using a copper - constantan thermocouple with an accuracy of 10K and was fed to another coordinate of the recording device (PDP-001). The heating rate was 0,3 K/min. The working volume of the chamber in which the thermolumination was carried out was hermetically sealed and purged with vapors of dry air, the humidity level in which did not exceed 0.05%. The source of exposure was cobalt ^{60} Co (power 0,15 x-ray / s). The measurements were carried out in the temperature range from 320-600 K. The curves of thermoluminescence are shown in fig. 1.

4. RESULTS AND DISCUSSION

It can be seen that all samples are characterized by peaks in the range of 500–525 K and about 580 K, which correspond to peaks of quartz and calcite. For samples exposed to a controlled dose of radiation, the intensity of the light sum increased and an additional peak appeared at a temperature of 400 K. The total value of the stored light sum was determined by the area under the curve of thermoluminescence. The age of the rocks was determined similarly to the formula given above:

$$t_1 = \frac{I_{icd} D_a}{I_{ind} D_a}$$

The annual dose of radioactive radiation included in this formula D_{an} was determined by the value of the natural background radiation. The accumulated dose D_{ac} was determined taking into account the power of the source. I_{icd} – the intensity controlled radiation dose rate (induced TSL), I_{inc} – the intensity of the uncontrolled radiation dose (natural background).

The age estimate taking into account the experimental data obtained is $2{,}6 \cdot 10^4$ years. The radiocarbon analysis of the same sample gives $2{,}1 \cdot 10^4$ the age of years. A good agreement of the results obtained by two different methods may indicate the validity of the assumption that the coefficient of proportionality is constant between the intensity of the TSL and the radiation dose power. This circumstance indicates the possibility of practical application of the samples under study to create dating sensors.

To determine the age of geological rocks, we studied the thermoluminescence of the natural light sum stored as a result of uncontrolled radioactive radiation, as well as after warming up

and exposure to a controlled irradiation dose. A good agreement was obtained between the results obtained by thermoluminescent and radiocarbon methods. It is shown that the discrepancy between the results obtained by these methods is less than that given by other authors. Obviously, this improvement was due to the inclusion of the "surface" component of thermoluminescence. The above dating method allows you to accurately determine the age of geological and archaeological objects and can find practical application for creating dating sensors.

REFERENCES

1. Hashimoto T. An overview of redthermoluminescence (RTL) studies on heated quartz and RTL application to dosimetry and dating // Geohronometria. 2008. Vol. 30 (1). P. 9–16. https://doi. org/10.2478/v10003-008-0011-z
2. Richter D., Richter A., Dornich K. Lexsyg smart—A luminescence detection system for dosimetry, material research and dating application. Geochronometria. 2015; 42:202–209. doi: 10.1515/geochr-2015-0022.
3. Murthy K.V.R. Thermoluminescence and its Applications: A Review. Defect Diffus. Forum. 2013; 347:35–73. doi: 10.4028/www.scientific.net/DDF.347.35.
4. Власов, В. К. Радиотермолюминесцентный метод датирования рыхлых отложений / В. К. Власов, О. А. Куликов. – М.: Издательство Московского университета, 1998. – 72 с.
5. Михо В.В., Дмитренко З.Ф. К вопросу о примененеии метода термовысвечивания для изучения параметров активных центров// Кинетика и катализ. 1998. – т.19. –№3. – С.720-724.
6. Федчук А.П., Михо В.В. Определение характера активных центров в окиси алюминия методом темровысвечивания // Кинетика и катализ. 1994. –Т.15. –№2. –С.534-535.
7. Танабе К. Твердые кислоты и основания. М.:Мир. 1993, 176 с.
8. Шелкопляс В. Н. Применение термолюминесцентного (ТЛ) метода для датирования плейстоценовых образований. // Хронология плейстоцена и климатическая стратиграфия. – Л. – 1993. – С. 121 – 127.
9. Хютт Г., Пуннинг Я.-М., Смирнов А. Методика термолюминесцентной датировки в геологии. // Изв. АН ЭССР. Сер.: химия, геолог. – 1997. – Т. 26, №4. – С. 284 – 288.
10. Чистяков В. К. Особенности природной и искусственной термолюминесценции апатита из интрузивных и метамерфических пород. // Изв. АН СССР. Сер.: геолог. – 1994. - № 8. – С. 81 – 90.
11. Комарова, Я. М. Термолюминесцентный метод датирования археологических объектов / Я. М. Комарова, Н. Л. Алукер, А. С. Сыроватко // Изв. ВУЗов. Физика. - 2011. - Т. 54. - № 2/2. - С. 191-195.
12. V.S. Grinevych, L.M. Filevska, V.A. Smyntyna, M.O. Stetsenko, S.P. Rudenko, L.S. Maksimenko, and B.K. Serdega. Characterization of SnO_2 Sensors Nanomaterials by Polarization Modulation Method. Springer Science+Business Media Dordrecht 2016 J. Bonca, S. Kruchinin (eds.), ˇ Nanomaterials for Security, NATO Science for Peace and Security Series A: Chemistry and Biology, DOI 10.1007/978-94-017-7593-9, p.259-266.
13. L.M. Filevska. Luminescence of nanoscale tin dioxide. Review. Photoelectronics. 27 (2018), p.52-59.
14. Лепіх Я.І., Лавренова Т.І., Садова Н.М., Борщак В.А. Балабан А.П., Затовська Н.П. Структурно-фазові перетворення і електрофізичні властивості композиційних матеріалів на базі системи " SiO_2-B_2O_3-Bi_2O_3-ZnO-BaO"//Sensor electronics and Microsystem Technologies. – 2018– Vol.15, № 4 – PP. 77-84.
15. Иванов В.П. Курс дозиметрии. - М.:Атомиздат, 1998. -391 с.13. https://www.ncbi.nlm.nih.gov/pmc/articles/PMC5744292/
16. Adrie J.J.Bos Thermoluminescence as a Research Tool to Investigate Luminescence Mechanisms. Material (Basel). 2017 Dec; 10(12): 1357. doi: 10.3390/ma10121357

UDC 550.93

L. N. Vilinskaya, G. M. Burlak, V. A. Borschak, M. I. Kutalova, N. P. Zatovskaya

FEATURES OF APPLICATION OF THE THERMOLUMINESCENT METHOD FOR DATING

To determine the age of geological rocks, we studied the thermoluminescence of the natural light sum stored as a result of uncontrolled radioactive radiation, as well as after warming up and exposure to a controlled irradiation dose. The magnitude of the stored light sum was determined from the area under the curve of thermoluminescence. It is shown that the thermoluminescent method allows one to accurately determine the age of geological objects and can find practical application for creating dating sensors.

Keywords: thermoluminescent method, dating, storage of light sum, thermoluminescence.

УДК 550.93

Л. Н. Вилинская, Г. М. Бурлак, В. А. Борщак, М. И. Куталова, Н. П. Затовская

ОСОБЕННОСТИ ПРИМЕНЕНИЯ ТЕРМОЛЮМИНЕСЦЕНТНОГО МЕТОДА ДЛЯ ДАТИРОВАНИЯ

Для определения возраста геологических пород проведено изучение термовысвечивания естественной светосуммы, запасенной в результате неконтролируемого радиоактивного излучения, а также после прогрева и воздействия контролируемой дозы облучения. Величина запасенной светосуммы определялась по площади под кривой термовысвечивания. Показано, что термолюминесцентный метод позволяет достаточно точно определять возраст геологических объектов и может найти практическое применение для создания сенсоров датирования.

Ключевые слова: термолюминесцентный метод, датирование, запасание светосуммы, термовысвечивание.

УДК 550.93

Л. М. Вілінська, Г. М. Бурлак, В. А. Борщак, М. І. Куталова, Н. П. Затовська

ОСОБЛИВОСТІ ЗАСТОСУВАННЯ ТЕРМОЛЮМИНЕСЦЕНТНОГО МЕТОДУ ДЛЯ ДАТУВАННЯ

Для визначення віку геологічних порід проведено вивчення термовисвітлення природної світлосуми, що запасена в результаті неконтрольованого радіоактивного випромінювання, а також після прогріву і впливу контрольованої дози опромінення. Величина запасеної світлосуми визначалася за площею під кривою термовисвітлення. Показано, що термолюмінесцентний метод дозволяє досить точно визначати вік геологічних об’єктів і може знайти практичне застосування для створення сенсорів датування.

Ключові слова: термолюмінесцентний метод, датування, запасання світлосуми, термовисвітлення.

UDC 621.315.592

S. S. Kulikov, YE. V. Brytavskyi, V. A. Borshchak, N. P. Zatovskaya,
M. I. Kutalova, Y. N. Karakis

Odessa I. I. Mechnikov National University, 42, Pastera Str; phone: 723-34-61 .

THE STUDY OF HOMOGENEOUS AND HETEROGENEOUS SENSITIZED CRYSTALS OF CADMIUM SULFIDE. PART III. OSCILLATIONS OF EXCITED CARRIERS

The processes at short-wave limit of the quenching of the photocurrent were studied. The possibility of creating a new type of device - a sensitive photometer (not on the intensity of light, but on its wavelength), and the combined temperature–voltage tester.

The process of hole oscillation under photoexcitation from R-centers is investigated. The quantum yield for infrared light is determined. The effect of the applied voltage on the form of the spectral distribution curves of the photocurrent quenching was found and explained. The concentration of R-centers in the samples is calculated.

This publication is a continuation of the reviews [1– 2]. For the sake of preservation of generality of work continuous numbering of sections is chosen. Numbers of formulas and figures are presented by sections. References in each article are given individually.

Cadmium sulfide crystals are used in our studies as a convenient model material. Obtained results and constructed models are also applied to other semiconductors.

4. Research of processes in the field of short-wave threshold of infrared quenching of photocurrent

Lets consider, that in a sensitive crystal under the action of light, the wavelength of which does not change from the maximum of its own excitation (520 *nm*), a photocurrent I_{excit} is formed. If at the same time the monochromatic light with controlled wavelength, hereinafter referred to as the main, is sent to sample, the quenching region of the flowing photocurrent I_{main} is less than the original: $I_{excit} > I_{main}$. With a decrease in the wavelength of the main light, it will also be intristic. Then, in the conditions of additional excitation $I_{main} > I_{excit.}$

As in the long-wave part of the spectrum $I_{excit} > I_{main}$, and in the shortwave $I_{main} > I_{excit.}$ then, according to the Bolzano-Cauchy theorem, there must be a point when $I_{main} = I_{excit.}$. Let's call this wavelength as shortwave threshold for the effect of IR-quenching of photocurrent or the point of bifurcation. The switching-on of basic light in this point of spectrum does not change photocurrent I_{excit} being already formed (see Fig. 4.1.B).

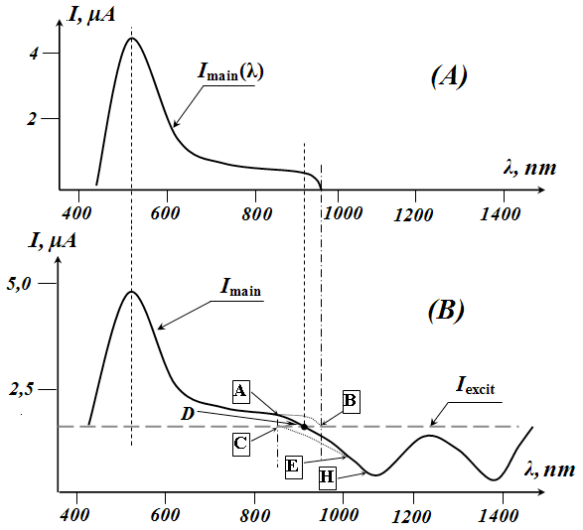

Fig. 4.1. The spectral distribution of the photocurrent under the action of only exciting light with λ=520 nm (A) and together the main and exciting light(B).

The processes occurring in the crystal have not been studied before and are studied for the first time [3,4].

4.1. On the balance of processes of excitation–quenching at the bifurcation point

There are two options. Exposure by the main light at the bifurcation point does not cause any changes. Its wavelength is too far from the field of its intristic excitation and does not lead to an increase in the concentration of the main charge carriers. At the same time, it is too small to change the concentration of minority carriers and does not cause the IR-quenching process.

Or both processes, although to a weak degree, are activated, but are equal to each other. In the latter case, as usual, when exposed to competing mechanisms, the current must be very sensitive to changes in external conditions – temperature, applied voltage, changes in the intensity of the main and excitation light.

Figure 4.1.B shows the change in photocurrent I_{main} under the action of the main light of different wavelengths. Here, for convenience, the photocurrent I_{excit} generated by the action of only light with a wavelength of 520 *nm* is shown.

In the direction of large wavelengths, photosensitivity was observed up to the boundary of the infrared part of the spectrum (~ 900 – 940 nm). In the region of wavelengths 600 – 850 nm, we observed almost a tabular part of the graph. Obviously, this area is formed due to emptying of the deep traps. These traps are also responsible for the relatively long relaxation of the photocurrent (up to 20 minutes at each point) described in chapter 3.1–3.2. All the results described below were obtained in stationary conditions. The kinetics of setting the values corresponded to [5–8].

The optimal intensity of the main and the excitation light to the curves of Fig. 4.1 in accordance with the data of Chapter 1, were selected as a baseline in the study of the effect of light fluxes on the spectral position of the bifurcation point (see below). At selected light intensities, the bifurcation point is shown in Fig. 4.1 hit at a wavelength of 930 nm.

1. If the processes of photoexcitation ended with a wavelength earlier than the bifurcation point, and the IR-quenching effect began later than it, the graph I_{main} (λ) would have the form shown in Fig. 4.1.B dotted line. In this case, in the vicinity of *D we would observe a more or less pronounced plateau coinciding with the value of I_{excit}. It is the absence of such a plateau that indicates that another possibility is being realized. In the bifurcation region, the sample is simultaneously excited by the main light and IR-quenching. At point D, these two processes are exactly compensated.

2. Figure 4.1.A at the same scale as 4.1.B the spectral distribution of the photocurrent is shown. As can be seen from the graph, the sample showed photosensitivity, though insignificant, up to wavelengths of ~ 1000 nm. The appearance of a longer-wave sensitivity relative to *D is explained as follows. The wavelength of the exciting light is too long. It is poorly absorbed and the number of photoexcited carriers is small. Obviously, in these circumstances, the filling of the R-centers by holes is minimal. The IR-quenching process is difficult. We observe long-wavelength edge of photo-excitation in absence of quenching. But in this case, at the point of bifurcation, photoexcitation is more pronounced.

3. To the left of the point D curve I_{main} (λ) changes the smoothness. Starting with wavelengths of about 880 nm, the I_{main} (λ) graph decreases more sharply to the bifurcation point. This can occur if the distribution of the photocurrent is already stepped in by infrared quenching.

It is impossible to measure the quenching curve in the area of the CE without excitation (similar to paragraph 2), since the quenching process essentially requires the participation of two light streams. However, this dependence can be calculated, assuming that the curve AB is a change in the photocurrent I_{excit} (λ) under the action of excitation only (see Fig. 4.1.A), whereas the ADE curve is the result of the combined action of excitation and quenching. Then $I_{CE}(\lambda) = I_{AB}(\lambda) - I_{ADE}(\lambda)$. The CE part of the graph in Fig. 4.1.B obtained by this method reflects the behavior of the curve I(λ) to the left of the point D, if there was no excitation process of the crystal.

We got the same result by another calculation method. This plot was selected EH curve I_{main} (λ)

Fig. 4.1.B. This plot was selected EH curve I_{main} (λ) Fig. 4.1.For this area is no longer affected by the excitation of the main light (curve AB, the end of the curve Fig. 4.1.A), but the mechanisms forming the minimum current behind the H-point are not yet essential. The expression for the trend line was used for calculations. On the site of the EH function I_{main} (λ) is approximated by the expression I (λ) = a λ^3 + b λ^2 + c λ + d, where a = 0,0002; b = – 0,5; c = 499,08; d = –165663. By extrapolating this dependence to the intersection with the value of I_{main}, we again obtain the curve CE (dotted line Fig.4.1.B).

Practically coinciding curves on the SE site indicate the existence of quenching in the spectral region of 900 – 920 nm even before the short-wave boundary of the IR effect.

4. In some cases, in the region of the bifurcation point, we observed a complex dependence of the I_{main} (λ) curve with one or even two inflection points. This can be easily explained by the fact that the simultaneous processes of quenching and excitation depend on the color of the light in different ways, both of which are nonlinear. The predominance of one of them for each wavelength of the incident light and generates a change in the nonlinearity of the graph.

Thus, all four of these arguments indicate that the region of the beginning of the infrared quenching of the photocurrent is characterized by a competition of excitation and quenching, and at the very point D the intensity of these processes are the same.

4.2. Dependence of the spectral position of the short–wave boundary of infrared quenching on external factors

With increasing temperature, the boundary of the effect of infrared quenching of the photocurrent λ_0 shifted towards large wavelengths (Fig. 4.2.A).

The operating temperature range was chosen in such a way that at the selected light intensities the effect of temperature quenching of the photocurrent was not affected. A noticeable decrease in the photocurrent was observed, starting with temperatures ~ 50 – 55 ^{O}C. Using subthreshold values of temperatures for this effect, the emission of holes from R-centers into the valence band was excluded from consideration.

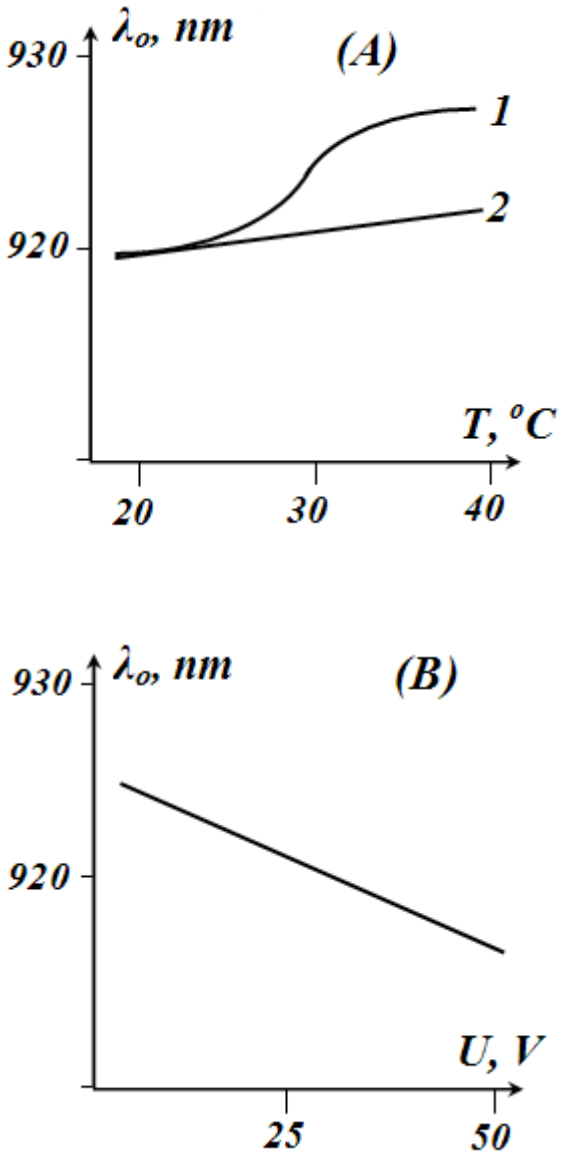

Fig. 4.2. The dependence of the coordinate of the bifurcation point on the operating temperature at high (2) and low (1) intensity of natural light (A) and the change of its position with the increase in the applied voltage (B).

However, thermal transitions occur. By absorbing phonons, equilibrium holes can pass from the basic levels of R -centers with an energy of 1.1 *eV* to excited R′- centers with an energy of 0.9 *eV*. In this case, the population of

R–states by holes decreases, and R´- states naturally increases. It has already been noted above that this process is responsible for the fact that the first maximum of optical quenching of the photocurrent with a wavelength of about ~1100 *nm* is always lower than the second, located at a wavelength of 1380–1400 *nm*.

The first minimum current (Fig. 4.1.B) as closer to the bifurcation point, has a major influence on the spectral position of the onset of the photocurrent IR-quenching effect. Moreover, in accordance with [9], with the change in temperature, the spectral position of this maximum did not change.

As the temperature increases from room temperature and above, the concentration of holes captured on the ground States of R-centers decreases. With a constant number of photons incident on them per unit time, a decrease in the population of these levels is accompanied by a decrease in the transitions of holes in the free state.

As a result, due to the weakening of the quenching mechanism, the equilibrium at the bifurcation point is disturbed, and it moves towards large wavelengths. Here, a new balance is achieved for less intensity of photoexcitation, but increased intensity of quenching. The shift will occur until the increase in the quenching rate compensates for the losses associated with the effect of temperature. The processes are nonlinear. This explains the deceleration of the wavelength increment at the point of branching with increasing temperature. The growth in terms of absolute values, the increment is affected to a lesser degree. Light intensity in the measurement of the dependence λ_o (T) (curve 1 Fig. 4.2.A) selected by us according to the figure. 1.1 chapter 1 [1]. With more significant illuminations, the step-like nature of the transition disappeared with additional light. The curve slightly increased (graph 2 Fig. 4.2.A) when values λ_o in the lower shelves. We explain this by changing the mechanism of emptying the ground state of R-centers.

At high intensities of its intristic light creates a lot of free holes. The filling of R-centers is significant. Their emission, and accordingly, the intensity of the quenching process is controlled only by the flow of IR photons. And the population remains stable. The flow of nonequilibrium holes on R-centers compensates for their knocking out by phonons.

On the contrary, at low light L_{excit}. and, hence, weak filling of R-centers, the quenching process is determined by the concentration of trapped holes, since their number is less than the density of the photon flux.

Thus, the form of the curve λ_o (T) is an indicator of the change of the described mechanisms.

The investigated samples had a linear current-voltage characteristic in displacements from 10 to 50 V over the whole range of the used intensities of the light of its own. Within these values, with increasing voltage, the bifurcation point shifted almost linearly towards short wavelengths.

The results obtained correspond to the model developed in [10].

Since the intensities of the main and additional light did not change during the experiment, the processes of photoexcitation of both the main (electrons through the forbidden zone) and non-main (holes from the R-centers) remain the same. Accordingly, the concentration of the captured charge on the R-centers remains unchanged.

If the applied voltage has almost no effect on the concentration of the free charge responsible for the formation of the current, it changes the speed of its movement, which is reflected in the current in accordance with the dependence $j = env$. It is taken into account that the current is formed by the main carriers, in our case – electrons.

However, this is not enough to change the balance of excitation and quenching processes at the bifurcation point. The current electrical voltage not only accelerates the free electrons, (the recorded current increases), but also the photoexcited holes (by increasing the recombination at the S-centers, the current must decrease). For these reasons, the coordinate of the bifurcation point with the change of voltage should not change.

But the processes overlaps with another one. Photoexcited holes are located in the vicinity of the original R-centers and have the ability to re-

turn there. The greater the applied voltage, the more effectively they get carried away from their traps (see chapter 5.1). This increases the quantum yield for IR light (See chapter 5.2) [11].

This process breaks the symmetry. The recombination at the S-centers is enhanced due to the additional charge. Due to enhanced quenching, the bifurcation point shifts to shorter wavelengths, where equilibrium is restored by a higher level of photoexcitation.

The behavior of the bifurcation point can serve as a criterion for changing the quantum yield from R-centers.

Note that the reasoning is valid only in the region of small intensities of light fluxes, when the number of absorbed light quanta at R-centers is less than the number of holes captured on them. In the opposite case, for example, the very large quenching of the light and a little exciting, $L_{excit} << L_{main}$, the observed pattern may be substantially adjusted by the rate of occupation of R-centers. The limits of applicability of light flux intensities are discussed in more detail in [10,11].

Changes in the position of the short-wave boundary of the IR effect with an increase in the intensity of the main color (horizontal columns

Table. 4.1.

Wavelength λ_0 branch points under various lighting conditions

		The intensity of the excitation light L_{excit}, *lx*		
		3	5	8
Main light intensity L_{main}	$7 \cdot 10^{13}$ $sm^{-2} \cdot s^{-1}$	920 *nm*	908,5 *nm*	897,7 *nm*
	$10 \cdot 10^{13}$ $sm^{-2} \cdot s^{-1}$	925,9 *nm*	915,5 *nm*	903,3 *nm*
	$13 \cdot 10^{13}$ $sm^{-2} \cdot s^{-1}$	930 *nm*	920 *nm*	906 *nm*

With increasing intensity of the exciting light (horizontal lines of table 4.1), the IR quenching boundary shifted towards shorter wavelengths [12,13]. These changes are easy to interpret for geometric reasons. The graph Fig. 4.1. would the increase in light intensity corresponds to an increase L_{excit}. horizontal line I_{excit}. The dependence of the I_{main} (λ) does not change. Therefore, the bifurcation point should move to the left.

Physically, this means that with the increase of the initial intensity of the natural light, the balance of excitation and quenching processes at the short-wave boundary of the effect is disturbed. There is an additional generation of electrons, while the number of holes knocked out from the R-centers remains the same, since the number of absorbed infrared photons has not changed. Since the intensity of the main light does not change, it is possible to restore the equilibrium only by shifting the bifurcation point to the short-wave part of the spectrum, where the light is better absorbed and the process of photoexcitation is greater.

of table 4.1) are not amenable to simple interpretation [12,13]. In this case, the horizontal line in Fig. 4.1.B remains unchanged, while the dependence of the I_{main} (λ) is nonlinearly modified. In the short–wave part of the graph, it increases due to additional absorption of photons of its own light, whereas in the long-wave part, where interband transitions do not occur, the photocurrent should decrease due to an increase in the number of infrared photons absorbed at the R-centers.

At the bifurcation point, the intensity of both processes-excitation and quenching-increases, but in different ways. The increase in the number of photons of its own light causes a direct increase in the concentration of electrons, and with it more or less a linear increase in the photocurrent.

The increase in the number of photons absorbed at the R-centers can affect the photocurrent only when the knocked holes fall on the S-centers and cause additional recombination of electrons. As shown in [13], this process may

be affected by the return of holes to the initial center immediately after excitation. At the same time, the quantum yield is generally reduced, and the process of exposure to IR photons is not so effective. As a result, the intensity of the quenching growth lags behind the growth of excitation. In addition, the number of incident photons is already greater than the number of holes on the centers at the used IR light intensities. Further increase in their number cannot cause an increase in the number of transitions. The resumption of the balance is possible in the longer wavelength region, when the process of photoexcitation is less, but the rate of quenching increases. Indeed, the shift of the bifurcation point to the right was observed experimentally.

Studies have shown that the very boundary of the beginning of the infrared quenching of the photocurrent carries important information about the nuances of the processes [20]. Previously, this aspect remained unexplored.

It is found that this spectral region is characterized by a competition of photoexcitation and photocurrent quenching. It is because of this that the wavelength of the short-wave edge of the IR quenching is sensitive to external influences.

In particular, its change with the applied voltage indicates that IR photons knocking holes from R-centers occurs in two stages-part of the photoexcited carriers can return to the original center, not participating in the effect of infrared quenching.

As the intensity of the additional light increases, the effect boundary shifts towards shorter wavelengths due to an increase in the concentration of the main carriers. On the contrary, the increase in the main light leads to the movement of the boundary to the right due to the predominance of the photoexcitation rate over the quenching due to the insufficiently effective ejection of holes from the R-levels.

Similar changes occur with increasing temperature. This is caused by a decrease in the population of the R-centers ground state holes [14].

The spectral position of the region of the infrared quenching can be the indicator of the occurrence of these processes.

Changing the position of the IR quenching edge can be used to create a new type of spectral-sensitive sensor [12,13,15]. Depending on the calibration applied, it can be used simultaneously to measure temperature and/or voltage and light intensity in the visible and IR region.

At the same time, since the difference current at the bifurcation point is zero, the sensitivity of such a device can be very significant. Depending on the doping of the initial crystal, it is possible to control the spectral position of the bifurcation point.

A more flexible option is also possible – since the spectral position of the bifurcation depends on the applied voltage, this point of increased sensitivity can be adjusted electrically in the finished sensor directly during operation.

The inverse problem is also feasible – with fixed parameters of external action, the coordinate of the point D can be used to calibrate the wavelength of radiation.

5. Experimental evidence of the holes oscillations under R-centers photoexcitation

The reason for the sliding of the short-wave threshold of the beginning of infrared quenching with external voltage (Chapter 4) is the possibility of repeated captures of holes knocked out by infrared photons from the centers of slow recombination. This is a natural assumption, since the newly activated hole is spatially in the area of the trap, the capture section of which has not changed. But with the departure of the hole changed the charge on the trap, and there were electric forces that contribute to the reverse capture of the already free hole. In addition, it is, as usual, beneficial to reduce their energy. Moreover, the probability of this event in these holes is much greater than that of other free charges of non-main carriers, which in the course of chaotic motion still need to meet with R-centers.

The possibility of re-capturing, as described In section 1.2, may significantly limit the applicability of the expression (1.9) to Q ($L_{quench.}$; L_{excit}) , especially in the region of low light intensities. For a small level of exciting light, the concentration of captured holes on the R-centers is too small, and with insufficient intensity of infrared radiation, they are too little knocked out.

Repeated captures begin to play a decisive role. Until the disappearance of the General effect of infrared quenching photocurrent, although both lights still continue to operate.

The existence of similar, probably multiple, oscillations of holes and the impact of these processes on the observed photovoltaic properties of the samples in the literature up to the present time was not considered. Although this issue has a wider importance, because it fundamentally applies to any emission from the traps.

The effect of infrared quenching in this case acts only as a convenient and sensitive tool to confirm this phenomenon. It is the combination of inherently effective hole traps and effective recombination S-centers that makes this process convex. The measured current consists of the main carriers – electrons. Holes knocked out from R-centers carry electrons to recombination, which is reflected in the magnitude of the flowing current. If there were only hole traps in the crystal and the current was determined only by free holes, then they could take part in the current transfer only up to the moment of repeated captures to the neighboring R-centers. Since the usual concentration of these centers is high ((~ 10^{15} cm^{-3}) and comparable, and at low light intensities even more concentration of free holes, such phenomena would be hardly noticeable due to the small free path.

5.1. Dependence of the spectral distribution of photocurrent quenching on the applied voltage

External voltage, on the contrary, prevents re-capture, because it helps to remove holes from the parent centers. Therefore, we used this parameter to test the assumption of oscillation.

For Fig. 5.1. the curve (b) is measured at the best ratio of the intensities of the exciting light to the quenching light (See chapter 1.1, Fig. 1.1), when the infrared quenching coefficient reached the highest value [9,16,17]. The sample was applied with 20 V. the range of voltages used was selected from the linearity of the current-voltage characteristics to avoid the additional influence of pre-breakdown phenomena.

As can be seen from the figure, the rise in voltage increases both the maximum $Q(\lambda)$. Moreover, this behavior was typical for all combinations L_{quench} and L_{excit} so far the effect of IR-quenching of the photocurrent was well observed.

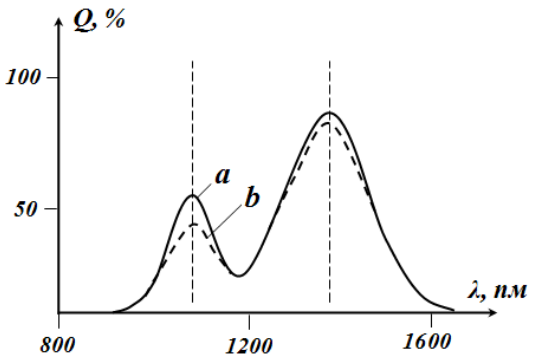

Fig. 5.1. Spectral distribution of the quenching value on the applied electric field: a) - 50 V is applied to the sample; b) - 20 V is applied to the sample.

In both cases, the second maximum was higher than the first one due to the thermal redistribution of holes between the centers of slow recombination. With an increase in the applied voltage, an increase in this difference was observed. But in different ways. For the maximum in the range of 1080–1100 nm it was more significant.

This is explained as follows. Since the temperature has not changed, the intensity of the hole transitions from R to R' - levels remains fixed. An increase in the applied voltage reduces the number of re-captured holes for both levels. Moreover, judging by the quantum yield (see chapter 5.2), it is an essential channel for the steady-state population of the centers. However, the decrease of this flow for the ground and excited States of R-centers affects differently. From the ground state (at a depth of 1.1 eV) holes are knocked out thermally and with an increase in voltage less return. Both mechanisms are aimed at reducing their concentration at this center. On the contrary, for R' -levels (0.9 eV), these mechanisms compete. If the stress reduces their population, the thermal swap still increas-

es. This camouflages the field effect on the population of the excited state of the R-centers. This is reflected in a smaller change in the long-wave maximum in Fig. 5.1.

It should be noted that with an increase in voltage, due to the movement of free holes, the hole component of the photocurrent increases. And after the capture in S-centres they are in accordance with the Bube-Rose mechanism needs to call it blanking out. Thus, the reduction of repeated hole captures and their participation in the current transfer is a competing mechanism with respect to the value of Q. Since the capture cross sections for holes and electrons at the centers of the first class are equal, the appearance of additional holes should cause an equal decrease in the concentration of electrons in the conduction band and a corresponding decrease in the photocurrent. At the same time, due to the increase in the drift velocity of both electrons and holes, as well as the increase in the concentration of free holes, the photocurrent should increase slightly. The degree of quenching, i.e. the value of the coefficient Q, decreases slightly.

Of course, removing the hole from the original R-center, the applied voltage contributes to its capture at the S-levels. Then the quenching value and, accordingly, the value of Q increase. However, during the drift, the holes can be captured at the other R centers. Moreover, the capture cross-sections for holes on the S- and R-centers are the same and the charge state of the R-centers (See chapter 2.1) contributes to this.

If the value of the quantum yield for infrared radiation would be about the same as the quantum yield for its own light, these two processes would compensate each other. However, the abnormally low β value for IR light [10,11,18] makes the inverse oscillation of the holes decisive for the useless absorption of long-wave photons. The application of external voltage breaks this mechanism and is effective, even if some part of the holes and returns to the other R-levels and again take part in the oscillations.

Thus, both changes in the spectral distribution of the infrared quenching coefficient – both the total increase in the value of Q with the applied voltage and the relatively larger jumps of the short-wave maximum-indicate in favor of the mechanism of repeated captures of holes on the R-centers.

Note in conclusion that in some situations the effect of repeated captures in the crystal can be eliminated automatically. Thus, when considering the migration–dependent relaxation of the photocurrent (chapters 3.1 and 3.2), the oscillation phenomenon was not manifested. In this case, it was due to the fact that R-centers accumulated in the area of spatial charge at the contacts. Inner field in SCR had contributed to the outflow of the embossed holes from the centers. The opposite is true. The fact that repeated captures didn't affect, serves as the proof of correctness of the constructed models, both relaxation, and re-capture.

5.2. Determination of quantum yield for infrared light

Oscillation of the release of capture did not occur in the externally recorded electric current, such as the coordinate of the charge carriers is not changed. For this reason, these stages of excitation remained unexplored.

In our case, the effect of infrared photocurrent quenching was chosen as a measurement tool. The quantum yield for monochromatic long-wave light was directly determined by experiment. It should be assumed that this parameter determines on the one hand the number of free media, and on the other – the number of photons spent on it. The difference is precisely related to the media returns to the original center, which are useless for current generation.

To determine the quantum yield of IR quenching, we applied the formula (1.9), [10,11] derived under the condition of significant light fluxes of exciting and suppressing light. Moreover, the intensity of the quenching is greater than the intensity of the excitation.

It means the number of quants trapped on the front surface of the crystal absorbed in the sample and created free carriers. Taking into account the quantum outputs for light fluxes, the expression for the quenching coefficient has the form

$$Q = \left[\left(1 - \frac{\tau_p}{\tau_n} \right) + \frac{L_{quench} \alpha \beta \tau_p}{L_{excit} \alpha' \beta' \tau_n} \right] \cdot 100\% \quad (5.1)$$

which assumes a linear Q-lux dependence in the infrared region.

Figure 5.2 shows the experimental dependence of Q factor on the intensity of the quenching light of a wavelength of 1100 nm with the fixed threads of the excitation light. The view of figure 5.2 corresponds to the section of the graph 1.1.b along the vertical line. The short-wave maximum of quenching is chosen as more sensitive to external influences (see Fig. 5.1).

As can be seen from the figure, in the case where the intensity of the exciting light is too small (curve 1) or too large (curve 5) compared to the intensity of the quenching light, the graphs did not contain linear sections. Obviously, for these curves the conditions of derivation of the formula (1.9) were not observed. Thus, these dependencies, (1) and (5) Fig. 5.2, define the limits of applicability of the expression for Q (L_{quench}; L_{excit}) (see also Section 1.2 and Fig.1.2).

The region of linear dependence was found for curves 2-4 in the range of dampening light intensities (12–25)·1015 s-1·mm-2 at exciting light intensities from 2.6 to 9,8 lx.

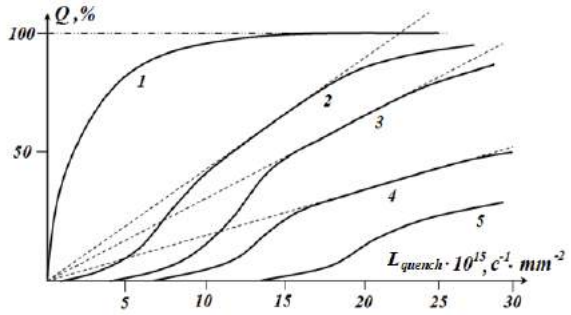

Fig. 5.2. The dependence of the
nching value on the number of infrared
ıs incident on the surface of the sample at
a fixed excitation level:
=1.2 *lx*; 2. L_{excit} =2.6 *lx*; 3. L_{excit} =4.25
4. L_{excit} =9.8 *lx*; 5. L_{excit} =19.4 *lx*.

It can be seen that as the intensity of the exciting light increases, the slope of the graphs 2-4 in the linear region decreases. Extrapolation of the linear sections of curves 2-4 fell into the origin of figure 5.2. According to the formula (5.1), this means that the first term in square brackets, with values, Lquench =0 is also equal . In such a case, at least for straight sections, it should . That is, the lifetime of free holes approximately corresponds to the lifetime of free electrons. This is the expected result, since recombination is mainly carried out through S-centers with the same capture cross-section for electrons and holes. Unfortunately, the details of changes in the relationship of the times of life at different intensities of own and exciting light have not been studied. At further calculations it was accepted $\frac{\tau_p}{\tau_n} = 1$.

The type of denominator of the second term in (5.1) is not convenient for experimental processing. So he was transformed, given n = L_{excit} $\alpha'\beta'\tau_n$,, where n is the concentration of the charge created by their own light. Then j=(enμ)E was used. Taking into account: $j = \frac{I_{excit}}{S}; E = \frac{U}{l}$, where I_{excit} –current flowing under the action of exciting light only, and *l=1,2 mm* – length of the sample between the contacts *S=1 mm²* – cross section of the sample, we obtain:

$$L_{excit} \alpha' \beta' \tau_n = I_{excit} D, \quad (5.2)$$

where the constant $D = \frac{l}{US\mu e}$.

The value of the voltage U=20 V was chosen as the minimum of those used to make the effect brighter, since a small voltage at least interferes with the oscillation (see section 5.1). The mobility value is taken $\mu = 210 \frac{cm^2}{V c}$.Thus, under the parameters used

$$D = 7{,}14 \cdot 10^{21} \text{ A}^{-1}\text{m}^{-1}. \quad (5.3)$$

After the above transformations, the formula (5.1) taking into account (5.2)–(5.3)

$$Q = \left[\frac{L_{quench} \alpha \tau}{I_{excit} D} \beta \right] \cdot 100\ \%$$

allows you to determine the coefficient of the angle of the curve Q (L_{quench} |L_{excit}):

$$\frac{\Delta Q}{L_{quench}} = \left[\frac{\alpha\,\tau}{I_{excit} D}\right]\beta \cdot 100\,\%\,. \qquad (5.4)$$

The coefficient α was determined by a spectrophotometer СФ-26 at a wavelength of 1100 nm. In the range of output slots of the spectrophotometer from 0.4 to 0.6 mm was obtained $\bar{\alpha}$=0.96. The lifetime of carriers was determined in two ways - by modulation of illumination and by the phase shift method [19], and was $8\cdot10^{-4}$ c.

With this in mind, it is determined: for curve 2 of figure 5.2 – β_2=0,026; for curve 3 – β_3=0,049; for curve 4 – β_4=0,072.

It is seen that the value β remains abnormally low in the entire region of the applied photoexcitation intensities. Moreover, the absorption coefficient of long-wave light is close to 1. This means that for the final release of each hole from the R-center, several tens of IR photons are consumed (in our case, from about 40 to 15). The hole repeatedly returns to the original level until the applied field drags it beyond the capture section. Indirectly, this is also evidenced by the changes in Q with the intensities of both light fluxes and the field considered above.

Some increase β with increasing photocurrent, and hence the intensity of their own light is associated with an increase in the population of R-centers. This increases the likelihood of media ejection and reduces the possibility of reseizures.

Thus, it is shown that within the limits of the applied combination of exciting factors – temperature, field and intensities of self and quenching light – when the lifetimes of nonequilibrium carriers of both signs were approximately equal, the calculated value of the quantum yield is in the range [0,026 – 0,072]. This, along with the Lux-ampere and field dependence Q, indicates the presence of a previously unexplored phase of charge excitation from deep traps – before taking part in the current transfer, they can repeatedly return to the initial center [15,18].

The proposed model allows estimating the concentration of the second class centers. For this purpose, the parameters of curve 4 were used at an extremely large, but still working, intensity of own light, or, what is the same, the maximum of the observed quantum yields. The abscissa of its deviation from linearity (taken L_{quench} =$27\cdot10^{15}$ $c^{-1}\cdot mm^{-2}$), the change of the growth mechanism β, is treated as the number of photons comparable to the concentration of R-centers. Then the calculation was carried out according to the same algorithm as in section 1.1. First, the proportion of photons from the whole beam that fall on the crystal surface was determined. This was done by the proportion between the light spot and the geometric dimensions of the front surface of the sample. Then it was assumed that the absorbed photons in the crystal are distributed uniformly and their density was calculated $N'' = 8,64\cdot10^{14}\ cm^{-3}$. The concentration of recombination R-centers in the investigated crystal is thus of order $9\cdot10^{14}\ cm^{-3}$.

REFERENCES

1. Simanovych N.S., Brytavskyi Ye.V., Kutalova M.I., Borshchak V.A., Karakis Y.N. “The study of heterogeneous sensitized crystals of cadmium sulfide. Part I. About charge state of the centers recombination” // “Photoelectronics”, n. 26. Odessa, “Одеський національний університет” 2017. s. 124 – 138 .

2. S.S.Kulikov, Ye.V. Brytavskyi, M.I., Kutalova, N.P. Zatovskaya, V.A. Borshchak, N.V. Konopel’skaya, Y.N. Karakis “The study of cadmium sulfide heterogeneously sensitized crystals. Part II. Relaxation characteristics” // “Photoelectronics”, n. 27. Odessa, “Одеський національний університет” 2018. s. 79 – 93 .

3. A.A.Dragoev, Yu.N.Karakis, M.I. Kutalova “Studies of processes within short-wave threshold of photocurrent infrared quenching” // Photoelectronics, n. 16. 2007. s. 60 – 64.

4. А.А.Драгоев “Вивчення умов початку інфрачервоного гасіння фотоструму” // Работа – призёр Областной сессии МАН. Мала Академія наук України. Одеське територіальне відділення. Секція “Фізика”. Одеса, 2007. 31 с.

5. Каракис К.Ю. “Релаксационные характеристики полупроводниковых кристаллов

с ИК-гашением фототока”// Одесса, Работа – лауреат Областного конкурса (III место) Малой академии наук, Областное территориальное отделение, Секция “Физика”. Одесса, 2001. с. 1–37.
6. Ю.Н.Каракис, Н.П.Затовская, В.В.Зотов, М.И.Куталова “Особенности релаксации фототока в кристаллах сульфида кадмия с запорными контактами” // 1-а Українська наукова конференція з фізики напівпровідників. Одеса, 10–14 вересня 2002. Тези доповідей. Т.2. – с.138.
7. К.Ю.Каракис, В.А.Борщак, В.В.Зотов, М.И.Куталова “Релаксационные характеристики кристаллов сульфида кадмия с ИК- гашением” // Фотоэлектроника вып.11. 2002. с.51 – 55.
8. Каракис Ю.Н., Борщак В.А., Затовская Н.П., Зотов В.В., Куталова М.И., Балабан А.П. “Исследование релаксации фототока в полупроводниковом устройстве” // Фотоэлектроника №12. 2003. с. 132 – 135.
9. M.A.Novikova, Yu.N.Karakis, M.I. Kutalova “Particularities of current transfer in the crystals with two types of Recombination centers” // Photoelectronics n.14. 2005. s. 58 –61.
10. A.A.Dragoev, Yu.N.Karakis, M.I. Kutalova “Peculiarities in photoexcitation of carriers from deep traps” // Photoelectronics n. 15. 2006. s. 54–56.
11. Драгоев А.А., Затовская Н.П., Каракис Ю.Н., Куталова М.И. “Управляемые электрическим полем датчики инфракрасного излучения” // Материалы 2 nd International Scientific and Technical Conference “Sensors Electronics and Microsystems Technology” Book of abstracts s. 115. Секция IV “Радіаційні, оптичні, та оптоелектричні сенсори”. Україна, Одеса, 26–30 червня 2006 р. “Астропринт”. 2006.
12. Зимина София Олеговна, Каракис Юрий Николаевич “Исследование полупроводникового спектрального калибратора с селективной чувствительностью” // Материалы международной заочной научно-практической конференции “Инновационные подходы и современная наука” – Новосибирск. 2012. с. 20-26.
13. Зимина С.О., Каракис Ю.Н. “Разработка физических основ схем регистрации в ближней инфракрасной области” // Международная конференция “Электронная техника и технологии”. Харьковский национальный университет радиоэлектроники. Харьков. 2011. Тезисы докладов. Том 1. “Электронные приборы и компоненты, включая микро- и наноэлектронные”. с. 106.
14. Melnik A.S., Karakis Y.N.. Kutalova M.I., Chemeresjuk G.G. “Features of thermo-optical transitions from the recombination centers excited states” // Photoelectronics n. 20. 2011. s. 23-28.
15. Софія Зіміна, Юрій Каракіс. “Спектрально–чутливий датчик світлових потоків, температури та напруги“ // International Conference of Students and Young Scientists in Theoretical and Experimental Physics HEUREKA – Lviv, Ukraine – 2011. – Book of abstracts. s. F3.
16. Новикова М.А. “Особливості інфрачервоного гасіння фотоструму у напівпровідниках CdS” // Работа – лауреат Областного конкурса (1 место) Малой академии наук, Областное территориальное отделение, Секция “Физика”. Одесса, 2005. с. 1 – 37.
17. M.A.Novikova “Change of Photoelectric Properties of Semiconductors as a Tool for the Control of Environmental Pollution by Extraneous Admixtures and IR-illumination” //Section of Environmental Science. Finalist of Intel International Science and Engineering Fair. USA, AZ, Phoenix, May 8 – 18. 2005.
18. А.А.Драгоев “Визначення квантового виходу інфрачервоного гасіння фототоку” // Робота – лауреат Областної сесії Малої Академії наук України. Одеське територіальне відділення. Секція “Фізика”. Одеса 2006. 32 с.
19. Чемересюк Г.Г., Каракис Ю.Н. Методические указания к лабораторным работам по спецпрактикуму “Фотоэлектрические процессы в полупроводниках. Часть I.” // Одесса. Издательство Одесского национального университета. 2011. с. 1 – 59.
20. 13. L.M. Filevska. Luminescence of

nanoscale tin dioxide. Review. Photoelectronics. 27 (2018), p.52-59.
21. 12. V.S. Grinevych, L.M. Filevska, V.A. Smyntyna, M.O. Stetsenko, S.P. Rudenko, L.S. Maksimenko, and B.K. Serdega. Characterization of SnO2 Sensors Nanomaterials by Polarization Modulation Method. Springer Science+Business Media Dordrecht 2016 J. Bonca, S. Kruchinin (eds.), ˇ Nanomaterials for Security, NATO Science for Peace and Security Series A: Chemistry and Biology, DOI 10.1007/978-94-017-7593-9, p.259-266.

UDC 621.315.592

S. S. Kulikov, Ye. V. Brytavskyi, V. A. Borshchak, N. P. Zatovskaya, M. I. Kutalova, Y. N. Karakis

THE STUDY OF HOMOGENEOUS AND HETEROGENEOUS SENSITIZED CRYSTALS OF CADMIUM SULFIDE. PART III. OSCILLATIONS OF EXCITED CARRIERS

The processes at short-wave limit of the quenching of the photocurrent were studied. The possibility of creating a new type of device - a sensitive photometer (not on the intensity of light, but on its wavelength), and the combined temperature–voltage tester.

The process of hole oscillation under photoexcitation from R-centers is investigated. The quantum yield for infrared light is determined. The effect of the applied voltage on the form of the spectral distribution curves of the photocurrent quenching was found and explained. The concentration of R-centers in the samples is calculated.

This publication is a continuation of the reviews [1–2]. For the sake of preservation of generality of work continuous numbering of sections is chosen. Numbers of formulas and figures are presented by sections. References in each article are given individually.

Cadmium sulfide crystals are used in our studies as a convenient model material. Obtained results and constructed models are also applied to other semiconductors.

УДК 621.315.592

С. С. Куликов, Е. В. Бритавский, В. А. Борщак, Н. П. Затовская, М. И. Куталова, Ю. Н. Каракис

ИССЛЕДОВАНИЕ ОДНОРОДНО И НЕОДНОРОДНО ОЧУВСТВЛЁННЫХ КРИСТАЛЛОВ СУЛЬФИДА КАДМИЯ. ЧАСТЬ III. ОСЦИЛЛЯЦИИ ВОЗБУЖДЁННЫХ НОСИТЕЛЕЙ

Изучены процессы на коротковолновой границе гашения фототока. Показана возможность создания прибора нового типа – как чувствительного фотометра (но не на интенсивность света, а на его длину волны), так и комбинированного тестера температура–напряжение.

Исследован процесс осцилляции дырок при фотовозбуждении с R-центров. Определён квантовый выход для инфракрасного света. Обнаружено и объяснено влияние приложенного напряжения на вид кривых спектрального распределения гашения фототока. Вычислена концентрация R-центров в образцах.

Настоящая публикация является продолжением обзоров. Ради сохранения общности работы нумерация разделов выбрана сквозной. Номера формул и рисунков представлены по разделам. Ссылки на литературу в каждой статье даются индивидуально.

Кристаллы сульфида кадмия использованы в наших исследованиях как удобный модельный материал. Полученные на них результаты и построенные модели распространяются также на другие полупроводниковые вещества.

Ключевые слова: сульфид кадмия, фотовозбуждение, гашение фототока

Інформація для авторів наукового збірника «Photoelectronics»

У збірнику "Photoelectronics " друкуються статті, що містять відомості про наукові дослідження і технічні розробки в напрямках:

*** фізика напівпровідників;**
*** гетеро- і низькорозмірні структури;**
*** фізика мікроелектронних приладів;**
*** лінійна і нелінійна оптика твердого тіла;**
*** оптоелектроніка та оптоелектронні прилади;**
*** квантова електроніка;**
*** сенсорика.**

Збірник "Photoelectronics видається англійською мовою. Рукопис подається автором у двох примірниках англійською і російською мовами.

Електронна копія статті повинна відповідати наступним вимогам:
1. Для тексту дозволяються наступні формати – MS Word (rtf, doc).
2. Рисунки приймаються у форматах – EPS. TIFF. BMP, PCX, JPG. GIF, CDR. WMF, MS Word I MS Giaf, Micro Calc Origin (opj).

Рукописи надсилаються за адресою:
Відп. секр. Куталовій М. І., вул. Пастера, 42. фіз. фак. ОНУ, м. Одеса, 65082
E-mail: photoelectronics@onu.du.ua
тел. 0482-726-63-56.

Збірники "Photoelectronics" знаходяться на сайті: http://photoelectronics.onu.edu.ua

До рукопису додаються:
1. Коди PAC і УДК. Допускається використання декількох шифрів, що розділяються комами.
2. Прізвища і ініціали авторів.
3. Установа, повна поштова адреса, номер телефону, номер факсу, адреси електронної пошти для кожного з авторів.
4. Назва статті.
5. Резюме обсягом до 200 слів пишеться англійською, російською і (для авторів з України) – українською мовами.

Текст друкувати шрифтом 14 пунктів через два інтервали на білому папері формату А4. Назва статті, а також заголовки підрозділів друкуються прописними літерами. .
Рівняння необхідно друкувати в редакторі формул MS Equation Editor. Необхідно давати визначення величин, що з'являються в тексті вперше.
Посилання на літературу друкувати через два інтервали, нумеруватися в квадратних дужках послідовно, у порядку їхньої появи в тексті статті. Посилатися необхідно на літературу, що видана пізніше 2000 року.
Підписи до рисунків і таблиць друкуються в тексті рукопису в порядку їхньої ілюстрації.
Резюме обсягом до 200 слів друкується англійською, російською і українською мовами (для авторів з України). Перед текстом резюме відповідною мовою вказуються УДК, прізвища та ініціали всіх авторів, назва статті.

Информация для авторов
Научного сборника «Photoelectronics »

В сборнике "Photoelectronics " печатаются статьи, которые содержат сведения о научных ис-следованиях и технических разработках в направлениях:

*** физика полупроводников;**
*** гетеро- и низкоразмерные структуры;**
*** физика микроэлектронных приборов;**
*** линейная и нелинейная оптика твердого тела;**
*** оптоэлектроника и оптоэлектронные приборы;**
*** квантовая электроника;**
*** сенсорика**

Сборник"Photoelectronics издаётся на английском языке. Рукопись подается автором в двух экземплярах на английском и русском языках.

Электронная копия статьи должна отвечать следующим требованиям:
1. Для текста допустимы следующие форматы - MS Word (rtf, doc).
2. Рисунки принимаются в форматах – EPS. TIFF. BMP, PCX, JPG. GIF, CDR. WMF, MS Word И MS Giaf, Micro Calc Origin (opj).

Рукописи присылаются по адресу:
Отв. секр. Куталовой М. И., ул. Пастера. 42. физ. фак. ОНУ, г. Одесса, 65026
E-mail:photoelectronics@onu.du.ua тел. 0482 - 726 6356 .

Статьи сб."Photoelectronics " находятся на сайте: http://photoelectronics.onu.edu.ua

К рукописи прилагается:
1. Коды PAC и УДК. Допускается использование нескольких шифров, которые разделяются запятой.
2. Фамилии и инициалы авторов.
3. Учреждение, полный почтовый адрес, номер телефона, номер факса, адреса электронной почты для каждого из авторов.
4. Название статьи.
5. Резюме объемом до 200 слов пишется на английском, русском языках и (для авторов из Украины) – на украинском.

Текст должен печататься шрифтом 14 пунктов через два интервала на белой бумаге формата А4. Название статьи, а также заголовки подразделов печатаются прописными буквами и отмечаются полужирным шрифтом.

Уравнения необходимо печатать в редакторе формул MS Equation Editor. Необходимо давать определение величин, которые появляются в тексте впервые.

Ссылки на литературу должны печататься через два интервала, нумероваться в квадратных скобках последовательно, в порядке их появления в тексте статьи. Ссылаться необходимо на литературу, которая издана позднее 2000 года.

Подписи к рисункам и таблицам печатаются в тексте рукописи в порядке их иллюстрации.

Резюме объемом до 200 слов печатается на английском, русском языках и на украинском (для авторов из Украины). Перед текстом резюме соответствующим языком указываются УДК, фамилии и инициалы всех авторов, название статьи.

Information for contributors of «Photoelectronics» articles

"Photoelectronics" Articles publishes the papers which contain information about scientific research and technical designs in the following areas:

- Physics of semiconductors;
- Physics of microelectronic devices;
- Linear and non-linear optics of solids;
- Optoelectronics and optoelectronic devices;
- Quantum electronics;
- Sensorics.

"Photoelectronics" Articles is defined by the decision of the Highest Certifying Commission as the specialized edition for physical-mathematical and technical sciences and published and printed at the expense of budget items of Odessa I.I. Mechnikov National University.

«Photoelectronics» Articles is published in English. Authors send two copies of papers in English. The texts are accompanied by 3.5» diskette with text file, tables and figures. Electronic copy of a material can be sent by e-mail to the Editorial Board and should meet the following requirements:

1.The following formats are applicable for texts – MS Word (rtf, doc).

2. Figures should be made in formats – EPS, TIFF, BMP, PCX, JPG, GIF, WMF, MS Word I MS Giaf, Micro Calc Origin (opj). Figures made by packets of mathematical and statistic processing should be converted into the foregoing graphic formats.

The papers should be sent to the address:

Kutalova M.I., Physical Faculty of Odessa I. I. Mechnikov National University, 42 Pastera str, 65026 Odessa, Ukraine, e-mail: wadz@mail.ru, tel. +38-0482-7266356. Information is on the site:

http://www.photoelectronics.onu.edu.ua

The title page should contain:

1. Codes of PACS
2. Surnames and initials of authors
3. TITLE OF PAPER
4. Name of institution, full postal address, number of telephone and fax, electronic address

An abstract of paper should be not more than 200 words. Before a text of summary a title of paper, surnames and initials of authors should be placed.

Equations are printed in MS Equation Editor.

References should be printed in double space and should be numbered in square brackets consecutively throughout the text. References for literature published in 2000-2009 years are preferential.

Illustrations will be scanned for digital reproduction. Only high-quality illustrations will be taken for publication. Legends and symbols should be printed inside. Neither negatives, nor slides will be taken for publication. All figures (illustrations) should be numbered in the sequence of their record in text.

For additional information please contact with the Editorial Board.

Верстка – О. І. Карлічук

Підп.до друку 24.12.2019.
Формат 60×84/8. Ум.-друк.арк. 17,21.
Тираж 300 прим. Замов. № ____.

Видавець і виготовлювач
«Одеський національний університет імені І. І. Мечникова»
Свідоцтво ДК № 4215 від 22.11.2011 р.

65082, м. Одеса, вул. Єлісаветинська, 12, Україна
Тел.: (048) 723 28 39, e-mail: druk@onu.edu.ua